

Institut für Informatik und Computational Science

# Global response to local extremes—a storyline approach on economic loss propagation from weather extremes

KUMULATIVE DISSERTATION

zur Erlangung des akademischen Grades „doctor rerum naturalium“  
(Dr. rer. nat.) in der Wissenschaftsdisziplin „Angewandte Informatik“

eingereicht an der



Mathematisch-  
Naturwissenschaftlichen  
Fakultät der Universität Potsdam

angefertigt am



Potsdam-Institut für  
Klimafolgenforschung

vorgelegt von

**ROBIN MIDDELANIS**

im April 2023.

Ort und Tag der Disputation: Potsdam, 6.10.2023

Betreuer der Arbeit: Prof. Dr. Niels Landwehr & Prof. Dr. Anders Levermann

Externer Gutachter: Prof. Dr. Elco Koks



This work is protected by copyright and/or related rights. You are free to use this work in any way that is permitted by the copyright and related rights legislation that applies to your use. For other uses you need to obtain permission from the rights-holder(s).

<https://rightsstatements.org/page/InC/1.0/?language=en>

Prüfungskommission:

Prof. Dr. Niels Landwehr (Hauptbetreuer & 1. Gutachter)

Prof. Dr. Anders Levermann (Zweitbetreuer & 2. Gutachter)

Prof. Dr. Elco Koks (3. Gutachter)

Prof. Dr. Torsten Schaub

Prof. Dr. Marina Höhne

Dr. Christian Otto

Published online on the

Publication Server of the University of Potsdam:

<https://doi.org/10.25932/publishup-61112>

<https://nbn-resolving.org/urn:nbn:de:kobv:517-opus4-611127>





# Abstract

Due to anthropogenic greenhouse gas emissions, Earth's average surface temperature is steadily increasing. As a consequence, many weather extremes are likely to become more frequent and intense. This poses a threat to natural and human systems, with local impacts capable of destroying exposed assets and infrastructure, and disrupting economic and societal activity. Yet, these effects are not locally confined to the directly affected regions, as they can trigger indirect economic repercussions through loss propagation along supply chains. As a result, local extremes yield a potentially global economic response. To build economic resilience and design effective adaptation measures that mitigate adverse socio-economic impacts of ongoing climate change, it is crucial to gain a comprehensive understanding of indirect impacts and the underlying economic mechanisms.

Presenting six articles in this thesis, I contribute towards this understanding. To this end, I expand on local impacts under current and future climate, the resulting global economic response, as well as the methods and tools to analyze this response.

Starting with a traditional assessment of weather extremes under climate change, the first article investigates extreme snowfall in the Northern Hemisphere until the end of the century. Analyzing an ensemble of global climate model projections reveals an increase of the most extreme snowfall, while mean snowfall decreases.

Assessing repercussions beyond local impacts, I employ numerical simulations to compute indirect economic effects from weather extremes with the numerical agent-based shock propagation model *Acclimate*. This model is used in conjunction with the recently emerged storyline framework, which involves analyzing the impacts of a particular reference extreme event and comparing them to impacts in plausible counterfactual scenarios under various climate or socio-economic conditions. Using this approach, I introduce three primary storylines that shed light on the complex mechanisms underlying economic loss propagation.

In the second and third articles of this thesis, I analyze storylines for the historical Hurricanes Sandy (2012) and Harvey (2017) in the USA. For this, I first estimate local economic output losses and then simulate the resulting global economic response with *Acclimate*. The storyline for Hurricane Sandy thereby focuses on global consumption price anomalies and the resulting changes in consumption. I find that the local economic disruption leads to a global wave-like economic price ripple, with upstream effects propagating in the

supplier direction and downstream effects in the buyer direction. Initially, an upstream demand reduction causes consumption price decreases, followed by a downstream supply shortage and increasing prices, before the anomalies decay in a normalization phase. A dominant upstream or downstream effect leads to net consumption gains or losses of a region, respectively. Moreover, I demonstrate that a longer direct economic shock intensifies the downstream effect for many regions, leading to an overall consumption loss.

The third article of my thesis builds upon the developed loss estimation method by incorporating projections to future global warming levels. I use these projections to explore how the global production response to Hurricane Harvey would change under further increased global warming. The results show that, while the USA is able to nationally offset direct losses in the reference configuration, other countries have to compensate for increasing shares of counterfactual future losses. This compensation is mainly achieved by large exporting countries, but gradually shifts towards smaller regions. These findings not only highlight the economy's ability to flexibly mitigate disaster losses to a certain extent, but also reveal the vulnerability and economic disadvantage of regions that are exposed to extreme weather events.

The storyline in the fourth article of my thesis investigates the interaction between global economic stress and the propagation of losses from weather extremes. I examine indirect impacts of weather extremes — tropical cyclones, heat stress, and river floods — worldwide under two different economic conditions: an unstressed economy and a globally stressed economy, as seen during the Covid-19 pandemic. I demonstrate that the adverse effects of weather extremes on global consumption are strongly amplified when the economy is under stress. Specifically, consumption losses in the USA and China double and triple, respectively, due to the global economy's decreased capacity for disaster loss compensation. An aggravated scarcity intensifies the price response, causing consumption losses to increase.

Advancing on the methods and tools used here, the final two articles in my thesis extend the agent-based model *Acclimate* and formalize the storyline approach. With the model extension described in the fifth article, regional consumers make rational choices on the goods bought such that their utility is maximized under a constrained budget. In an out-of-equilibrium economy, these rational consumers are shown to temporarily increase consumption of certain goods in spite of rising prices.

The sixth article of my thesis proposes a formalization of the storyline framework, drawing on multiple studies including storylines presented in this thesis. The proposed guideline defines eight central elements that can be used to construct a storyline.

Overall, this thesis contributes towards a better understanding of economic repercussions of weather extremes. It achieves this by providing assessments of local direct impacts, highlighting mechanisms and impacts of loss propagation, and advancing on methods and tools used.

# Zusammenfassung

Mit dem kontinuierlichen Anstieg der globalen Mitteltemperatur aufgrund anthropogener Treibhausgasemissionen kann die Intensität und Häufigkeit vieler Wetterextreme zunehmen. Diese haben das Potential sowohl natürliche als auch menschliche Systeme stark zu beeinträchtigen. So hat die Zerstörung von Vermögenswerten und Infrastruktur sowie die Unterbrechung gesellschaftlicher und ökonomischer Abläufe oft negative wirtschaftliche Konsequenzen für direkt betroffene Regionen. Die Auswirkungen sind jedoch nicht lokal begrenzt, sondern können sich entlang von Lieferketten ausbreiten und somit auch indirekte Folgen in anderen Regionen haben – bis hin zu einer potenziell globalen wirtschaftlichen Reaktion. Daher sind Strategien zur Anpassung an veränderliche Klimabedingungen notwendig, um die Resilienz globaler Handelsketten zu stärken und dadurch negative sozioökonomische Folgen abzumildern. Hierfür ist ein besseres Verständnis lokaler Auswirkungen sowie ökonomischer Mechanismen zur Schadensausbreitung und deren Folgen erforderlich.

Die vorliegende Dissertation umfasst insgesamt sechs Artikel, die zu diesem Verständnis beitragen. In diesen Studien werden zunächst lokale Auswirkungen von Wetterextremen unter gegenwärtigen und zukünftigen klimatischen Bedingungen untersucht. Weiterhin werden die globalen wirtschaftlichen Auswirkungen lokaler Wetterextreme sowie die darunterliegenden ökonomischen Effekte analysiert. In diesem Zusammenhang trägt diese Arbeit ferner zu der Weiterentwicklung der verwendeten Methoden und Ansätze bei.

Der erste Artikel widmet sich zunächst der Betrachtung von extremem Schneefall in der nördlichen Hemisphäre unter dem Einfluss des Klimawandels. Zu diesem Zweck wird ein Ensemble von Projektionen globaler Klimamodelle bis zum Ende des Jahrhunderts analysiert. Die Projektionen zeigen dabei eine Verstärkung von extremen Schneefallereignissen, während die mittlere Schneefallintensität abnimmt.

Um indirekte Auswirkungen von Wetterextremen zu erforschen, wird weiterhin das numerische agentenbasierte Modell *Acclimate* verwendet, welches die Ausbreitung ökonomischer Verlustkaskaden im globalen Versorgungsnetzwerk simuliert. In mehreren sogenannten Storylines werden die Auswirkungen eines historischen Referenzereignisses analysiert und mit den potentiellen Auswirkungen dieses Ereignisses unter plausiblen alternativen klimatischen oder sozioökonomischen Bedingungen verglichen. In dieser Dis-

sertation werden drei zentrale Storylines vorgestellt, die jeweils unterschiedliche Aspekte der Schadensausbreitung von Wetterextremen untersuchen.

Im zweiten und dritten Artikel dieser Arbeit werden dazu Storylines für die historischen Hurrikane Sandy (2012) und Harvey (2017) in den USA untersucht. Hierfür werden zunächst die lokalen ökonomischen Verluste durch diese Hurrikane ermittelt, welche als direkte wirtschaftliche Schockereignisse in *Acclimate* zur Berechnung der globalen Reaktion verwendet werden. Hierbei untersucht die Studie zu Hurricane Sandy globale Konsumpreisanomalien und damit einhergehende Auswirkungen auf das Konsumverhalten. Der direkte Schock löst hier eine wellenartige Veränderung globaler Konsumpreise mit drei Phasen aus, welche aus gegenläufigen Effekte aufwärts und abwärts der Lieferketten resultiert – sogenannten Upstream- und Downstream-Effekten. Zunächst steigt der Konsum aufgrund sinkender Preise durch Upstream-Effekte, bevor Preise aufgrund von Güterknappheit durch Downstream-Effekte wieder ansteigen und der Konsum abfällt. In einer Normalisierungsphase klingen diese Anomalien wieder ab. Ein länger anhaltender direkter wirtschaftlicher Schock verstärkt die Downstream-Phase und führt so in vielen Regionen insgesamt zu einem Konsumverlust.

Die entwickelte Methode zur Berechnung direkter Verluste wird im dritten Artikel erweitert, indem Verstärkungen unter dem Einfluss des fortschreitenden Klimawandels berücksichtigt werden. Unter Nutzung dieser verstärkten direkten Verluste wird die Veränderung globaler Produktionsanomalien in Reaktion auf Hurricane Harvey simuliert. Die Ergebnisse zeigen, dass die USA bei zunehmender Erwärmung nicht mehr in der Lage sein werden, direkte Produktionsverluste auf nationaler Ebene auszugleichen. Stattdessen muss ein zunehmender Anteil dieser Verluste durch andere, insbesondere exportstarke Länder ausgeglichen werden. Der Anteil kleinerer Regionen an dieser ausgleichenden Produktion nimmt jedoch mit zunehmenden direkten Verlusten zu. Diese Produktionsverschiebungen verdeutlichen die Möglichkeit der globalen Wirtschaft, lokale Katastrophenverluste weitgehend flexibel abzumildern. Gleichzeitig veranschaulichen sie den Wettbewerbsnachteil direkt betroffener Wirtschaftsregionen.

Die Storyline im vierten Artikel befasst sich mit dem Einfluss einer globalen wirtschaftlichen Krise auf die Schadensausbreitung von tropischen Wirbelstürmen, Hitzestress und Flussüberschwemmungen weltweit. Hierfür werden die indirekten Auswirkungen dieser Extreme unter dem Einfluss der global reduzierten wirtschaftlichen Aktivität während der Covid-19-Pandemie, sowie bei „normaler“ globaler Wirtschaftsleistung simuliert. Der Vergleich beider Szenarien zeigt bei global gestörter Wirtschaft eine deutliche Verstärkung negativer Konsumauswirkungen durch die simulierten Extreme. Konsumverluste steigen besonders stark in den USA und China an, wo sie sich verdoppeln bzw. verdreifachen. Diese Veränderungen resultieren aus der global verminderten wirtschaftlichen Kapazität, die für den Ausgleich der Produktionsverluste von Wetterextremen zur Verfügung steht. Dies verstärkt die Extremewetter-bedingte Güterknappheit, was zu Preisanstiegen und erhöhten Konsumverlusten führt.

Abschließend werden in den letzten beiden Artikeln die in der Arbeit verwendeten Methoden und Ansätze erweitert. Hierfür wird das Modell *Acclimate* im fünften Artikel weiterentwickelt, indem Konsumenten als rational agierende Agenten modelliert werden. Mit dieser Erweiterung treffen lokale Verbraucher Entscheidungen über die konsumierten Güter so, dass diese den Nutzen eines begrenzten Budgets maximieren. Die entstehende Dynamik kann außerhalb eines wirtschaftlichen Gleichgewichts dazu führen, dass bestimmte Güter temporär trotz erhöhter Preise stärker nachgefragt werden.

Der sechste Artikel formalisiert den Storyline-Ansatz und präsentiert einen Leitfaden für die Erstellung von Storylines. Dieser basiert auf den Ergebnissen mehrerer Studien, die diesen Ansatz verfolgen; einschließlich Storylines aus der vorliegenden Arbeit. Es werden insgesamt acht Elemente definiert, anhand derer eine Storyline-Studie erstellt werden kann.

Insgesamt trägt diese Arbeit zu einem umfassenderen Verständnis der ökonomischen Auswirkungen von Wetterextremen bei. Hierfür werden lokale Auswirkungen von Extremen unter gegenwärtigen und zukünftigen klimatischen Bedingungen untersucht, sowie wichtige ökonomische Mechanismen und Auswirkungen der resultierenden Schadensausbreitung aufgedeckt. Neben diesen Erkenntnissen werden überdies Weiterentwicklungen der Methoden und Ansätze präsentiert, die weiterführende Analysen ermöglichen.



# Contents

INTRODUCTION	I
1 Climate change impacts . . . . .	I
2 Global response to local extremes . . . . .	3
3 The storyline approach . . . . .	5
4 Scope of this thesis . . . . .	6
5 Article contributions . . . . .	13
ARTICLES	17
1 The intensification of snowfall extremes . . . . .	19
2 The global economic response to Hurricane Sandy . . . . .	29
3 The projected compensation response to Hurricane Harvey . . . . .	41
4 The response to extremes under global economic stress . . . . .	53
5 The utility maximizing consumer . . . . .	71
6 The formalization of storylines . . . . .	97
DISCUSSION AND CONCLUSIONS	131
1 Assessing current and future local impacts . . . . .	131
2 Simulating the global economic response . . . . .	133
3 Advancing on methods and tools . . . . .	136
4 Storylines for assessing the economic response . . . . .	138
5 Conclusions . . . . .	140
REFERENCES	141
APPENDICES	149





# Introduction

## I Climate change impacts

Anthropogenic greenhouse gas emissions alter the radiation balance of the planet. As a result, Earth's mean surface temperature has already increased by about 1.2°C compared to pre-industrial times (1850-1900) and continues to increase further (IPCC 2023). A stabilization of the energy balance and thus, of the climate, can only be achieved by ceasing emissions (Fankhauser et al. 2022). Until this target of net zero emissions is reached, greenhouse gases will further continue to accumulate in the atmosphere (Friedlingstein et al. 2022).

The resulting changes within the climate system threaten the functioning of natural and human systems on multiple levels. Slow-onset changes like sea level rise (Marzeion and Levermann 2014), generally increasing temperatures (Tebaldi et al. 2021), and changes in wet and dry weather patterns (Konapala et al. 2020) have demonstrably negative implications for societies. Empirical findings already point out adverse impacts on human behaviour (Stechemesser, Levermann, and Wenz 2022) and conflict (Burke, Hsiang, and Miguel 2015a), labor (Dasgupta et al. 2021), and the economy overall (Kotz, Levermann, and Wenz 2022; Kotz, Wenz, et al. 2021; Burke, Hsiang, and Miguel 2015b). In addition to these slow-onset condition changes, climate change affects the frequency and intensity of abrupt extreme weather events such as droughts (Trenberth et al. 2014), extreme precipitation (Donat et al. 2016; Lehmann, Coumou, and Frieler 2015) and river floods (Willner, Levermann, et al. 2018), and heat waves (Suarez-Gutierrez et al. 2018). Such events cause loss of lives (Vicedo-Cabrera et al. 2021), migration (Hoffmann et al. 2020), physical damages (Guha-Sapir, Below, and Hoyois 2023), and health issues (Patz et al. 2005). Accordingly, the international community has agreed to confine global warming to "well below 2°C" within the century, compared to pre-industrial levels (Paris Agreement 2015). At the same time, societies will need to adapt to negative impacts that cannot be mitigated. This requires a good understanding of the climate's response to further emissions, as well as the socio-economic response to ongoing climate change.

## INTRODUCTION

Numerical models can be used to simulate the climate system and its reaction to continued greenhouse gas emissions in the future. Commonly, several of these climate models are combined into ensembles that are driven by standardized pathways of possible future global emissions (Eyring et al. 2016). This way, the state of the climate and many of its slow-onset changes can be projected with some certainty until the end of the century and beyond (IPCC 2021). Forecasts of extreme events on annual or even decadal time scales, on the other hand, are often subject to significant uncertainty due to the seemingly chaotic nature of weather and resulting large natural variability. Nonetheless, changing distributions of intensity and frequency can often be observed in trends or derived from simulations (Rahmstorf and Coumou 2011).

One particularly destructive type of weather extremes are tropical cyclones, also called hurricanes in the Atlantic and northeast Pacific Ocean when exceeding a certain wind speed threshold. These low-pressure weather systems evolve from evaporation over warm ocean waters in the tropics. Rising upwards, the moist air cools and clouds form due to condensation. As a result of the Coriolis force due to Earth's rotation, this self-sustained system rotates counter-clockwise on the Northern and clockwise on the Southern Hemisphere. When tropical cyclones make landfall, they can cause huge damages through strong wind, extreme precipitation, and storm surges (DWD 2017). Even though suggested by theory (Emanuel 1987), there is only little evidence for trends of tropical cyclone activity with climate change so far (Kossin et al. 2020; Knutson, Camargo, et al. 2019). Nevertheless, a distribution shift towards stronger tropical cyclones is expected under further global warming (Knutson, Camargo, et al. 2020). Even if storm intensity remains unchanged, climate change will likely exacerbate the impacts of tropical cyclones; rising sea levels increase the risk for severe storm surges (Walsh et al. 2016) and warmer temperatures increase the likelihood for extreme precipitation from tropical cyclones (Emanuel 2017).

Thus, even though the intensification of tropical cyclones with climate change is subject to ongoing research, their already large impacts (Weinkle et al. 2018), as those of other extremes, must be expected to further intensify in the absence of adequate adaptation measures. Understanding these impacts under current and future warming therefore is paramount for the development of such adaptation measures. With this thesis, I contribute towards this understanding by analyzing the current and future risks that weather extremes pose for societies. To this end, I investigate economic repercussions from tropical cyclones specifically, and weather extremes more generally. As outlined in the next section, these repercussions are not locally confined, but may evoke a potentially global response in the economic network. In my thesis, I focus on this systemic form of risk and assess how it is influenced by a changing climate as well as altered socio-economic conditions.

## 2 Global response to local extremes

Economic risk from weather extremes is determined by the vulnerability of human structures and their exposure to hazards. Accordingly, the economic cost of a disaster is most commonly reported as the estimated value of destroyed assets, referred to as damages (Van der Veen 2004). However, the economic impact of disasters extends beyond this cost of reconstruction. If during and after a disaster, production assets like machines, buildings, and land are affected, or the workforce is reduced, business interruption (Okuyama and Chang 2012; Rose 2004a) results in economic losses in the form of missed output (Okuyama and Santos 2014). These output losses are often referred to as *first-order* losses (Rose 2004b) in the regions that are physically exposed to a hazard. In the densely connected (Hummels, Ishii, and Yi 2001) and globalized economy, these first-order losses are not confined to the region of the extreme event but can propagate through the economic network along supply chains (Acemoglu et al. 2012), leading to *higher-order* effects (Rose 2004b). On the one hand, losses can propagate upstream if the locally hampered production affects the demand for goods from other regions or sectors. On the other hand, downstream propagation of losses occurs when the lost production is missing elsewhere in the economic network. In a market environment, the resulting mismatch of supply and demand is resolved by price adjustments, which in turn again affect production, demand, and consumption. The resulting complex cascades can be far-reaching and therefore constitute a form of systemic risk (Hochrainer-Stigler et al. 2020). This complexity makes an assessment of total impacts, that is, aggregated impacts of any order, challenging (Przyluski and Hallegatte 2011). However, it has been shown that higher-order effects can contribute significantly to the overall impacts from weather extremes (Willner, Otto, and Levermann 2018; Hallegatte 2008). Moreover, increasing impacts under climate change likely affect the respective systemic risks within the economic network. This raises the need for adaptation of the economy, and in particular the economic network, to global warming (Levermann 2014). To this end, a thorough understanding of future losses, as well as of the mechanisms by which these losses propagate in the economic network, is essential to increase economic resilience and suppress adverse repercussions in the future (Wenz and Willner 2022).

Economic models can be used to gain an understanding of this complexity. Early work has been done by Leontief (1970), who pioneered with the development of input-output (IO) models. These models link final consumption to the corresponding optimal levels of production through a technology matrix. This matrix defines the production function for each sector in the economy, i.e., how the outputs from one sector depend on inputs from other sectors. While first-order losses can well be calculated using IO models, they likely overestimate higher-order impacts due to the inflexibility of the economic network. As opposed to IO models, computable general equilibrium (CGE) models allow for a high degree of flexibility of the modeled economy (Botzen, Deschenes, and Sanders 2020). This

type of models derives a solution in response to an economic shock by adjusting economic variables like production, allocation of goods, and prices such that the economy reaches a new general equilibrium state. As such, they are well-suited for modeling long-term economic adjustments to economic shocks, but likely underestimate short-term impacts of unanticipated shocks. Besides IO and CGE models, agent-based models can simulate the complex interactions from loss propagation in the economic network. Such models aim to explain macro-economic dynamics by the interplay of individual agents equipped with micro-economic behavioral rules (Wenz and Willner 2022). While these models are difficult to calibrate and validate (Fagiolo, Windrum, and Moneta 2006), they have been shown to reproduce macro-economic behaviour (Mandel 2012).

In this thesis, I apply the method of agent-based modeling to simulate economic loss propagation from weather extremes in general, and tropical cyclones in particular. To this end, I use and extend the dynamic agent-based shock model *Acclimate* (Otto et al. 2017). Agents in this model are producing sectors or representative consumers on a regional level. The model dynamics emerges from the interplay of micro-economic agents following local optimization principles. Producing agents maximize their profits, while representative consumers decide on consumption levels based on price elasticities. The model computes daily perturbations of quantities of production, consumption, and trade as well as their prices in response to local economic shocks. These shocks are defined by a time-dependent reduction in production capacity of agents in regions that are geographically exposed to hazards. In the remainder of this thesis, the production equivalent of these capacity decreases are called *direct* losses. Anomalies within the economic network in response to these direct losses are referred to as *indirect* impacts. The economic network of the model is given by the Eora (Lenzen, Kanemoto, et al. 2012) multi-region input-output table, globally resolving 26 producing sectors as well as final consumption (simply consumption hereafter) on a country level. Disaggregation (Wenz, Willner, et al. 2015) yields state and province data for the USA and China, respectively. Thus, the model resolves over 7,000 agents with more than 1.8 million trade links.

Using this model, I simulate the complex interactions that result from loss propagation in the economic network to assess the impacts of weather extremes and the resulting systemic form of economic risk. Yet, besides the complexity of economic loss propagation itself, additional uncertainties arise with respect to future socio-economic development and exposure (O'Neill et al. 2014), as well as the impacts of extreme events at a regional scale under future climate. These uncertainties need to be addressed without losing informativeness of the obtained results. In this thesis, I address these issues by using the *Acclimate* model within a *storyline* framework.

### 3 The storyline approach

Traditional assessments of future impacts from extreme weather use large ensembles of climate model simulations (O'Neill et al. 2016) under different socio-economic pathways (O'Neill et al. 2014), often in combination with statistical (e.g. Villarini and Vecchi 2012) or dynamical (e.g. Knutson, Sirutis, et al. 2013) downscaling methods to produce likelihood statements of impacts conditional on the state of the climate system. While such analyses are useful to detect large-scale trends under climate change with a certain degree of confidence, their results often cannot provide practitioners with a good understanding of very rare but extreme risks. Yet, these extreme risks typically constitute benchmarks to be considered when designing adaptation measures (Hazeleger et al. 2015). Studying the interactions of systemic risks within the traditional approach is further complicated due to the involved complex impact chains, where uncertainties quickly add up. It has therefore been argued that within the traditional approach, "reliability is achieved at the price of informativeness" (Shepherd 2019), especially with regards to cases of extreme risk. However, recently the need has been raised for more research on bad-to-worst case fat-tail scenarios (Kemp et al. 2022).

As an alternative, a storyline-centric approach (Lloyd and Shepherd 2020; Shepherd et al. 2018) has been proposed to study the unfolding of impacts from weather extremes under different plausible conditions. Shepherd (2016) compares this approach to the investigation of accidents. These are often complex cascades of cause and effect, making them hard to predict due to the multitude of factors involved. But for a given specific incident, the impact chain can be analyzed and the influence of changes to this impact chain can be assessed. Analogously, the risks of specific weather extremes often cannot easily be predicted due to complex impact cascades, as in the case of loss propagation in the economic network. However, given a specific extreme event in the past, it can be analyzed how the impacts of the event unfolded. Elements in the impact chain can then be altered to represent changing climatic and socio-economic conditions, allowing to study how the the outcome of the event is affected.

Thus, storylines construct a narrative to answer a specific type of questions. Rather than asking "what will be the impact?" as in the traditional approach, the relevant question is reframed to "how would the observed impact change under different conditions?" (Shepherd 2019). To this end, self-contained impact chains of a historical event are analyzed under observed or plausible future conditions (Sillmann et al. 2021), framed as the *reference* and one or more *counterfactual* scenarios. The reference scenario is given by the unfolding of impacts from the observed event, with observed boundary conditions. Counterfactuals are then constructed for this event by imposing changed boundary conditions on the reference (Hazeleger et al. 2015). The impacts in the counterfactual scenario are conditional

on the existence of the event, hence they need not consider the possibility of changed hazard likelihood.

Storylines are particularly useful to analyze the unfolding of impacts from very rare extreme events or those where specific atmospheric conditions were central to the observed impacts (IPCC 2021). As such, they are well-suited to analyze the systemic risks of economic loss propagation from weather extremes, like major tropical cyclones. In this thesis, I construct three central storylines to assess indirect economic effects from tropical cyclones specifically, and weather extremes more generally. Within these storylines, I design counterfactual scenarios for changed climatic and socio-economic boundary conditions. Framing the overall structure of this thesis, I further contribute to the formalization of storylines, informed by the experience gathered in the particular storyline studies.

## 4 Scope of this thesis

Against the backdrop of increasing damages from weather extremes, a thorough understanding of current and future losses, and their propagation is essential for the development of effective adaptation and mitigation strategies that reduce future economic risk. Yet due to the involved complexity at multiple levels, this understanding is still incomplete. My thesis contributes to fill this gap by expanding on

1. the local impacts under current and future climate,
2. the resulting global economic response, and
3. the methods and tools to analyze this response.

To this end, this thesis builds on six scientific articles (figure 1). First, I apply the commonly used probabilistic approach in article 1 to investigate the intensification of snowfall extremes in the Northern Hemisphere until the end of the century. Then, using the storyline framework, I assess the global economic response to weather extremes generally, and tropical cyclones specifically, in articles 2–4. To this end, I construct a storyline for the 2012 landfall of Hurricane Sandy in article 2 and analyze the resulting global response in terms of consumption and consumption prices. I then present a storyline for the 2017 landfall of Hurricane Harvey in article 3, whereby counterfactuals are constructed to analyze the global production response under additional global warming. With the storyline in article 4, I analyze how the economic response to weather extremes worldwide is affected when the global economy is under stress as during the Covid-19 pandemic. Improving on the agent-based model that is used throughout the three constructed storylines, I present and apply an extension to *Acclimate* in article 5. Finally, drawing on multiple studies including storylines presented in this thesis, a formalization of the storyline approach is presented in article 6.



## 4.1 Assessing current and future local impacts

Any economic impact of weather extremes is rooted in the physical forces that these extremes exert onto exposed structures. Therefore, assessing economic impacts of arbitrary order often necessitates the quantification of these physical impacts. Besides characterizing the hazard intensity directly, proxy variables of the socio-economic impact can also be used to measure a hazard's impact. In the latter case, the observed impacts not only measure the physical intensity of the hazard, but also incorporate economic vulnerability and exposure to the hazard. Here, I use both metrics — physical and socio-economic — to quantify the current and future local impacts of snowfall extremes and tropical cyclones.

To assess the physical intensity of snowfall extremes under future climate, the traditional approach as described above is used in [article 1](#). Snowstorms cause severe damages ([Changnon and Changnon 2006](#)) and thus, potentially higher-order economic repercussions. Under climate change, increasing temperatures and more precipitation through intensified evaporation have opposing effects on the occurrence of snowfall ([O’Gorman 2014](#)). Here, an ensemble of climate model projections from phase six of the Coupled Model Intercomparison Project ([Eyring et al. 2016](#)) is used to investigate the possible intensification of snowfall extremes in the Northern Hemisphere until the end of the century. To this end, extreme daily snowfall percentiles are compared between a historical climate (1851–1920), and climate projections under a strong global warming scenario. In addition, the *expected extreme magnitude* is proposed as a measure that calculates the mean of snowfall extremes exceeding some percentile. The results of [article 1](#) indicate a regionally heterogeneous intensification of snowfall extremes in the Northern Hemisphere under future warming, while mean snowfall decreases.

Estimating hazard impacts through socio-economic proxy variables, I propose a method to derive local economic output losses due to a major tropical cyclone. Resulting in huge damages ([NOAA 2023](#); [Weinkle et al. 2018](#)), these hazards range among the costliest meteorological disasters. Therefore, their economic effects are relatively well studied and impacts have been found to have long-lasting ([Hsiang and Jina 2014](#)) adverse effects on the exposed economy ([Barton-Henry and Wenz 2022](#); [Strobl 2011](#)). However, an estimate of the local economic losses resulting from an individual hazard is often not readily available. To estimate these losses, many disaster studies use reported damages, thereby possibly missing spillover effects from the interaction between damaged and undamaged assets in the immediate aftermath of the disaster ([Hallegatte and Vogt-Schilb 2019](#)). In [article 2](#), I approach this issue by proposing a method to estimate locally confined *total* economic losses, i.e., losses of any order that occur within the geographic region that is exposed to the tropical cyclone. An initial decrease in production capacity is estimated from the exposed gross domestic product and the duration of a subsequent exponential decay is derived from observed unemployment claims. The approach unfolds its strength by its

simplicity that allows for a high degree of flexibility with regards to the hazard. It can easily be adapted to other tropical cyclones or, more generally, natural disasters, for which an estimate of the exposed area and a proxy for the duration of the decay exist.

Expanding on this method, I propose a means to project direct tropical cyclone losses to future warming levels in [article 3](#). Such projections require an understanding of how the severity of the tropical cyclones may be influenced by future climate change. As outlined above, the influence on tropical cyclone intensity is still strongly debated. However, it is possible to attribute the severity of the impacts from individual historical tropical cyclones to their climatological boundary conditions, which are themselves influenced by climate change. For example, it has been shown that anthropogenic sea level rise has increased the damages of Hurricane Sandy ([Strauss et al. 2021](#)). Similarly, precipitation of tropical cyclones increases with higher atmospheric temperatures ([Reed, Wehner, and Zarzycki 2022](#)), which has been shown for individual historic storms ([Reed, Wehner, Stansfield, et al. 2021](#); [Patricola and Wehner 2018](#)). Thus, in [article 3](#) I project direct losses to future levels of global warming using a simple but effective scaling approach. Thereby, the initial shock intensity and duration of the economic shock are scaled with expected increases in precipitation intensity and the exposed area of the hurricane, respectively.

## 4.2 Simulating the global economic response

Using direct loss estimates of an individual observed tropical cyclone, I construct a storyline to assess the global economic response to a major hurricane in the United States. Within two additional storylines, I investigate how such a response may change under further global warming and assess how loss propagation from tropical cyclones, heat stress, and river floods worldwide is affected by global economic background stress.

Indirect economic effects from a single historical tropical cyclone have been modelled previously. For instance, [Hallegatte \(2008\)](#) finds that total losses in Louisiana resulting from Hurricane Katrina (2005) significantly exceed direct losses and nonlinearly increase with these beyond a certain threshold. Similarly significant relationships between total and direct losses are found by [Lenzen, Malik, et al. \(2019\)](#), who simulate indirect economic and labor impacts on Australian states in response to the landfall of Tropical Cyclone Debbie (2017). Given these findings on indirect impacts at a regional and national level, propagation effects likely also occur at a global scale; but this global perspective is still missing in the literature. Moreover, even though the importance of prices in the aftermath of natural disasters has been acknowledged for some time ([Hallegatte and Przulski 2010](#)), post-disaster price dynamics emerging from complex network interactions are still subject to uncertainty ([Parker 2018](#)). [Article 2](#) addresses these gaps by assessing the global economic impact on consumption and consumption prices resulting from a single historical major tropical cyclone. To this end, I construct a storyline for the 2012 landfall of Hurricane



Sandy in the United States, the second-costliest storm on record at the time (NOAA 2022). Using estimated local losses as a direct shock in the *Acclimate* model, I simulate the global economic response to Hurricane Sandy. Analyzing this response, I focus on the price dynamics in the aftermath of the hazard and its repercussions on consumption. In particular, I compute the anomalies of consumption quantities in the aftermath of the landfall and the aggregate net effect on consumption for all simulated regions. Thus, I discover a three-phase economic price ripple in the simulated consumption price dynamics. In addition to the main analysis of the reference scenario, counterfactuals probe the sensitivity of the economic response to varying parameters of the direct economic shock. These reveal regionally heterogeneous changes in the price ripple and overall consumption response.

The expected increases of tropical cyclone impacts under further global warming will likely change the resulting global economic response. Using projected direct losses from Hurricane Harvey, I assess qualitative changes in the resulting response under climate change counterfactuals in [article 3](#). To this end, I compute the production anomaly of not directly affected regions over the duration of one year and investigate to what extent these regions are able to compensate adverse repercussions on production. Here, compensation is defined as the production increase in response to hurricane's direct production shock. The construction of climate counterfactuals distinguishes this study from previous work on loss propagation and allows for an exploration of qualitative changes in compensation mechanisms. In particular, I quantify the compensation shares of not directly affected regions under climate change and thus show that the USA will no longer be able to nationally offset the direct hurricane losses at a certain level of additional global warming. Instead, other countries take over larger shares of compensation, measured as the share of the total global production increase in response to the hurricane in the USA.

Economic repercussions from loss propagation reveal the vulnerability of economies (Briguglio et al. 2009) to climate hazards, even if they are not directly exposed. This vulnerability has increased with the density of the economic network (Wenz and Levermann 2016), but is determined by a multitude of socio-economic factors (IPCC 2012). In particular, it can be influenced by consecutive disasters if the impacts from two or more events coincide in time or space (de Ruiter et al. 2020). It has been shown that the concurrency of multiple disaster types amplifies their adverse effects on consumption through loss propagation (Kuhla et al. 2021). Global economic crises, like the recent Covid-19 pandemic, likely further affect economic vulnerability to loss propagation. Despite recent and overlapping global crises, the impact of interaction with loss propagation from weather extremes has not yet been quantified. I address this research gap in [article 4](#), where I investigate how the global economic response to tropical cyclones, heat stress, and river floods worldwide is affected when the global economy is under stress as during the Covid-19 pandemic. By disrupting international supply chains, the pandemic has been shown to cause adverse indirect economic effects at a global scale (Pichler et al. 2022; Verschuur, Koks, and Hall

2021; Bonadio et al. 2021; Guan et al. 2020). This disruption likely also altered economic vulnerability to extreme weather events. To assess this influence, I compute the global economic response to climate extremes worldwide under two scenarios. A reference scenario is designed to simulate loss propagation of weather extremes in a global economy that is under stress due to the pandemic. For this, I estimate the reduced economic activity due to containment measures against the Covid-19 virus at daily resolution and regional level, using the stringency index from the Oxford Covid-19 Government Response Tracker project (Hale et al. 2021). In a counterfactual scenario, loss propagation from the same extremes is simulated, but within a global economy that is at full capacity. Direct loss time series for these extremes — tropical cyclones, heat stress, and river floods worldwide — are used from Kuhla et al. (2021), based on a global climate model ensemble. The results of [article 4](#) show that aggregated consumption losses over a two-year period significantly increase when the global economy is under stress due to the pandemic. Losses increase particularly strong in China and the USA, where they triple and double, respectively, in comparison to an unstressed economy.

In the storylines described above, consumption anomalies emerge from price changes of goods in the economic network. There, the consumption response to price changes is determined by prescribed price elasticities, defined as the ratio of relative changes in consumed quantity to relative price changes. In [article 5](#), a utility function is introduced for *Acclimate* consumers, such that they instead determine their consumption by locally maximizing their utility under a constrained budget (see also next section). Thus, *market-emerging elasticities* result from price and consumption changes in an out-of-equilibrium state, as demonstrated in simulations for tropical cyclones, heat stress, and river floods over a time span of 20 years. This yields temporarily positive price elasticities for certain goods under rational consumer behaviour, whereby consumption of goods increases despite higher prices.

### 4.3 Advancing on methods and tools

The previous section has introduced studies that investigate the systemic form of economic risks from loss propagation in the global economic network. In these studies, I employ the *Acclimate* model as a primary tool for numerical simulations within the applied storyline framework. In addition to using these, this thesis also advances on both the employed tool and the applied framework.

In the original *Acclimate* model version as used in the constructed storylines, the representation of consumers is rather simplistic. First, representative consumers are aggregated at a regional level, ignoring the role of different income groups. Second, as commonly modeled, the consumption reaction to prices is determined solely by prescribed price elasticities, i.e., consumers simply decrease or increase the consumption of a certain good with

higher or lower prices, according to the prescribed elasticities. While these simplifications are justifiable for the conducted analyses of regionally aggregated consumption, a more nuanced representation of consumer behaviour is desirable. In [article 5](#), an extension to the *Acclimate* model is proposed and applied, allowing for a more realistic and detailed representation of consumption. In particular, consumers are disaggregated into five income groups per region and locally maximize a utility function that allows for substitution between different goods. This way, consumers in the extended model version make a rational choice on the bought goods, expressing preferences of some goods over others given their respective prices. The model extension is applied to a time series of economic shocks from weather extremes, simulating the resulting consumption behaviour. As a result, consumption price elasticities emerge from market dynamics rather than being prescribed endogenously.

With the previously introduced storylines, I add to an ever-growing and diverse landscape of studies that apply this framework (e.g. [Ciullo et al. 2021](#); [Wiel, Lenderink, and Vries 2021](#); [Young et al. 2021](#); [Reed, Stansfield, et al. 2020](#); [Mindlin et al. 2020](#); [Zappa and Shepherd 2017](#)). There is an increasing number of storylines with a focus on interdisciplinary impact chains that go beyond the biophysical consequences of extreme events. This includes general perspectives on systemic risk ([Ringsmuth et al. 2022](#)), as well as more specifically, risk to infrastructure ([Koks et al. 2022](#)), or the economy ([Zhang, Wiel, et al. 2022](#)), including storylines from this thesis ([Middelanis, Willner, Otto, and Levermann 2022a](#); [Middelanis, Willner, Otto, Kuhla, et al. 2021a](#)). This development has widened the space of application for storyline assessments with diverse socio-economic impact channels and counterfactuals. While the common idea of analyzing the unfolding of impacts from a past or plausible future event ([Shepherd et al. 2018](#); [Hazeleger et al. 2015](#)) prevails in all studies, this widened scope makes a formalization and standardization of the framework desirable. In particular, concrete guidelines for the construction of storylines are still missing. Embedded in a growing research community, these guidelines are provided in the formal description of storylines as presented in [article 6](#). To this end, distinct design steps are described and illustrated with different storylines, including those described in [articles 2 and 3](#). The formalization yields a set of eight common elements that can be used to construct storylines. These elements define steps for the selection of a historic hazard region and event, the definition of a transmission pathway and impact metric to other regions, the creation of counterfactuals under changed climatic and socio-economic conditions, and their comparison to the selected reference. Thus, with the studies presented in this thesis, I apply the storyline framework and further actively add to its formalization, contributing the gained results and experience.

INTRODUCTION

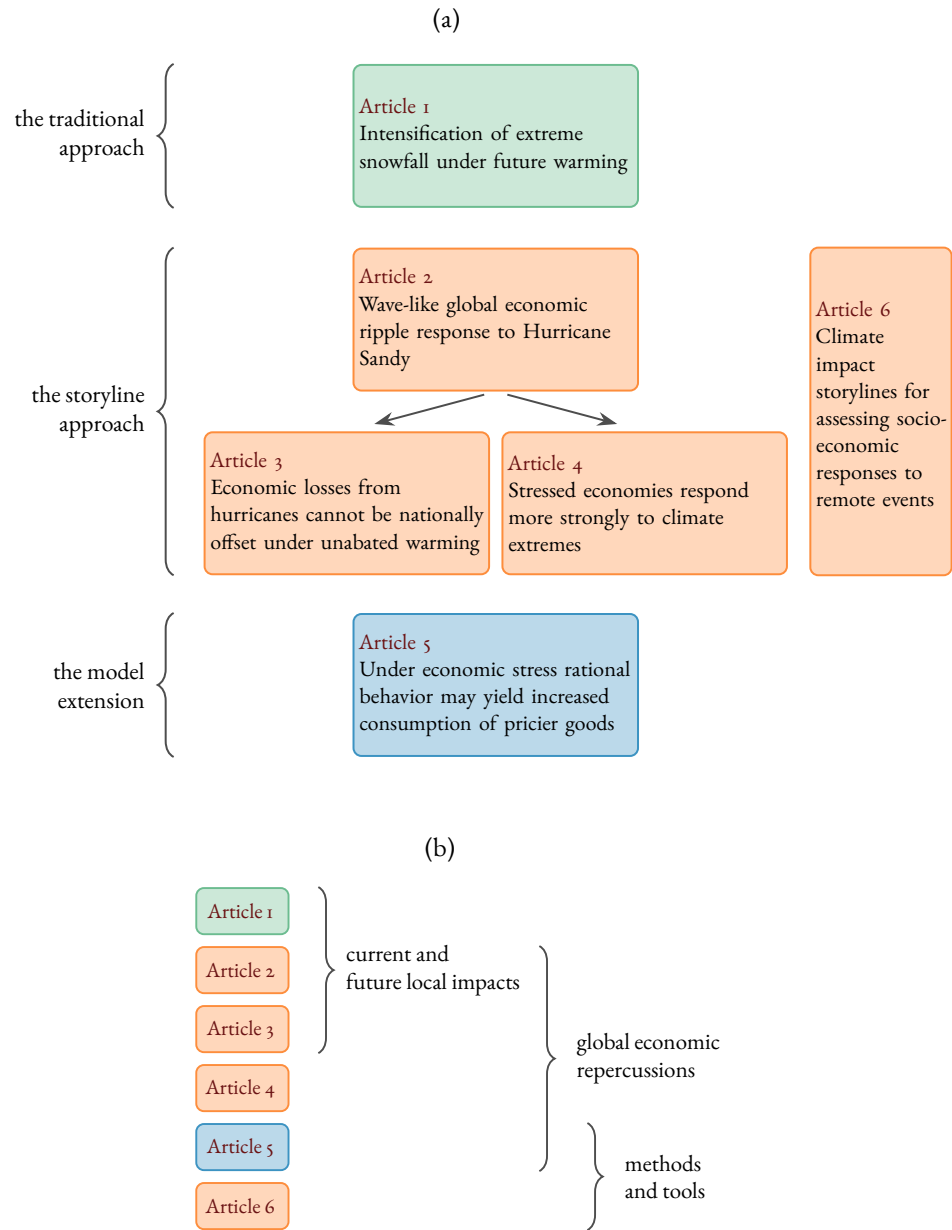


Figure 1: Schema of the thesis. (a) Overview of the articles and the corresponding approaches. (b) Article contributions to extreme weather impact assessments.

## 5 Article contributions

This thesis builds on six scientific articles (figure 1). In the following, an overview of these articles with author contributions is presented. Four of them have been published or accepted for publication in renowned scientific journals, one is currently under review and one has been submitted.

### ARTICLE 1

#### Regions of intensification of extreme snowfall under future warming

L. Quante, S. N. Willner, R. Middelani, A. Levermann

In this article, the intensification of snowfall extremes in the Northern Hemisphere until the end of the century is analyzed, using data from phase six of the Coupled Model Intercomparison Project. I analyzed, interpreted, and discussed the results together with all authors and contributed to the writing of the manuscript.

This article has been published in *Scientific Reports* (2021),  
<https://doi.org/10.1038/s41598-021-95979-4>.

### ARTICLE 2

#### Wave-like global economic ripple response to Hurricane Sandy

R. Middelani, S. N. Willner, C. Otto, K. Kuhla, L. Quante, A. Levermann

This study estimates direct economic losses in the United States from the 2012 landfall of Hurricane Sandy. These losses are used to simulate the global economic response to the hurricane using the *Acclimate* model, investigating global consumption prices and consumption. I designed the research method with the help of S. Willner and C. Otto. I conducted the analysis and led the research process. I wrote the manuscript with contributions from my co-authors and led the discussion of the results.

This article has been published in *Environmental Research Letters* (2021),  
<https://doi.org/10.1088/1748-9326/ac39c0>.

## INTRODUCTION

### ARTICLE 3

Economic losses from hurricanes cannot be nationally offset under unabated warming

R. Middelanis, S. N. Willner, C. Otto, A. Levermann

This article extends the previously presented method and projects hurricane loss estimates of the 2017 landfall of Hurricane Harvey to counterfactual climate scenarios. Using *Acclimate*, the resulting production anomalies are simulated and analyzed. I designed the method and conducted the analysis. I analyzed and interpreted the results with the help of S. Willner and A. Levermann. I wrote the manuscript with contributions from all authors and led the discussion of the results.

This article has been published in *Environmental Research Letters* (2022), <https://doi.org/10.1088/1748-9326/ac90d8>.

### ARTICLE 4

Stressed economies respond more strongly to climate extremes

R. Middelanis, S. N. Willner, K. Kuhla, L. Quante, C. Otto, A. Levermann

This article analyzes the interaction of global economic stress with loss propagation from tropical cyclones, heat, and river floods. I led the study and conducted the analysis. I designed the research together with S. Willner and A. Levermann. I wrote the manuscript with contributions from all authors and led the discussion of the results.

This article is under review in *Communications Earth and Environment*.

### ARTICLE 5

Under economic stress rational behavior may yield increased consumption of pricier goods

L. Quante, , C. Otto, S. N. Willner, R. Middelanis, A. Levermann

In this article, an extension to the *Acclimate* model is presented and applied, where consumers are modeled as utility-maximizing agents with a constrained budget. I discussed the results with all authors and contributed to the writing of the manuscript. Discussing the research, I developed the notion of market-emerging elasticities together with L. Quante.

This article has been submitted to *Nature Human Behaviour*.

**ARTICLE 6****Climate impact storylines for assessing socio-economic responses to remote events**

B. Van den Hurk, M. Baldissera Pacchetti, A. Ciullo, L. Coulter, S. Dessai, E. Ercin, H. Goulart, R. Hamed, S. Hochrainer, E. Koks, P. Kubiczek, A. Levermann, R. Mechler, M. van Meersbergen, B. Mester, R. Middelani, K. Minderhoud, J. Mysiak, S. Nirandjan, C. Otto, P. Sayers, J. Sillman, J. Schewe, T. G. Shepherd, D. Stuparu, K. Witpas

This article provides a formalization of the storyline approach. For this, it draws on a multitude of storyline assessments, including storylines presented in this thesis. I provided the storylines on tropical cyclone landfalls in the USA. I further contributed to the discussion of the storyline approach and helped writing the manuscript.

This article has been accepted for publication in *Climate Risk Management*.





# Articles

In this chapter, the six articles of this thesis are presented. Four of them have been published or accepted for publication in renowned scientific journals, one is currently under review and one has been submitted. All articles are self-contained in presenting their own introductions, methods, results, discussions, and references. Supplementary information is available for articles 1–5, provided in the [Appendix](#).



# The intensification of snowfall extremes

1

This article has been published in *Scientific Reports* as:

L. Quante, S. N. Willner, R. Middelani, A. Levermann (2021). “Regions of intensification of extreme snowfall under future warming”. In: *Scientific Reports* under the terms of the Creative Commons Attribution 4.0 licence.

DOI: [10.1038/s41598-021-95979-4](https://doi.org/10.1038/s41598-021-95979-4)

**ABSTRACT:** Due to climate change the frequency and character of precipitation are changing as the hydrological cycle intensifies. With regards to snowfall, global warming has two opposing influences; increasing humidity enables intense snowfall, whereas higher temperatures decrease the likelihood of snowfall. Here we show an intensification of extreme snowfall across large areas of the Northern Hemisphere under future warming. This is robust across an ensemble of global climate models when they are bias-corrected with observational data. While mean daily snowfall decreases, both the 99th and the 99.9th percentiles of daily snowfall increase in many regions in the next decades, especially for Northern America and Asia. Additionally, the average intensity of snowfall events exceeding these percentiles as experienced historically increases in many regions. This is likely to pose a challenge to municipalities in mid to high latitudes. Overall, extreme snowfall events are likely to become an increasingly important impact of climate change in the next decades, even if they will become rarer, but not necessarily less intense, in the second half of the century.

# Regions of intensification of extreme snowfall under future warming

Lennart Quante<sup>1,2</sup>, Sven N. Willner<sup>1</sup>, Robin Middelanis<sup>1,2</sup> & Anders Levermann<sup>1,2,3</sup>

Due to climate change the frequency and character of precipitation are changing as the hydrological cycle intensifies. With regards to snowfall, global warming has two opposing influences; increasing humidity enables intense snowfall, whereas higher temperatures decrease the likelihood of snowfall. Here we show an intensification of extreme snowfall across large areas of the Northern Hemisphere under future warming. This is robust across an ensemble of global climate models when they are bias-corrected with observational data. While mean daily snowfall decreases, both the 99th and the 99.9th percentiles of daily snowfall increase in many regions in the next decades, especially for Northern America and Asia. Additionally, the average intensity of snowfall events exceeding these percentiles as experienced historically increases in many regions. This is likely to pose a challenge to municipalities in mid to high latitudes. Overall, extreme snowfall events are likely to become an increasingly important impact of climate change in the next decades, even if they will become rarer, but not necessarily less intense, in the second half of the century.

Global warming caused by persisting greenhouse gas emissions<sup>1</sup> is expected to cause an increasing number of extreme weather events<sup>2,3</sup>. The intensification of precipitation events<sup>4</sup> is one of the main consequences of global warming. One of the main driving factors for this is the increase of global mean temperature of around 1 °C over the last century and the projected future increase of a similar magnitude in the next decades. Rising temperatures lead to higher evaporation and thus enable more global precipitation. Since higher temperatures also increase atmospheric water vapour, this may lead to more intense extreme rainfall events<sup>1</sup>.

Snowfall and its extremes are a special case of precipitation, since the intensification of the hydrological cycle allows for potentially more snowfall, as long as temperatures remain sufficiently cold for snowfall to occur. These opposing forces lead to a contrast between a substantial decrease of mean snowfall and a much less pronounced decrease of extreme snow events<sup>5</sup>. These results based on empirical percentiles and generalised extreme value distribution analysis emerge very pronounced under a high emissions scenario (RCP8.5). O’Gorman<sup>5</sup> thereby presents a physical theory complementing these findings to show that snowfall extremes occur close to an optimal temperature  $T_m$  and thus the change of extreme events related to warming is argued to be differing from the decrease of mean snowfall. A regional comparison<sup>6</sup> for RCP8.5 shows a general decrease in daily snowfall events in most regions, with exceptions in regions with sufficiently cold climate even under global warming. Reductions of snowfall also cause reduced mountain snow pack under RCP8.5 in North-Western America, leading up to a possible disruption of agriculture due to lack of predictability of melt water occurrence<sup>7</sup>. Further, down-scaled regional climate models show a decreasing size and frequency of snow storms in eastern North America<sup>8</sup> under RCP8.5.

Even with medium emissions (RCP4.5) a reduction of annual mean snowfall is observed with increases in high latitude regions<sup>9</sup>. And also for a strong CO<sub>2</sub> doubling experiment a weaker decrease of wind-driven heavy snowfall events is found when compared to the decrease of mean snowfall<sup>10</sup>. Adding to these model-based analyses of future snowfall, snow mass shows continental contrasts. North America displays decreasing trends of snow mass, while for Eurasia no trend is found using satellite data for the recent past (1980–2018)<sup>11</sup>.

For the latest round of the Climate Model Intercomparison Project, CMIP6, it has been shown that, for a fixed snow threshold and conversion ratio between liquid and solid precipitation, there is an increase in the occurrence of high snowfall events that can be attributed to anthropogenic greenhouse gas emissions in most parts of Asia, North America, and Greenland. By contrast, decreases of intense snowfall days are described for the remaining

<sup>1</sup>Potsdam Institute for Climate Impact Research, Telegrafenberg A56, Potsdam, Germany. <sup>2</sup>Potsdam University, Karl-Liebknecht Str. 24, Potsdam, Germany. <sup>3</sup>Columbia University, LDEO, Palisades, NY, USA. ✉email: sven.willner@pik-potsdam.de; anders.levermann@pik-potsdam.de

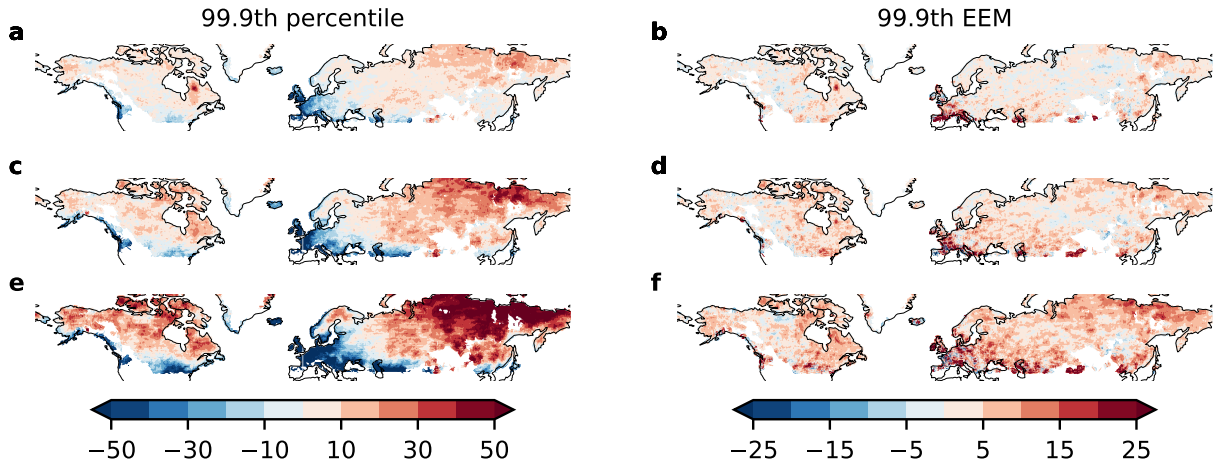


**Figure 1.** Intensification of extreme daily snowfall throughout the century for high-latitudes, decreasing percentiles, particularly in the second half of the century for mid-latitudes, especially Western Europe. Values are relative to the historical baseline (1851–1920). Relative change (in %) of (a,c,e) 99.9th percentile, and (b,d,f) 99.9th expected extreme magnitude; (a,b) 2021–2030, (c,d) 2051–2060, (e,f) 2091–2100. Maps created using the cartopy 0.17<sup>24</sup> library based on GSHHG shapes<sup>25</sup>.

regions under the stronger warming of SSP5-RCP8.5 compared to SSP1-RCP2.6<sup>12</sup>. Moreover, recently a linear relationship between increasing global surface air temperature and decreasing spring snow cover has been shown by comparing recent global climate model results from CMIP6 to historical data<sup>13</sup>.

Despite the dire long-term prospects of snowfall under global warming in mid-latitudes, extreme snow events remain a major damaging category of extreme weather events, especially in the Northern Hemisphere. Here, snow and winter storms have caused 21.6bn USD of insured losses (in prices of 2000) in the United States from 1949 to 2000, accounting for roughly 4% of all storm induced insured losses<sup>14</sup>. Such damage due to extreme snowfall increased in the United States during the second half of the twentieth century<sup>14</sup>. However, this effect arises primarily because of a growing population and increasing value of assets at risk.

Here, we show a regionally diverging intensification of extreme snowfall events compared to the historical climate until the end of the century. First, we find that, under a strong global warming scenario (SSP5-RCP8.5), extreme percentiles increase for already snow-prone regions also in mid-latitudes. In contrast to this, mean daily snowfall decreases in most areas of the Northern Hemisphere except for high latitudes.

Second, we show that extreme snowfall intensifies at least until the middle of the century as indicated by an increase of the 99.9th percentile of daily snowfall (commonly measured in  $\text{kg}/(\text{m}^2\text{s})$ ) as well as of the expected magnitude of extreme events exceeding the historic 99.9th percentile. This is pronounced for high-latitude regions, which face intensifying extreme snow events throughout the century. Mid-latitude regions like Western Europe show increasing expected magnitude of extreme events, i.e. the average of events exceeding the historical 99.9th percentile increases. While we observe a decreasing frequency of extreme snowfall events towards the end of the century, this analysis of the most extreme snowfall events indicates that the remaining events might be more extreme than historical experienced (Fig. 1).

This study is based on most up-to-date climate projections from the Sixth Coupled Model Intercomparison Project (CMIP6)<sup>15</sup>. By contrast, CMIP5 data has been shown to underestimate extreme snowfall events and to overestimate average snowfall when compared to observations<sup>16</sup>. Thus, we here use an ensemble of bias-corrected model output<sup>17,18</sup> from the ISIMIP project with improved representation of extremes. This bias-correction combines a parametric quantile mapping approach to adjust biases in all quantiles of a distribution and to preserve trends in the individual quantiles as described in detail in<sup>17,19</sup>. Using an ensemble of ten model outputs, we compare extreme daily snowfall percentiles of the Northern Hemisphere land mass above  $40^\circ\text{N}$  for a historical climate (1851–1920) to a strong global warming scenario (SSP5-RCP8.5; we further provide analyses of SSP1-RCP2.6 and SSP3-RCP7.0 scenarios in the supplement). Furthermore, we introduce the measure of *expected extreme magnitude (EEM)* inspired by the financial risk measure of conditional value at risk<sup>20–22</sup>. We define expected extreme magnitude as the mean of all events above a certain percentile from the historical baseline. Thus, it reflects changes in the tail of the distribution, i.e., for the intensity of extreme events. We overall contribute to the discussion of appropriate measures for extreme precipitation<sup>23</sup> and suggest the expected extreme magnitude to enable a substantial extension of the analysis of extreme event risk in general. Details are given in the methods, Eq. (2).

Since one of the main biases of global circulation models consists in the underestimation of extreme precipitation events<sup>16</sup>, we are confident that using the bias-corrected data yields a more realistic representation of the extreme percentiles we analyse in our study. As shown in Figs. S7–S11, CMIP model data without bias correction from the GCM MPI ESM1-2-HR leads to quite consistent trends in the mean and EEM, while the single model percentile is more noisy and an increase can not be observed as clearly as for the bias corrected data.

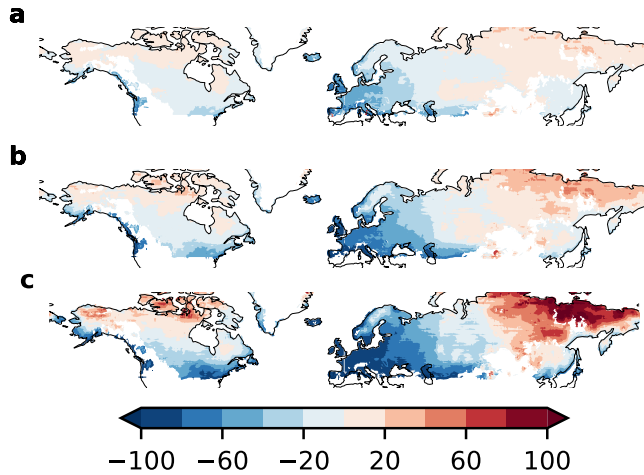


**Figure 2.** Strong increase in mean daily snowfall in high latitudes of North America and North-East Asia, decreases in mid-latitudes of North America and Western Eurasia relative to historical baseline (1851–1920), (0% points = baseline) (a) 2021–2030, (b) 2051–2060, (c) 2091–2100. Maps created using the cartopy 0.17<sup>24</sup> library based on GSHHG shapes<sup>25</sup>.

### Global changes of daily snowfall

We find that, for the first half of the 21st century, the 99.9th percentile of daily snowfall, i.e., the largest daily snowfall in 1000 days, increases for large areas of the Northern Hemisphere by 10–20 percentage points until the decade of 2051–2060, while some areas, e.g. in Western Europe, show decreasing extreme percentiles (all percentages are relative to the historical baseline (1851–1920) values, Fig. 1, first column). Towards the end of the century (2091–2100), this trend diverges into sharply decreasing 99.9th percentiles for lower latitudes like Western Europe and parts of North America (up to  $\sim -50\%$  points), and further increasing percentiles (more than  $\sim 30\%$  points) in high latitudes. These trends are well grounded in the model ensemble as shown in Fig. S4.

Substantiating these trends, the expected extreme magnitude, i.e., the average of daily snowfall events exceeding the historical 99.9th percentile (for details see the methods, Eq. (2)), increases by 5–10% points until the middle of the century (Fig. 1, second column). This indicates the strengthening of extreme snowfall events. The continued increase until the end of the century to 10–15% points of the baseline level shows that even with rarer extreme events as indicated by decreasing percentiles, the remaining extreme snowfall events are projected to intensify compared to the historical baseline. These findings are not as robust with respect to model agreement as the analysis of the percentile, due to the inherent high uncertainties in tail risk analysis. Nonetheless, the overall trends are still supported by acceptable model agreement (Fig. S5). We advise caution interpreting the results for regions with an observed strong decrease of the percentile like Western Europe.

In contrast to this increase in extreme snowfall statistics, the mean daily snowfall diverges already in the near future. While snow-prone regions in high latitudes exhibit an increase of mean daily snowfall by 20% points until the middle of the century, we observe a sharp decrease for lower latitudes ( $\sim -20\%$  points; Fig. 2). These trends continue until the end of the century, yielding decreases of up to 80% points in large parts of Europe and parts of North America, while high-latitude regions like Siberia show a similar increase of around at least 50% points. Again, these trends are well grounded in the model ensemble as shown in Fig. S3.

Possibly due to the improved representation of extreme events in our bias-corrected data<sup>17,18</sup>, we find that the contrast between mean and extreme snowfall might be stronger than discussed previously<sup>5,6</sup>. This is supported by the 99th percentile statistics (Fig. S2). Here, the contrast between higher and lower latitudes is already evident in the middle of the century, with strong decreases in parts of Europe and North America. Nonetheless, the expected extreme magnitude increases by at least roughly 5% points, in support of our claim that extreme snowfall events become more intense, even if their frequency declines as indicated by decreasing percentiles.

In Fig. 3, we show the area-averaged model ensemble projections for an elevation below 1000 m as high-elevation areas show generally differing snow patterns. While global trends are dampened in comparison to the most volatile regions in Fig. 1, the described divergence between non-decreasing percentiles as well as slightly increasing expected extreme magnitude of daily snowfall and decreasing mean snowfall remains. We observe a decrease of the global mean daily snowfall by almost 20% points until the end of the century, contrasting a stagnating 99.9th percentile with no clear trend. Some intensification of extreme snowfall events is shown by the increase of 99.9th expected extreme magnitude of daily snowfall by around 4% points. While these trends are heterogeneous between regions, they are still observable in averages for the Northern Hemisphere north of 40°N with narrow likely ranges (Fig. 3, 16.6th to 83.3rd percentiles) in our ensemble of ten bias-corrected climate models<sup>17,18</sup>. This indicates that the trends observed in the simulations are well grounded in our ensemble.

To evaluate the possible impacts of this intensification on damages suffered by humans, we analyse the share of the population exposed to increasing or decreasing percentiles of daily snowfall sorted by bins. Until the middle of the century, the population exposed to a strongly increasing 99.9th percentile of daily snowfall (more than 5 percentage points compared to baseline levels) grows slightly by about 10 percentage points, while the population

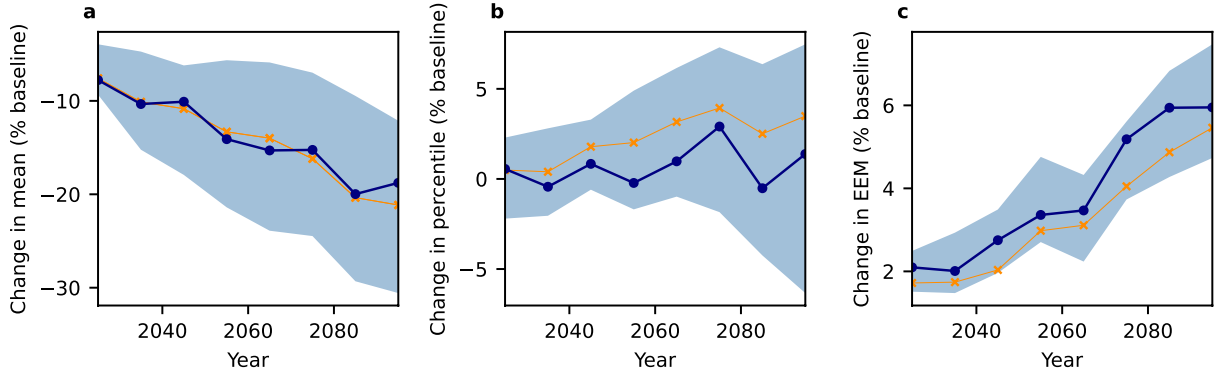


**Figure 3.** Contrasting global trends of mean daily snowfall and extreme snowfall measures (elevation below 1000 m, decadal statistics, Northern Hemisphere north of 40 °N, SSP5-RCP8.5). All values are area-weighted and relative to the baseline (1851–1920) climate. (a) Mean, (b) 99.9th percentile, (c) expected extreme magnitude above the 99.9th baseline percentile. Blue line shows the model ensemble median, shaded areas denote the likely range (16.7th to 83.3rd percentiles). Orange line shows statistics for all ten models combined into one time series ensemble.

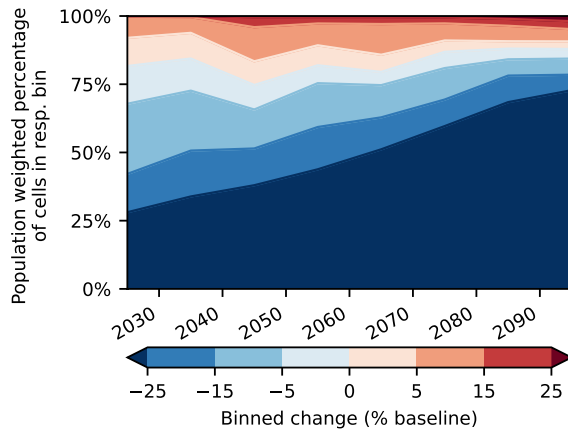


**Figure 4.** Population exposed to strongly intensifying and decreasing snowfall events grows in the next decades before a majority of population is experiencing decreasing extreme events at the end of the century. Global population weighted trend of 99.9th percentile (elevation below 1000 m, decadal statistics, Northern Hemisphere north of 40 °N, SSP5-RCP8.5). Binned according to change relative to the baseline (1851–1920) climate. Coloured area represents the population weighted percentage of cells in the respective bin. Population is fixed to a 2020 estimate.

experiencing very strongly (more than 15 percentage points compared to baseline levels) decreasing snowfall events grows by about 10%. Due to the concentration of intensifying daily snowfall events in higher latitudes, this trend is continued till the end of the century and the population experiencing decreasing extreme snowfall grows up to 85% (Fig. 4). Nonetheless, the population weighting shows a still considerable intensification of extreme snowfall in the coming decades, almost doubling the amount of people exposed to strongly intensifying extreme snowfall events, while in the second half of the century decreasing extreme snowfall events will be experienced by an increasing majority of the population. Complementing area weighted analysis is included in the supplement (Fig. S12), showing continuous increase of the area where extreme percentiles intensify very strongly (more than 15 percentage points compared to baseline levels) until the end of the century.

**Regional divergence due to temperature shifts.** Since we observe not only a divergence between mean and extreme snowfall but also between different regions, we present some more details on three selected regions: the east coast of North America (1), Western Europe (2), and Northern Asia (3) (Fig. S1)—note that only land cells are considered.

As shown in Fig. 5, these regions’ snowfall diverges in its response to global warming. While Western Europe exhibits the sharpest decline in average mean snowfall (~ -90% points) and 99.9th percentile (~ -80% points), the few remaining extreme events do not decrease in intensity as shown by the very uncertain, but slight intensification trend (~ +5% points). The east coast of North America exhibits a much less pronounced decrease of

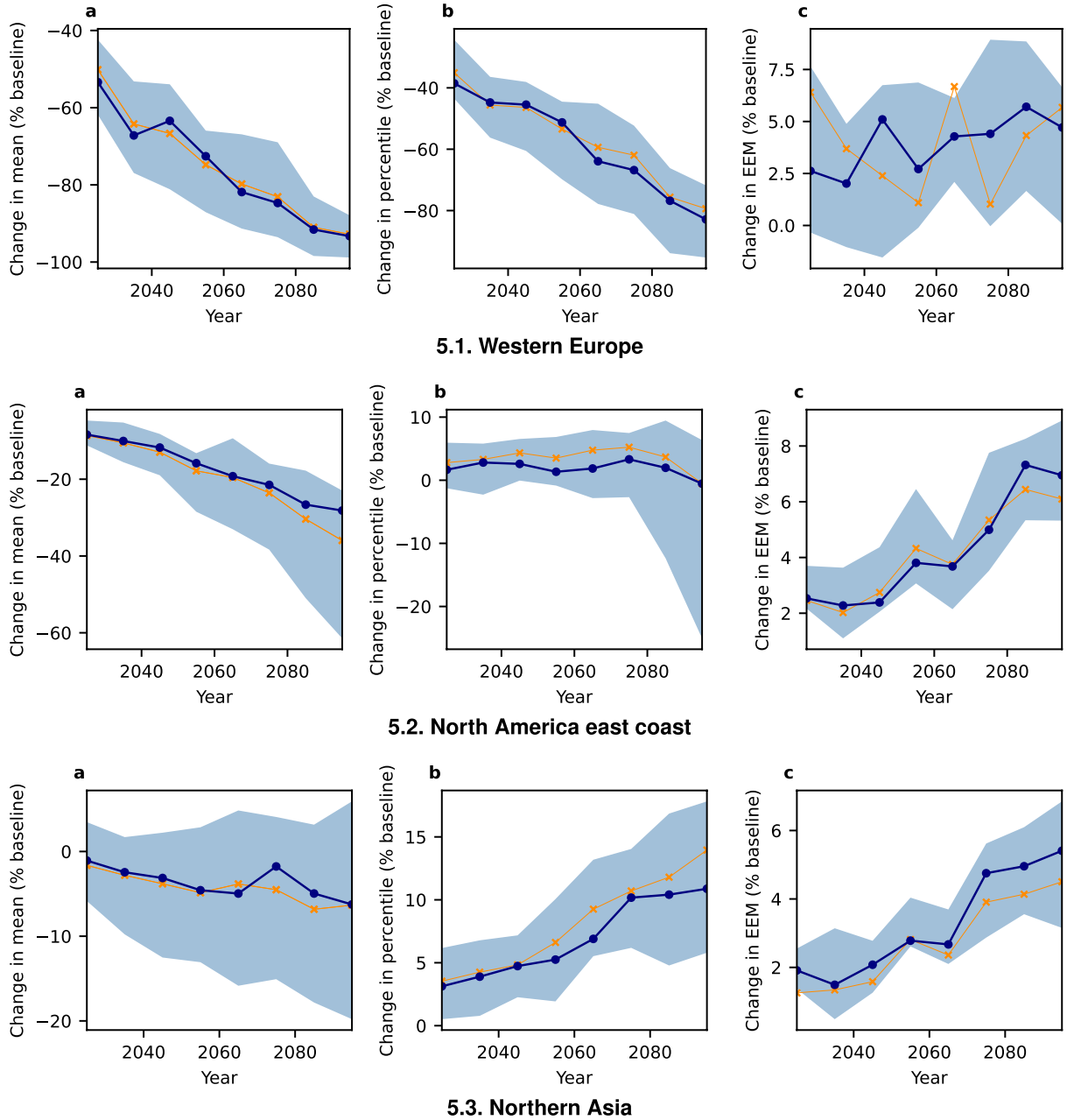


**Figure 5.** Regional differences of changes in daily snowfall statistics (elevation below 1000 m, decadal statistics, SSP5-RCP8.5). All values are relative to the baseline (1851–1920) climate. (a) Mean, (b) 99.9th percentile, (c) expected extreme magnitude above the 99.9th baseline percentile. Blue line shows the model ensemble median, shaded areas denote the likely range (16.7th to 83.3rd percentiles). Orange line shows statistics for all ten models combined into one time series ensemble.

mean snowfall ( $\sim -30\%$  points), while the average percentile remains almost constant. The expected extreme magnitude increases slightly ( $\sim 5\%$  points). Snowfall in the higher latitude region of Northern Asia is intensifying with regards to all extreme measures. By contrast, the mean snowfall decreases slightly ( $\sim -5\%$  points). While percentiles of extreme snowfall increase ( $\sim 10\%$  points), the average extreme events show a small increase ( $\sim +6\%$  points). Due to the large magnitude of change, the ensemble does exhibit relatively large uncertainty, but for mean snowfall and the general trends regarding percentiles and expected extreme magnitude, most models show good agreement (Figs. S3–S5). Similar, but slightly weaker trends can be observed for SSP3-RCP7.0 (Fig. S16), whereas SSP1-RCP2.6 induces no clear trend (Fig. S21).

We find evidence for the existence of an optimal temperature  $T_m$  for extreme snowfall in agreement with previous studies on earlier climate projections<sup>5</sup>. For that, we contrast the change of days with surface temperatures below freezing point, respectively, in the bin of  $[-2.5^\circ\text{C}, -1.5^\circ\text{C}]$  around the proposed<sup>5</sup>  $T_m = -2^\circ\text{C}$ . We thereby



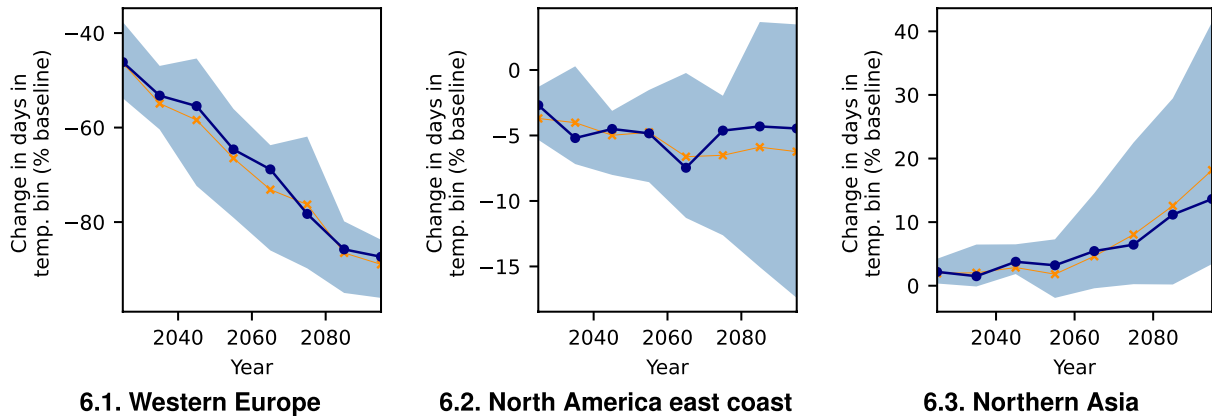


**Figure 6.** Regional differences in the trend of number of days with surface temperature between  $-2.5^{\circ}\text{C}$  and  $-1.5^{\circ}\text{C}$  (elevation below 1000 m, decadal statistics, SSP5-RCP8.5). All values are relative to the baseline (1851–1920) climate. Blue line shows the model ensemble median, shaded areas denote the likely range (16.7th to 83.3rd percentiles). Orange line shows statistics for all ten models combined into one time series ensemble.

show differences between the considered regions (Fig. 6). While for Western Europe the number of days in the range of  $T_m$  is reduced from  $\sim 45\%$  of the historical baseline level in 2020 to  $\sim 10\%$  in the decade 2091–2100, for the North American east coast these days remain at about  $\sim 95\%$  of the baseline level. For Northern Asia we even observe a small increase to  $\sim 110\%$  in these extreme snowfall prone days. In contrast to this, freezing days in Western Europe are reduced from  $\sim 50\%$  baseline level to  $\sim 10\%$ , the North American east coast shows a much less pronounced reduction from  $\sim 90\%$  to  $\sim 60\%$ , while in Northern Asia freezing days only recede from  $\sim 90\%$  to  $\sim 65\%$  (Fig. S23). Similarly, slightly weaker trends can be observed for SSP3-RCP7.0 (Fig. S17), whereas SSP1-RCP2.6 causes no clear trend (Fig. S22).

We thus conclude that the increase of temperatures renders snowfall so much less likely in Western Europe, that the already observed<sup>26</sup> and predicted<sup>3,4,27</sup> intensification of the hydrological cycle does not result in increasing frequency of extreme snowfall events—the increased overall precipitation is not realised as snowfall but as rain. Nonetheless, it leads to a strengthening of the remaining events as indicated by the slight increase in expected extreme magnitude. By contrast, for the east coast of North America as well as Northern Asia, sufficient temperature conditions remain for extreme snowfall to occur. Thus, for these regions we observe intensifying extreme events. On the global scale, we observe an almost steady number of days in the optimal temperature bin with a considerable model spread, whereas freezing days decrease (Fig. S24). These findings indicate that global warming decreases the number of days with sufficiently cold temperatures for snow, while days close to the theorised optimal temperature<sup>5</sup> of  $\sim -2^{\circ}\text{C}$  reduce not as much in regions with intensifying extreme snowfall.

## Discussion

In this study, we show that daily extreme snowfall events are projected to intensify in many regions in the latest climate model projections. We introduce the measure of expected extreme magnitude of snowfall events and show increasing tail risk of daily snowfall events. Thus, our analysis of bias corrected CMIP6 data<sup>17,18</sup> shows substantial evidence for intensifying extreme snowfall under strong global warming (SSP5-RCP8.5).

The exclusive consideration of SSP5-RCP8.5 might constitute a limitation<sup>28</sup>, but in the short to medium run assuming no meaningful mitigation might be appropriate, as commented recently<sup>29</sup>. Moreover, slower warming in lower emissions scenarios shows similar trends of intensification of extreme snowfall events, as shown in the supplement for SSP3-RCP7.0 (Figs. S13–S17) in contrast to relatively small changes for SSP1-RCP2.6 (Figs. S18–S22).

We find increasing percentiles and expected extreme magnitude of daily snowfall for large areas until at least the middle of the 21st century. In contrast to this, mean daily snowfall decreases sharply. Analysing the observed changes weighted by population we find an increasing share of population exposed to strongly intensifying extreme snowfall events in the next decades, while the share of the population exposed to decreasing extreme snowfall grows as well, especially in the second half of the century to lead to a majority of the population being exposed to decreasing extreme snowfall percentiles at the end of the century. We also observe a regional divergence between warmer regions like Western Europe, moderate regions like the North American east coast, and snow-prone regions like Northern Asia. As an explanation for this divergence, we suggest changes in the number of days with potentially optimal temperature conditions for extreme snowfall events. These lead to increasing humidity and hence more intense extreme snowfall events. Thus, for snow-prone high-latitude regions, higher temperatures enable more extreme snowfall events until the end of the century.

The divergence between extreme events and mean daily snowfall is in line with previous studies<sup>5,6,12</sup>. The global circulation model data used in this study offer only a coarse resolution of  $0.5^{\circ} \times 0.5^{\circ}$  compared to studies using regionalised climate models<sup>8</sup>, thus we are not able to conclude anything about the regional occurrence of snowstorms or similar local extreme events. Due to the bias-correction of our data we are optimistic to provide enhanced results compared to previous studies of CMIP5 data<sup>5,6,9,10</sup>. Our model ensemble shows good agreement on the described intensification of daily snowfall events. Thus, future research might combine the data

from global climate models and regionalised climate models to fully estimate future extreme snowfall events like regional snowstorms. Finally, the introduced concept of tail risk sensitive analysis utilising the expected extreme magnitude could be applied to estimate potential impacts of extreme events in general and to the identification of optimal adaptation policies.

In summary, we show that there is substantial evidence that global warming and the resulting changes of the hydrological cycle may lead to intensification of daily snowfall extreme events in the coming decades. These changes diverge between regions and the immediate and more distant future. In particular, there is a contrast between decreasing extreme snowfall percentiles in lower latitude regions like Western Europe and higher latitude regions experiencing increasing extreme snowfall percentiles.

## Methods

**Definition of expected extreme magnitude (EEM).** We aim to improve upon exclusive consideration of the  $i$ th percentile  $p_i$  of the random variable of daily values for a weather event  $D$ . To this end, we define the measure of *expected extreme magnitude (EEM)* on level  $i$  as the conditional expectation of a weather event  $D$  given that  $D$  exceeds  $p_i$ , the  $i$ th percentile of  $D$ :

$$EEM_i := \mathbb{E}[D|D \geq p_i], \quad (1)$$

i.e. the mean magnitude of the events exceeding the  $i$ th percentile.

This conditional expectation with respect to the percentile is known in the field of financial risk management as *conditional Value at Risk*<sup>20,21</sup> or *Expected Shortfall*<sup>22</sup>. It is commonly applied as a risk measure for the loss distribution  $L$  of a financial portfolio. By building on the common risk measure *Value at Risk*, the  $i$ th percentile of  $L$ , it measures the risk based on all potential losses exceeding the  $i$ th percentile. Due to the consideration of all realisations of the analysed random variable above the specified percentile, it is sensitive to changes of risk in the tail of the distribution.

We simplify Eq. (1) according to our application, keeping the percentile fixed as the control climate baseline percentile  $\tilde{p}_i$ . Thus,  $\tilde{p}_i$  is deterministic and in our application expected extreme magnitude is simplified to the average of weather events  $\{D_j\}_{j \in 1, \dots, N}$  that exceed the baseline  $i$ th percentile  $\tilde{p}_i$ :

$$EEM_i = \frac{\sum_{j \in 1, \dots, N} [D_j | D_j \geq \tilde{p}_i]}{N}, \quad (2)$$

where  $N$  is the number of all considered realisations of  $D$ .

This enables a comparison of the expected magnitude of extreme events under future climate scenarios to the expected magnitude of the historical baseline scenario. Since in contrast to a financial portfolio, we are not able to influence the distribution of weather events  $D$  by reallocating assets, the baseline percentile constitutes a valid threshold also for future time periods.

This simplification is not without caveats, since the probabilistic interpretation of the events exceeding the  $i$ th percentile of the analysed period is replaced by a comparison with the events exceeding the  $i$ th percentile of the (historical) baseline. Nonetheless, since preparation against extreme snowfall events is based on historical experiences, we strongly favor the fixed baseline percentile approach to the changing percentile threshold as it would be used for conditional Value at Risk due to the following arguments. As can be seen in Fig. S6, using the changing future percentiles as a baseline, i.e. just as for the original conditional Value at Risk, yields a measure which tracks changes in the percentile quite closely. Our definition of EEM enables a complementary analysis adding important insights about the most extreme snowfall events. Even if they become rarer as follows from decreasing percentiles, the remaining events are intensifying and thus EEM uncovers important information that would be lost using the changing percentile as a threshold. Moreover, for increasing percentiles our definition of EEM yields conservative estimates of intensification.

In future applications of this measure, an advanced modelling of the distribution of daily weather extremes  $D$  might enable an application of Eq. (1) for the management of extreme weather risks. For example, adaptation policies could be optimised by modelling the expected impacts of weather extremes after implementation of these policies and adaptation priorities could be identified following the maximisation of the expected reduction of extreme damages. There remain substantial challenges to this approach, since caution is required to model the relevant tails of the distributions accurately and the numerical simulation of conditional expectations is challenging due to their path-dependency, rendering standard Monte-Carlo methods computationally infeasible.

**Calculation of daily snowfall from climate model output.** To ensure a robust measurement of daily snowfall per grid cell, we have applied the following simple transformation to model output precipitation ( $pr$ ) based on surface temperature ( $tas$ ). Snowfall ( $prsn$ ) is assumed to occur if and only if the surface temperature is below  $0^\circ\text{C}$ , i.e.

$$prsn := \mathbb{1}_{tas \leq 0^\circ\text{C}} pr, \quad (3)$$

as also commonly used by hydrological models.

*Auxiliary data used.* For population weighted analysis, all grid cell data are weighted by 2020 population data<sup>30</sup> to show trends in impacts on human activities. The weights are scaled to the total population of the analysed area. This introduces a limitation, because we do not consider population development for the historical data

and under different scenarios, e.g. SSPs. Thus, our analysis focuses on the changes of extreme snowfall without considering population shifts.

For elevation data, we use data from the global land data assimilation project<sup>31</sup>.

*Calculation of snowfall statistics.* All statistics (mean, percentiles, expected extreme magnitude) are calculated per grid cell, using the 0.5° resolution of the ISIMIP data<sup>17–19</sup>, for  $T = 10$  year windows of the analysed time frames. All percentiles are estimated based on standard percentile estimation techniques implemented in `scipy`<sup>32</sup>. The analysis was facilitated by the IRIS python package<sup>33</sup>.

Area averages are calculated from ocean-masked data, weighting the grid cell data by area with weights given by

$$r^2(lon_1 - lon_0)(\sin(lat_1) - \sin(lat_0)), \quad (4)$$

where  $r$  denotes the radius of the earth, approximated as 6,367,470 m<sup>33</sup>.

The baseline values are calculated as an average of decadal data from the baseline period of 1851–1920. These are used as basic values for all baseline relative percentages.

## Code availability

All code used for analysis and data that support the findings of this study are available from the corresponding author upon request.

Received: 22 January 2021; Accepted: 27 July 2021

Published online: 17 August 2021

## References

1. Stocker, T. F. *et al.* (eds) *IPCC Climate Change 2013 the Physical Science Basis. Working Group I Contribution to the Fifth Assessment Report of the Intergovernmental Panel on Climate Change* (Cambridge University Press, 2013). <https://doi.org/10.1017/CBO9781107415324>.
2. Field, C. *et al.* (eds) *Managing the Risks of Extreme Events and Disasters to Advance Climate Change Adaptation. A Special Report of Working Groups I and II of the Intergovernmental Panel on Climate Change* Vol. 9781107025 (Cambridge University Press, 2012). <https://doi.org/10.1017/CBO9781139177245>.
3. Coumou, D. & Rahmstorf, S. A decade of weather extremes. *Nat. Clim. Change* **2**, 491–496 (2012). <https://doi.org/10.1038/nclimate1452>.
4. O’Gorman, P. A. & Schneider, T. The physical basis for increases in precipitation extremes in simulations of 21st-century climate change. *Proc. Natl. Acad. Sci. USA* **106**, 14773–14777. <https://doi.org/10.1073/pnas.0907610106> (2009).
5. O’Gorman, P. A. Contrasting responses of mean and extreme snowfall to climate change. *Nature* **512**, 416–418. <https://doi.org/10.1038/nature13625> (2014).
6. Danco, J. F., Deangelis, A. M., Raney, B. K. & Broccoli, A. J. Effects of a warming climate on daily snowfall events in the Northern Hemisphere. *J. Clim.* **29**, 6295–6318. <https://doi.org/10.1175/JCLI-D-15-0687.1> (2016).
7. Livneh, B. & Badger, A. M. Drought less predictable under declining future snowpack. *Nat. Clim. Change* **10**, 452–458. <https://doi.org/10.1038/s41558-020-0754-8> (2020).
8. Ashley, W. S., Haberlie, A. M. & Gensini, V. A. Reduced frequency and size of late-twenty-first-century snowstorms over North America. *Nat. Clim. Change* <https://doi.org/10.1038/s41558-020-0774-4> (2020).
9. Krasting, J. P., Broccoli, A. J., Dixon, K. W. & Lanzante, J. R. Future changes in northern hemisphere snowfall. *J. Clim.* **26**, 7813–7828. <https://doi.org/10.1175/JCLI-D-12-00832.1> (2013).
10. Janoski, T. P., Broccoli, A. J., Kapnick, S. B. & Johnso, N. C. Effects of climate change on wind-driven heavy-snowfall events over eastern North America. *J. Clim.* **31**, 9037–9054. <https://doi.org/10.1175/JCLI-D-17-0756.1> (2018).
11. Pulliaainen, J. Patterns and trends of Northern Hemisphere snow mass from 1980 to 2018. *Nature* **581**, 294–298. <https://doi.org/10.1038/s41586-020-2258-0> (2020).
12. Chen, H., Sun, J. & Lin, W. Anthropogenic influence would increase intense snowfall events over parts of the Northern Hemisphere in the future. *Environ. Res. Lett.* <https://doi.org/10.1088/1748-9326/abb93> (2020).
13. Mudryk, L. *et al.* Historical Northern Hemisphere snow cover trends and projected changes in the CMIP-6 multi-model ensemble. *Cryosphere Discuss.* <https://doi.org/10.5194/tc-2019-320> (2020).
14. Changnon, S. A. & Changnon, D. A spatial and temporal analysis of damaging snowstorms in the United States. *Nat. Hazards* **37**, 373–389. <https://doi.org/10.1007/s11069-005-6581-4> (2006).
15. Eyring, V. *et al.* Overview of the Coupled Model Intercomparison Project Phase 6 (CMIP6) experimental design and organization. *Geosci. Model Dev.* <https://doi.org/10.5194/gmd-9-1937-2016> (2016).
16. AnnaThomas, M. *et al.* Snowfall distribution and its response to the Arctic Oscillation: An evaluation of HighResMIP models in the Arctic using CPR/CloudSat observations. *Geosci. Model Dev.* **12**, 3759–3772. <https://doi.org/10.5194/gmd-12-3759-2019> (2019).
17. Lange, S. Trend-preserving bias adjustment and statistical downscaling with ISIMIP3BASD (v1.0). *Geosci. Model Dev. Discuss.* <https://doi.org/10.5194/gmd-2019-36> (2019).
18. Lange, S. ISIMIP3BASD (2021). <https://zenodo.org/record/4686991>. <https://doi.org/10.5281/zenodo.4686991>.
19. Lange, S. ISIMIP3b bias adjustment fact sheet (2021). <https://www.isimip.org/gettingstarted/isimip3b-bias-correction/>.
20. Artzner, P., Delbaen, F., Eber, J. M. & Heath, D. Coherent measures of risk. *Math. Financ.* <https://doi.org/10.1111/1467-9965.00068> (1999).
21. Rockafellar, R. T. & Uryasev, S. Optimization of conditional value-at-risk. *J. Risk* <https://doi.org/10.21314/jor.2000.038> (2000).
22. Tasche, D. Expected shortfall and beyond. *J. Bank. Financ.* [https://doi.org/10.1016/S0378-4266\(02\)00272-8](https://doi.org/10.1016/S0378-4266(02)00272-8) (2002).
23. Schär, C. *et al.* Percentile indices for assessing changes in heavy precipitation events. *Clim. Change* <https://doi.org/10.1007/s10584-016-1669-2> (2016).
24. Met Office. Cartopy: A cartographic python library with a Matplotlib interface. <https://scitools.org.uk/cartopy>.
25. Wessel, P. gshhg—A Global Self-consistent, Hierarchical, High-resolution Geography Database. <https://www.soest.hawaii.edu/pwessel/gshhg/>.
26. Fischer, E. M. & Knutti, R. Observed heavy precipitation increase confirms theory and early models. *Nat. Clim. Change* **6**, 986–991. <https://doi.org/10.1038/nclimate3110> (2016).

27. Prein, A. F. & Heymsfield, A. J. Increased melting level height impacts surface precipitation phase and intensity. *Nat. Clim. Change* <https://doi.org/10.1038/s41558-020-0825-x> (2020).
28. Peters, G. P. & Hausfather, Z. Emissions—the “business as usual” story is misleading. *Nature* **577**, 618–620 (2020).
29. Schwalm, C. R., Glendon, S. & Duffy, P. B. RCP8.5 tracks cumulative CO<sub>2</sub> emissions. *Proc. Natl. Acad. Sci. USA* **2020**, 8–9. <https://doi.org/10.1073/pnas.2007117117> (2020).
30. Center for International Earth Science Information Network-CIESIN-Columbia University. *Gridded Population of the World, Version 4 (GPWv4): Population Count* (NASA Socioeconomic Data and Applications Center (SEDAC), 2016). <https://doi.org/10.7927/H4X63JVC>.
31. Rodell, M. *et al.* The global land data assimilation system. *Bull. Am. Meteorol. Soc.* **85**, 381–394. <https://doi.org/10.1175/BAMS-85-3-381> (2004).
32. Cunnane, C. Unbiased plotting positions—a review. *J. Hydrol.* [https://doi.org/10.1016/0022-1694\(78\)90017-3](https://doi.org/10.1016/0022-1694(78)90017-3) (1978).
33. Met Office. Iris: A Python library for analysing and visualising meteorological and oceanographic data sets. <http://scitools.org.uk/>. Edition: v2.4. Exeter, Devon.

### Acknowledgements

This research has received funding from the German Federal Ministry of Education and Research (BMBF) under the research projects CLIC (01LA1817C) and QUIDIC (01LP1907A) and the Horizon 2020 Framework Programme of the European Union (Grant agreement 820712). The authors gratefully acknowledge the European Regional Development Fund (ERDF), the German Federal Ministry of Education and Research, and the Land Brandenburg for supporting this project by providing resources on the high-performance computer system at the Potsdam Institute for Climate Impact Research.

### Author contributions

L.Q., S.W., and A.L. designed the research. L.Q. conducted the analysis, L.Q., S.W., R.M., and A.L. analysed and interpreted the results. L.Q. and S.W. wrote the manuscript with contributions from all authors. All authors discussed the results.

### Funding

Open Access funding enabled and organized by Projekt DEAL.

### Competing interests

The authors declare no competing interests.

### Additional information

**Supplementary information** The online version contains supplementary material available at <https://doi.org/10.1038/s41598-021-95979-4>.

**Correspondence** and requests for materials should be addressed to S.N.W. or A.L.

**Reprints and permissions information** is available at [www.nature.com/reprints](http://www.nature.com/reprints).

**Publisher’s note** Springer Nature remains neutral with regard to jurisdictional claims in published maps and institutional affiliations.



**Open Access** This article is licensed under a Creative Commons Attribution 4.0 International License, which permits use, sharing, adaptation, distribution and reproduction in any medium or format, as long as you give appropriate credit to the original author(s) and the source, provide a link to the Creative Commons licence, and indicate if changes were made. The images or other third party material in this article are included in the article’s Creative Commons licence, unless indicated otherwise in a credit line to the material. If material is not included in the article’s Creative Commons licence and your intended use is not permitted by statutory regulation or exceeds the permitted use, you will need to obtain permission directly from the copyright holder. To view a copy of this licence, visit <http://creativecommons.org/licenses/by/4.0/>.

© The Author(s) 2021

# The global economic response to Hurricane Sandy

# 2

This article has been published in *Environmental Research Letters* as:







R. Middelani, S. N. Willner, C. Otto, K. Kuhla, L. Quante, A. Levermann (2021). “Wave-like global economic ripple response to Hurricane Sandy”. In: *Environmental Research Letters*

under the terms of the [Creative Commons Attribution 4.0 licence](#).

DOI: [10.1088/1748-9326/ac39c0](https://doi.org/10.1088/1748-9326/ac39c0)

**ABSTRACT:** Tropical cyclones range among the costliest disasters on Earth. Their economic repercussions along the supply and trade network also affect remote economies that are not directly affected. We here simulate possible global repercussions on consumption for the example case of Hurricane Sandy in the US (2012) using the shock-propagation model Acclimate. The modeled shock yields a global three-phase ripple: an initial production demand reduction and associated consumption price decrease, followed by a supply shortage with increasing prices, and finally a recovery phase. Regions with strong trade relations to the US experience strong magnitudes of the ripple. A dominating demand reduction or supply shortage leads to overall consumption gains or losses of a region, respectively. While finding these repercussions in historic data is challenging due to strong volatility of economic interactions, numerical models like ours can help to identify them by approaching the problem from an exploratory angle, isolating the effect of interest. For this, our model simulates the economic interactions of over 7000 regional economic sectors, interlinked through about 1.8 million trade relations. Under global warming, the wave-like structures of the economic response to major hurricanes like the one simulated here are likely to intensify and potentially overlap with other weather extremes.

# Wave-like global economic ripple response to Hurricane Sandy

Robin Middelanis<sup>1,2</sup> , Sven N Willner<sup>1,\*</sup> , Christian Otto<sup>1</sup> , Kilian Kuhla<sup>1,2</sup> , Lennart Quante<sup>1,2</sup>   
and Anders Levermann<sup>1,2,3</sup> 

<sup>1</sup> Potsdam Institute for Climate Impact Research, Telegrafenberg A56, Potsdam, Germany

<sup>2</sup> University of Potsdam, Potsdam, Germany

<sup>3</sup> Columbia University, New York, NY, United States of America

\* Author to whom any correspondence should be addressed.

E-mail: [sven.willner@pik-potsdam.de](mailto:sven.willner@pik-potsdam.de)

**Keywords:** supply chains, Hurricane Sandy, economic ripples, extreme weather impacts, loss propagation, natural disasters

Supplementary material for this article is available [online](#)

---

## Abstract

Tropical cyclones range among the costliest disasters on Earth. Their economic repercussions along the supply and trade network also affect remote economies that are not directly affected. We here simulate possible global repercussions on consumption for the example case of Hurricane Sandy in the US (2012) using the shock-propagation model *Acclimate*. The modeled shock yields a global three-phase ripple: an initial production demand reduction and associated consumption price decrease, followed by a supply shortage with increasing prices, and finally a recovery phase. Regions with strong trade relations to the US experience strong magnitudes of the ripple. A dominating demand reduction or supply shortage leads to overall consumption gains or losses of a region, respectively. While finding these repercussions in historic data is challenging due to strong volatility of economic interactions, numerical models like ours can help to identify them by approaching the problem from an exploratory angle, isolating the effect of interest. For this, our model simulates the economic interactions of over 7000 regional economic sectors, interlinked through about 1.8 million trade relations. Under global warming, the wave-like structures of the economic response to major hurricanes like the one simulated here are likely to intensify and potentially overlap with other weather extremes.

---

## 1. Introduction

Globally, tropical cyclones range among the costliest and deadliest natural disasters. While they constitute only 16.5% of all recorded billion-dollar events in the United States between 1980 and 2018, they are responsible for more than half of the costs resulting from all extreme weather events combined [1, 2]. Their frequency is expected to decrease or to remain static under global warming but most projections anticipate an increase in intensity of the most extreme tropical cyclones [3], especially in the Atlantic basin [4] (where tropical cyclones are called hurricanes). In consequence, economic losses in hurricane-prone regions are expected to increase in the future due to climate change [5–8] through higher storm intensity [9] and sea level rise [10] but also due to changes in the economic values at risk [11, 12]. Local economies

can be affected through destroyed capital stock (stock losses or damages) or through lost production output (flow losses). Since we do not consider damages in this work, we here generally imply lost production in the notion of loss. In particular, we refer to losses in a region that is directly affected by a hurricane as direct losses. However, losses can spread through the supply network, which is then referred to as higher-order losses [13–15]. We here refer to the latter as indirect losses. These may represent a substantial or even dominant share of total economic disaster losses [16–18]. Indirect losses can result from supply shortages due to direct losses that propagate downstream along supply chains. Direct losses and an associated production decrease may also lead to reduced demand (production demand, generally in contrast to final demand for household consumption) which propagates upstream in the



supply network. These downstream and upstream effects are also called forward and backward propagation [19] or ripple effects [20]. Here, we investigate the possible ripple response to Hurricane Sandy (2012) and its effect on global consumption expenditure.

There is good consensus in the literature that extreme weather events have adverse effects on household consumption [21], which is commonly used in economic models as a measure for societal welfare [22] and is therefore often regarded in disaster impact analyses. In this study, we refer to the latter as final consumption or simply consumption where we also include government spending. In a globalized world, local disasters can have global economic repercussions [23], one prime example being the COVID-19 pandemic [24] with huge estimated indirect consumption losses worldwide [25]. However, most studies [26–29] on the impacts of historic extreme weather events focus on the local economic impacts of the disaster and therefore miss the global dimension [23].

With this work, we choose a different scope of analysis and investigate a single historic hurricane’s possible impact on consumption on a global scale. We simulate the potential global indirect impacts on consumption that a major hurricane in the United States can have globally, using an agent-based network model. We choose a modeling approach because this allows us to investigate aspects of higher-order effects of a single event that cannot be found in historic data. While local effects of hurricanes are — in large parts — well-studied [30–32], higher-order effects and the way they propagate in the trade network are still poorly understood. Lenzen [14] conducted a study on the higher-order indirect effects of a single hurricane in Australia but focus on national spillover effects. Other studies [7, 33, 34] give a global perspective but cannot link effects to single historic events or do not consider indirect losses. We here propose one means to study loss propagation and global effects on consumption after a single historic major hurricane. As a case study, we choose Hurricane Sandy which made landfall in the US in 2012.

Sandy severely hit the US and in particular the states of New York (NY) and New Jersey (NJ) in 2012. It was the fourth-costliest hurricane in history and caused an estimated total damage of \$65bn [35] (in 2012 US Dollar), predominantly by driving a storm surge into the coastlines of NY and NJ [36]. Given the magnitude of this local economic shock and the importance of the economically strong regions of NY and NJ in the global trade network, Hurricane Sandy most likely also entailed indirect effect in regions not directly affected. To understand how these repercussions may have spread in the global supply and trade network, we here simulate global consumption expenditure across the global economy in the direct

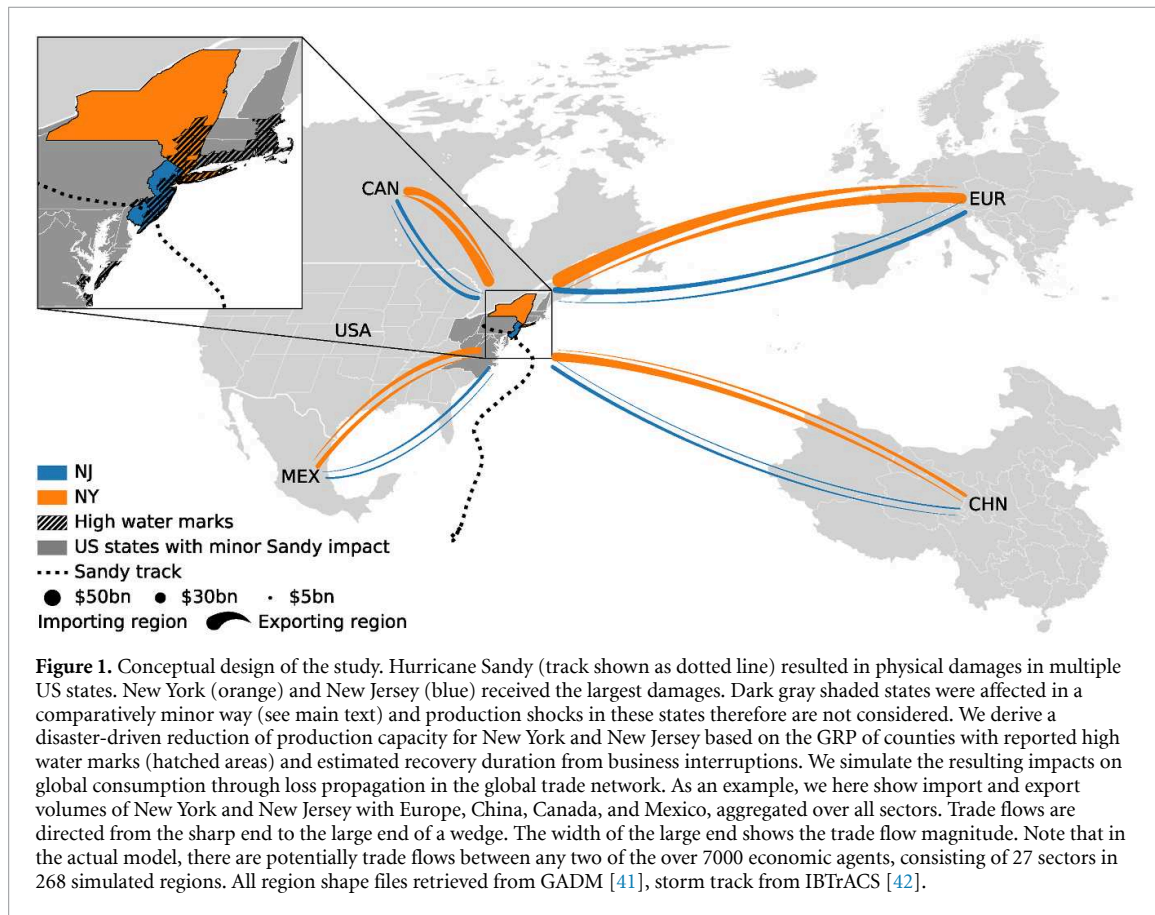
aftermath of the strong economic shock in NY and NJ after Sandy.

We thereby add to the discussion on the welfare impacts of extreme weather events in two major points. First, by taking a modeling approach, we can go beyond a local case study and simulate consumption impacts globally as a result of production shortages and price effects propagating in the global supply network. This allows us to investigate effects that are otherwise hidden in coarse and noisy data. We find that although directly affected regions show the strongest effects, we observe an overall impact on consumption on the global level. Regions with strong trade relations to the US are affected most. Second, our approach allows us to analyze the underlying propagation effects inside our model that lead to the observed global consumption anomalies. The propagation follows a three-phase ripple of prices. An initial upstream effect results in price decreases and associated consumption increases. The following downstream effect leads to price increases and reduced consumption, followed by a normalization phase.

## 2. Method overview

Our simulations are carried out using the dynamic agent-based model *Acclimate* [37] which models loss-propagation on the global supply network, assuming a demand-driven economy. In this model, economic sectors (in case of the United States and China on a state and province level respectively, otherwise on a national level) are modeled as agents that are interlinked through trade flows, with each agent maximizing its own profit. The economy of each region is divided into 27 sectors, including the final consumer. With a total of 268 modeled regions, this results in over 7000 agents. By applying an external shock in the form of a reduction in the production capacity of one or more agents, the initial baseline state of equilibrium can be disturbed. We model this production shock to represent the direct losses due to Hurricane Sandy in the affected areas of New York and New Jersey. We use a disaggregated [38] version of the EORA MRIO dataset for the year 2012 [39] as economic baseline. *Acclimate* then simulates anomalies around this baseline state that result from the production capacity reduction by profit-maximization of each individual agent on a daily time scale. Prices in the model are endogenous variables which account for local scarcities and transport costs. They always reflect price changes relative to baseline prices and do not represent absolute prices of traded goods (which are unknown since they are not contained in the EORA dataset).

The conceptual approach of this study is summarized in figure 1. We model the direct economic impact from Hurricane Sandy for NY and NJ only (orange and blue, respectively), although another ten



states and the District of Columbia (DC) were also affected (hatched areas). However, NY and NJ were most affected, receiving more than 96% of Congress' Disaster Relief Appropriations Act funds from January 2013 (\$50.5bn in total) [40]. And according to estimates of the National Oceanic and Atmospheric Administration [1], the damage share for all other areas is less than 5% of the total damage. We derive production shocks for NY and NJ (supplementary figure 1, supplementary table 1 (available online at [stacks.iop.org/ERL/16/124049/mmedia](http://stacks.iop.org/ERL/16/124049/mmedia))) based on estimated business interruption (BI) due to the disaster. In this, we assume all sectors to be affected in the same way. While this is generally a strong assumption, we find it reasonable for the short time in the immediate aftermath of the hurricane. We then analyze the resulting global levels of final consumption and related prices as well as production levels, production prices, and demands communicated in the network to assess the higher-order repercussions of Hurricane Sandy. These result from the inter-linkages of NY and NJ within the global trade network (exemplary trade flows in figure 1). For a detailed description of the approach, see appendix A.

### 3. Three-phase consumption ripple

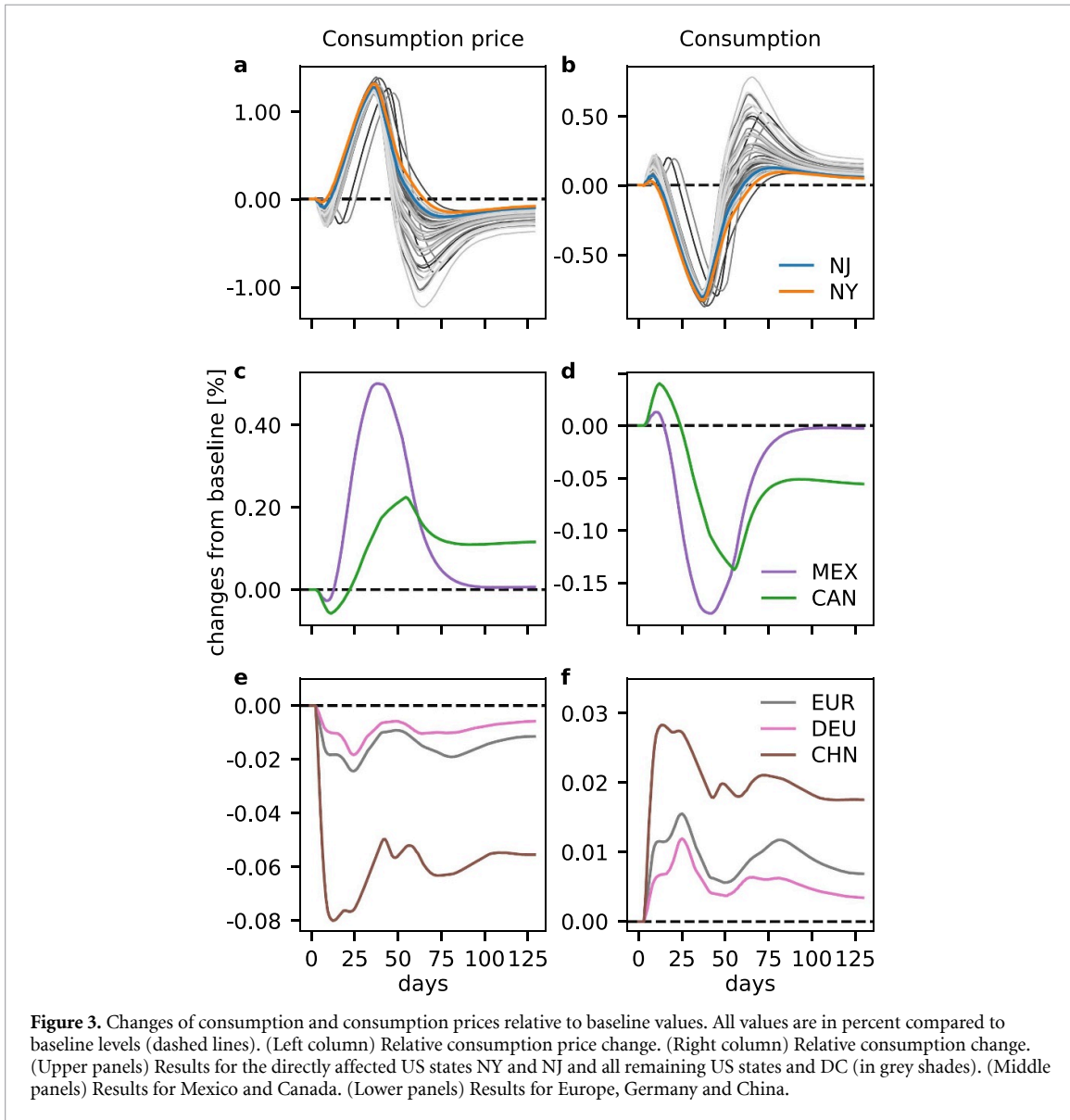
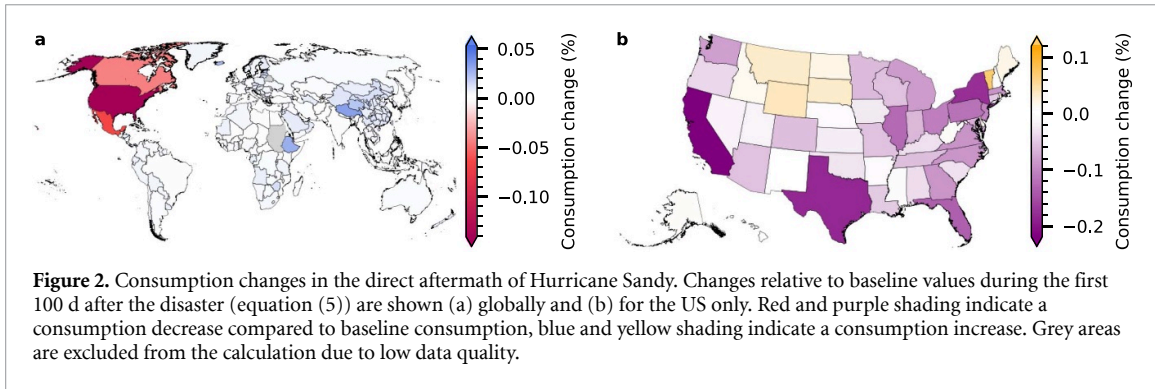
We compute the relative consumption change in the first 100 d after the disaster for all regions globally

(figure 2, supplementary table 2). A region's consumption change is computed as the ratio between the absolute aggregated difference from baseline consumption and the consumption that these regions would exhibit in the unperturbed baseline scenario during this time (equation (5) in appendix A).

A normalisation of consumption and consumption prices in the United States of America occurs about 100 d after the event (figure 3). On a national level, the US show the strongest consumption decrease of all regions within our study. However, on a US state level we find both consumption increases as well as losses (figure 2(b)) in our simulations. Within the US, there is a strong correlation between the gross regional production (GRP) of a state and its consumption change. Economically strong states like California, Texas, or Florida exhibit strong consumption decreases whereas consumption increases in states with a lower GRP like Vermont, Wyoming, or Montana.

Both increases and reductions in consumption are a result of consumption price changes. The consumption level depends directly on the consumption price with sector and region specific consumption price elasticities (see appendix A, supplementary tables 2–4). The latter reflect the sensitivity of consumption (quantity) to price changes. Of course, post-disaster price elasticities might deviate from those during normal times. However, this is





difficult to estimate and only relevant for the final consumption in the directly affected states NY and NJ. Consumption in all other regions can be assumed to follow normal elasticities. Previous sensitivity analysis [43] on model-internal price elasticities showed that this parameter choice has no significant impact on results derived via *Acclimate*.

In all regions, we observe an initial consumption price drop directly after the disaster, resulting in a consumption level above baseline. This initial price drop results from a reduction in the (production) demand of the directly affected states of NY and NJ and its quick upstream propagation along the global supply chains. Therefore, reducing demand

instantaneously results in a situation of surplus supply, which causes prices to decline and consumption to rise. However, direct production losses in NY and NJ simultaneously propagate downstream through the global supply network and result in scarcity situations also in other regions that are not directly affected. As a result, shortly after the initial small consumption increase, consumption prices rise again with prices in US states reaching values above baseline level only few days after the hurricane and a maximum peak at over +1.3% about 30 d after the disaster. In case of the United States, the initial price drop associated with increased consumption is therefore quickly reversed by a scarcity driven price inflation resulting in a reduction in consumption. While the upstream effect happens without time delay, the downstream propagation of scarcities is initially buffered by the agents' inventories but also by transport chains through which goods are delivered. Therefore, in contrast to demand shortages propagating upstream, the downstream propagation of scarcities only shows effects with some lag time. The persisting shortage of supply leads to price inflation of intermediate goods that are passed on to the final consumers. As a consequence, the latter have to decrease their consumption. A normalization of US prices and consumption occurs about 100 d after the event. While the US are most impacted by the event, changes from the baseline economic state due to the hurricane event occur globally. A similar development with an initial small consumption increase followed by a stronger counter effect of decreasing consumption can be observed — yet with smaller magnitude — in Mexico and Canada, which have strong trade relations with the United States.

Generally, consumption shows a three-phase wave pattern of an initial price drop due to upstream effects, followed by a price increase attributable to downstream effects and finally a normalization phase where prices develop back towards baseline values. Depending on how strong the upstream and downstream effects are with regards to a particular region, average prices range above or below baseline. For example, the upstream effect for Canada and Mexico is small compared to the downstream effect, leading to higher average prices. In Europe and its strongest economy Germany as well as China, the initial price drop due to the fast upstream effect is large enough to permanently keep prices below baseline (figure 3(e)).

#### 4. Regions' trade with the US

In the simulated disaster aftermath, the magnitude of the effect on a region's consumption depends on the trade relations of that region with the US (i.e. the sum of all imports and exports, figure 4(a)), following a power law relationship. Both high import and export trade flows result in a strong consumption changes

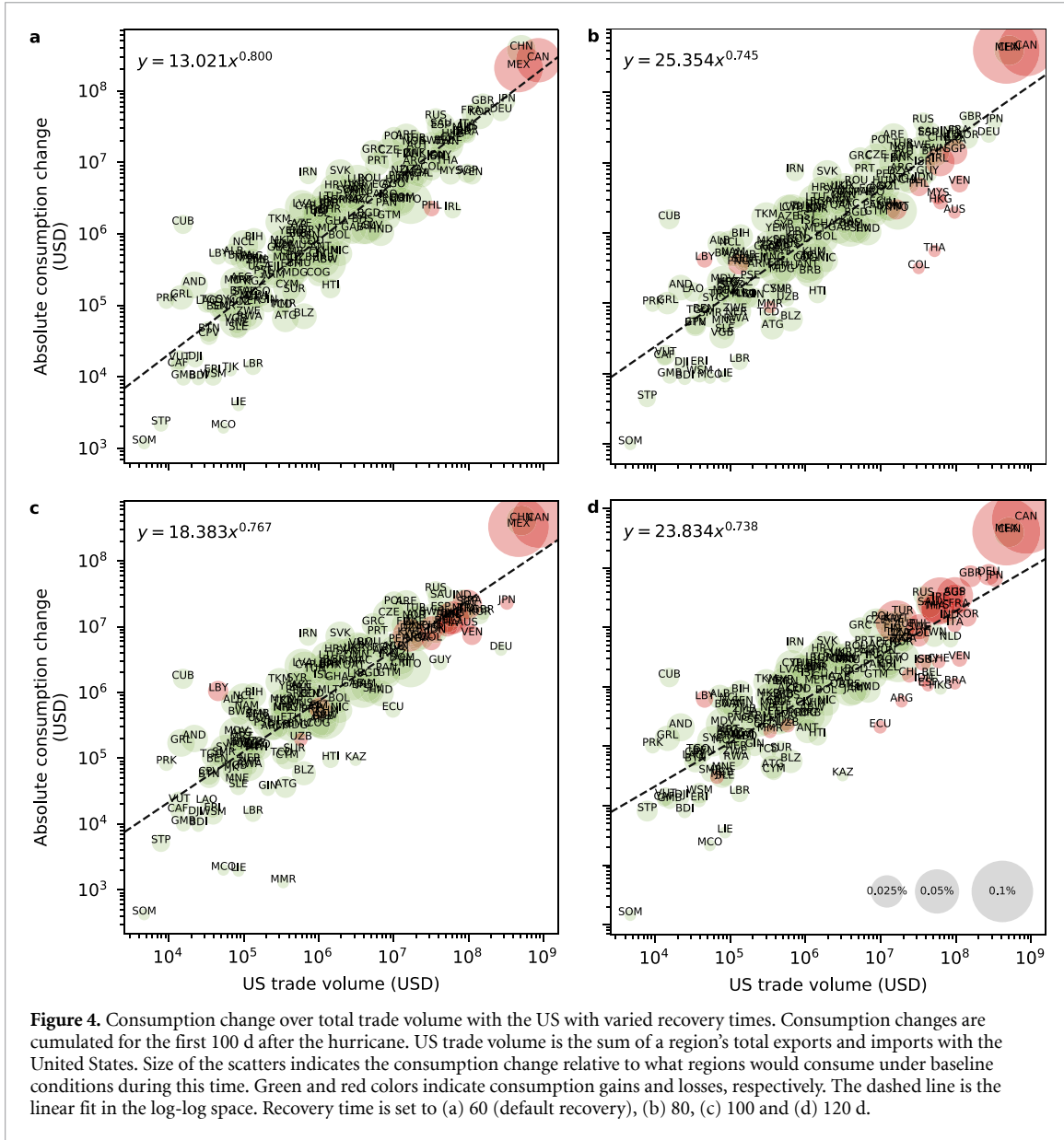
(supplementary figure 2). Linear regression in the log-log space indicates an exponent that is below 1, i.e. the absolute consumption difference increases less than linearly with growing trade volume with the US. Regions with strong trade relations experience a stronger price effect. However, due to the prescribed negative price elasticities, this price effect affects consumption less than linearly.

Whether or not a region experiences total gains or losses in consumption depends on the country-specific shape of the three-phase ripple, i.e. whether the upstream or downstream effects is dominant. To show this, we analyze additional simulations with longer recovery times (80, 100, 120 d, figure 4), which mainly intensifies the slower propagating downstream effect (supplementary figure 3). Initially, most regions (with the exception of Mexico, Canada and the Philippines) show consumption gains. With longer duration, the latter decrease and consumption losses increase. With a recovery time extension of 20 d (figure 4(b)), additional regions transition from gains to losses (e.g. Australia, Venezuela, Ireland, Singapore, Hong Kong). The initially small consumption loss increases with further recovery time extension (panels (c) and (d)). Likewise, regions like Canada, Mexico and the Philippines that show losses already with the original recovery time further increase their losses. In the case of Mexico and Canada, this can supposedly be explained by the geographic and economic proximity of the regions to the US, resulting in a faster downstream propagation to these countries. This suggests that each region has an individual threshold where the direct impact in NY and NJ becomes too strong and a dominating downstream effect results in overall consumption losses. This threshold is already crossed for the Philippines as well as Mexico and Canada with the original recovery time of 60 d.

Generally, the consumption reaction of all regions to the shock duration in NY and NJ appears to follow an inverted U-shape. Without a shock, all regions consume at their baseline level. Short shocks result in consumption gains that increase with the shock duration at first. At some point—depending on the trade relations with the US—consumption gains decrease and eventually transition into losses. Regions with a large trade volume tend to transition sooner than those with smaller trade to the US.

#### 5. Price dynamics

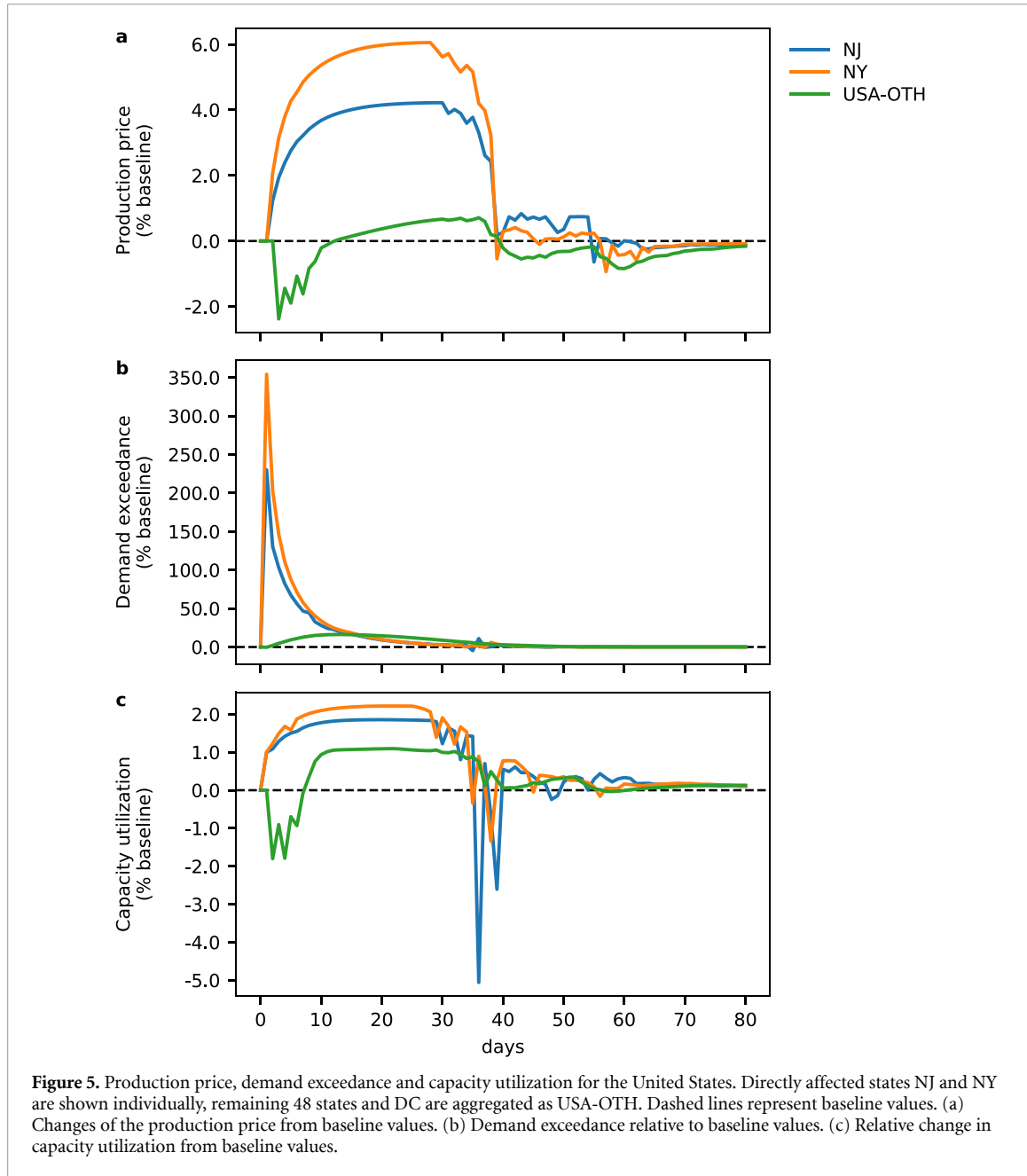
So far we analyzed the consumption price and resulting consumption levels on a regional level and found a three-phased ripple that can result in both overall gains and losses of consumption. In the following, we investigate the underlying price dynamics that lead this ripple which originates in the directly affected regions NY and NJ. For this, we look at changes of



production prices and levels of incoming demand as well as changes of the capacity utilization in NY and NJ as well as the rest of the US. We use the economic notion of capacity utilization [44] that is defined as the ratio of actual output to the output that would minimize production costs. This measure quantifies if and by how much a region is in a state of overproduction, relative to the actual production capacity. For the directly affected regions, we need to first adjust production capacity for the applied production shock. We also calculate the similarly adjusted demand exceedance which indicates if fulfilling the entire incoming demand at a given time step would drive the agent into overproduction, i.e. by how much current incoming demand exceeds the production capacity (for both adjusted capacity utilization and demand exceedance see appendix A). Time series for production prices, demand exceedance and capacity utilization in our simulations are shown in figure 5

for the directly affected US states NJ and NY as well as an aggregate over all other US states and DC. We refer to the latter in the following as USA-OTH.

In the *Acclimate* model, production prices and ultimately consumption prices are driven by the demand that agents receive. In the immediate aftermath of the disaster, NY and NJ cannot satisfy their incoming demand due to the applied external reduction of production capacity. This is reflected by a high demand exceedance. As a result, the directly affected states switch to overproduction directly after the disaster, similarly indicated by an increased capacity utilization. At the same time, NY and NJ reduce their demand towards other regions. Due to the resulting initial upstream propagation, the remainder of the US does not fully use the available production capacity and production prices decrease at first (note that the apparent contradiction for the pooled region USA-OTH of positive demand exceedance



and simultaneous low capacity utilization during the first days after the disaster is simply a result of the aggregation that we perform over the US regions and their individual sectors, see appendix A). However, the longer the disruption prevails, the more of the lost production in NY and NJ propagates downstream in the economic network, resulting in scarcity of goods. This scarcity is compensated by other US states and also the latter eventually switch to overproduction. Yet, overproduction comes at the cost of production prices increasing super-linearly with the production level and average prices rise above baseline levels during this upstream phase. In the situation of scarcity in the disaster aftermath, agents in the network are willing to pay these higher-than-usual prices and producing agents keep their increased production level.

We observe this behavior of rising production prices until about 45 d after the disaster, when production prices rapidly drop again. This drop marks the beginning of the normalization phase. Note that it coincides with a change of the capacity utilization change from positive to negative values, causing agents to switch from an overproduction state to a normal production regime. The sudden price drop results from the fact that now production prices no longer depend super-linearly on the produced quantity. Two factors lead to the end of the overproduction regime: (1) many purchasing firms decide simultaneously to reduce their demand due to the high level of prices, and (2) the reduction of production capacity in the directly affected states is released enough so that the new, reduced incoming demand can be satisfied without overproduction.

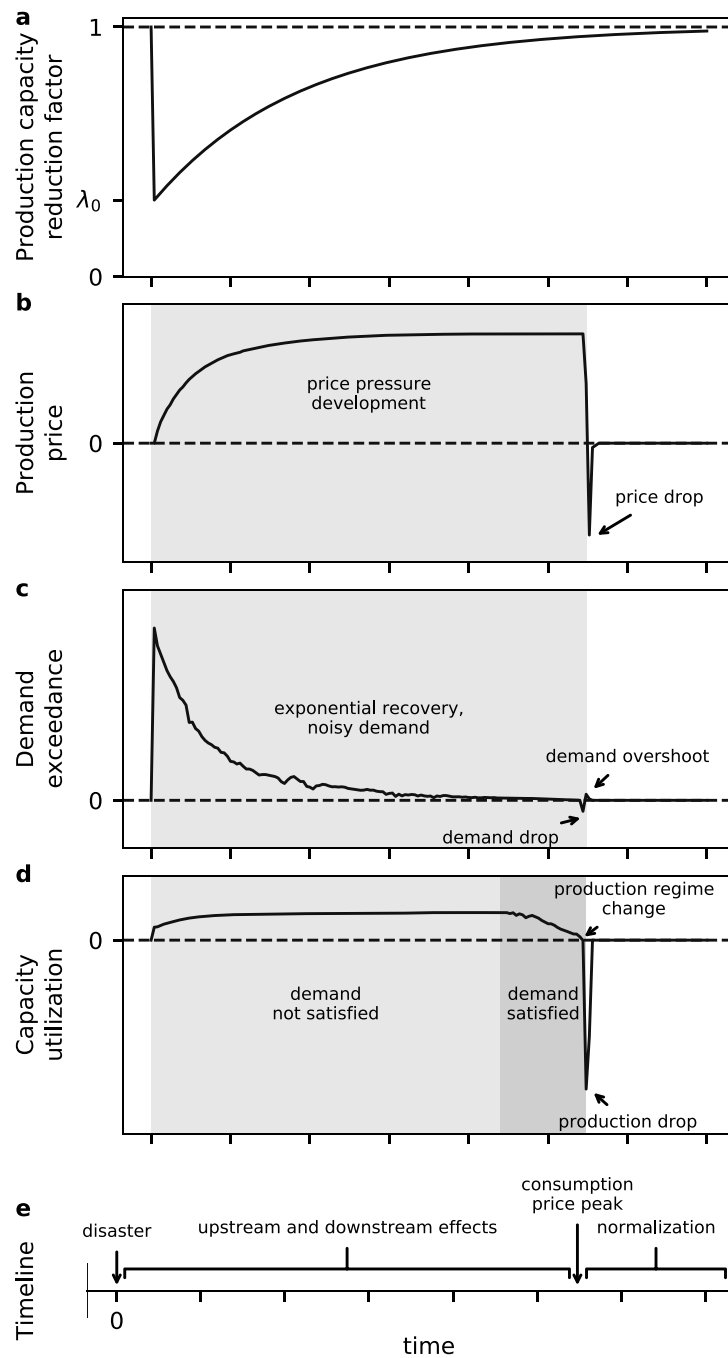


**Figure 6.** Schematic time evolution of a directly affected agent. Dashed lines represent baseline values. Explicit values and durations are not given because magnitudes and time scales differ between disasters. (a) Production capacity reduction factor with initial production shock  $\lambda_0$ . (b) Relative production price change. Grey shaded area denotes the price pressure development time until the price drop. (c) Demand exceedance. Grey shaded area denotes the time during which the economic shock has not decayed enough for demand variations to end the overproduction regime. Noise is due to demand fluctuation from the profit maximization and associated demand shifts of all agents. When the production capacity has recovered enough, this noise can be strong enough to make an agent switch from an overproduction to a normal production regime (production regime change). (d) Relative change in capacity utilization. Light grey area denotes the time during which the agent does not fulfill the incoming demand while in a state of overproduction. The dark grey shaded area is the time during which the entire demand can be satisfied with overproduction. (e) Timeline with the initial disaster impact, the consumption price peak and upstream, downstream and normalization phases.

As can be seen in figure 5, the demand exceedance for NY and NJ decreases exponentially after the disaster, which is simply due to the defined exponential economic recovery. About 45 d after the event, when we observe the production price drop, the production capacity reduction has released enough for smaller

demand variations to cause the demand exceedance to drop below 0. Such variations are a result of the complex dynamics of the model. Since each agent may redistribute its demand in each time step and will do so in order to maximize its profit, the incoming demand (and hence, the demand exceedance) is

subject to some fluctuation. The price tension that previously built up in the network releases and prices drop back towards baseline levels.

A schematic time evolution for the analyzed quantities of a directly affected agent is shown in figure 6 (panels (a)–(d)) with coincident events and phases in the aftermath of the hurricane (panel (d)). While we expect the general behavior of directly affected agents to may be similar for other natural disasters that show an exponential BI recovery, time scales and magnitudes may well be different and are therefore omitted in the figure.

## 6. Discussion

In this study, we modeled the impact that a severe disaster like Hurricane Sandy (2012) can have on global consumption, resulting from economic forward and backward loss propagation in the global supply network. We find a three-phase economic ripple in the supply chain network. This ripple is characterized by an initial upstream effect and resulting consumption increase, followed by an opposing and slower downstream effect and associated reduced consumption. The last phase is a price normalization.

The magnitude of consumption effects on a region depends on its trade volume with the US. Whether a region experiences overall gains or losses depends on which of the upstream or downstream effect during the ripple is dominating. In our simulations, most regions experience slight consumption gains. With longer duration of the direct impact, these regions show a tendency of decreasing consumption gains and eventually a transition to consumption losses. Many regions experience these losses already with an additional recovery time of only 20 d. This is important for two reasons. First, direct losses of hurricanes must be expected to increase in the future due to climate change [8, 45], resulting in potentially longer recovery durations. Second, the recovery from BI was particularly quick after Hurricane Sandy and it can take much longer for other economies subjected to different natural disasters to recover. In the case of Hurricane Katrina in 2005, the economic activity recovered to pre-disaster levels only about one year later [46].

Of course, results from socioeconomic models like the one used in this study are subject to uncertainties due to the necessary assumptions on which the model builds. In particular, these uncertainties concern the absolute magnitudes of the reported results which may appear small at first sight. We emphasize that these values result from only one local, isolated extreme weather event and are therefore still considerable. Previous research [47] has also shown that economic ripples from disasters can amplify each other. More importantly however, we stress the *qualitative* nature and importance of our findings regarding the economic ripple. Our finding of a three-phase

ripple and related consumption changes is qualitatively robust against variations of the local production disruption (supplementary figures 3–5).

While we focused on the specific regions of New York and New Jersey in the United States for this study, similar ripple waves can be expected for major shocks in other regions of the world. Besides hurricanes, we also expect other categories of extreme weather events to have similar economic impacts on consumption. Consecutive and compound events (e.g. the 2020 flood in China and the concurrent heat wave in Europe as recent examples) will likely further increase the magnitudes of the observed indirect effects. Since all these extremes are projected to intensify—at least on a local level—under global warming [48], we believe that modeling approaches like the one we conducted here can contribute valuable insights for necessary mitigation by allowing to simulate and better understand higher-order effects that otherwise cannot be studied.

## Data availability statement

The data that support the findings of this study are available from the corresponding author upon request. GADM region shape files can be found at [www.gadm.org](http://www.gadm.org). Storm track retrieved from IBTrACS database at <http://ibtracs.unca.edu/>.

The data that support the findings of this study will be openly available following an embargo at the DOI: [10.5281/zenodo.5682128](https://doi.org/10.5281/zenodo.5682128). Data will be available from 01 December 2021.

## Code availability

The implementation of the *Acclimate* model is available as open source on <https://github.com/acclimate/acclimate> with identifier [10.5281/zenodo.853345](https://doi.org/10.5281/zenodo.853345). The code for data processing and analysis scripts is available from the corresponding author upon request.

## Acknowledgments

This research has received funding from the Horizon 2020 Framework Programme of the European Union project RECEIPT (Grant Agreement 820712), the German Academic Scholarship Foundation and the German Federal Ministry of Education and Research (BMBF) under the research projects CLIC (01LA1817C), SLICE (01LA1829A), and QUIDIC (01LP1907A). The authors gratefully acknowledge the European Regional Development Fund (ERDF), the German Federal Ministry of Education and Research, and the Land Brandenburg for supporting this project by providing resources on the high performance computer system at the Potsdam Institute for Climate Impact Research.



## Author contributions

R M, S W, and C O designed the method. S W and C O developed the Acclimate model. K K provided the price elasticities. R M conducted the analysis. R M, S W, C O, and A L analysed and interpreted the results. R M, S W, C O, K K, L Q, and A L discussed the results and wrote the manuscript.

## Conflict of interest

The authors declare that they have no competing interests.

## ORCID iDs

Robin Middelanis  <https://orcid.org/0000-0001-8848-3745>

Sven N Willner  <https://orcid.org/0000-0001-6798-6247>

Christian Otto  <https://orcid.org/0000-0001-5500-6774>

Kilian Kuhla  <https://orcid.org/0000-0002-8698-1246>

Lennart Quante  <https://orcid.org/0000-0003-4942-8254>

Anders Levermann  <https://orcid.org/0000-0003-4432-4704>

## References

- [1] NOAA National Centers for Environmental Information (NCEI) 2020 U.S. billion-dollar weather and climate disasters (available at: [www.ncdc.noaa.gov/billions/](http://www.ncdc.noaa.gov/billions/)) (Accessed 10 June 2020)
- [2] Münchener Rückversicherungs-Gesellschaft 2020 NatCatSERVICE (available at: <https://natcatservice.munichre.com/>) (Accessed 20 March 2020)
- [3] Nicholls N *et al* 2012 Changes in climate extremes and their impacts on the natural physical environment *Managing the Risks of Extreme Events and Disasters to Advance Climate Change Adaptation* (Cambridge: Cambridge University Press) pp 109–230
- [4] Walsh K J *et al* 2016 Tropical cyclones and climate change *Wiley Interdiscip. Rev. Clim. Change* **7** 65–89
- [5] Knutson T R *et al* 2010 Tropical cyclones and climate change *Nat. Geosci.* **3** 157–63
- [6] Hallegatte S 2012 The rising costs of hurricanes *Nat. Clim. Change* **2** 148–9
- [7] Mendelsohn R, Emanuel K, Chonabayashi S and Bakkensen L 2012 The impact of climate change on global tropical cyclone damage *Nat. Clim. Change* **2** 205–9
- [8] Knutson T *et al* 2020 Tropical cyclones and climate change assessment: part II: projected response to anthropogenic warming *Bull. Am. Meteorol. Soc.* **101** E303–22
- [9] Emanuel K 2011 Global warming effects on us hurricane damage *Weather Clim. Soc.* **3** 261–8
- [10] Maloney M C and Preston B L 2014 A geospatial dataset for us hurricane storm surge and sea-level rise vulnerability: development and case study applications *Clim. Risk Manage.* **2** 26–41
- [11] Pielke Jr R A *et al* 2008 Normalized hurricane damage in the United States: 1900–2005 *Nat. Hazards Rev.* **9** 29–42
- [12] Weinkle J *et al* 2018 Normalized hurricane damage in the continental united states 1900–2017 *Nat. Sustain.* **1** 808–13
- [13] Rose A 2004 Economic principles, issues and research priorities in hazard loss estimation *Modeling Spatial and Economic Impacts of Disasters* (Berlin: Springer) pp 13–36
- [14] Lenzen M *et al* 2019 Economic damage and spillovers from a tropical cyclone *Nat. Hazards Earth Syst. Sci.* **19** 137–51
- [15] Inoue H and Todo Y 2019 Firm-level propagation of shocks through supply-chain networks *Nat. Sustain.* **2** 841–7
- [16] Hallegatte S 2008 An adaptive regional input–output model and its application to the assessment of the economic cost of Katrina *Risk Anal.* **28** 779–99
- [17] Noy I 2009 The macroeconomic consequences of disasters *J. Dev. Econ.* **88** 221–31
- [18] Willner S N, Otto C and Levermann A 2018 Global economic response to river floods *Nat. Clim. Change* **8** 594–8
- [19] Okuyama Y and Santos J R 2014 Disaster impact and input–output analysis *Econ. Syst. Res.* **26** 1–12
- [20] Hallegatte S 2014 Economic resilience : definition and measurement. policy research working Paper (World Bank) **6852** (<https://openknowledge.worldbank.org/handle/10986/18341>)
- [21] Hallegatte S and Przulski V 2010 The economics of natural disasters: concepts and methods *Policy Research Working Paper* No. WPS 5507
- [22] Deaton A and Zaidi S 2002 Guidelines for constructing consumption aggregates for welfare analysis. working paper (World Bank) **135** (<https://openknowledge.worldbank.org/handle/10986/14101>)
- [23] Levermann A 2014 Climate economics: make supply chains climate-smart *Nature* **506** 27–29
- [24] Guan D *et al* 2020 Global supply-chain effects of covid-19 control measures *Nat. Hum. Behav.* **4** 577–87
- [25] Lenzen M *et al* 2020 Global socio-economic losses and environmental gains from the coronavirus pandemic *PLoS One* **15** e0235654
- [26] Sawada Y 2007 The impact of natural and manmade disasters on household welfare *Agric. Econ.* **37** 59–73
- [27] Pauw K, Thurlow J, Bachu M and Van Seventer D E 2011 The economic costs of extreme weather events: a hydrometeorological CGE analysis for Malawi *Environ. Dev. Econ.* **16** 177–98
- [28] Markhvida M, Walsh B, Hallegatte S and Baker J 2020 Quantification of disaster impacts through household well-being losses *Nat. Sustain.* **3** 538–47
- [29] Walsh B and Hallegatte S 2020 Measuring natural risks in the Philippines: socioeconomic resilience and wellbeing losses *Econ. Disasters Clim. Change* **4** 249–93
- [30] Strobl E 2011 The economic growth impact of hurricanes: evidence from us coastal counties *Rev. Econ. Stat.* **93** 575–89
- [31] Hsiang S M and Jina A S 2014 The causal effect of environmental catastrophe on long-run economic growth: evidence from 6,700 cyclones *Technical Report* (National Bureau of Economic Research)
- [32] Elliott R J, Liu Y, Strobl E and Tong M 2019 Estimating the direct and indirect impact of typhoons on plant performance: evidence from Chinese manufacturers *J. Environ. Econ. Manage.* **98** 102252
- [33] Neumayer E, Plümper T and Barthel F 2014 The political economy of natural disaster damage *Glob. Environ. Change* **24** 8–19
- [34] Bakkensen L and Barrage L 2018 Climate shocks, cyclones, and economic growth: bridging the micro-macro gap *Technical Report* (National Bureau of Economic Research)
- [35] National Hurricane Center 2018 Costliest us tropical cyclones tables updated (available at: [www.nhc.noaa.gov/news/UpdatedCostliest.pdf](http://www.nhc.noaa.gov/news/UpdatedCostliest.pdf)) (Accessed 25 July 2020)
- [36] Blake E S, Kimberlain T B, Berg R J, Cangialosi J P and Beven J L 2013 Tropical Cyclone Report: Hurricane Sandy **12** (National Hurricane Center) 1–10
- [37] Otto C, Willner S N, Wenz L, Frierler K and Levermann A 2017 Modeling loss-propagation in the global supply network: the dynamic agent-based model acclimate *J. Econ. Dyn. Control* **83** 232–69

- [38] Wenz L *et al* 2015 Regional and sectoral disaggregation of multi-regional input–output tables—a flexible algorithm *Econ. Syst. Res.* **27** 194–212
- [39] Lenzen M, Kanemoto K, Moran D and Geschke A 2012 Mapping the structure of the world economy *Environ. Sci. Technol.* **46** 8374–81
- [40] Henry D K *et al* 2013 *Economic Impact of Hurricane Sandy: Potential Economic Activity Lost and Gained in New Jersey and New York* (Washington, DC: US Department of Commerce)
- [41] Global Administrative Areas 2018 GADM database of global administrative areas, version 3.6 (available at: [www.gadm.org](http://www.gadm.org)) (Accessed 16 December 2020)
- [42] Knapp K R, Diamond H J, Kossin J P, Kruk M C and Schreck C J 2018 Int. best track archive for climate stewardship (IBTrACS) project, version 4 (NOAA National Centers for Environmental Information) (available at: <https://doi.org/10.25921/82ty-9e16>) (Accessed 8 August 2020)
- [43] Kuhla K, Willner S N, Otto C, Wenz L and Levermann A 2021 Future heat stress to reduce people’s purchasing power *PLoS One* **16** e0251210
- [44] Berndt E R and Morrison C J 1981 Capacity utilization measures: underlying economic theory and an alternative approach *Am. Econ. Rev.* **71** 48–52
- [45] Grinsted A, Moore J C and Jevrejeva S 2013 Projected atlantic hurricane surge threat from rising temperatures *Proc. Natl Acad. Sci.* **110** 5369–73
- [46] Federal Reserve Bank of Philadelphia 2005 Coincident economic activity index for Louisiana (FRED, Federal Reserve Bank of St. Louis) (available at: <https://fred.stlouisfed.org/series/LAPHCI>) (Accessed 27 April 2021)
- [47] Kuhla K, Willner S N, Otto C, Geiger T and Levermann A 2021 Ripple resonance amplifies economic welfare loss from weather extremes *Environ. Res. Lett.* **16** 114010
- [48] Rahmstorf S and Coumou D 2011 Increase of extreme events in a warming world *Proc. Natl Acad. Sci.* **108** 17905–9



# The projected compensation response to Hurricane Harvey

3

This article has been published in *Environmental Research Letters* as:

R. Middelani, S. N. Willner, C. Otto, A. Levermann (2022). “Economic losses from hurricanes cannot be nationally offset under unabated warming”. In: *Environmental Research Letters*

under the terms of the [Creative Commons Attribution 4.0 licence](#).

DOI: [10.1088/1748-9326/ac90d8](https://doi.org/10.1088/1748-9326/ac90d8)

**ABSTRACT:** Tropical cyclones range among the costliest of all meteorological events worldwide and planetary scale warming provides more energy and moisture to these storms. Modeling the national and global economic repercussions of 2017’s Hurricane Harvey, we find a qualitative change in the global economic response in an increasingly warmer world. While the United States were able to balance regional production failures by the original 2017 hurricane, this option becomes less viable under future warming. In our simulations of over 7,000 regional economic sectors with more than 1.8 million supply chain connections, the US are not able to offset the losses by use of national efforts with intensifying hurricanes under unabated warming. At a certain warming level other countries have to step in to supply the necessary goods for production, which gives US economic sectors a competitive disadvantage. In the highly localized mining and quarrying sector — which here also comprises the oil and gas production industry — this disadvantage emerges already with the original Hurricane Harvey and intensifies under warming. Eventually, also other regions reach their limit of what they can offset. While we chose the example of a specific hurricane impacting a specific region, the mechanism is likely applicable to other climate-related events in other regions and other sectors. It is thus likely that the regional economic sectors that are best adapted to climate change gain significant advantage over their competitors under future warming.

# Economic losses from hurricanes cannot be nationally offset under unabated warming

Robin Middelanis<sup>1,2</sup> , Sven N Willner<sup>1</sup> , Christian Otto<sup>1</sup>  and Anders Levermann<sup>1,3,4,\*</sup> 

<sup>1</sup> Potsdam Institute for Climate Impact Research, Telegrafenberg A56, Potsdam 14473, Germany

<sup>2</sup> Department of Computer Science, University of Potsdam, An der Bahn 2, Potsdam 14476, Germany

<sup>3</sup> Institute of Physics and Astronomy, University of Potsdam, Karl-Liebknecht-Straße 24/25, Potsdam 14476, Germany

<sup>4</sup> Lamont-Doherty Earth Observatory, Columbia University, Palisades, NY, 10964, USA

\* Author to whom any correspondence should be addressed.

E-mail: [anders.levermann@pik-potsdam.de](mailto:anders.levermann@pik-potsdam.de)

**Keywords:** natural disasters, supply chains, higher-order impacts, Hurricane Harvey, tropical cyclones, extreme weather impacts

Supplementary material for this article is available [online](#)

## Abstract

Tropical cyclones range among the costliest of all meteorological events worldwide and planetary scale warming provides more energy and moisture to these storms. Modelling the national and global economic repercussions of 2017's Hurricane Harvey, we find a qualitative change in the global economic response in an increasingly warmer world. While the United States were able to balance regional production failures by the original 2017 hurricane, this option becomes less viable under future warming. In our simulations of over 7000 regional economic sectors with more than 1.8 million supply chain connections, the US are not able to offset the losses by use of national efforts with intensifying hurricanes under unabated warming. At a certain warming level other countries have to step in to supply the necessary goods for production, which gives US economic sectors a competitive disadvantage. In the highly localized mining and quarrying sector—which here also comprises the oil and gas production industry—this disadvantage emerges already with the original Hurricane Harvey and intensifies under warming. Eventually, also other regions reach their limit of what they can offset. While we chose the example of a specific hurricane impacting a specific region, the mechanism is likely applicable to other climate-related events in other regions and other sectors. It is thus likely that the regional economic sectors that are best adapted to climate change gain significant advantage over their competitors under future warming.

With annual global damages amounting to \$26bn [1], tropical cyclones (TCs) range among the costliest and most harmful natural disasters. In the US, they have caused more than half of all damages attributed to extreme weather since 1980 [2]. One particularly destructive hurricane was Harvey in 2017. It made landfall along the Texas coast on 26 August 2017 as a category 4 TC on the Saffir–Simpson scale. Stalling for four days, the storm released torrential rainfall and flooded large areas, predominantly in the state of Texas but also in Louisiana [3]. Harvey resulted in 89 deaths and caused an estimated total damage of \$125bn (in 2017 dollars). Adjusting for price inflation, this makes Harvey the second-costliest hurricane on record after Katrina (2005) [2].

Natural disasters like Hurricane Harvey not only cause dramatic loss of life and damages in

capital stock locally (denoted ‘damages’ hereafter). Losses of local production from business interruption (denoted ‘direct losses’ hereafter) also propagate through the global supply chain network and lead to higher-order effects and associated economic repercussions (denoted ‘indirect’ or ‘higher-order’ effects) elsewhere in the world [4–6]. Analyses of such indirect effects from individual historic TCs [7, 8] suggest that also Harvey's economic repercussions extended well beyond the directly affected area within the US.

With intensifying weather extremes due to anthropogenic climate change [9], the damages, direct losses and thus indirect repercussions from TCs can be expected to increase in the future [1, 10–12]. It has already been shown that a significant share of Harvey's economic costs can be attributed to the ~1 °C global warming in 2017 [13]. Even though TC

frequency is believed to decrease or remain stable, the Intergovernmental Panel on Climate Change (IPCC) projects an increase in intensity and precipitation of the most severe TCs [14–16], and particularly those with a genesis in the North Atlantic basin [17]. In addition to changed climatic conditions [18], increased economic values at risk are another factor for exacerbated future TC damages [19, 20].

On the 16th anniversary of Hurricane Katrina, Hurricane Ida made landfall in Louisiana on 29 August 2021 [21]. Even though among the five costliest US hurricanes on record [22], Ida’s damages did not match those of Katrina, which has been attributed to the improved New Orleans levee system after the latter. While there are meteorological differences between the two storms, this example highlights the importance to assess possible impacts of past events under future conditions so that appropriate countermeasures can be taken. Here, we aim to assess possible economic repercussions of Hurricane Harvey under further global warming. To approach this, we use a *storyline* method [23–25] and construct *counterfactual* scenarios of Hurricane Harvey under future climate conditions. The storyline approach aims to generate and assess plausible effect chains that probabilistic approaches would typically fail to cover due to the relatively rare occurrence of extreme events like Hurricane Harvey. Previous studies (e.g. [26–29]) that show exacerbated economic repercussions from TCs under climate change often use large ensembles of simulated TCs or try to detect trends in historic observations. Here we focus on a single historic event and the economic repercussions it could result in under different climate.

## 1. Method overview

We generate counterfactuals for an additional increase in global warming of up to 4 °C after 2017. These counterfactuals are based on a conceptualization [30] of the original (i.e. unscaled) Hurricane Harvey, modelled as a decrease in productive capacity (the direct economic shock). Note that this shock only models short-term business interruption and does not cover reconstruction efforts or externalities on, e.g. the transport sector (see supplement A: methods and [30] for details). The original scenario is then projected to future climate (scaled or counterfactual scenarios). We generally assume a shock for the US states Texas and Louisiana with exponential decay, deriving the initial shock intensity from the share of the economy that is geographically exposed to the hurricane. For the latter, gross regional product on a county level is used as a proxy. The duration of the shock is estimated from reported initial unemployment claims in the state of Texas after Hurricane Harvey.

Projections are based on the expectation that precipitation will increase with global warming and

that hurricanes may grow larger [12, 31–33] and have longer decay time on land [34], affecting larger areas. According to the Clausius–Clapeyron equation, warming of 1 °C yields an additional 7% of possible air moisture [35] and thus potential precipitation. However, precipitation increase from hurricanes due to climate change must be assumed to be much higher [36] and previous studies [35, 37, 38] confirm this for the case of Hurricane Harvey. We therefore here use the average best estimate of the three studies on Harvey, i.e. about 19% °C<sup>-1</sup> warming [13]. Assuming that damages increase linearly with precipitation and that recovery time from business interruption is proportional to damages, we scale the original hurricane’s recovery time with the precipitation increase. Likewise, we scale the initial shock intensity with the increase in exposed gross regional product resulting from larger affected areas. The size of TCs is typically determined as radii of various wind speeds [39] and it is uncertain whether and how it is affected by climate change [16]. However, some studies find a moderate increase in wind speed radii with larger temperatures [40, 41]. We therefore here assume three scenarios A, B and C with no, moderate (5 km °C<sup>-1</sup>) and strong (10 km °C<sup>-1</sup>) increases in radius of affected area by flooding from Hurricane Harvey. Along these three scenarios, we vary parameters slightly for points in steps of 1 °C to obtain estimates for variability of the dynamics in our model at these points.

Higher-order effects of natural disasters are often analysed, i.a. using computable general equilibrium (CGE) or I–O (input–output) models. For this study, we use the agent-based model *Acclimate* [42]. A full review of the variety of models and their applications is beyond the scope of this study and can be found in the literature [4, 43, 44] but we here give a brief reasoning of the model choice and basic functioning. For all details on the model, please see the model publication [42]. Unlike CGE models [44], *Acclimate* does not require market equilibrium. This is particularly important in the immediate aftermath of a disaster [7] which we focus on here. At the same time, there is only one equilibrium and the model cannot capture longer-term structural network adaptation or economic growth. Like I–O models, *Acclimate* assumes a fixed-proportion production function. However, it is less rigid than I–O models [43, 44] in that it can respond to price changes and adjust each agent’s production capacities. The economic and spatial resolution of *Acclimate* is in principle only bound by data availability for the underlying baseline network, theoretically allowing the simulation of single firms as agents. Here, as baseline, we use a disaggregated [45] version of the EORA multi-region input–output (MRIO) database [46] for the year 2015. With a total of 268 regions and 27 sectors, this results in over 7000 economic agents that are connected through a dense network of more than 1.8 million trade relations.

Agents in Acclimate represent economic sectors of entire regions (countries, generally and states or provinces for the US and China, respectively). Their rationale is, for an agent-based model, rather sophisticated with a local optimization scheme. This is guided by prices, in particular, extra unit production costs when firms use additional idle capacities and costs that arise through deviating from baseline supply relations. Additionally, agents can resort to inventories, storages, when needed. The dynamics of the model accordingly depends not only on the structure of the underlying network, but also on the parameterization of emerging local price changes as well as storage sizes and usage time frames. For this model parameterization we overall stick to the parameters values that have been identified in the model description publication [42] (supplementary table 4). However, for key price and storage parameters we conduct a sensitivity analysis over a wide value range in supplement B: sensitivity analysis.

In this paper, we analyse how net production changes globally in the direct aftermath of the disaster. Hereafter, we refer to net production volumes, i.e. the difference of an agent's outputs to its inputs, simply as 'production'. We assess if and how direct production losses in Texas and Louisiana can be balanced out by other regions. We thereby define production increases by other regions as compensation efforts for direct losses, or simply as compensation. Note that compensation here should not be confused with wages, a notion common in other branches of economics. We find that while the United States are able to compensate for direct local production losses from the original 2017 hurricane, this is no longer possible with further global warming. Losses in the US cannot be offset by national efforts with intensifying hurricanes under unabated warming. At a certain warming level, other countries and regions step in to supply the necessary goods for production. In the highly localized mining and quarrying sector (which here also comprises oil and gas production), this happens already with the original Hurricane Harvey and intensifies under warming. Eventually, also other regions reach limits of what they can offset, suggesting an individual threshold for compensation capabilities. Our results show that countries have an interest to adapt their economies such that they are able to compensate for direct losses from extreme weather in order to keep a competitive advantage. One possible way of adaptation is regional distribution of production capacities. For sectors where this proves challenging, sufficient buffers are necessary to reduce dependencies on other regions for compensation.

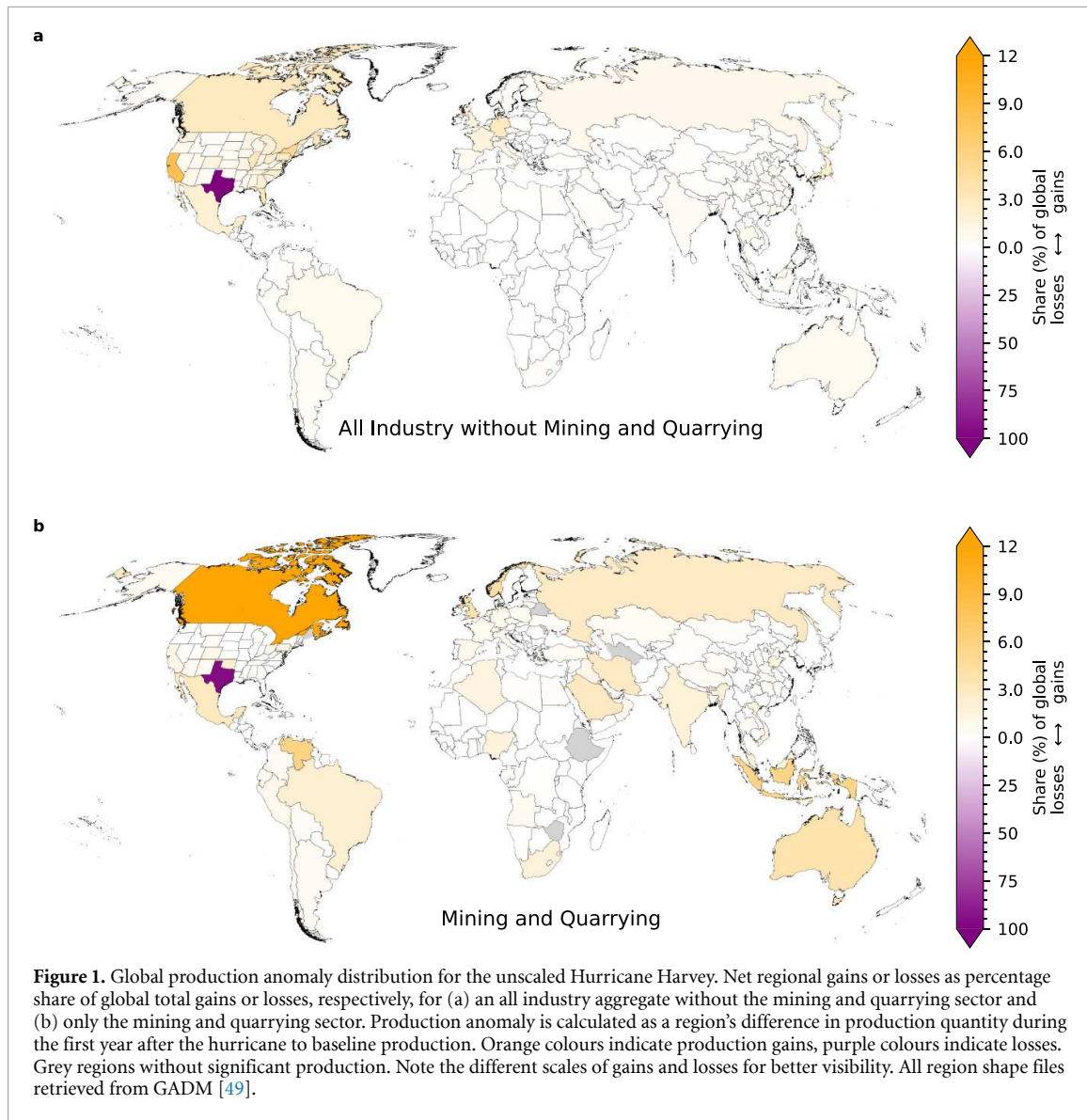
## 2. US unable to compensate for losses under climate change

We first investigate how global production changes during the first year after the original, unscaled

hurricane. For this, we aggregate each region's difference from baseline production during this time and find that—all sectors combined—production gains outweigh losses on a global level. The latter are almost exclusively direct losses in Texas (99.6% of all losses) while indirect losses after the disaster can be regarded as negligible. California, New York and Florida as the economically strongest US states show the largest share of gains. Even though directly affected by the hurricane, Louisiana can compensate for local direct losses. In total, losses in Texas are about equal to the gains in all other US states, meaning that the country can overall compensate for these losses. However, while other regions in the world experience production increases due to the temporary scarcity of goods, the US does not profit from this stimulus due to the compensation efforts.

While the US can overall compensate for direct losses in Texas, this is not achieved on the individual level of the mining and quarrying sector which is highly concentrated in Texas. Texas is responsible for over 42% of US crude oil production and over 25% of US natural gas production<sup>5</sup>. We compare how production is redistributed globally in this sector after the hurricane, compared to an aggregate of all other economic sectors. For each region, we calculate the share of global production gains or losses, respectively, depending on whether a region experiences an overall increase or decrease in production compared to baseline. Results are shown (again for the time of one year after the hurricane) in figure 1. We observe that the lost production in Texas results in a much different production distribution for the different sectors. Only about 11.5% of global production gains in the mining and quarrying sector are realized within the US as opposed to about 62.8% for the aggregated remaining sectors. At the same time, mining and quarrying gains realized within the US do not outweigh losses in Texas, resulting in a net production loss of the country in this sector. To offset this loss on a global scale, demand and thus production are shifted from the US to other strong mining and quarrying export regions (figure 1(b), supplementary table 2). The degree to which production is shifted to these regions is significantly higher than with regards to the aggregated remaining sectors. We note that also strong coal-producing regions like Australia, Indonesia and India show increased production in this sector, even though Texas and Louisiana are responsible for only small shares of total US coal production [47, 48]. The reason for this lies in the economic baseline data we use for our model. In this data, mining and quarrying does not only contain monetary flows for oil and gas trade but also other fossil energy resources and their production like coal.

<sup>5</sup> [www.eia.gov/state/print.php?sid=TX](http://www.eia.gov/state/print.php?sid=TX).

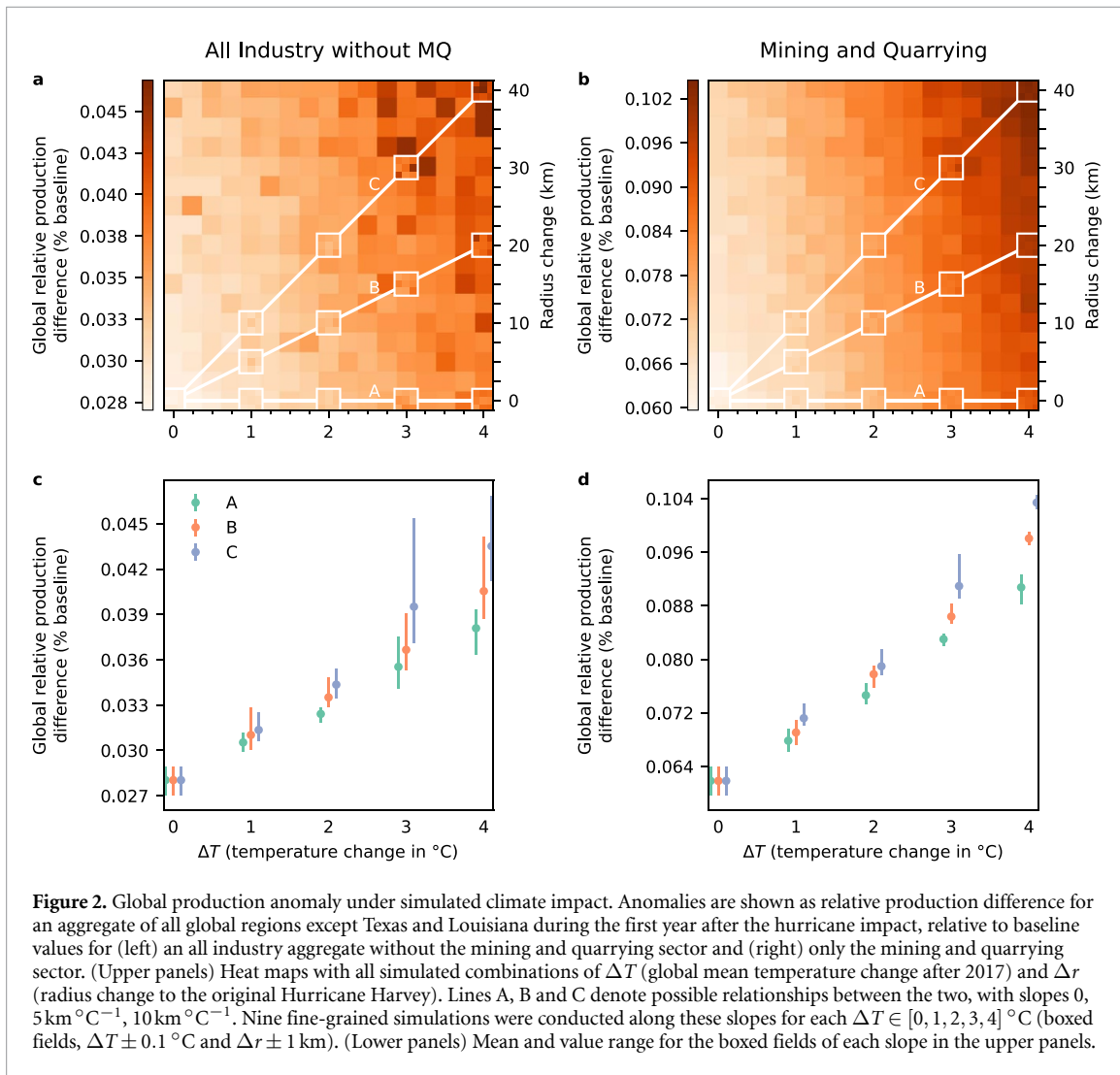


We observe that production gains outside of Texas grow when projecting the original, unscaled direct economic impact of the hurricane to future climate. In figure 2 we show the relative production difference on a global scale for all simulated scenarios, excluding Texas and Louisiana as directly affected regions. We find that, for all assumed temperature-radius relationships, global production increases roughly linearly with global warming. Notably, the relative production increase of the mining and quarrying sector is slightly more than twice the relative increase of the rest of the industry. This factor is a result of the respective sector shares of global exports from Texas (supplementary table 3), which are almost twice as high for the mining and quarrying sector as for the aggregated other sectors. While global production excluding the directly affected US-states increases with all assumed temperature-radius relationships, the steepness of the slopes for this relationship has

an impact on the change of absolute production values. However, the qualitative result of linearly increasing global production is robust against variation of the assumed slopes and the dominant factor for production increase is the change in temperature, given the moderate radius increases. Results are also robust against slight variation of radius and temperature (boxed fields in upper panels and error bars in lower panels of figure 2).

On a global level, the increasing gains offset direct losses under all temperature increases and assumed slopes (figure 3), resulting in net production gains (grey shading in upper panels) in all sectors. Gains in all sectors—both the aggregated sectors and mining and quarrying—increase at a slower pace than losses throughout all simulated scenarios, resulting in a slight decrease of net gains. The United States, on the other hand, can only just compensate for losses in all sectors excluding mining and quarrying under





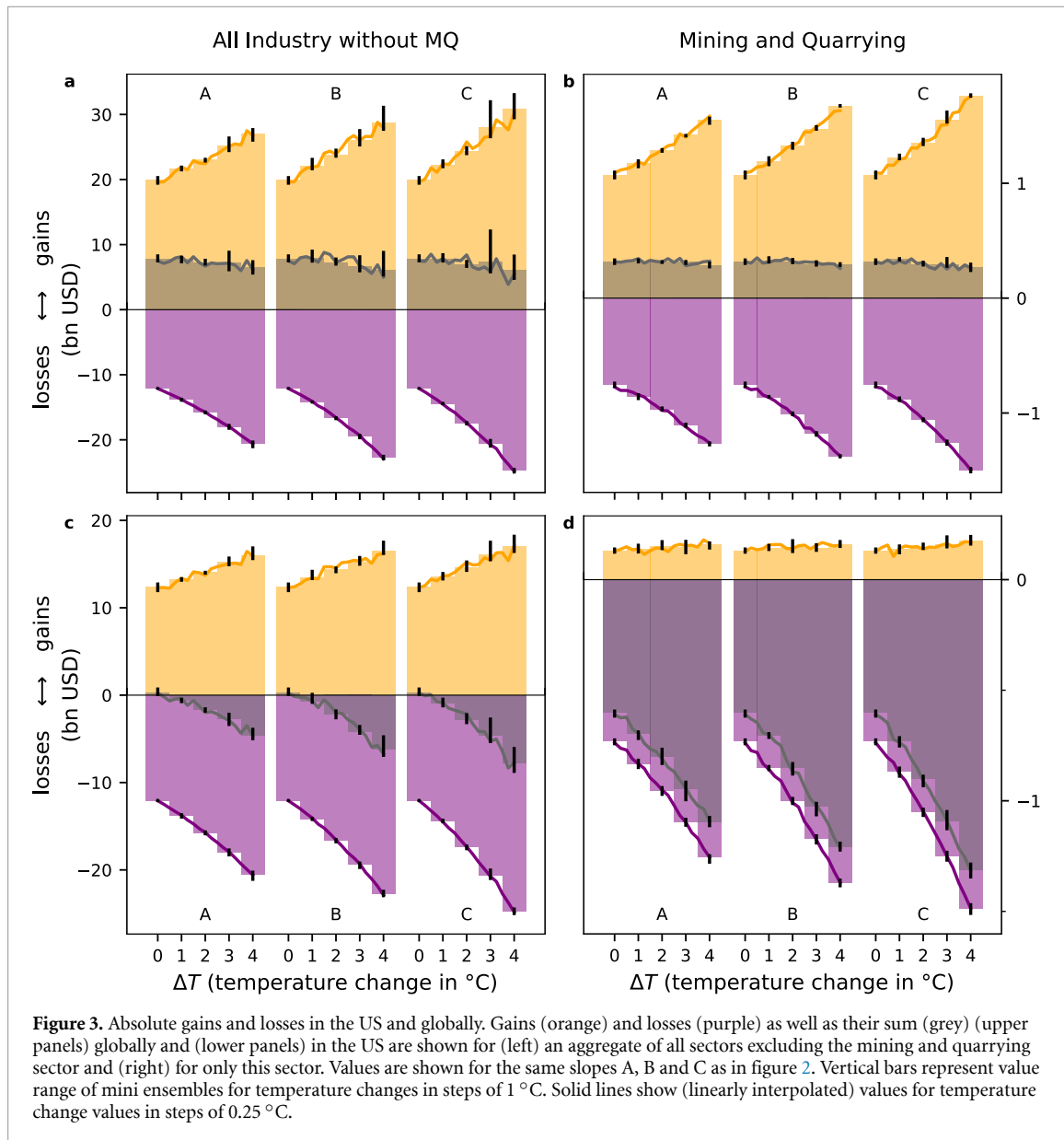
the original, unscaled hurricane scenario. Under all considered slopes, future warming results in net losses (panel (c)). As stated above, the US can in no scenario compensate for mining and quarrying losses on a national level (panel (d)) and net losses in this sector intensify under future warming. In particular, unlike the other sectors, mining and quarrying gains in the US only increase moderately compared to the losses in this sector. This suggests that other US states have reached a limit to which they can compensate for losses in Texas, even in the unscaled scenario.

### 3. Remote regions reach compensation limit under climate change

We further investigate which regions compensate for losses in Texas under climate change, both in the mining and quarrying sector and the aggregate of all other sectors. For this, we calculate the shares of global gains for different groups of regions (figure 4), which we group according to their total export volume excluding the mining and quarrying sector (AI-MQ) as well as the export volume only in the latter. Regions are

grouped such that they make up 50%, 75% and 95% of global exports. In addition to this, we also explicitly show shares for the US which ranges in the top 50% exporters for the aggregate of all industries except mining and quarrying sector and in the top 75% of mining and quarrying exporters. For each of these groups and all considered radius-temperature relationships, we calculate absolute gains and the share of global gains in the according sector (or sector group, respectively) that the regions were grouped by. Absolute gains and shares of the respective other sectors can be found in the supplements (supplementary figures 1 and 2).

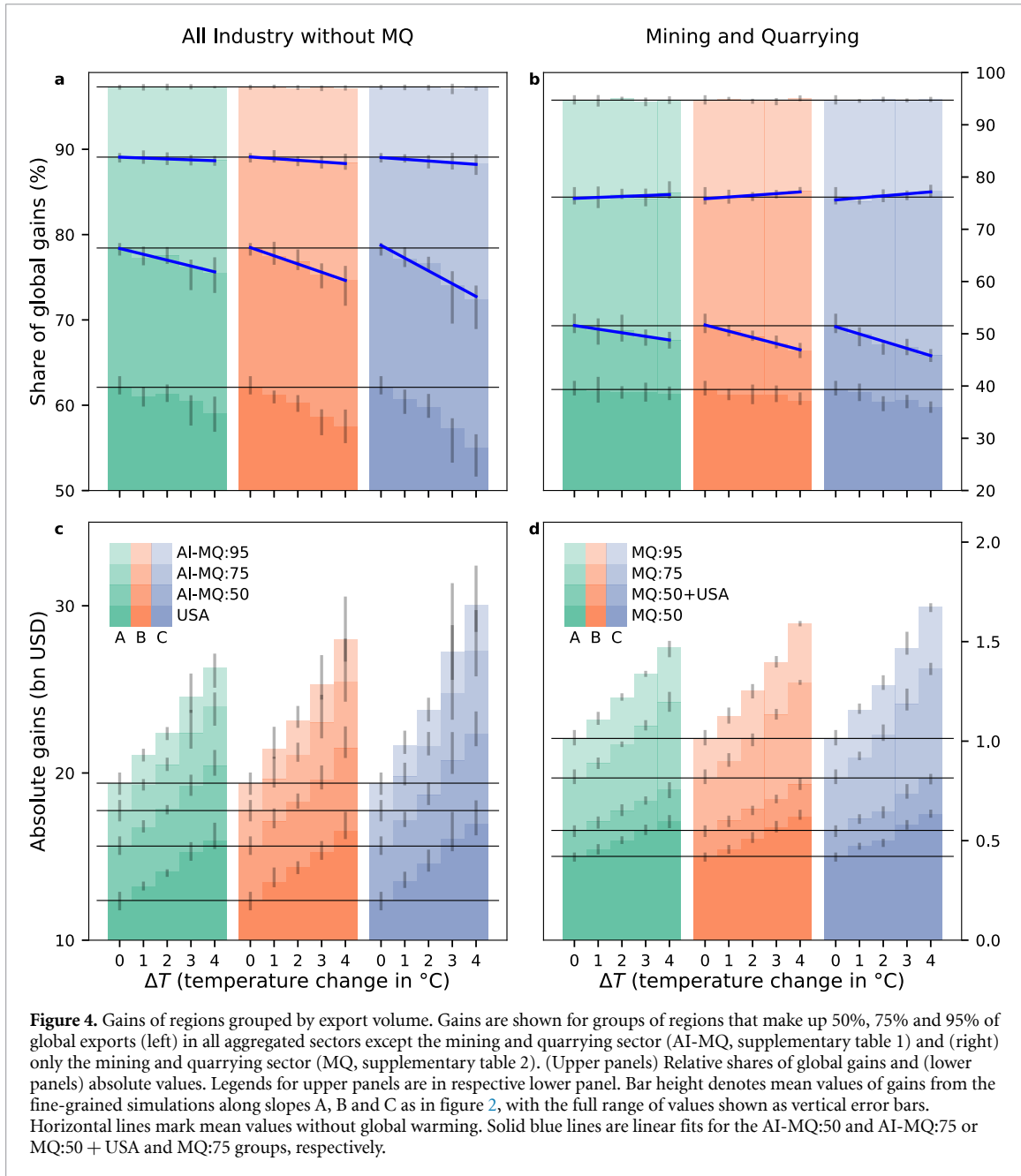
We find that while global gains continually increase for each of the considered region groups with global warming (lower panels), there is a shift in gain distribution towards smaller regions (i.e. regions with less exports in the baseline state, upper panels). This shift is most prominent with the strongest assumed radius-temperature relationship (scenario C) although shifts can be observed across all slopes with similar qualitative behaviour. Most prominently, the mining and quarrying exporters that are in



the top 75% group but not in the 50% + USA group increase their share of gains in this sector under climate change (panel (b), blue trend lines) while shares of the largest exporters (top 50%) generally decrease, both in this sector as well as the other sectors (panel (a)). This suggests that the degree to which large exporters can (cost-efficiently) compensate for losses in Texas diminishes with a stronger climate-induced direct impact. The latter reach their compensation limits and other (smaller) regions take up increasing shares of compensation. This shift from (export-wise) larger regions to smaller regions is more pronounced for the mining and quarrying sector than the remaining aggregated sectors, suggesting that large exporters in this sector reach their compensation limits earlier. This behaviour can be explained with the high regional aggregation of this sector both in the US and globally and the larger relative share of global

production that is lost with the direct impact. Therefore, the degree to which the remaining US states can profit from global gains is also smaller in the mining and quarrying sector compared to the other sectors and gains are mostly realized outside of the US. However, we observe the same qualitative behaviour of increasing gain shares for smaller exporters in the top 75% group also in the aggregated remaining sectors (trends in panel (a)). It is less pronounced for these sectors (because regional aggregation is not as high as for the mining and quarrying sector) but is generally applicable to all sectors.

While gains (i.e. compensation efforts) outside of Texas generally increase both in the US and the rest of the world, we now quantify the degree to which these gains balance out losses. We define the compensation to loss ratio (CLR) as the ratio between a region's or region group's gains and losses, considering a specific

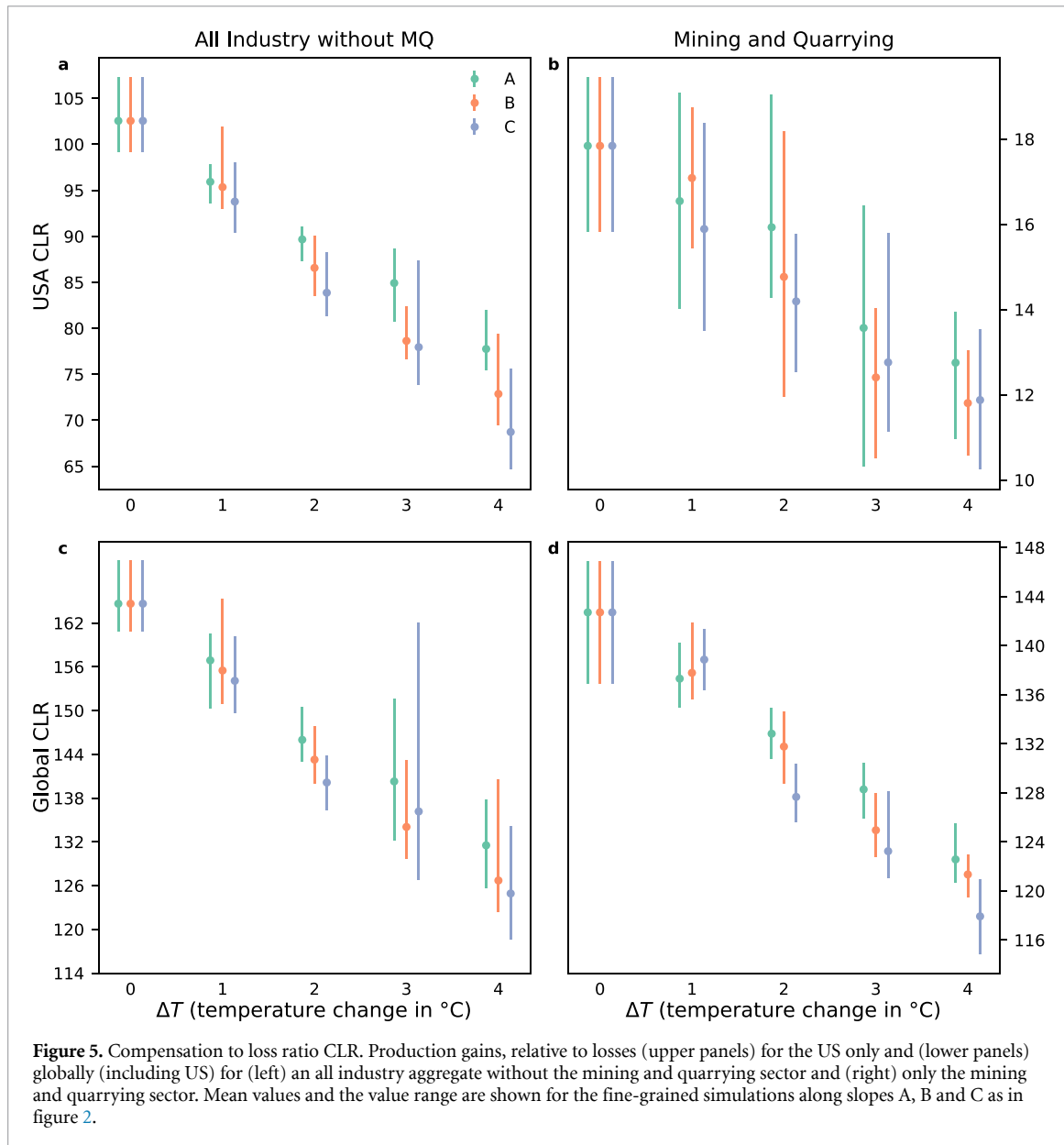


sector or a group of sectors. A CLR above 100% means that losses are (over-) compensated, a negative CLR below this threshold indicates that losses are not (fully) offset. We compute the CLR on a US and global level (figure 5), again for the aggregate of all sectors except mining and quarrying as well as only this sector. As previously shown, for the US as a whole, direct losses in the aggregated sectors can be compensated for in the unscaled scenario, while this is no longer the case with climate change (CLR below 100%, panel (a)). This finding is consistent along all assumed slopes for the radius increase although full compensation lies within the range of uncertainty until 1°C of additional warming after 2017 (i.e. ~2°C compared to pre-industrial temperatures) for scenario A. For the mining and quarrying sector (panel (b)), the CLR on a US level lies continually

at ~18% or below. Production in this sector being highly regionally aggregated in Texas, other US states have not the capacity to compensate for direct losses under any of the considered scenarios.

On a global level, gains outweigh losses both for the aggregated sectors as well as the mining and quarrying sector. This is reflected in a CLR well above 100% with all considered scenarios (lower panels in figure 5), albeit with decreasing trend for ongoing global warming. Hence, while the economic system of the US is not capable to compensate for losses, the world as the superordinate economic system is. Globally, the CLR in the mining and quarrying sector for the unscaled scenario starts at a much lower value than in the aggregated other sectors, which is due to the relatively larger importance of Texas in this sector on a global level. Therefore, to compensate for losses





in Texas in mining and quarrying, other regions reach their compensation limits earlier in this sector than in the aggregated remaining sectors.

#### 4. Discussion

Our findings from simulating the projected global economic impact of Hurricane Harvey under climate change illustrate how direct production losses from a strong local economic shock are offset, i.e. compensated for, in the global economic system. We find that the US, as the directly affected country, cannot compensate for direct losses of the hurricane under further global warming, leaving the US at a competitive disadvantage. Other regions take over to offset these losses until reaching their own compensation limits, with compensation shares gradually shifting from large to smaller exporters as global warming continues.

These are not hard limits, but rather a matter of cost effectiveness. In the model used here, marginal production costs increase in production extension (i.e. production above baseline), making compensation efforts more expensive. This reflects the fact that, in practice, a region cannot increase production infinitely but is bound by production capacity which in turn is limited by, e.g. availability of labour and production assets. A sensitivity analysis of some important model parameters like the price increase in production extension is provided in supplement B: sensitivity analysis. We find that our results are robust to these parameter variations. Changes in magnitudes of gains and losses are small compared to the changes resulting from climate variation.

Of course, the modelling of the shock is rather stylized and the direct impact may vary in reality, both with regards to the unscaled scenario as well as the scaled scenarios. In particular, the quantitative

relationship between radius of the hurricane and temperature is unknown, although it is likely for a hurricane like Harvey to grow larger under progressing climate change. For this reason, we assumed different possible relationships between temperature increase and radius change and found our results to be qualitatively consistent across these relationships, with slightly different magnitude. Main driver in the magnitude of the results is the change in temperature and associated precipitation increase.

Applying the same direct impact to all sectors is a strong simplification. However, we do not claim to have modelled the economic shock exactly like it happened historically. Rather, we were interested in the global economic repercussions to a shock with magnitudes like Hurricane Harvey and how these change under global warming in a storyline/counterfactual approach. In particular, we chose to investigate the mining and quarrying sector in comparison to the remaining economy. Of course, this sector will likely play a very different role in the future and we emphasize that it was chosen due to its strong regional concentration in Texas and the US. Even though this may change in the future, findings may be generalized to any such high regionally concentrated economic sector. We argue that applying identical shocks to this sector as to all others is a reasonable approach to investigate how the underlying structural differences regarding the sectors impact the economic response.

A source of uncertainty is the EORA MRIO table which we use as underlying network, comprising 26 industry sectors and final consumption. While more detailed MRIO tables are available for specific regions, global coverage inevitably comes at the cost of lower sectoral detail. As a result, e.g. production of oil, natural gas, and coal are all contained in the mining and quarrying sector, making these goods interchangeable in the model. In this comparably coarse resolution the model assumptions of goods being perfect complements and the network structure itself being fixed (i.e. demand and supply can only be shifted between existing supply relations without creating new ones) are reasonable.

Accordingly, the amounts of compensation globally and in the US should be regarded with care due to uncertainties in the modelling of the direct impact as well as the used model. However, we stress the qualitative findings of our research and their relevance to disaster impact analysis. Stronger direct impacts from major hurricanes like Harvey under climate change (with otherwise unaltered socioeconomic conditions) will at some point exceed the compensation capabilities of the US. The exact temperature, however, is subject to uncertainties. While we investigated a specific TC in the United States, our findings are likely applicable for any country that is threatened by major localized extreme weather events. These countries will be in a position of

economic disadvantage, especially with regards to sectors with strong exposure and high level of regional concentration. Besides climate mitigation, economic adaptation in the form of regional distribution of production capacities is therefore advised. For sectors where this proves challenging, sufficient buffers are necessary to reduce dependencies on other regions for compensation.

We here looked into the temporary global redistribution of production volumes in the disaster aftermath. It has been shown that hurricanes can also affect growth patterns [50] with long-lasting effects [51], which we cannot model here due to a static economic baseline. However, shifts in production towards other regions may steer investments, thereby perpetuating these regions' economic advantages. We plan to investigate this in the future by implementing an investment scheme and thus adding endogenous growth to our model.

### Data availability statement

The data that support the findings of this study are available from the corresponding author upon request. GADM region shape files can be found at <http://www.gadm.org>. Storm track retrieved from IBTrACS database at <http://ibtracs.unca.edu/>.

The data that support the findings of this study will be openly available following an embargo at the following URL/DOI: [10.5281/zenodo.5848439](https://doi.org/10.5281/zenodo.5848439).

### Acknowledgments

We thank Michael Wehner and three anonymous reviewers for their very constructive and valuable feedback to this work. This research has received funding from the Horizon 2020 Framework Programme of the European Union project RECEIPT (Grant Agreement 820712) and the German Federal Ministry of Education and Research (BMBF) under the research projects CLIC (01LA1817C), SLICE (01LA1829A), and QUIDIC (01LP1907A).

### Code availability

The implementation of the *Acclimate* model is available as open source on <https://github.com/acclimate/acclimate> with identifier [10.5281/zenodo.853345](https://doi.org/10.5281/zenodo.853345). The code for data processing and analysis scripts is available from the corresponding author upon request.

### Author contribution


R M designed the method and conducted the analysis. S W and C O developed the *Acclimate* model. R M, S W, and A L analysed and interpreted the results. R M wrote the manuscript with contributions from all authors. All authors discussed the results.

## Conflict of interest

The authors declare that they have no competing interests.

## ORCID iDs

Robin Middelani  <https://orcid.org/0000-0001-8848-3745>

Sven N Willner  <https://orcid.org/0000-0001-6798-6247>

Christian Otto  <https://orcid.org/0000-0001-5500-6774>

Anders Levermann  <https://orcid.org/0000-0003-4432-4704>

## References

- Mendelsohn R, Emanuel K, Chonabayashi S and Bakkensen L 2012 The impact of climate change on global tropical cyclone damage *Nat. Clim. Change* **2** 205–9
- Smith A B 2020 U.S. Billion-dollar Weather and Climate Disasters, 1980 - present (NCEI Accession 0209268). NOAA National Centers for Environmental Information (<https://doi.org/10.25921/stkw-7w73>)
- Blake E S and Zelinsky D A 2018 *National hurricane center tropical cyclone report: Hurricane Harvey* AL092017 National Hurricane Center (available at: [www.nhc.noaa.gov/data/tcr/AL092017\\_Harvey.pdf](http://www.nhc.noaa.gov/data/tcr/AL092017_Harvey.pdf)) (Accessed 12 October 2021)
- Rose A 2004 Economic principles, issues and research priorities in hazard loss estimation *Modeling Spatial and Economic Impacts of Disasters* ed Y Okuyama and S E Chang Advances in Spatial Science (Berlin: Springer) pp 13–36
- Acemoglu D, Carvalho V M, Ozdaglar A and Tahbaz-Salehi A 2012 The network origins of aggregate fluctuations *Econometrica* **80** 1977–2016
- Levermann A 2014 Climate economics: make supply chains climate-smart *Nature* **506** 27–29
- Hallegatte S 2008 An adaptive regional input-output model and its application to the assessment of the economic cost of Katrina *Risk Anal.: Int. J.* **28** 779–99
- Lenzen M, Malik A, Kenway S, Daniels P, Lam K L and Geschke A 2019 Economic damage and spillovers from a tropical cyclone *Nat. Hazards Earth Syst. Sci.* **19** 137–51
- Robinson A, Lehmann J, Barriopedro D, Rahmstorf S and Coumou D 2021 Increasing heat and rainfall extremes now far outside the historical climate *npj Clim. Atmos. Sci.* **4** 1–4
- Knutson T R, McBride J L, Chan J, Emanuel K, Holland G, Landsea C, Held I, Kossin J P, Srivastava A and Sugi M 2010 Tropical cyclones and climate change *Nat. Geosci.* **3** 157–63
- Hallegatte S 2012 The rising costs of hurricanes *Nat. Clim. Change* **2** 148–9
- Knutson T *et al* 2020 Tropical cyclones and climate change assessment: part II: projected response to anthropogenic warming *Bull. Am. Meteorol. Soc.* **101** E303–22
- Wehner M and Sampson C 2021 Attributable human-induced changes in the magnitude of flooding in the Houston, Texas region during Hurricane Harvey *Clim. Change* **166** 1–13
- Seneviratne S I *et al* 2012 Changes in climate extremes and their impacts on the natural physical environment *Managing the Risks of Extreme Events and Disasters to Advance Climate Change Adaptation* ed C B Field *et al* (Cambridge: Cambridge University Press) pp 109–230
- Christensen J H *et al* 2013 Climate phenomena and their relevance for future regional climate change *Climate Change 2013 the Physical Science Basis: Working Group I Contribution to the Fifth Assessment Report of the Intergovernmental Panel on Climate Change* ed T F Stocker, D Qin, G Plattner, M Tignor, S K Allen, J Boschung, A Nauels, Y Xia, V Bex and P M Midgley (Cambridge: Cambridge University Press) pp 1217–308
- Seneviratne S I *et al* 2021 Weather and Climate Extreme Events in a Changing Climate *Climate Change 2021: The Physical Science Basis. Contribution of Working Group I to the Sixth Assessment Report of the Intergovernmental Panel on Climate Change* ed V P Masson-Delmotte *et al* (Cambridge: Cambridge University Press) pp 1513–766
- Walsh K J *et al* 2016 Tropical cyclones and climate change *Wiley Interdiscip. Rev.: Clim. Change* **7** 65–89
- Emanuel K 2017 Assessing the present and future probability of Hurricane Harvey's rainfall *Proc. Natl Acad. Sci.* **114** 12681–4
- Pielke R A, Gratz J, Landsea C W, Collins D, Saunders M A and Musulin R 2008 Normalized hurricane damage in the United States: 1900–2005 *Nat. Hazards Rev.* **9** 29–42
- Weinkle J, Landsea C, Collins D, Musulin R, Crompton R P, Klotzbach P J and Pielke R 2018 Normalized hurricane damage in the continental United States 1900–2017 *Nat. Sustain.* **1** 808–13
- BevenII J L, Hagen A and Berg R 2021 *National hurricane center tropical cyclone report: Hurricane Ida* AL092021 National Hurricane Center (available at: [www.nhc.noaa.gov/data/tcr/AL092021\\_Ida.pdf](http://www.nhc.noaa.gov/data/tcr/AL092021_Ida.pdf)) (Accessed 18 April 2022)
- NOAA 2022 Costliest U.S. tropical cyclones (available at: [www.ncei.noaa.gov/access/billions/dcmi.pdf](http://www.ncei.noaa.gov/access/billions/dcmi.pdf)) (Accessed 18 May 2022)
- Shepherd T G, Boyd E, Cabel R A, Chapman S C, Dessai S, Dima-West I M, Fowler H J, James R, Maraun D, Martius O *et al* 2018 Storylines: an alternative approach to representing uncertainty in physical aspects of climate change *Clim. Change* **151** 555–71
- Sillmann J, Shepherd T G, van den Hurk B, Hazeleger W, Martius O, Slingo J and Zscheischler J 2021 Event-based storylines to address climate risk *Earth's Future* **9** e2020EF001783
- van den Hurk B *et al* 2022 Climate impact storylines for assessing socio-economic responses to remote events *Climate Risk Management* CLRM-D-22-00088 (available at: <https://ssrn.com/abstract=4090562>) (Accessed 2 May 2022)
- Narita D, Tol R S J and Anthoff D 2010 Economic costs of extratropical storms under climate change: an application of FUND *J. Environ. Plan. Manage.* **53** 371–84
- Emanuel K 2011 Global warming effects on US hurricane damage *Weather Clim. Soc.* **3** 261–8
- Estrada F, Botzen W J W and Tol R S J 2015 Economic losses from US hurricanes consistent with an influence from climate change *Nat. Geosci.* **8** 880–4
- Bakkensen L A, Park D-S R and Sarkar R S R 2018 Climate costs of tropical cyclone losses also depend on rain *Environ. Res. Lett.* **13** 074034
- Middelani R, Willner S N, Otto C, Kuhla K, Quante L and Levermann A 2021 Wave-like global economic ripple response to Hurricane Sandy *Environ. Res. Lett.* **16** 124049
- Lin Y, Zhao M and Zhang M 2015 Tropical cyclone rainfall area controlled by relative sea surface temperature *Nat. Commun.* **6** 1–7
- Sun Y, Zhong Z, Li T, Yi L, Hu Y, Wan H, Chen H, Liao Q, Ma C and Li Q 2017 Impact of ocean warming on tropical cyclone size and its destructiveness *Sci. Rep.* **7** 1–10
- Xu Z, Sun Y, Li T, Zhong Z, Liu J and Ma C 2020 Tropical cyclone size change under ocean warming and associated responses of tropical cyclone destructiveness: idealized experiments *J. Meteorol. Res.* **34** 163–75
- Li L and Chakraborty P 2020 Slower decay of landfalling hurricanes in a warming world *Nature* **587** 230–4
- van Oldenborgh G J, van der Wiel K, Sebastian A, Singh R, Arrighi J, Otto F, Haustein K, Li S, Vecchi G and Cullen H 2017 Attribution of extreme rainfall from Hurricane Harvey, august 2017 *Environ. Res. Lett.* **12** 124009

- [36] Patricola C M and Wehner M F 2018 Anthropogenic influences on major tropical cyclone events *Nature* **563** 339–46
- [37] Risser M D and Wehner M F 2017 Attributable human-induced changes in the likelihood and magnitude of the observed extreme precipitation during Hurricane Harvey *Geophys. Res. Lett.* **44** 12–457
- [38] Wang S-Y S, Zhao L, Yoon J-H, Klotzbach P and Gillies R R 2018 Quantitative attribution of climate effects on Hurricane Harvey's extreme rainfall in Texas *Environ. Res. Lett.* **13** 054014
- [39] Chavas D R, Lin N and Emanuel K 2015 A model for the complete radial structure of the tropical cyclone wind field. Part I: comparison with observed structure *J. Atmos. Sci.* **72** 3647–62
- [40] Reed K A, Stansfield A, Wehner M and Zarzycki C 2020 Forecasted attribution of the human influence on Hurricane Florence *Sci. Adv.* **6** eeaw9253
- [41] Wehner M 2021 Simulated changes in tropical cyclone size, accumulated cyclone energy and power dissipation index in a warmer climate *Oceans* **2** 688–99
- [42] Otto C, Willner S, Wenz L, Frieler K and Levermann A 2017 Modeling loss-propagation in the global supply network: the dynamic agent-based model acclimate *J. Econ. Dyn. Control* **83** 232–69
- [43] Okuyama Y and Santos J R 2014 Disaster impact and input–output analysis *Econ. Syst. Res.* **26** 1–12
- [44] Botzen W W, Deschenes O and Sanders M 2020 The economic impacts of natural disasters: a review of models and empirical studies *Rev. Environ. Econ. Policy* **13** 167–88
- [45] Wenz L, Willner S N, Radebach A, Bierkandt R, Steckel J C and Levermann A 2015 Regional and sectoral disaggregation of multi-regional input–output tables—a flexible algorithm *Econ. Syst. Res.* **27** 194–212
- [46] Lenzen M, Kanemoto K, Moran D and Geschke A 2012 Mapping the structure of the world economy *Environ. Sci. Technol.* **46** 8374–81
- [47] U.S. Energy Information Administration (EIA) 2021 Texas state energy profile (available at: [www.eia.gov/state/print.php?sid=TX](http://www.eia.gov/state/print.php?sid=TX)) (Accessed 10 August 2021)
- [48] U.S. Energy Information Administration (EIA) 2021 Louisiana state energy profile (available at: [www.eia.gov/state/print.php?sid=LA](http://www.eia.gov/state/print.php?sid=LA)) (Accessed 10 August 2021)
- [49] Global Administrative Areas 2018 GADM database of global administrative areas, version 3.6 (available at: [www.gadm.org](http://www.gadm.org)) (Accessed 16 December 2020)
- [50] Strobl E 2011 The economic growth impact of hurricanes: evidence from US coastal counties *Rev. Econ. Stat.* **93** 575–89
- [51] Hsiang S M and Jina A S 2014 The causal effect of environmental catastrophe on long-run economic growth: evidence from 6,700 cyclones *Technical Report* (National Bureau of Economic Research)

# The response to extremes under global economic stress

# 4

This article is under review in *Communications Earth and Environment* as:

R. Middelani, S. N. Willner, K. Kuhla, L. Quante, C. Otto, A. Levermann (2023). “Stressed economies respond more strongly to climate extremes”. In review at *Communications Earth and Environment*.

**ABSTRACT:** Economies experience stress for various reasons such as the global Covid-19 pandemic beginning in 2020. The associated lock-downs caused local economic losses and the disruption of international supply chains. In addition, such stress alters the effects of short-term shocks as caused by climate extremes, especially their propagation through the economic network and the resulting repercussions. Here we show that the combined adverse impacts of tropical cyclones, river floods, and heat stress on global consumption is strongly enhanced when the economy is under stress. This increase results from aggravated scarcity causing higher consumer prices. Modeling climate impacts during Covid-19, we find that in a stressed economy with the current network structure, consumption losses due to climate extremes double in the US and triple in China. The simulated effects intensify when climate shocks grow stronger. Our results emphasize the amplifying role of the interaction between climate change and its socioeconomic backdrop.

Emissions of greenhouse gases (GHG) due to human activity have increased Earth's mean temperature by more than 1°C compared to pre-industrial levels (IPCC 2021). As a result, intensity and frequency of extreme weather events have increased (Seneviratne et al. 2021; Robinson et al. 2021) with adverse impacts on society (IPCC 2022). Events like tropical cyclones (TCs) (Strobl 2011; Middelanis, Willner, Otto, Kuhla, et al. 2021), heat waves (Burke, Hsiang, and Miguel 2015), and river floods (Willner, Otto, and Levermann 2018) can hamper economic output, causing *direct* local economic shocks. This shock can propagate through the economic network (Acemoglu et al. 2012), resulting in indirect effects onto production, final consumption (simply consumption hereafter) and prices elsewhere (Hallegatte 2008; Middelanis, Willner, Otto, and Levermann 2022). Quantifying the total effect, that is, the sum of direct and indirect economic impacts, is a difficult task due to uncertainty associated with the direct shock as well as the resulting complex interactions in the economic network (Levermann 2014). For example, concurrency of multiple types of extreme events can reinforce their indirect impacts (Kuhla et al. 2021). Complexity is further increased through the interaction with a multitude of socio-economic factors that determine economic vulnerability and resilience (Cardona et al. 2012). Most studies assess indirect economic effects of climate extremes in an isolated fashion, not considering interaction with major concurrent socioeconomic events. However, global economic stress, induced by, e.g., major international conflicts and crises, may well reduce the economic capacity to cope with shocks induced by climate extremes.

In recent years, the most severe global economic shock resulted from the Covid-19 pandemic of 2020 and onward. Over 630 million confirmed cases and more than 6.5 million deaths globally have been reported to the World Health Organization (World Health Organization 2022). Most governments have taken a wide range of measures against the spreading of the virus. These unprecedented societal interruptions have taken their toll on economic activity (Deb et al. 2022). The gross domestic product (GDP) decreased globally by 3.3% in 2020 (World Bank 2010) with adverse effects on consumption (Martin et al. 2020; World Bank 2018). It has been shown that economic impacts from the pandemic propagated through disruption of the economic network (Verschuur, Koks, and Hall 2021; Guan et al. 2020; Bonadio et al. 2021; Pichler et al. 2022). Thus, the pandemic likely also altered the propagation of shocks from weather extremes. While most climate-related research on Covid-19 focuses on the accompanying beneficial reduction of GHG emissions (Forster et al. 2020; Le Quéré et al. 2021), little research exists on possible amplifications of adverse climate impacts through the pandemic.

We here assess how economies react to shocks from climate extremes when subjected to economic stress on a global scale, using the Covid-19 pandemic and its economic repercussions as an example for global stress. To this end, we use a global agent-based loss propagation model with myopic profit-optimizing producers (Otto et al. 2017), which simulates perturbations of quantities of trade, production, consumption, and their prices on the economic network (given by the EORA (Lenzen et al. 2012) multi-region input-



output table) in response to direct local economic shocks. The model computes the interaction of over 7,000 agents with more than 1.8 million trade links on a daily time scale.

Inspired by the storyline approach (Van den Hurk et al. 2023), we define a 'stressed economy' and an 'unstressed economy' scenario and simulate indirect economic impacts from climate extremes under both scenarios. The scenarios are defined by their respective *baselines*, i.e., an economic reference simulation without climate shocks. The unstressed baseline is a simulation with full economic capacity of all agents without stress impacts from the pandemic. In contrast to this, the stressed baseline experiences regionally decreased economic activity. Since the pandemic entails both a supply and demand shock (Rio-Chanona et al. 2020; Brinca, Duarte, and Faria-e-Castro 2020), both productive capacity and demand by final consumers are reduced for the stressed baseline. We derive this reduction in economic activity using the daily stringency index from the Oxford Covid-19 Government Response Tracker project (Hale et al. 2021) (methods, equation (1)), a compound indicator for the strictness of government measures in response to Covid-19. We calibrate the decrease in economic activity such that our model best reproduces observed GDP for the United States (US) and European Union (EU, 27 countries of the European Union as of 2020 after withdrawal of the United Kingdom) during the years 2020 and 2021 (Supplementary Figs. 1 and 2, Supplementary Tbl. 1).

Under both scenarios, we simulate global impacts on consumption induced by heat stress, river flooding, and TCs. We utilize an ensemble of 200 region and sector-specific production shock time series by Kuhla et al. 2021 based on projections of four CMIP5 global circulation models (GCMs) and representative concentration pathways 2.6 and 6.0. Regional heat stress-induced production reduction is based on empirical evidence (Hsiang 2010) of sector-dependent productivity loss linear to daily mean temperatures above 27°C. Further, production capacity is reduced in regions that experience floods or a TC wind speed above 64 kn. Flooded areas are derived from a river routing model (Yamazaki et al. 2011), driven by discharge time series from the used GCMs which are coupled with five hydrological models. Five wind field realizations are computed from a probabilistic TC emulator (Geiger, Frieler, and Bresch 2018; Geiger, Gütschow, et al. 2021) driven by the used GCMs. The resulting direct shocks directly limit productive capacity of exposed sectors and regions for the time of the disaster; final consumption is not directly affected. For more details see Kuhla et al. 2021 or methods.

We assess the impact of climate extremes on global consumption and prices under both scenarios with respect to their baselines. In this, different goods and services are aggregated across economic sectors (simply 'goods' in the following). All results are shown as mean values of the ensemble. Where provided, ensemble ranges denote the 66% range (the 16.7 and 83.3 percentiles). Aggregated numbers are aggregates over the two-year period of 2020 and 2021. Our simulations are conducted on a 2015 economic network and therefore, absolute values are in US dollars of this year.

## Consumption losses from climate extremes increase under global economic stress

We aggregate consumption losses for the EU, US, China (CHN), and the rest of the world (ROW). Lost consumption in response to climate extremes is the difference in consumption quantities to the respective scenario baseline consumption. Fig. 1 shows consumption losses for both scenarios (panel a) and the relative loss increase from the unstressed to the stressed scenario (panel b) as well as the regional absolute increase relative to the unstressed baseline consumption (panel c).

Globally, losses amount to \$314bn in the unstressed and \$430bn in the stressed scenario, hence an increase of 37%. In both cases, ROW shows the largest consumption losses, also when normalizing to baseline consumption (Supplementary Fig. 3). However, comparing between the scenarios, the impact of the global economic stress is strongest in the other regions, with consumption losses almost tripling in China, doubling in the US and increasing by 35% in the EU. This pronounced increase for the US and China persists when normalizing to the unstressed baseline consumption of these regions, showing that the increase of consumption losses is substantial. Hence, vulnerability to consumption losses from climate extremes is strongly increased in the US and China when the global economy is under stress. For example, while absolute consumption losses in the EU exceed those of the US in the unstressed scenario, they are about equal in the stressed case. Notably, there are also few ROW regions where consumption losses decrease with the stressed scenario (green regions in Fig. 1c). While these regions are better off in the stressed compared to the unstressed scenario, they are nonetheless among the regions with largest consumption losses in both cases.

## Loss increases result from amplified price response

In both scenarios, production capacity is reduced in regions that suffer from a direct climate shock. This has effects on both their demand and the supply they can provide as well as the prices charged for produced goods. Reduced production capacity can — to a certain extent — be compensated through production extension. In production extension, marginal production costs increase, resulting in higher prices of the supplied goods. The amount of lost production from the shock that is not compensated this way results in decreased supply on the downstream side and reduced demand for intermediate goods on the upstream side. Perturbations to the baseline are eventually passed on to final consumers in the form of prices who react by adjusting their purchasing behaviour. Through differing exposure to climate extremes as well as economic linkages, prices and price changes can be regionally heterogeneous, resulting in regionally different consumption behaviour. Fig. 2 shows the temporal evolution (panels a, c-f) of consumption price changes and the two-year average deviation (panel b) from the respective baseline price in response to the simulated climate extremes.



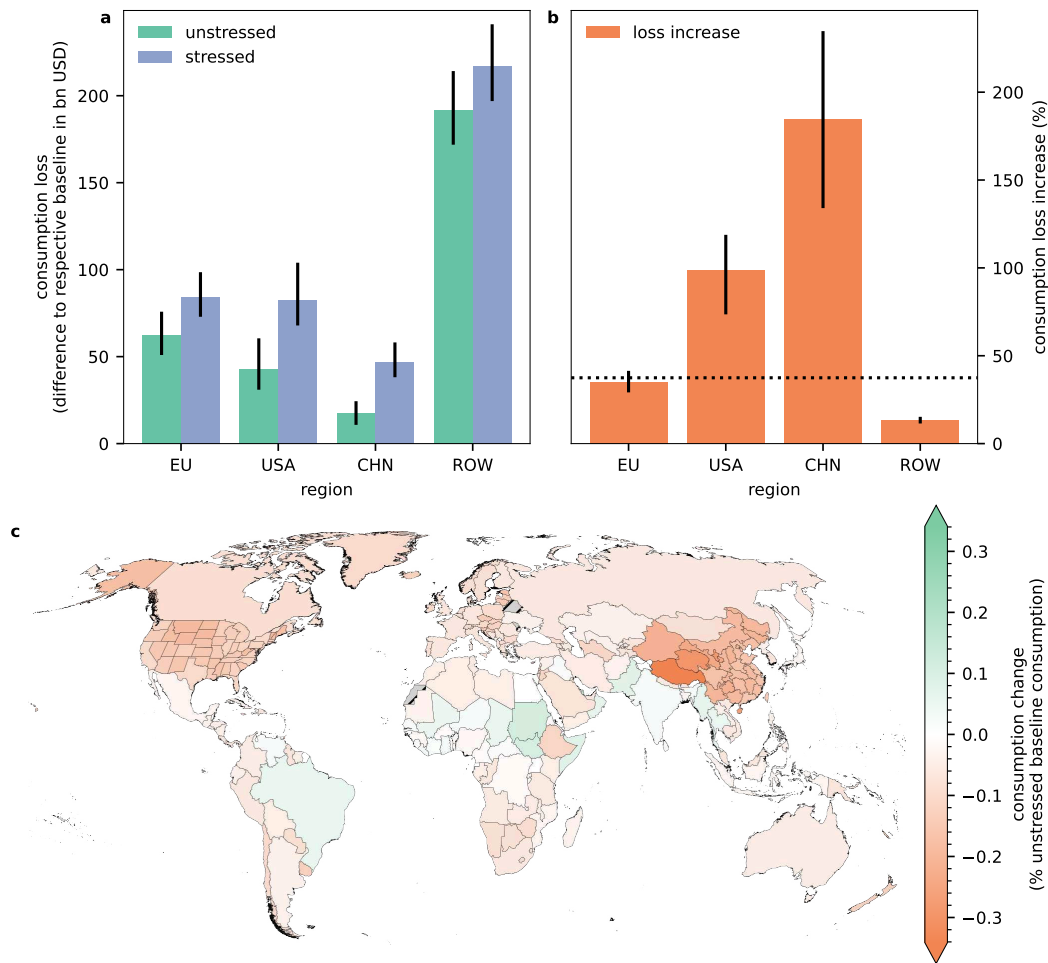


**Figure 1: Consumption losses from climate extremes intensify within a stressed economy.** (a) Climate extreme-induced absolute consumption losses for the EU, US, and China under unstressed and stressed scenario. (b) Stressed consumption loss increase relative to unstressed scenario: losses double in the US and triple in China. Dotted line denotes mean global loss increase. (c) Regional absolute consumption loss increase relative to unstressed baseline consumption, showing that loss increases especially in the US and China are substantial. Normalization to stressed baseline consumption yields similar results (Supplementary Fig. 4). All panels show ensemble means, error bars in panels a and b denote the 66% ensemble range. Grey regions with low data quality or without data.

All regions show seasonal price behaviour with peaks in the northern hemisphere summer, resulting from the seasonality in the climate extremes, in particular, heat stress. Globally, consumption prices increase by up to 1.8% in the stressed but only up to 1.3% in the unstressed scenario. Comparing price spikes of 2020 and 2021 reveals that this amplification abates with the global economic stress (dashed lines in Fig. 2a). The difference

of price increases ('price gap', difference of percentage points, "pp", price increase between scenarios) leads to larger consumption losses in the stressed scenario (Supplementary Fig. 5), rather than the absolute consumption prices. For example, the price gap for China is about 0.5pp, resulting in the largest consumption loss increase in the simulations (Fig. 1b). By contrast, ROW consumption prices in the stressed scenario are at the same level as those in China, but increase only slightly compared to the unstressed scenario. Therefore, consumption losses only increase moderately in ROW compared to other regions. However, it should be noted that ROW is only in a better position in a sense that the consumption loss increase between scenarios is small (Fig. 1b) and not with regards to absolute consumption losses. Put differently, adverse consumption impacts from climate extremes in ROW regions are strongest, but intensify least with global economic stress. The US and China show the opposite behaviour. Here, consumption losses are smallest but increase the most under global economic stress.

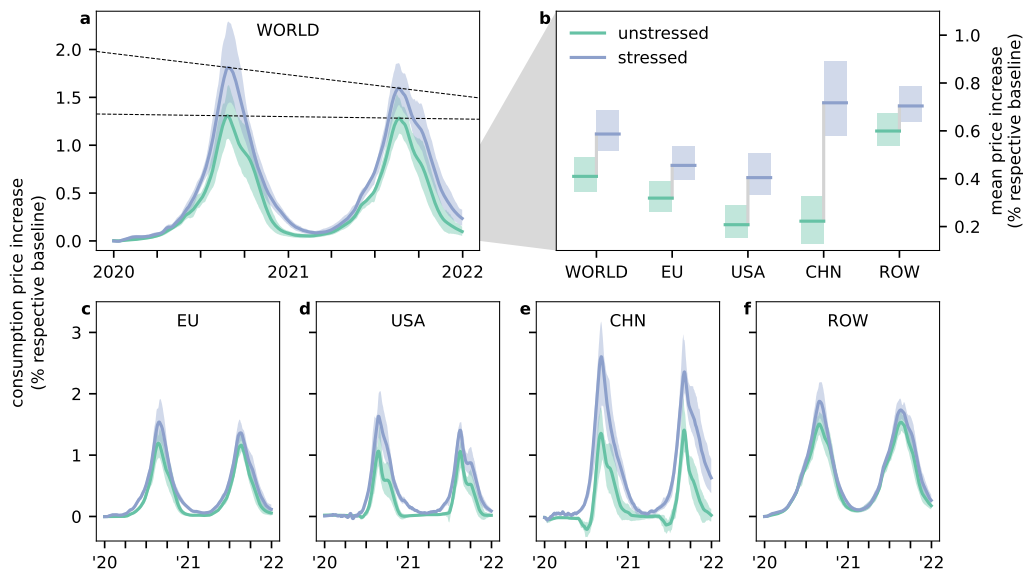


Figure 2: **Economic stress triggers more intense price response.** Mean consumption price increase across all consumed goods relative to respective baseline prices is shown for the unstressed and stressed scenarios (a) globally and for (c-f) the EU, US, China, and the rest of the world. (b) Temporally averaged price increases for the same regions across all goods consumed throughout the years 2020 and 2021. The difference of price increases between scenarios — the price gap — results in observed increases of consumption losses. Solid lines show the ensemble means, shaded areas denote the 66% ensemble range. Dashed lines in panel a show trends in the price peaks from the first and second year for both scenarios.

## Aggravated supply-demand mismatch leads to higher prices

Price increases result from scarcity of goods in response to production losses due to climate extremes. This scarcity emerges from a mismatch of supply and demand and it is resolved by prices. We calculate the difference in demand for intermediate production goods (firm-to-firm demand) to the respective baseline demand. We express the demand difference relative to the unstressed baseline demand, which yields the region-specific demand response to the climate extremes (Fig. 3a).

Regardless whether economies are under global stress or not, the same climate extremes evoke similar demand increases. However, in the stressed scenario, production capacity is globally hampered. With a similar increase in demand, yet lower capacity to supply goods, the imbalance between supply and demand is stronger than in the unstressed scenario. To fulfill the same demand, economies would need to extend their production beyond baseline levels further than in the unstressed case. This aggravated supply-demand mismatch is resolved by a stronger price signal and final consumers cut their consumption according to their price elasticities. Since final consumption is primarily satisfied domestically (Supplementary Fig. 6), the demand responses have a strong influence on regional consumption prices. Simulated consumption loss increases correspond to regional demand responses (Fig. 1b, Fig. 3a); China and the US, where consumption losses increase most with the stressed scenario, exhibit the strongest demand responses.

In the globalized economic network, demand for intermediate production goods is not only satisfied domestically but it is also directed to other regions, globally. Therefore, while demand responses are generally reactions to climate extremes, on a regional level, they can be more specifically a reaction to climate shocks both locally and elsewhere, with an indefinite number of involved trade links. A region's vulnerability to consumption losses from climate extremes thus not only depends on how its economy can cope with local direct climate shocks, but also how it reacts to shocks of trade partners. Fig. 3b displays the direct and weighted remote climate shocks. The direct shock is expressed as the share of global unstressed baseline production that is locally obstructed due to climate extremes. The weighted remote shock for a region (methods, equation (4)) is the average over all other regions' direct shocks, weighted with the trade volume (imports and exports) with these regions. As such, it only includes direct supplier-buyer relationships, tier one, as a first-order measure for indirect shocks from trade partners. Note that we here show shock magnitudes under the unstressed scenario, and that there is small variation between scenarios because global economic stress due to the pandemic is regionally heterogeneous. However, differences are small and lie well within ensemble uncertainty (Supplementary Fig. 7). While the EU, US, and China are economically strongly interlinked, the remaining ROW regions are a large and not structurally coherent group of countries. Therefore, ROW trade volumes should be interpreted with care and shocks are only shown for the sake of completeness.

The direct climate shock is small in the EU, compared to the other regions. The US and China show stronger direct shocks, with the shock in China about twice as strong as in the US. The weighted remote shock is pronounced for all three regions due to overall large direct shocks in ROW. It is strongest in the EU, due to the significant direct shocks in the US and China. The computed demand response in the EU therefore results to a large extent from shocks to its trade partners. Possibly, buyers from affected regions switch to the EU as a supplier, requiring the EU to ramp up production and, in turn, demand. Simultaneously, EU demand that is usually directed to affected regions cannot be completely fulfilled anymore, further increasing scarcity. In the US and China, also direct shocks are significant. These two regions — due to geographical exposure to hazards and exposure in the economic network to weighted remote shocks — experience the strongest aggravation of scarcity among scenarios, resulting in the largest price and consumption difference between scenarios.

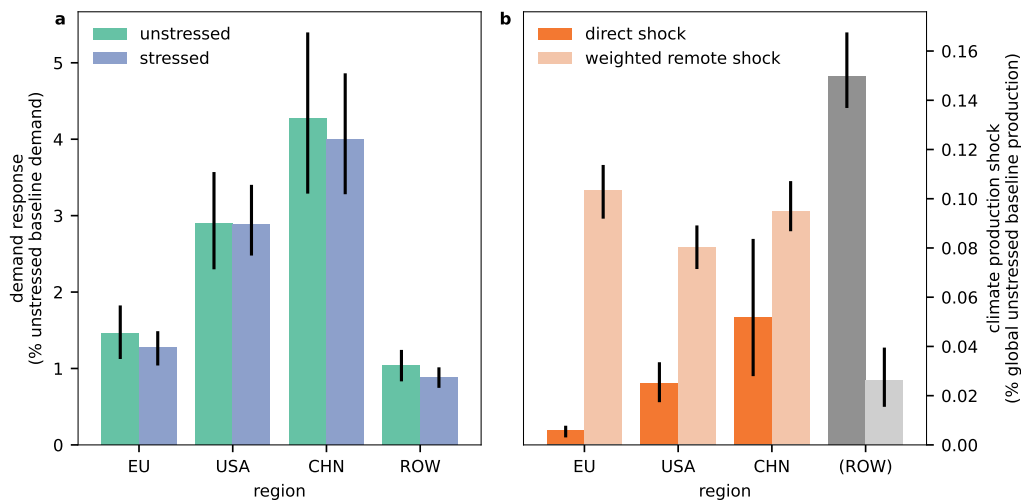


Figure 3: **Demand responses to direct and weighted remote shocks are similar between scenarios. (a)** Demand response for the EU, the US, China and the rest of the world to the simulated climate extremes under both scenarios, expressed in percent of unstressed baseline consumption to obtain identical scales of quantities. **(b)** Direct and weighted remote shock for the same regions in the unstressed scenario. Shock magnitudes are similar for the stressed scenario but vary slightly within ensemble uncertainty due to regional heterogeneity of the global economic stress (Supplementary Fig. 7). Values for ROW are shown for completeness but should be interpreted with care due to the large number of aggregated regions. Error bars denote the 66% ensemble range.

## Price gap increases with stronger climate shocks

Exposure to direct and weighted remote shocks changes with spatial and temporal variability within the ensemble of simulated climate extremes. While both shock types are correlated (Supplementary Fig. 8), their difference in magnitudes across the considered regions (Fig. 3b) suggests individual effects. Fig. 4 shows the price gap between the scenarios in relation to the direct and weighted remote climate shock magnitude. Shocks are normalized to global unstressed baseline production, but results are similar when normalizing shocks to global stressed production (Supplementary Fig. 9). Again, ROW is only shown for completeness and should be interpreted carefully, especially with regards to the weighted remote shock.

With more intense direct and weighted remote climate shocks, the price gap widens in the EU, the US, and China. Importantly, this does not merely indicate an increase in consumption losses with stronger climate extremes. Moreover, it entails a stronger amplification of consumption losses between scenarios, which again results from an aggravated supply-demand mismatch. However, unlike the change between scenarios, the increased scarcity with stronger climate extremes does not result from altered supply capacity. Varying the intensity of climate shocks evokes demand response changes (Supplementary Fig. 10), causing larger price gaps with stronger shocks. Hence, while global economic stress affects the supply-side of the supply-demand mismatch, the strength of climate extremes affects its demand-side. This effect on the demand response is regionally heterogeneous and differs between direct and weighted remote shock, which suggests different regional vulnerability (in terms of consumption price reaction) with regards to changes in the two climate shock types. For example, the price gap increase is most pronounced for the US with regards to the direct climate shock, while China exhibits the strongest reaction to a variation of the weighted remote climate shock.

## Discussion

Our findings show that regional economies are more vulnerable to consumption losses from climate extremes when the global economy is under stress, as simulated here with the example of the Covid-19 pandemic. The simulated loss increases result from stronger price responses to climate extremes in the stressed scenario. Under global economic stress, economies have less production capacity and thus, scarcity emerging from lost production due to the climate extremes is more pronounced. This leads to higher prices of final consumption and decreases in consumed quantities. Thus, while the pandemic had temporary (Tollefson 2021) mitigating effects through reduction of greenhouse gases, it nonetheless reinforced adverse economic ramifications of climate change.

In this study, we cover one (economic) dimension of how a global pandemic can amplify adverse repercussions from climate extremes, not taking into account other possible impacts. For example, loss of life from climate extremes could be influenced by the

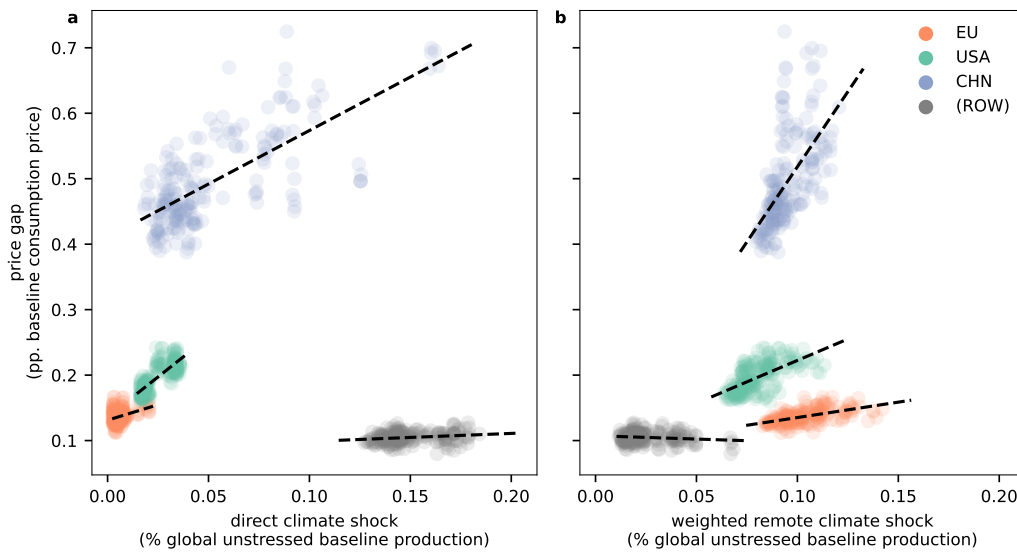


Figure 4: **Price gap increases with climate shock intensity.** Price gap for the EU, US, China and rest of the world **(a)** with regards to the direct climate shock and **(b)** the weighted remote climate shock, expressed as share of unstressed global baseline production. Normalization to stressed baseline production yields similar results ([Supplementary Fig. 9](#)). Points represent individual simulations from the ensemble, dashed lines are linear fits. Values for ROW are shown for completeness but should be interpreted with care due to the large number of aggregated regions.

pandemic due to stress exerted on health care systems. However, restricting our focus to economic impacts, we argue that the effects shown here likely also apply to other crises that globally reduce economic activity.

Due to the uncertainty of future global economic stressors and structure of the economic network, we refrained from simulating scenarios under future climate conditions. However, with likely increasing number ([Rahmstorf and Coumou 2011](#); [Coumou and Rahmstorf 2012](#)) and intensity ([Seneviratne et al. 2021](#)) of weather extremes with climate change, the effects computed here are also likely to intensify in the absence of adaptation. This expectation is substantiated with our finding of responses to more intense climate extremes, both locally and remote.

Using the stringency index necessarily introduces uncertainties in the economic stress due to the pandemic. Not all factors of government strictness that determine economic activity can be included in a single index and economies react differently to restrictions. However, our calibration to observed GDP warrants that the overall global economic stress situation is well reproduced. Remaining uncertainties can be justified, given that Covid-19 serves predominantly as an example of global economic stress and we do not focus on

specific conditions of this pandemic. Similarly, the modeling chain of climate extremes as well as necessary assumptions on the economic behaviour of agents in our model add to the uncertainty of the results. Nonetheless, such micro-economic assumptions on agent behaviour are useful to model macro-economic behaviour (Farmer and Foley 2009). In this, we stress the qualitative nature of our results regarding the underlying economic effects.

Many previous studies have investigated propagation of climate impacts in the economic network. Furthermore, the need for analyses of impacts from consecutive disasters, including the spreading of diseases, has been raised (de Ruiter et al. 2020). Our study addresses this need, thus adding on the literature of indirect impacts from climate extremes. We show that adverse effects from climate extremes are amplified by global economic stress. At the same time, this amplification is enhanced by stronger climate extremes. This mutual impact reveals that cause and effect of interacting disasters are not easily disentangled, adding an additional layer of complexity to the assessment of total impacts from climate extremes. We therefore stress the importance of further research focusing on the superposition of multiple crises.

Overall, our study shows that mitigation of and adaptation to climate risks not only entails the protection of regions prone to hazards. Moreover, also the protection against shocks originating in other regions through resilient trade relations is necessary. In any case, the full impact of disasters can only be assessed by including the broader economic and societal backdrop against which the extremes unfold.



## Methods

### Economic model

We conduct our simulations using the agent-based global loss propagation model *Acclimate* (Otto et al. 2017). As an anomaly model it simulates the dynamics of deviations in trade, production, consumption, and prices from an economic equilibrium in response to local economic shocks, which are characterized by time-dependent reduction in economic activity (i.e., production or final consumption). The equilibrium is given by a multi-regional input-output table. Agents represent economic sectors on a regional level. They locally maximize their profit on a daily basis, adjusting production and supply distribution according to prices and incoming demand. The model design allows for a disequilibrium of demand and supply (resulting in price changes), enabling simulation of shocks on short and medium time scales. An economic shock is modeled as a time-dependent reduction in productive capacity of individual agents, represented by a factor  $0 \leq f(t) \leq 1$ . To avoid possible artifacts from the simulation start, all simulations are preceded by a transient artificial global shock of 2.5% to all agents for ten days and subsequent return to equilibrium for 90 days.

### Economic data

As economic equilibrium for the *Acclimate* model, we use the EORA multi-region input-output table (Lenzen et al. 2012) of the year 2015. We disaggregate (Wenz et al. 2015) the United States (US) and China into states and provinces using subnational GDP for the year 2015 on a state (Bureau of Economic Analysis 2017) and province (National Bureau of Statistics of China 2017) level as a proxy. In total, we thus resolve 268 regions with 26 producing sectors and the final consumption sector, resulting in over 7,000 agents with more than 1.8 million trade relations. Data for Belarus is excluded from all analyses due to low data quality.

We use historical GDP for the United States and European Union (EU, 27 countries of the European Union as of 2020 after withdrawal of the United Kingdom) for the years 2010 through 2021. US seasonally adjusted quarterly GDP is obtained from the Federal Reserve Bank of St. Louis (Bureau of Economic Analysis 2022). EU seasonally and calendar adjusted quarterly GDP is retrieved from Eurostat (Eurostat 2022). GDP data are linearly detrended for the two years preceding the pandemic (i.e., 2018 and 2019), using the `detrend` function from the `scipy.signal` Python package (Supplementary Fig. 2a). Losses in GDP are then expressed as percentage deviations from this trend during the years 2020 and 2021 (Supplementary Fig. 2b). Detrending is necessary because our model does not endogenously simulate economic growth.



## Scenario definition

We define an unstressed and a stressed scenario, denoted with the superscripts  $(\cdot)^-$  and  $(\cdot)^+$  in the following. These scenarios define the economic backdrop against which changes of final consumption resulting from climate extremes are simulated. Both scenarios have an economic reference simulation, or 'baseline', denoted by  $(\cdot)^{ref-}$  and  $(\cdot)^{ref+}$ , respectively. Economic shocks under both scenarios are defined as time-dependent factors  $f$  by which economic activity of a specific agent is reduced. In the unstressed case, the reference  $ref-$  is a simulation with only the transient shock and no climate or COVID-related disturbance, i.e.  $f^{ref-}(t) := f^{transient}(t)$ . The stressed reference  $ref+$  is a simulation with only the transient and COVID production shock, hence  $f^{ref+}(t) := f^{transient}(t) \cdot f^{covid}(t)$ . Under both scenarios, we simulate a climate shock ensemble by applying the climate production shock in addition to the baseline, i.e.  $f^-(t) := f^{ref-}(t) \cdot f^{climate}(t)$  and  $f^+(t) := f^{ref+}(t) \cdot f^{climate}(t)$ . We simulate 200 realizations of climate extreme production shocks, resulting in a total of 402 simulations including the baseline simulation runs.

## Global economic stress

We use a simple but reasonable approach to derive the stressed baseline. This baseline is defined by the time-dependent factor  $f_a^{covid}$  by which economic activity of agent  $a$  is reduced due to the global economic stress resulting from the pandemic. We use the stringency index from the Oxford Covid-19 Government Response Tracker project (Hale et al. 2021) which combines a total of 9 indicators into a single index that represents the stringency of government containment and closure responses ('lockdown policies'), bounded between 0 and 100. It is available for a total of 186 countries with subnational resolution for some countries, including the United States (state-level) and China (province-level). The used indicators (school closures, workplace closing, cancellation of public events, restrictions on gatherings, public transportation, stay at home order, restrictions on internal movement, international travel controls, and public information campaigns) are normalized to values between 0 and 100 and then averaged to obtain the overall stringency index (see Hale et al. 2021 for more details). While the stringency index is continually calculated also beyond the year 2021, we limit our analysis to the years 2020 and 2021 to set a focus on the period of strongest restrictions and economic stress.

We use the most recent implementation of the 'average stringency index' that incorporates differences in policies for vaccinated and non-vaccinated people. Where available, population shares of (non)-vaccinated people are used as weights to calculate the average stringency (otherwise both are equally weighted). Since this new implementation was not available for Chinese provinces at the time we conducted our research, we resort to the legacy stringency for Chinese provinces.

We derive the factor  $f_a^{covid}$  by which economic activity of agent  $a$  is reduced due to the global economic stress, by convolving first difference of the stringency,  $\Delta s$ , with a response function  $r$ . Note that all agents, both producing agents and final consumption, are affected in this way, because the pandemic entails both a supply and demand shock (Rio-Chanona et al. 2020; Brinca, Duarte, and Faria-e-Castro 2020). The convolution reads

$$\begin{aligned} f_a^{covid}(t) &= \max \{0, \min \{1, 1 - (\Delta s_a * r)(t)\}\} \\ &= \max \left\{ 0, \min \left\{ 1, 1 - \sum_{k=0}^t \Delta s_a(k) \cdot r(t-k) \right\} \right\}, \end{aligned} \quad (1)$$

where  $s_a$  is the stringency in agent  $a$ 's region and  $t$  is the number of days since 01 Jan 2020. We use the same exponential response function for all agents, given by

$$r(t) = \alpha \cdot e^{-t/\tau}. \quad (2)$$

This approach implies a shock of strength  $\alpha \cdot \Delta s$  with each change in stringency and subsequent exponential decay of this individual shock with time constant  $\tau$ . In this, we assume that economies reduce (increase) their economic activity whenever the stringency increases (decreases) and that economies adapt to these changes over time. We set the condition  $0 \leq f^{covid} \leq 1$ , assuming that adaptation does not lead to increased economic activity compared to unstressed levels on the regarded time scales.

Parameters  $\alpha$  and  $\tau$  are calibrated using the *Acclimate* model such that the deviations in quarterly gross domestic product (GDP) from equilibrium best reproduce the observed decrease in GDP for the US and the EU during the years 2020 and 2021. GDP for these regions represents over 40% of global GDP (World Bank 2014) and is available at relatively high temporal resolution (quarters). From a set of model runs with  $\alpha \in [0.15, 0.16, \dots, 0.25]$  and  $\tau \in [6, 9, 12, 15, 18]$  months, the parameter set ( $\alpha = 0.22, \tau = 9$ ) is chosen (highlighted in [Supplementary Fig. 1](#)) as the set with lowest mean squared error (MSE) to historical GDP deviation ([Supplementary Tbl. 1](#)).

## Climate extremes production shock

For the economic shock of climate extremes, given by the share of production capacity that remains during the hazards,  $f_a^{climate}(t) \in [0, 1]$ , we use sector-specific daily productivity reduction factors for compound climate extremes in the years 2020 and 2021 by Kuhla et al. 2021. We here give a brief description of this factor while we refer to Kuhla et al. 2021 for full detail. The used factor comprises productivity reduction of producing agents due to heat stress, river flooding, and tropical cyclones, globally. It builds on

representative concentration pathways (RCPs) projections 2.6 and 6.0 from four CMIP5 general circulation models (GCMs) which have been bias-corrected (Hempel et al. 2013) within phase 2b of the ISIMIP project (Frieler et al. 2017). We choose GCM runs driven by two different RCPs to obtain a larger ensemble and thus capture climate variability and model uncertainty. Since projections of the models for the considered time span are largely determined by historic emissions, differences between RCPs are within model uncertainty.

The share of productive capacity that is lost due to each disaster category is first estimated on a grid level. For heat stress, a linear empirical relationship (Hsiang 2010) of productivity and temperatures above 27°C is used. Flooded areas are computed by a river routing model (Yamazaki et al. 2011) which is driven by outputs from five hydrological models within the ISIMIP2b framework coupled with each projection of the four GCMs. For tropical cyclones (TC), a probabilistic TC emulator (Geiger, Frieler, and Bresch 2018; Geiger, Gütschow, et al. 2021) is driven by the used GCM projections to produce five TC realizations for each GCM projection. Cells exposed to a wind speed above 64kn or flooding are considered non-productive (i.e., the share production capacity lost due to the disaster is set to one) as long as the hazard persists, with subsequent exponential recovery.

A cell's overall loss in production capacity is then calculated as the sum over the shares of production lost due to the three individual disaster categories, with the constraint that the sum cannot exceed one. Population-weighted averaging over grid cells yields the production capacity loss of an entire region. The difference of this loss share to one is the remaining production capacity.

Using four GCMs with two RCPs, driving five hydrological models and five TC realizations yields an ensemble of  $4 \times 2 \times 5 \times 5 = 200$  climate production shocks.

We compute the direct shock  $F_r$  of region  $r$  as the share of global production that is lost within this region due to the climate extremes as

$$F_r = \frac{\sum_{t=0}^T \sum_{a \in R} (f_a^{ref}(t) - f_a(t)) X_a^*(t)}{\sum_{t=0}^T \sum_{a \in A} X_a^{ref}(t)}, \quad (3)$$

with  $R$  the set of agents in region  $r$ ,  $A$  the set of all agents,  $X^*$  the production in equilibrium, and  $X^{ref}$  the production in the respective reference scenario. The weighted remote shock  $\hat{F}_r$  is calculated as the average over all other regions' direct shock, weighted with the trade volume with these regions:

$$\hat{F}_r = \frac{\sum_{r' \neq r} F_{r'} * t(r, r')}{\sum_{r' \neq r} t(r, r')}, \quad (4)$$

where  $t(r, r')$  is the trade volume between region  $r$  and  $r'$ .

## References

- Acemoglu, D. et al. (2012). “The network origins of aggregate fluctuations”. In: *Econometrica* 80.5, pp. 1977–2016.
- Bonadio, B. et al. (2021). “Global supply chains in the pandemic”. In: *Journal of international economics* 133, p. 103534.
- Brinca, P., J. B. Duarte, and M. Faria-e-Castro (2020). “Is the COVID-19 pandemic a supply or a demand shock?” In: *Available at SSRN 3612307*.
- Bureau of Economic Analysis (2017). *Gross domestic product (GDP) by state*. Accessed on 07 Jul 2017.
- (2022). *Gross Domestic Product [GDP]*. retrieved from FRED, Federal Reserve Bank of St. Louis. Accessed on 02 Aug 2022.
- Burke, M., S. M. Hsiang, and E. Miguel (2015). “Global non-linear effect of temperature on economic production”. In: *Nature* 527.7577, pp. 235–239.
- Cardona, O. D. et al. (2012). “Determinants of risk: exposure and vulnerability”. In: *Managing the risks of extreme events and disasters to advance climate change adaptation: special report of the intergovernmental panel on climate change*. Cambridge University Press, pp. 65–108.
- Coumou, D. and S. Rahmstorf (2012). “A decade of weather extremes”. In: *Nature climate change* 2.7, pp. 491–496.
- de Ruiter, M. C. et al. (2020). “Why we can no longer ignore consecutive disasters”. In: *Earth’s future* 8.3, e2019EF001425.
- Deb, P. et al. (2022). “The economic effects of COVID-19 containment measures”. In: *Open Economies Review* 33.1, pp. 1–32.
- Eurostat (2022). *GDP and main components (output, expenditure and income) [NAMQ\_10\_GDP]*. Accessed on 02 Aug 2022.
- Farmer, J. D. and D. Foley (2009). “The economy needs agent-based modelling”. In: *Nature* 460.7256, pp. 685–686.
- Forster, P. M. et al. (2020). “Current and future global climate impacts resulting from COVID-19”. In: *Nature Climate Change* 10.10, pp. 913–919.
- Frieler, K. et al. (2017). “Assessing the impacts of 1.5 C global warming—simulation protocol of the Inter-Sectoral Impact Model Intercomparison Project (ISIMIP2b)”. In: *Geoscientific Model Development* 10.12, pp. 4321–4345.
- Geiger, T., K. Frieler, and D. N. Bresch (2018). “A global historical data set of tropical cyclone exposure (TCE-DAT)”. In: *Earth System Science Data* 10.1, pp. 185–194.
- Geiger, T., J. Gütschow, et al. (2021). “Double benefit of limiting global warming for tropical cyclone exposure”. In: *Nature Climate Change* 11.10, pp. 861–866.
- Guan, D. et al. (2020). “Global supply-chain effects of COVID-19 control measures”. In: *Nature human behaviour* 4.6, pp. 577–587.

- Hale, T. et al. (2021). “A global panel database of pandemic policies (Oxford COVID-19 Government Response Tracker)”. In: *Nature Human Behaviour* 5.4, pp. 529–538.
- Hallegatte, S. (2008). “An adaptive regional input-output model and its application to the assessment of the economic cost of Katrina”. In: *Risk Analysis: An International Journal* 28.3, pp. 779–799.
- Hempel, S. et al. (2013). “A trend-preserving bias correction—the ISI-MIP approach”. In: *Earth System Dynamics* 4.2, pp. 219–236.
- Hsiang, S. M. (2010). “Temperatures and cyclones strongly associated with economic production in the Caribbean and Central America”. In: *Proceedings of the National Academy of sciences* 107.35, pp. 15367–15372.
- IPCC (2021). “Changing State of the Climate System”. In: *Climate Change 2021: The Physical Science Basis. Contribution of Working Group I to the Sixth Assessment Report of the Intergovernmental Panel on Climate Change*. Cambridge, United Kingdom and New York, NY, USA: Cambridge University Press, pp. 287–422. [10.1017/9781009157896.004](https://doi.org/10.1017/9781009157896.004).
- (2022). *Climate Change 2022: Impacts, Adaptation and Vulnerability. Contribution of Working Group II to the Sixth Assessment Report of the Intergovernmental Panel on Climate Change*. Cambridge, UK and New York, USA: Cambridge University Press.
- Kuhla, K. et al. (2021). “Ripple resonance amplifies economic welfare loss from weather extremes”. In: *Environmental Research Letters* 16.11, p. 114010.
- Le Quéré, C. et al. (2021). “Fossil CO<sub>2</sub> emissions in the post-COVID-19 era”. In: *Nature Climate Change* 11.3, pp. 197–199.
- Lenzen, M. et al. (2012). “Mapping the structure of the world economy”. In: *Environmental science & technology* 46.15, pp. 8374–8381.
- Levermann, A. (2014). “Climate economics: Make supply chains climate-smart”. In: *Nature* 506.7486, pp. 27–29.
- Martin, A. et al. (2020). “Socio-economic impacts of COVID-19 on household consumption and poverty”. In: *Economics of disasters and climate change* 4.3, pp. 453–479.
- Middelanis, R., S. N. Willner, C. Otto, K. Kuhla, et al. (2021). “Wave-like global economic ripple response to Hurricane Sandy”. In: *Environmental Research Letters* 16.12, p. 124049.
- Middelanis, R., S. N. Willner, C. Otto, and A. Levermann (2022). “Economic losses from hurricanes cannot be nationally offset under unabated warming”. In: *Environmental Research Letters* 17.10, p. 104013.
- National Bureau of Statistics of China (2017). *Gross Regional Product by Province*. Accessed on 07 Jul 2017.
- Otto, C. et al. (Oct. 2017). “Modeling loss-propagation in the global supply network: The dynamic agent-based model acclimate”. In: *Journal of Economic Dynamics and Control* 83, pp. 232–269. [10.1016/j.jedc.2017.08.001](https://doi.org/10.1016/j.jedc.2017.08.001).
- Pichler, A. et al. (2022). “Forecasting the propagation of pandemic shocks with a dynamic input-output model”. In: *Journal of Economic Dynamics and Control* 144, p. 104527.

- Rahmstorf, S. and D. Coumou (2011). “Increase of extreme events in a warming world”. In: *Proceedings of the National Academy of Sciences* 108.44, pp. 17905–17909.
- Rio-Chanona, R. M. del et al. (2020). “Supply and demand shocks in the COVID-19 pandemic: An industry and occupation perspective”. In: *Oxford Review of Economic Policy* 36.Supplement\_1, S94–S137.
- Robinson, A. et al. (2021). “Increasing heat and rainfall extremes now far outside the historical climate”. In: *npj Climate and Atmospheric Science* 4.1, pp. 1–4.
- Seneviratne, S. et al. (2021). “Chapter 11: Weather and climate extreme events in a changing climate”. In: *Climate Change 2021: The Physical Science Basis. Contribution of Working Group I to the Sixth Assessment Report of the Intergovernmental Panel on Climate Change*. Ed. by V. Masson-Delmotte et al. Cambridge, United Kingdom and New York, NY, USA: Cambridge University Press. Chap. 11, pp. 1513–1766. [10.1017/9781009157896.013](https://doi.org/10.1017/9781009157896.013).
- Strobl, E. (2011). “The economic growth impact of hurricanes: Evidence from US coastal counties”. In: *Review of Economics and Statistics* 93.2, pp. 575–589.
- Tollefson, J. (2021). “COVID curbed 2020 carbon emissions-but not by much”. In: *Nature* 589.343.
- Van den Hurk, B. et al. (2023). “Climate impact storylines for assessing socio-economic responses to remote events”. In: *Climate Risk Management*. In press.
- Verschuur, J., E. E. Koks, and J. W. Hall (2021). “Observed impacts of the COVID-19 pandemic on global trade”. In: *Nature Human Behaviour* 5.3, pp. 305–307.
- Wenz, L. et al. (2015). “Regional and sectoral disaggregation of multi-regional input–output tables—a flexible algorithm”. In: *Economic Systems Research* 27.2, pp. 194–212.
- Willner, S. N., C. Otto, and A. Levermann (2018). “Global economic response to river floods”. In: *Nature Climate Change* 8.7, pp. 594–598.
- World Bank (2010). *annual GDP growth*. Accessed 11 Nov 2022.
- (2014). *GDP (current USD)*. Accessed 02 Dec 2022.
- (2018). *annual final consumption expenditure growth*. Accessed 02 Jan 2023.
- World Health Organization (2022). *WHO COVID-19 Dashboard*. Accessed 11 Nov 2022. Geneva.
- Yamazaki, D. et al. (2011). “A physically based description of floodplain inundation dynamics in a global river routing model”. In: *Water Resources Research* 47.4.

# The utility maximizing consumer

# 5

This article has been submitted to *Nature Human Behaviour* as:

L. Quante, , C. Otto, S. N. Willner, R. Middelanis, A. Levermann (2023). “Under economic stress rational behavior may yield increased consumption of pricier goods”. Submitted to *Nature Human Behaviour*.

**ABSTRACT:** The behavior of consumers is one of the elementary market forces. Thus, changes in consumed quantity in response to changing prices are an important determinant of economic behavior. Here, we show analytically under minimal assumptions that in an out-of-equilibrium market it can be rational to buy more of a good in spite of increasing prices. When rational consumers maximize their utility, consumption is driven by two factors, the relative price change of goods and their substitutability. Influenced by heterogeneous prices between suppliers and goods, the budget-driven preference for goods with the least price increase is competing with the utility-driven substitution of goods. This leads to a stabilizing feedback loop emerging from any utility function that is strictly monotonically increasing. We illustrate this feedback dynamics in an agent-based model with utility-optimizing consumers under regionally heterogeneous weather-induced supply failures. The resulting relation between changes in prices and quantities are predominantly in line with macro economic observations, but a positive correlation between price and quantity emerges in out-of-equilibrium situations. Thus, in a stressed economy rational consumers might buy more of pricier goods in spite of budget constraints.



## Introduction

A major goal of economic science is the bridging of the micro-macro gap by explaining macroeconomic observations based on microeconomic processes. Here, price elasticity as a determinant of consumer behavior is an important link connecting the microeconomic decisions of consumers with their macroeconomic outcomes. Consumption price elasticity measures the relation between changes of consumed quantity and changes in prices, i. e. negative price elasticity corresponds to the standard case of reducing consumption with increasing prices, i. e. the consumed quantity of a good is negatively correlated to its price, while positive price elasticity indicates increased consumption in spite of increasing prices, i. e. the consumed quantity of a good is positively correlated to its price.

Global economic stress situations like the financial crisis 2007–2009 [Claessens et al. 2010](#); [Mishkin 2011](#) or the global supply chain disruptions during the COVID-19 pandemic [Guan et al. 2020](#); [Bonadio et al. 2021](#) induce a complex response from the global economic system. But also more localized impact channels disrupt economic activity — e. g., local epidemic outbreaks [Siu and Wong 2004](#); [Beutels et al. 2009](#) or extreme weather events — and can have global repercussions [Hallegatte et al. 2011](#); [Willner, Otto, and Levermann 2018](#); [Kuhla, Willner, Otto, Geiger, et al. 2021](#); [Middelani et al. 2021](#).

Empirical studies are often hampered by ample confounding factors rendering the observation of time evolution in price elasticities difficult. This challenge can only be tackled by large-scale field experiments as, for instance, conducted by [Jensen and Miller](#) in their study showing evidence of Giffen good behavior in a real world setting [Jensen and Miller 2008](#) distributing vouchers for necessities in two Chinese provinces. Gaining a better theoretical understanding on the formation of price elasticities is, thus, an important factor to consider. However, there is little model-based research into price elasticity, one example being a study by [He et al.](#) on the case of electricity markets based on a CGE model [He et al. 2011](#).

In this study, we focus on analyzing the dynamic behavior of consumption price elasticity in response to economic stress, i. e. non-equilibrium situations induced by extreme weather events. To this end, we study the economic repercussions of extreme weather events as local events that can be regionally [Kornhuber et al. 2018](#) or seasonally [Pfleiderer et al. 2019](#) synchronized and cause global economic repercussions [Willner, Otto, and Levermann 2018](#). Since under ongoing global warming, extreme weather events become more frequent and intense [Masson-Delmotte et al. 2021](#), a better understanding of their economic repercussions is quintessential to address adaptation and mitigation challenge [Pörtner et al. 2022](#). Adding to more traditional approaches using integrated assessment models (IAMs) or econometrics, agent-based modeling of the economics of climate change is an important complementary approach. Examples of use include agent-based IAMs [Lamperti et al. 2020](#) or agent-based supply chain models [Hallegatte 2008](#) to analyze global

effects under climate stress Hallegatte et al. 2011. In the numerical experiments in this study, we use the global agent-based supply chain model *Acclimate* Otto et al. 2017. Allowing to describe the out-of-equilibrium dynamics in the aftermath of economic shocks, it has already been applied to analyze the propagation of indirect losses induced by extreme weather events in the global supply network Willner, Otto, and Levermann 2018; Kuhla, Willner, Otto, Wenz, et al. 2021; Kuhla, Willner, Otto, Geiger, et al. 2021; Middelanis et al. 2021. We here present a substantially extended version of the model. Going beyond the (rather strong but common) assumption of constant price elasticities, we introduce a utility maximization principle for consumers that allows for an endogenous description of time varying price elasticities emerging for the internal market dynamics. We show that, during the out-of-equilibrium transition phase in the aftermath of economic shocks, positive price elasticities can emerge entailing a self-stabilizing feedback mechanism that drives the economy back into equilibrium. We further provide an analytical description of this feedback mechanism in a simplified model for a rational utility maximizing consumer where the dynamics of price elasticities arise from the relative price changes of goods as well as from their substitutability. We finally show that the simplified analytical model can quantitatively reproduce the *market emerging elasticities* of the complex *Acclimate* model.

## Results

A common way of modeling a consumer's decision is defining a utility function  $U(x_1, \dots, x_N)$  depending on the consumption of  $N$  goods  $x_i, i = 1, \dots, N$  and constrained by a budget  $B$ . The consumer's choice of a set of goods  $(x_1, \dots, x_N)$  is now made by maximizing the utility given by  $U(x_1, \dots, x_N)$ . To align our analysis with the anomaly modeling of *Acclimate*, we refer — without loss of generality — to the undisturbed state of the economy as 'baseline' in the following analysis. We assume that the consumer's budget  $B \equiv B^*$  is constant at baseline level with

$$B^* = \sum_{i=1}^N x_i^* = \sum_{i=1}^N p_i x_i, \quad (1)$$

where  $p_i$  denotes prices relative to the baseline,  $x_i^*$  baseline consumption, and  $x_i$  current consumption of good  $i$ . Thus increased spending for one good necessitates reduced spending for all other goods and vice versa. Using Lagrangian multiplier optimization leads to the following set of equations for any utility function  $U(x_1, \dots, x_N)$ :

$$\frac{\partial U}{\partial x_i} = \lambda p_i x_i \forall i \in 1, \dots, N \quad (2)$$

Defining  $q_i := \frac{x_i}{x_i^*}$  as the relative change of quantity compared to baseline and using the budget constraint [equation \(1\)](#), we derive the following relation between relative quantities and relative prices,

$$q_i = \frac{\frac{\partial U}{\partial x_i} \sum_{j \neq i}^N (p_j q_j x_j^*)}{p_i x_i^* \sum_{j \neq i}^N \frac{\partial U}{\partial x_j}}, \quad (3)$$

and the optimal *market-emergent elasticity* is given by

$$\epsilon_i = \frac{q_i - 1}{p_i - 1} = \left( \frac{\frac{\partial U}{\partial x_i} \sum_{j \neq i}^N (p_j q_j x_j^*)}{p_i x_i^* \sum_{j \neq i}^N \frac{\partial U}{\partial x_j}} - 1 \right) / (p_i - 1). \quad (4)$$

### Analytical description of price elasticity dynamics

This market-emergent price elasticity characterizes the re-balancing of budget-shares in response to price changes. If a good has a price elasticity of  $-1$ , its budget share is constant. For a good with positive price elasticity, the share of the budget spent on this good is increased if prices rise and decreased if prices fall.

### Feedback mechanism driving market emergence of elasticities

We analyze the price elasticity emerging from utility maximization as derived in [equation \(4\)](#). Without loss of generality, we assume all quantities to be normalized such that  $x_i^* \equiv 1$  and  $x_i = q_i$ . For that, we define the substitution-weighted relative price  $R_i$  for good  $i$  which is a measure for the relative price deviation of good  $i$  to all other goods. Relative prices favor consumption of good  $i$  if  $R_i > 1$ . For any utility function, we can define  $R_i$  – which might still depend on  $q_i$  – from [equation \(3\)](#) as

$$R_i(q_i) := \frac{\frac{\partial U}{\partial q_i}(q_i)}{\sum_{j \neq i}^N \frac{\partial U}{\partial q_j}(q_j)} \left( \sum_{j \neq i}^N (p_j q_j) \right). \quad (5)$$

With this definition of  $R_i$ , we can write [equation \(3\)](#) as  $q_i = \frac{R_i(q_i)}{p_i}$  and thus

$$\epsilon_i = \frac{\frac{R_i(q_i)}{p_i} - 1}{p_i - 1}. \quad (6)$$

Note that  $\epsilon_i$  is well-defined for  $p_i \neq 1$  and that this condition is fulfilled for any deviation from undisturbed baseline prices. Since  $R_i$  might depend on  $q_i$  through the partial derivative  $\frac{\partial U}{\partial q_i}$ , we discuss the necessary assumptions regarding  $U(q_1, \dots, q_N)$  for our feedback elaborations:

## Assumptions on the utility function

For any strictly monotonous increasing utility function, i. e.,  $\frac{\partial U}{\partial q_i} > 0 \forall i \in 1, \dots, N$ , our following elaborations on feedback processes hold generally. This is satisfied as long as the standard assumption of non-saturation is fulfilled and thus – all else being equal – marginally increasing consumption of one good always increases utility.

**DIMINISHING MARGINAL UTILITY** While it reinforces the feedback through the term  $\frac{\frac{\partial U}{\partial q_i}}{\sum_{j \neq i}^N \frac{\partial U}{\partial q_j}}$ , diminishing marginal utility is not strictly required since price-quantity interactions can still yield dynamic behavior via  $\sum_{j \neq i}^N (p_j q_j)$  in equation (5). Nonetheless, in most situations of economic stress, diminishing marginal utility — especially as soon as some baseline consumption  $q_i^*$  is fulfilled — is a realistic assumption on consumers utility functions.

**PARTIALLY SATURATING UTILITY FUNCTIONS** To relax the assumption of non-saturation, we first consider partially non-saturating utility functions, e. g., a monotonous increasing utility function that saturates for a certain consumption level  $q_i^S$  such that  $\frac{\partial U}{\partial q_i} = 0$  for all  $q_i \geq q_i^S$ . In this case, our argument holds true up to  $q_i^S$ . Thus, since we discuss the impact of shocks on consumption behavior, it is a reasonable condition for saturating utility functions that the most scarce goods are not saturated. If other goods  $q_j$  for  $j \in \{1, \dots, i-1, i+1, \dots, N\}$  do saturate, this only eliminates the utility driven feedback from changes in the saturated goods back to good  $i$ . Even in the extreme case of all goods but good  $i$  being saturated and equation (5) thus being ill-defined due to division by zero, optimization of utility would still yield increasing consumption of good  $i$  and reduction of saturated goods, as long as this yields a positive change of utility. If all goods are in a saturated state, trivially consumption will not change.

**MINIMUM CONSUMPTION LEVELS** Another general class of utility functions might prescribe a minimum level of consumption  $q_i^M$  for specific goods such that  $U(q_1, \dots, q_i, \dots, q_N) \equiv 0$ , if  $q_i < q_i^M$ . While this introduces a discontinuity in the utility plane, optimization would yield a consumption above minimum levels if possible and for the further distribution between goods. As soon as all minimum consumption levels can be obtained, the presented feedback mechanism would depend upon the properties of the utility function.

**OTHER PREFERENCE ORDERS** In the presence of lexicographic preferences, i. e., a strict hierarchy between the goods  $1 < 2 < \dots < N$  such that any amount of good  $i+1$  is better than any amount of good  $i$ , there is no real balancing of consumption between different goods. We acknowledge that lexicographic preferences might be important

for decisions between similar, different quality goods Encarnación 1964; Fishburn 1975. Nonetheless, we posit that for the question of substitution between different more or less complementary goods which is our main concern with respect to the dynamics of price elasticity, assuming balancing between different goods reflects realistic consumers behavior better than lexicographic preferences.

**OPTIMIZATION UNDER A BUDGET CONSTRAINT** Another essential assumption for our analytical derivation is that the budget  $B$  is fixed for all time steps. This is a strong simplification of reality, where consumers might have differing levels of savings to draw from in times of need. Still, here we are mainly interested in the dynamic response due to diverging price changes between goods, for which this simplification is reasonable. In future work, this aspect should be expanded upon, including a labor market and savings component.

**EXAMPLE OF A CES UTILITY FUNCTION** To illustrate our theoretical elaboration with a concrete example, we use a one-level constant elasticity of substitution (CES) utility function with elasticity of substitution  $\sigma$  as an explicit example. Note that our main subject of study is the price elasticity  $\epsilon$  of goods, while the specification of a constant elasticity of substitution  $\sigma$  specifies the degree of substitution under the CES utility function. Wherever we refer to “elasticity” without specification, we discuss price elasticity.

$$U(x_1, \dots, x_N) = \left[ \sum_{i=1}^N \left( a_i^{\frac{1}{\sigma}} x_i^{\frac{\sigma-1}{\sigma}} \right) \right]^{\frac{\sigma}{\sigma-1}} \quad (7)$$

Here,  $a_i^*$  denotes the baseline share of consumption of good  $i$ , defined as  $a_i^* := \frac{x_i^*}{\sum_{j=1}^N x_j^*}$ .

Its partial derivative with respect to  $x_i$ , the consumption of good  $i$ , reads

$$\frac{\partial U}{\partial x_i} = a_i^{\frac{1}{\sigma}} x_i^{-\frac{1}{\sigma}} \left[ \sum_{j=1}^N \left( a_j^{\frac{1}{\sigma}} x_j^{\frac{\sigma-1}{\sigma}} \right) \right]^{\frac{1}{\sigma-1}}. \quad (8)$$

The following relation between the relative price change of good  $i$ ,  $p_i$ , and relative quantity change  $q_i$  holds in each time step (detailed calculation in the methods):

$$q_i = \left( R_i \cdot \frac{1}{p_i} \right)^{\frac{1}{1+\frac{1}{\sigma}}}, \quad (9)$$

where

$$R_i := \frac{\sum_{j \neq i}^N (p_j q_j x_j^*)}{\sum_{j \neq i}^N q_j^{-\frac{1}{\sigma}}} \frac{1}{x_i^*}. \quad (10)$$

For this utility function, we can derive an  $R_i$  that is independent of  $q_i$ , but our following general analysis does not depend on this analytical simplification.

### Mechanisms resulting in positive price elasticities

Returning to the general case, we identify  $R_i$  as central to the relation between  $p_i$  and  $q_i$ , such that a self-regulating feedback loop evolves as sketched in Fig. 1. If  $R_i$  depends on  $q_i$  through  $\frac{\partial U}{\partial q_i}$ , the assumption of diminishing marginal utility ensures that the feedback loop is reinforced by decreasing  $\frac{\partial U}{\partial q_i}$  with increasing  $q_i$ . If this assumption does not hold true, non-decreasing marginal utility would potentially weaken the feedback loop and destabilize it. While this might introduce more complicated dynamics, for the return to optimal consumption levels after a shock either saturation or diminishing marginal utility would ensure a stable feedback such that  $R_i \rightarrow 1$ . If relative prices favor good  $i$

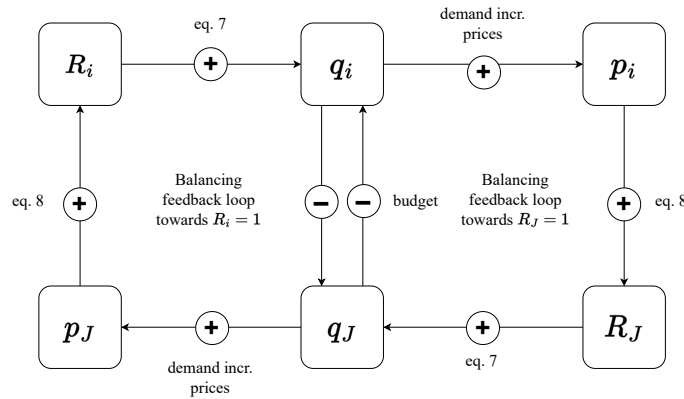


Figure 1: **Changes of  $R_i$  drive a self-regulating feedback loop.** Schematic feedback loop with  $J$  defined as the combination of all other goods, i. e.,  $J := \{1, \dots, i - 1, i + 1, \dots, N\}$ , resulting in two interconnected negative feedback loops.

(case  $R_i > 1$ ), the increased consumption decreases the consumption of the other goods, which decreases the prices  $p_j$  for  $j \in \{1, \dots, i - 1, i + 1, \dots, N\}$ , thus decreasing  $R_i$  and thereby the increased consumption is slowly pulled back to baseline state. In supplementary figure S1 we sketch a flow-chart of the feedback processes. Since this applies to all goods in parallel, complex patterns might emerge, but the whole system relaxes back to baseline levels in the aftermath of a disturbance. This effect is symmetric for price

decreases followed by demand reduction if a good is unfavorable, i. e., less important for utility than combined other goods (case  $R_i < 1$ ).

Since shifts in  $R_i$  move the demand curve, the actually realized demand curve can deviate from the expected curve. An example is illustrated in Fig. 2. Depending on

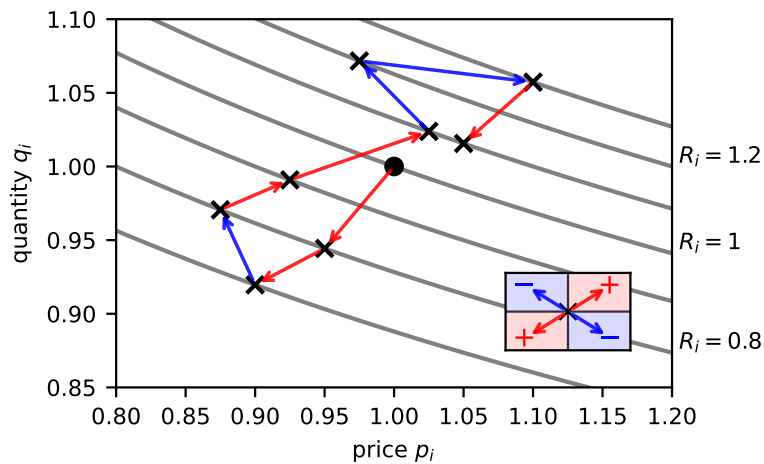


Figure 2: **Effect of the time dependence of  $R_i$  on the demand curve of good  $i$ .** Illustrative projection of trajectory on (relative) price–quantity plane in the aftermath of a shock pushing the system out of the equilibrium point at  $(1, 1)$ . Arrows indicate the movement in price–quantity space induced by changes in  $R_i$ . The inset shows the sign of price elasticity depending on the relative movement in price–quantity space; red and blue colors indicate positive and negative elasticities, respectively.

the change in  $R_i$ , the resulting demand trajectory can yield positive or negative *market emergent price elasticities*. While these do not indicate the 1:1-dependency of price to quantity as in the case of classical constant price elasticity derived under ceteris paribus assumptions, the incorporation of the relative price effect gives a more complete, realistic picture of consumption behavior.

Our analysis of emerging price elasticity implies a dynamic behavior driven by  $R_i$ , where the market interactions of relative prices can lead to counter-intuitive positive price elasticity for individual goods. The market forces are influenced by higher-order effects and yield results apparently contradicting the fundamental laws of the market — where increasing prices are assumed to cause decreasing demand. Importantly, the consumers in this framework do not use any further behavioral component to determine consumption, such that the resulting *market emerging elasticity* is solely driven by the standard economic assumption of utility maximization.



RELATION TO OTHER TYPES OF POSITIVE PRICE ELASTICITIES There are two general cases of positive price elasticity — Veblen goods and Giffen goods. Veblen goods are based on the perception of secondary utility by the consumers Veblen 1899; Basmann, Molina, and Slottje 1988; Bagwell and Bernheim 1996, most often thought to be some sort of luxury, i. e. a utility function that increases with increasing price of a good. In our setting without such behavioral assumptions about perception of luxury, Veblen goods cannot exist.

Compared to the classical example of Giffen goods Jensen and Miller 2008, positive price elasticities do not occur due to substitution of high-quality goods by lower-quality goods, but emerge from relative price effects in non-equilibrium states of the economy. While there is a certain similarity of Giffen behavior and our dynamic elasticities, an important distinction is that Giffen goods are assumed to have a constantly positive price elasticity, i. e. for decreasing prices consumption will always decrease. Moreover, the textbook and empirically studied example Jensen and Miller 2008 depends on two-dimensions of utility from goods: calories as the primary driver of utility and taste respectively variety of food as a secondary component of utility. In contrast to imposing specific conditions on individual goods, we study within our dynamic framework changes of price elasticity based on the reallocation of budget towards other goods, as described in our discussion of the emerging feedback loop.

More specifically, we can compare the potentially resulting elasticity for a good  $i$   $\epsilon_i$  depending on  $p_i$  and  $R_i$  following equation (6). For the case of Giffen goods, price elasticity is constrained to be negative in any case, such that our dynamic analysis adds a substantial component of market induced “Giffen-like” behavior.

The phase-diagram of price  $p_i$  and its relative position  $R_i$  in the price landscape (Fig. 3) illustrate the connection between our more general case of positive price elasticity emerging from market interaction and a prescribed positive elasticity due to specific properties of Giffen goods. For the case of the Giffen good, the attainable values are constrained to the red area of positive price elasticity by the assumption that a Giffen good always exhibits positive price elasticities.

Following from equation (6), we can derive the following condition for the emergence of positive elasticity:

$$\begin{aligned} \operatorname{sgn} \left( \frac{R_i(q_i)}{p_i} - 1 \right) &= \operatorname{sgn} (p_i - 1) \\ \Leftrightarrow \left( \frac{R_i(q_i)}{p_i} > 1 \wedge p_i > 1 \right) \vee \left( \frac{R_i(q_i)}{p_i} < 1 \wedge p_i < 1 \right) & \quad (\text{II}) \end{aligned}$$

This equation (II) shows, that positive elasticity will emerge, if either the price of good  $i$  is increasing, and its price weighted relative value compared to all other goods is increasing more strongly, i. e.  $\frac{R_i(q_i)}{p_i} > 1$  or if the price of good  $i$  is decreasing, and its price

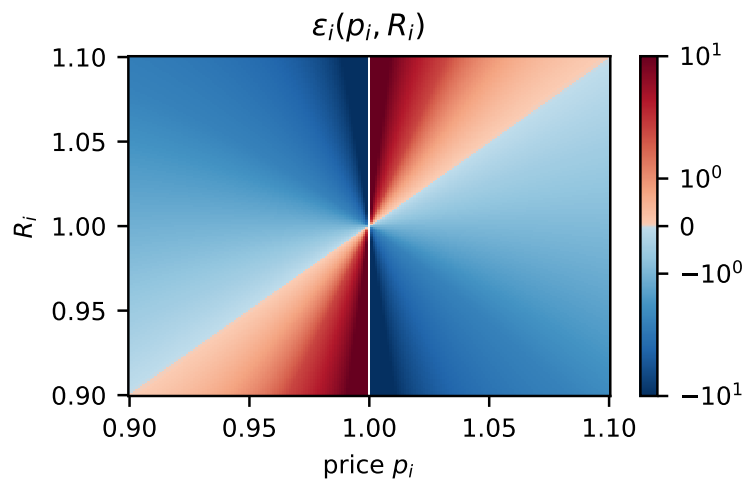


Figure 3: **Elasticity resulting from different values of  $p_i$  and  $R_i$  plotted in  $p_i - R_i$  space.** For Giffen goods,  $R_i$  is constrained by definition such that only positive elasticities in the red area are attainable. In our more general case, market circumstances might yield a dynamic transition between positive elasticities and negative elasticities.

weighted relative value compared to all other goods is decreasing even more, i. e.  $\frac{R_i(q_i)}{p_i} < p_i < 1$ .

While the result of positive elasticity is the same in our market oriented perspective, it is an important extension of this classical example to consider emerging positive elasticities due to market interactions, not just inherent properties of individual goods. In Fig. 4 we show, that for all types of goods positive elasticities are attained in a dynamic trajectory. Thus, the influence of the market circumstances on the emergence of price elasticity is more dynamic than in the static case of the Giffen good. This perspective extends the assumption based positive price elasticity of Giffen goods to a market based emergence thereof.

### Utility maximization in *Acclimate*

To explore the described theoretical feedback processes in a numerical experiment, we use the agent-based global supply chain model *Acclimate* and extend its consumer module with the maximization of a two-layer CES utility function. In contrast to our explanatory example of a simple CES utility function, we use a two-level CES utility function since the 26 classes of goods are not equally substitutable for one another. For this, we define three consumption baskets to classify goods as 'necessary', 'relevant', and 'other goods', each with varying degrees of substitutability. We thereby follow the classification used previously to map consumption price elasticities from the Global Trade Analysis Project

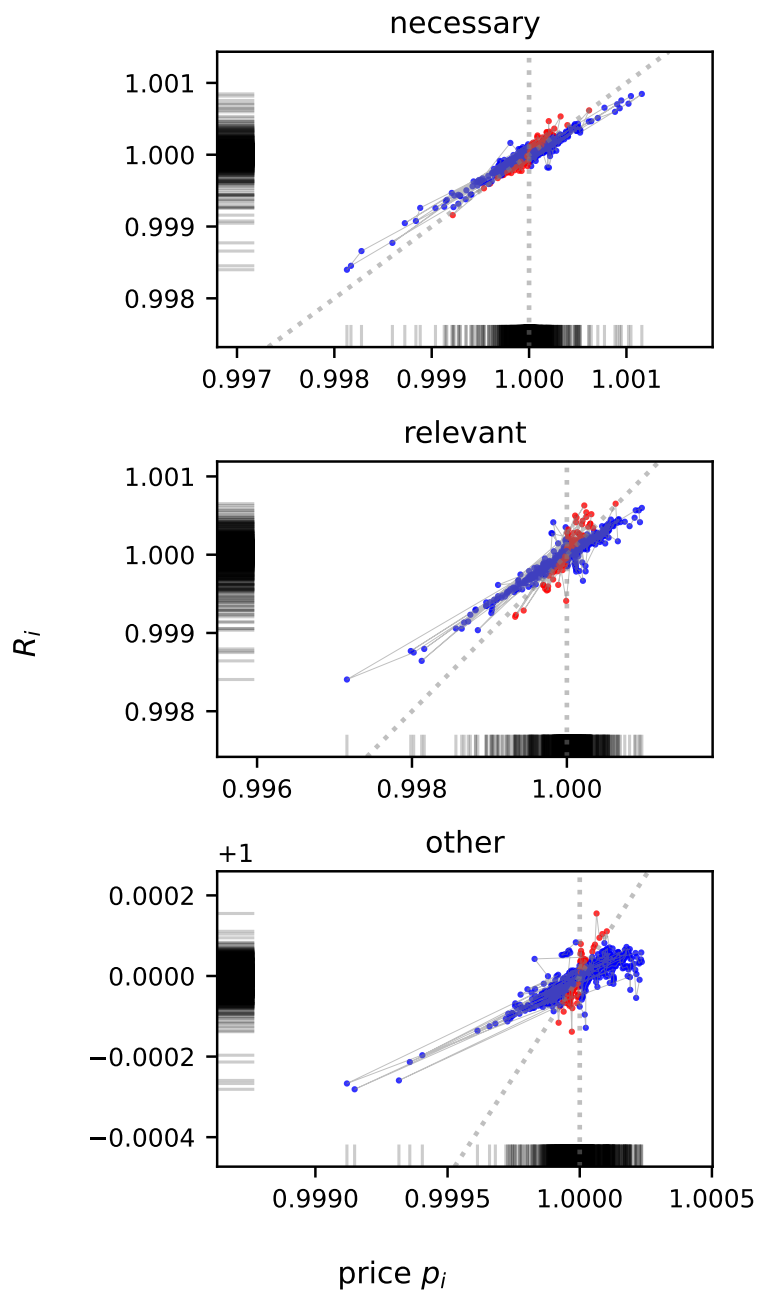


Figure 4: **Example trajectories in  $p_i - R_i$  space:** This sample from model results shows, that the dynamic switch between negative (blue) and positive elasticity (red) occurs in our modeling exercise. Sample for first income quintile in Germany for the years 2021-2025.

(GTAP) Huff et al. 2012 to the Eora sectors. For details we refer to the methods, where we also provide an analysis of the two-level  $R_i$  (equation (23)).

Using a shock scenario for economic disturbances after extreme weather events, we can readily estimate the *market emergent price elasticity* — i. e., elasticity including market substitution effects, not using ceteris paribus assumptions — of consumption flows per region and income group based on our previous theoretical analysis. While we run the experiment for 20 years, our results focus on the short-term response to extreme weather shocks. Instead of aiming to predict the consumption patterns for the next twenty years, we focus on understanding the characteristics of the response to short-term seasonality and variability of extreme weather events. Since *Acclimate* is designed to explore the complexity of short-term out-of-equilibrium dynamics, we consider it well suited for this modeling exercise.

With respect to our modeling results we focus on the data of consumer agents from the three biggest economic blocks: China, the USA, and the EU28. Since China and the USA are resolved on sub-national level and the EU28 is naturally partitioned into countries, we thus show data for an ensemble of 550 consumer agents (31 provinces of China, 51 states of the US, and 28 EU28 countries with 5 income groups each).

## Comparing analytical expectations and modeling results

To compare analytical expected emerging elasticities and results from *Acclimate*, we generate a random distribution of substitution-weighted relative prices of all other goods  $R_i$  to plot corresponding distributions of theoretical emerging elasticity  $\epsilon_i$  depending on price change  $p_i$ . For this, we draw a uniform sample of price change  $p_i \in [-0.01, 0.01] \setminus (-0.0001, 0.0001)$ , excluding values close to 0 as price elasticity is ill-defined there. We assume  $R_i$  to be normally distributed with mean  $\mu = 1$ . Further, we assume variance  $\nu$  to be decreasing for an increasing inter-basket substitution coefficient in the utility function since a higher substitution between goods should lead to a less volatile  $R_i$ . The resulting distribution of price elasticity  $\epsilon_i$  with respect to price change  $p_i$  shows that reduced substitutability, conventionally assumed for elementary goods, results in a price elasticity closer to 0 and thus also more frequent emergence of positive price elasticities ( $(A,B,C)$  in Fig. 5). Comparing the numerical to the analytical results in Fig. 5, we observe that the simulated two-level behavior follows the theoretical prediction. In particular, increases in elasticity of substitution  $\sigma$  shift the emerging price elasticity for relevant and other goods to more negative values. In line with the analytical findings, positive price elasticities occur dynamically for all classes of goods. Since these positive elasticities are concentrated in periods of economic stress Fig. 6, we show the possibility of temporary positive price elasticity emerging from market conditions, not the inherent properties of a certain good as in the classical Giffen good case. So while these concepts yield similar outcomes, the driving mechanisms are distinct, since we focus on interactions between goods. The elasticity of substitution influences the likelihood

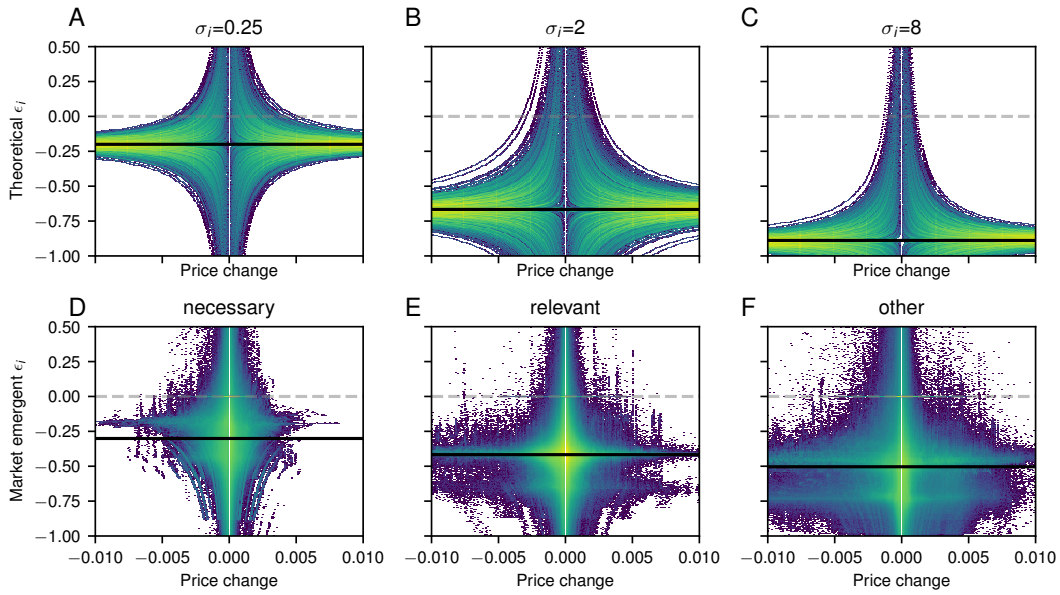


Figure 5: **Results of the full model are qualitatively in line with elasticity distributions randomly drawn from simplified theory. Analytical approximation** in (A,B,C) shows the effect of  $\sigma_i$  corresponding to the baskets of 'necessary' (first column), 'relevant' (second column), and 'other' (third column) goods on the expected elasticity distribution for randomly fluctuating  $R_i$ .  $R_i$  is assumed to be normally distributed with mean 1 and variance  $\nu$  that decreases with increasing  $\sigma_i$  to reflect the dampening effect of higher substitutability on  $R_i$ 's volatility, i. e., (A)  $\nu = 16 \cdot 10^{-4}$ , (B)  $\nu = 8 \cdot 10^{-4}$  and (C)  $\nu = 4 \cdot 10^{-4}$ . **Full model results** in (D,E,F) show the corresponding modeling results for (A) 'necessary' basket, (B) 'relevant' basket and (C) 'other' basket. Solid black line shows median elasticity. Distributions are plotted with log-scaling.

for Giffen like behavior via equations (9) and (10), but still a wide variety of goods show positive elasticities under stressed market conditions. Deviations in median price elasticity compared to the theoretical analysis are induced by the lack of two-level structure in the theoretical example, while they also might point to higher-order effects regulating the price elasticity dynamics. These are likely driven by the network interactions and complexities not accounted for in the simplified, randomized parameter draw for (A,B,C) in Fig. 5.

### Volatility clustering of consumption price elasticity

To analyze the temporal dynamics of the simulated processes, we show a 5-year time series sample from our 20 years of simulations in Fig. 6. While the consumption price elasticity emerging from *Acclimate* is fluctuating around its median, the economic stress in the agents trade network is dominated by heat stress in the northern hemisphere summertime

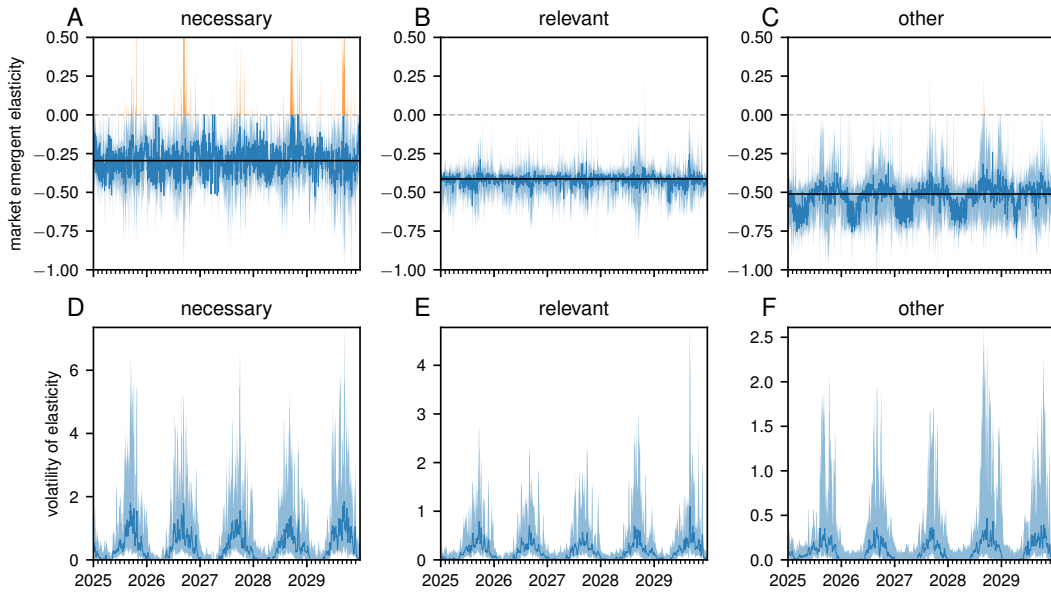


Figure 6: **Dynamics of price elasticity are stronger in periods of economic stress** (*A,B,C*) show sample time-series of the market emerging elasticity for the respective consumption basket. Orange lines highlights positive elasticities. (*D,E,F*) show the corresponding 7-day volatility of market emerging elasticity. Solid blue lines show the median over the ensemble of all considered consumer agents, while shaded areas indicate the 16.66-83.33 percentile intervals. The solid black line in (*A,B,C*) shows the ensemble median over time. The definition of our volatility measure is given in the methods (equation (24)).

and, thus, induces a seasonal clustering of volatility of elasticity. This link between external forcing and the reaction of the utility maximizing consumers shows the dynamic nature of price elasticity under economic stress. While in this specific example, we recover the seasonal pattern of heat stress on the Northern Hemisphere, the described feedback mechanisms might drive volatility clustering of consumption price elasticities in any type of clustered economic stress. Further, this observation shows that exogenous shocks and not endogenous consumption changes dominate the price dynamics leading to the market emergence of positive consumption price elasticities.

## Discussion and conclusion

We show analytically that consumption price elasticities are dynamic in response to economic shocks and demonstrate this behavior extending a numerical agent-based model of the world economy.

Based on the analysis of market emergent price elasticities resulting from utility maximization under a constraint budget, we show that substitution effects and relative price changes introduce a self regulating feedback loop. This leads to positive price elasticities manifesting from increasing demand in spite of increasing prices driven by utility maximizing consumers without behavioral assumptions. Thus, the case of Veblen goods whose utility increases with higher prices is not connected to the explored mechanisms. We further show that the marked driven emergence of positive price elasticities discussed in the paper is a substantial extension of the classical example of Giffen goods. For the latter, positive elasticities emerge from the assumptions on the specific good, while in our analysis positive elasticities are a result of market circumstances, which may occur for any good.

Thus, our results are consistent with standard assumptions of rational decision making. These theoretical results are reproduced in a complex agent-based supply chain model and show the need to consider complexity additional to *ceteris paribus* analyses in economic modeling. The qualitative differences we observe between baskets of goods indicate the need for an extension of existing models of price elasticity by heterogeneous modeling approaches.

We also observe an additional temporal component in our dynamic heterogeneous modeling experiments - seasonal economic stress induces seasonality in the volatility of price elasticity. While periods of volatility clustering is well-explored for financial markets and numerous behavioral explanations are discussed using agent-based modeling [Lux and Marchesi 2000](#); [Cont 2007](#); [Schmitt and Westerhoff 2017](#), in our case the connection between high volatility and economic stress provides a direct explanation. Additionally, this direct mechanism is potentially reinforced by the agents' herding behavior in our model due to utility functions of the same form. This stresses the importance of the development of methods to model the dynamics of consumption price elasticity overcoming the assumption of static elasticity. While simpler input-output models augmented by utility maximizing consumers could also be used to reproduce our analytical findings, we prefer to demonstrate that the analytically derived dynamics are also observable in a complex agent-based model. This strengthens the robustness of our results with respect to complex interaction mechanics, while it is also practical since we are able to use an already published scenario of extreme weather impacts [Kuhla, Willner, Otto, Geiger, et al. 2021](#). Most importantly, *Aclimate* allows us to study the effects of heterogeneity in shocks, response of profit maximizing producers and consumption behavior of different income groups, such that our numerical experiments offer insights on temporal dynamics of the described feedback mechanism in a realistic shock scenario.

Even though there are discussions about the exact effects of the COVID-19 pandemic on supply chains [Guan et al. 2020](#); [Bonadio et al. 2021](#); [Verschuur, Koks, and Hall 2021](#); [Wang et al. 2021](#), it clearly showed that global economic connections foster the transmission and synchronization of economic stress. Even if this motivates initiatives to decouple



economies, a full decoupling — with uncertain benefits, would be economically costly, if not infeasible. Moreover, for the pandemic scenario, there is evidence that decoupling rather reinforces negative consequences of regional lock-downs [Bonadio et al. 2021](#). Thus, the observation of increased complexity of consumption price elasticity in a state of synchronized economic stress should be considered when modeling the global impacts of economic crisis scenarios. A more dynamic modeling of economic systems might reveal an overall tendency of economic systems to exhibit volatility clustering, which could be used as a potential early warning signal or a measure of economic stress.

We cannot provide a full assessment of potential inflationary pressure of economic shocks on the global economy due to a lack of a labor market and monetary policy agents in the current version of *Acclimate*. Nevertheless, our results might show one cause of such an inflationary pressure: Dynamic price elasticities inducing price increases due to positive price elasticity causing increased demand in spite of increasing prices. Further, these dynamics suggest that any such exercise would need to consider the dynamic response to market conditions of consumption agents carefully — assumptions about static price elasticities might underestimate the persistence of demand for elementary goods. Recent studies are so far unclear about whether climate change induced inflation is persistent [Mukherjee and Ouattara 2021](#) or decays after an initial shock [Faccia, Parker, and Stracca 2021](#). Regarding supply chain disruptions during COVID-19, there is some evidence for the US [LaBelle and Santacreu 2022](#) and Euro area [Giovanni et al. 2022](#) that bottlenecks in global supply chains contributed to the observed inflation, thus underlining the necessity for global trade sensitive modeling of economic activity.

In the following we discuss some limitations: First, for our modeling exercise we assume fixed substitution coefficients between different goods. While this is a reasonable assumption on short time scales, one could also investigate models with a more flexible substitutability between goods. Second, our analysis is based on a fixed consumption budget since our modeling approach does not consider for example income driven by a labor market model. Third, our numerical modeling results are limited to one specific utility function due to constraints on computational effort, such that a wider comparison of different utility functions is omitted. While alternative forms might lead to slightly different behavior, we choose the nested CES structure since its limited number of parameters enables its application in our global modeling exercises.

In future research the presented methods for modeling consumption behavior in response to economic shocks will be applied to analyze the inequalities of impacts of climate change on different income groups.

We conclude that the analytical description of the dynamics of price elasticity of utility maximizing consumers and their numerical modeling enables the exploration of the interactions of micro and macroeconomic processes driven by economic stress. The potential emergence of positive price elasticities shows that classic economic *ceteris paribus*

analysis should be complemented by dynamic modeling to describe periods of economic stress.

## Methods

### Derivation of optimum conditions

Starting with [equation \(1\)](#), it follows, that

$$\lambda \left( B^* - \sum_{j \neq i}^N p_j x_j \right) = \frac{\partial U}{\partial x_i} \quad (12)$$

$$\Leftrightarrow \lambda = \frac{\sum_{i=1}^N \frac{\partial U}{\partial x_i}}{B^*}, \quad (13)$$

and with the baseline relative change of quantity  $q_i := \frac{x_i}{x_i^*}$ ,

$$\frac{\partial U}{\partial x_i} (B^* - p_i x_i) = p_i x_i \sum_{j \neq i}^N \frac{\partial U}{\partial x_j} \quad (14)$$

$$\Leftrightarrow \frac{\frac{\partial U}{\partial x_i}}{\sum_{j \neq i}^N \frac{\partial U}{\partial x_j}} = \frac{p_i q_i x_i^*}{\sum_{j \neq i}^N (p_j q_j x_j^*)}. \quad (15)$$

Hence, [equation \(3\)](#) follows.

### Derivation of $R_i$ for simple CES function

$$\begin{aligned} q_i &= \frac{\frac{\partial U}{\partial x_i}}{\sum_{j \neq i}^N \frac{\partial U}{\partial x_j}} \frac{\sum_{j \neq i}^N p_j q_j x_j^*}{p_i x_i^*} \\ \Leftrightarrow q_i &= \frac{x_i^{*\frac{1}{\sigma}} x_i^{-\frac{1}{\sigma}}}{\sum_{j \neq i}^N x_j^{*\frac{1}{\sigma}} x_j^{-\frac{1}{\sigma}}} \frac{\sum_{j \neq i}^N p_j q_j x_j^*}{p_i x_i^*} \\ \Leftrightarrow q_i^{1+\frac{1}{\sigma}} &= \frac{\sum_{j \neq i}^N p_j q_j x_j^*}{\sum_{j \neq i}^N q_j^{-\frac{1}{\sigma}} x_j^*} \frac{1}{x_i^*} \frac{1}{p_i}, \end{aligned} \quad (16)$$

thus [equation \(9\)](#) and [equation \(10\)](#) follow.

### *Acclimate*

*Acclimate* is an agent-based model of the world economy using baseline data from the Eora Lenzen et al. 2013 multi-regional input output (MRIO) tables. We provide a sketch

of its general structure in the supplementary materials, figure S2. Since we disaggregate China to province and the USA to state level resolution [Wenz et al. 2015](#), we obtain a network with 264 regions (excluding regions with poor data quality). Disaggregating consumption demand based on world bank development indicator income shares [Bank 2021](#) and the assumption that all income quintiles consume equal amounts of food, we obtain 1320 individual consumption agents. These operate as consumers of final demand in a network with 6243 firm agents, which represent one of the 26 Eora sectors in each region. In total, our simulations are based on the modeling of 7563 individual agents under consecutive extreme event forcing of heat stress, river floods, and tropical cyclones as in [Kuhla, Willner, Otto, Geiger, et al. 2021](#) for a time-period of twenty years. These shocks reduce productive capacity according to empirically derived damage functions as shown in Fig. 5 A of [Kuhla, Willner, Otto, Geiger, et al. 2021](#), a short summary of the different categories of extreme weather shocks is given in section two of [Kuhla, Willner, Otto, Geiger, et al. 2021](#). Propagating through the prescribed supply and demand connections of the economic input-output network. These propagation effects cause downstream supply and upstream demand changes as analyzed with the story-line approach for the case of Hurricane Sandy [Middelanis et al. 2021](#). The prices anomalies emerging from the balance between supply and demand changes result in changing consumption patterns - for the previous *Acclimate* studies just based on fixed price elasticities, which motivated the development of the here presented utility maximization extension. To summarize, consumers are exposed to the results of the firms profit optimizing demand and supply adjustments, for details see the model description [Otto et al. 2017](#), resulting in a change of price and available quantity. The thereby induced consumption changes feed back into the propagation interactions between all the agents. Thus our extension with different consumer groups per region might also introduce intra-consumer interactions

In the following, we present the new consumption decision dynamics and analyze the expected emerging price elasticity. Extending the existing *Acclimate* model by utility maximizing consumers enables us to evaluate differentiated trends in consumer behavior after economic shocks. For this, we endow each consumer agent with a nested CES utility function to maximize and observe the reaction to economic shocks. Noteworthy, there are no assumptions on behavioral drivers for the consumption decision, but pure *Homo oeconomicus* utility maximization. The two-level utility function considers goods in three broad baskets of *necessary*, *relevant* and *other* goods. The composition of the baskets based on the Eora sectors can be found in the supplementary materials, table S1. We use a plausible set of global parameters for the CES utility function to demonstrate the concept and its effects.

### Utility function for *Acclimate* consumers

The utility function for a consumer in region  $r$  and income quintile  $q$  is given by

$$U_{rq} = \left( \sum_{i=1}^B \left( b_i \cdot \frac{1}{\theta} \left[ \sum_{k=1}^{m_i} \left( a_k \frac{1}{\sigma_i} x_{k \rightarrow rq} \frac{\sigma_i - 1}{\sigma_i} \right) \right]^{\frac{\sigma_i - 1}{\theta}} \right)^{\frac{\theta - 1}{\theta - 1}} \right)^{\frac{\theta}{\theta - 1}} \quad (17)$$

Each consumer optimizes their utility for  $B$  consumption baskets. Within each basket of goods, the varying  $\sigma_i$  for  $i \in 1, \dots, B$  allows for a varying degree of intra-basket substitution, while  $\theta$  controls inter-basket substitution. The share factors of good  $k$  in basket  $i$  for  $k = 1, \dots, m_i$  are chosen such that

$$a_k = \frac{x_{k \rightarrow rq}^*}{\sum_{i=1}^{m_i} x_{i \rightarrow rq}^*}, \quad (18)$$

while the basket share factors  $b_j$  for  $j = 1, \dots, B$  are chosen such that

$$b_j = \frac{\sum_{i=1}^{m_i} x_{i \rightarrow rq}^*}{\sum_{i=1}^M x_{i \rightarrow rq}^*}, \quad (19)$$

For the application of equations (17) to (19) in *Acclimate* we use  $B = 3$  with three baskets classified as *necessary*, *relevant*, and *other* goods. We refer to the SI, supplementary table 1, for the exact basket specification, resulting in 5 'necessary', 12 'relevant', and 9 'other' goods. We choose  $\sigma_{necessary} = 0.25$ ,  $\sigma_{relevant} = 2$ ,  $\sigma_{other} = 8$ , and  $\theta = 0.5$  for our trial simulations.

To summarize, the local utility optimization of each agent's consumption reacting to economic shocks and the calculation of market emergent price elasticities, as summarized in supplementary figure S3, enables to study changes of consumption price elasticity based on utility maximization.

**DERIVATION OF  $R_i$  FOR *ACCLIMATE* TWO-LEVEL CES FUNCTION** The partial derivative of the two-level CES utility function with  $M$  goods in  $B$  different baskets used in *Acclimate* is given by

$$\begin{aligned}
 f_k(x_1, \dots, x_M) &:= b_k^{\frac{1}{\theta}} \sum_{i \in B_k} \left( a_i^{\frac{1}{\sigma_k}} x_i^{\frac{\sigma_k-1}{\sigma_k}} \right) \\
 g(x_1, \dots, x_M) &:= \sum_{i=1}^B f_i(x_1, \dots, x_M)^{\frac{\sigma_i}{\sigma_i-1}} \\
 h(x_1, \dots, x_M) &:= g(x_1, \dots, x_M)^{\frac{\theta-1}{\theta}} \\
 U(x_1, \dots, x_M) &= h(x_1, \dots, x_M)^{\frac{\theta}{\theta-1}}
 \end{aligned}$$

For  $x_i \in B_j$ ,  $\mathbb{X} := (x_1, \dots, x_M)$  and  $\mathbb{X}_j := \{x_i | x_i \in B_j\}$  the partial derivative is

$$\frac{dU}{dx_i} = h(\mathbb{X})^{-\frac{1}{\theta-1}} g(\mathbb{X})^{-\frac{1}{\theta}} f_j(\mathbb{X}_j)^{-\frac{1}{\sigma_j-1}} b_j^{\frac{1}{\theta}} a_i^{\frac{1}{\sigma_j}} x_i^{-\frac{1}{\sigma_j}}. \quad (20)$$

Thus, expanding equation (4) with  $x_i \in B_l$  and  $x_j \in B_{k_j}$  yields

$$R_i = \quad (21)$$

$$\frac{f_l(\mathbb{X}_l)^{-\frac{1}{\sigma_l-1}} b_l^{\frac{1}{\theta}} (\sum_{n=1}^{m_l} x_n^*)^{-\frac{1}{\sigma_l}}}{\sum_{j \neq i}^M \left( f_{k_j}(\mathbb{X}_{k_j})^{-\frac{1}{\sigma_{k_j}-1}} b_{k_j}^{\frac{1}{\theta}} (\sum_{n=1}^{m_{k_j}} x_n^*)^{-\frac{1}{\sigma_j}} q_j^{-\frac{1}{\sigma_{k_j}}} \right)} \quad (22)$$

$$\frac{\sum_{j \neq i}^M (p_j q_j x_j^*)}{x_i^*}. \quad (23)$$

$q_i^{1+\frac{1}{\sigma_i}} = R_i \frac{1}{p_i}$  thus implies

$$\epsilon_i = \frac{\left( R_i \frac{1}{p_i} \right)^{1+\frac{1}{\sigma_i}} - 1}{p_i - 1}.$$

## Economic shock scenario

As a shock scenario for our trial simulation runs, we use one realization of the combined river flood, heat stress, and tropical cyclone shocks spanning the double decade 2020–2039 as presented in Kuhla, Willner, Otto, Geiger, et al. 2021.

### Definition of volatility measure

We measure volatility  $\nu_w$  as the 7-day rolling standard deviation of relative changes of  $\epsilon_i$  at time  $t$ . The latter are given by

$$\delta_{\epsilon_i}(t) := \frac{\epsilon_i(t-1) - \epsilon_i(t)}{\epsilon_i(t-1)}$$

for window size  $w$ . Then, the rolling mean reads

$$\bar{\delta}_{\epsilon_i}(t) := \frac{\sum_{k=t-w+1}^t \delta_{\epsilon_i}(k)}{w},$$

and the resulting volatility

$$\nu_w(t) := \sqrt{\frac{\sum_{k=t-w+1}^t (\delta_{\epsilon_i}(k) - \bar{\delta}_{\epsilon_i}(t))^2}{w}}. \quad (24)$$

We choose  $w = 7$  to analyze the small-scale dynamics of *market emergent price elasticity*.



## References

- Bagwell, L. S. and B. D. Bernheim (1996). “Veblen Effects in a Theory of Conspicuous Consumption”. In: *The American Economic Review* 86.3, pp. 349–373.
- Bank, W. (Mar. 2021). *World Development Indicators DataBank*.
- Basmann, R. L., D. J. Molina, and D. J. Slottje (1988). “A Note on Measuring Veblen’s Theory of Conspicuous Consumption”. In: *The Review of Economics and Statistics* 70.3, pp. 531–535. [10.2307/1926796](https://doi.org/10.2307/1926796).
- Beutels, P. et al. (2009). “The economic impact of SARS in Beijing, China”. en. In: *Tropical Medicine & International Health* 14.S1, pp. 85–91. [10.1111/j.1365-3156.2008.02210.x](https://doi.org/10.1111/j.1365-3156.2008.02210.x).
- Bonadio, B. et al. (Nov. 2021). “Global supply chains in the pandemic”. en. In: *Journal of International Economics* 133, p. 103534. [10.1016/j.jinteco.2021.103534](https://doi.org/10.1016/j.jinteco.2021.103534).
- Claessens, S. et al. (Apr. 2010). “Cross-country experiences and policy implications from the global financial crisis”. In: *Economic Policy* 25.62, pp. 267–293. [10.1111/j.1468-0327.2010.00244.x](https://doi.org/10.1111/j.1468-0327.2010.00244.x).
- Cont, R. (2007). “Volatility Clustering in Financial Markets: Empirical Facts and Agent-Based Models”. en. In: *Long Memory in Economics*. Ed. by G. Teyssi ere and A. P. Kirman. Berlin, Heidelberg: Springer, pp. 289–309.
- Encarnaci on, J. (1964). “A Note on Lexicographical Preferences”. In: *Econometrica* 32.1/2, pp. 215–217. [10.2307/1913748](https://doi.org/10.2307/1913748).
- Faccia, D., M. Parker, and L. Stracca (Dec. 2021). *Feeling the Heat: Extreme Temperatures and Price Stability*. en. SSRN Scholarly Paper. Rochester, NY. [10.2139/ssrn.3981219](https://doi.org/10.2139/ssrn.3981219).
- Fishburn, P. C. (July 1975). “Axioms for Lexicographic Preferences<sub>12</sub>”. In: *The Review of Economic Studies* 42.3, pp. 415–419. [10.2307/2296854](https://doi.org/10.2307/2296854).
- Giovanni, J. di et al. (July 2022). *Global Supply Chain Pressures, International Trade, and Inflation*. Working Paper. [10.3386/w30240](https://doi.org/10.3386/w30240).
- Guan, D. et al. (June 2020). “Global supply-chain effects of COVID-19 control measures”. en. In: *Nature Human Behaviour* 4.6, pp. 577–587. [10.1038/s41562-020-0896-8](https://doi.org/10.1038/s41562-020-0896-8).
- Hallegatte, S. (2008). “An adaptive regional input-output model and its application to the assessment of the economic cost of Katrina”. In: *Risk Analysis* 28.3, pp. 779–799. [10.1111/j.1539-6924.2008.01046.x](https://doi.org/10.1111/j.1539-6924.2008.01046.x).
- Hallegatte, S. et al. (Jan. 2011). “Assessing climate change impacts, sea level rise and storm surge risk in port cities: a case study on Copenhagen”. en. In: *Climatic Change* 104.1, pp. 113–137. [10.1007/s10584-010-9978-3](https://doi.org/10.1007/s10584-010-9978-3).
- He, Y. X. et al. (Feb. 2011). “Electricity demand price elasticity in China based on computable general equilibrium model analysis”. en. In: *Energy* 36.2, pp. 1115–1123. [10.1016/j.energy.2010.11.038](https://doi.org/10.1016/j.energy.2010.11.038).

- Huff, K. M. et al. (2012). “GTAP behavioral parameters”. In: *Global Trade Analysis*, pp. 124–148. 10.1017/cbo9781139174688.005.
- Jensen, R. T. and N. H. Miller (Sept. 2008). “Giffen Behavior and Subsistence Consumption”. en. In: *American Economic Review* 98.4, pp. 1553–1577. 10.1257/aer.98.4.1553.
- Kornhuber, K. et al. (2018). “Amplified Rossby waves enhance risk of concurrent heatwaves in major breadbasket regions”. In: *Nature Climate Change*, pp. 2–9. 10.1038/s41558-019-0637-z.
- Kuhla, K., S. N. Willner, C. Otto, T. Geiger, et al. (Oct. 2021). “Ripple resonance amplifies economic welfare loss from weather extremes”. en. In: *Environmental Research Letters* 16.11, p. 114010. 10.1088/1748-9326/ac2932.
- Kuhla, K., S. N. Willner, C. Otto, L. Wenz, et al. (June 2021). “Future heat stress to reduce people’s purchasing power”. en. In: *PLOS ONE* 16.6, e0251210. 10.1371/journal.pone.0251210.
- LaBelle, J. and A. M. Santacreu (2022). *Global Supply Chain Disruptions and Inflation During the Covid-19 Pandemic*. en. SSRN Scholarly Paper. Rochester, NY.
- Lamperti, F. et al. (Apr. 2020). “Climate change and green transitions in an agent-based integrated assessment model”. en. In: *Technological Forecasting and Social Change* 153, p. 119806. 10.1016/j.techfore.2019.119806.
- Lenzen, M. et al. (2013). “BUILDING EORA: A GLOBAL MULTI-REGION INPUT–OUTPUT DATABASE AT HIGH COUNTRY AND SECTOR RESOLUTION”. In: *Economic Systems Research* 25.1, pp. 20–49. 10.1080/09535314.2013.769938.
- Lux, T. and M. Marchesi (Oct. 2000). “Volatility clustering in financial markets: a microsimulation of interacting agents”. In: *International Journal of Theoretical and Applied Finance* 03.04, pp. 675–702. 10.1142/S0219024900000826.
- Masson-Delmotte, V. et al. (2021). *Climate Change 2021: The Physical Science Basis. Contribution of Working Group I to the Sixth Assessment Report of the Intergovernmental Panel on Climate Change*. IPCC. Cambridge University Press.
- Middelanis, R. et al. (2021). “Wave-like global economic ripple response to Hurricane Sandy”. en. In: *Environmental Research Letters*. 10.1088/1748-9326/ac39c0.
- Mishkin, F. S. (Mar. 2011). “Over the Cliff: From the Subprime to the Global Financial Crisis”. en. In: *Journal of Economic Perspectives* 25.1, pp. 49–70. 10.1257/jep.25.1.49.
- Mukherjee, K. and B. Ouattara (Aug. 2021). “Climate and monetary policy: do temperature shocks lead to inflationary pressures?” en. In: *Climatic Change* 167.3, p. 32. 10.1007/s10584-021-03149-2.
- Otto, C. et al. (Oct. 2017). “Modeling loss-propagation in the global supply network: The dynamic agent-based model acclimate”. In: *Journal of Economic Dynamics and Control* 83, pp. 232–269. 10.1016/j.jedc.2017.08.001.
- Pfleiderer, P. et al. (Sept. 2019). “Summer weather becomes more persistent in a 2 °C world”. en. In: *Nature Climate Change* 9.9, pp. 666–671. 10.1038/s41558-019-0555-0.

- Pörtner, H.-O. et al., eds. (2022). *IPCC, 2022: Climate Change 2022: Impacts, Adaptation, and Vulnerability. Contribution of Working Group II to the Sixth Assessment Report of the Intergovernmental Panel on Climate Change*. Cambridge University Press. Cambridge University Press.
- Schmitt, N. and F. Westerhoff (Aug. 2017). “Herding behaviour and volatility clustering in financial markets”. In: *Quantitative Finance* 17.8, pp. 1187–1203. 10.1080/14697688.2016.1267391.
- Siu, A. and Y. C. R. Wong (Jan. 2004). “Economic Impact of SARS: The Case of Hong Kong\*”. In: *Asian Economic Papers* 3.1, pp. 62–83. 10.1162/1535351041747996.
- Veblen, T. (1899). *The Theory of the Leisure Class*. en. Oxford World’s Classics.
- Verschuur, J., E. E. Koks, and J. W. Hall (Mar. 2021). “Observed impacts of the COVID-19 pandemic on global trade”. en. In: *Nature Human Behaviour* 5.3, pp. 305–307. 10.1038/s41562-021-01060-5.
- Wang, D. et al. (Mar. 2021). “Reply to: Observed impacts of the COVID-19 pandemic on global trade”. en. In: *Nature Human Behaviour* 5.3, pp. 308–309. 10.1038/s41562-021-01061-4.
- Wenz, L. et al. (Apr. 2015). “Regional and Sectoral Disaggregation of Multi-Regional Input–Output Tables – a Flexible Algorithm”. In: *Economic Systems Research* 27.2, pp. 194–212. 10.1080/09535314.2014.987731.
- Willner, S. N., C. Otto, and A. Levermann (July 2018). “Global economic response to river floods”. In: *Nature Climate Change* 8.7, pp. 594–598. 10.1038/s41558-018-0173-2.



# The formalization of storylines

# 6

This article has been accepted for publication in *Climate Risk Management* as:

B. Van den Hurk, M. Baldissera Pacchetti, A. Ciullo, L. Coulter, S. Dessai, E. Ercin, H. Goulart, R. Hamed, S. Hochrainer, E. Koks, P. Kubiczek, A. Levermann, R. Mechler, M. van Meersbergen, B. Mester, R. Middelani, K. Minderhoud, J. Mysiak, S. Nirandjan, C. Otto, P. Sayers, J. Sillman, J. Schewe, T. G. Shepherd, D. Stuparu, K. Witpas (2022). “Climate Impact Storylines for Assessing Socio-Economic Responses to Remote Events”. In press at *Climate Risk Management*.

**ABSTRACT:** Modelling complex interactions involving climatic features, socio-economic vulnerability or responses, and long impact transmissions is associated with substantial uncertainty. Physical climate storylines are proposed as an approach to explore complex impact transmission pathways and possible alternative unfoldings of event cascades under future climate conditions. These storylines are particularly useful for climate risk assessment for complex domains, including event cascades crossing multiple disciplinary or geographical borders. For an effective role in climate risks assessments, development guidelines are needed to consistently develop and interpret the storyline event analyses. This paper elaborates on the suitability of physical climate storyline approaches involving climate event induced shocks propagating into societal impacts. It proposes a set of common elements to construct the event storylines. In addition, criteria for their application for climate risk assessment are given, referring to the need for storylines to be physically plausible, relevant for the specific context, and risk-informative. Apart from an illustrative gallery of storyline examples found in literature, three examples of varying scope and complexity are presented in detail, all involving the potential impact on European socio-economic sectors induced by remote climate change features occurring far outside the geographical domain of the European mainland. The storyline examples illustrate the application of the proposed storyline components and evaluate the suitability of the criteria defined in this paper. It thereby contributes to a rigorous design and application of event-based climate storyline approaches.

## 1. Introduction

In the modern, highly connected and globalized world, the assessment of impacts of past and projected climate change on nature and society needs to extend beyond the local perspective in which adverse climate features are linked to immediate, localized consequences (Hedlund et al., 2018). Impacts from fast (extreme weather) and slow-onset events (van der Geest and van den Berg, 2021) at any location on the planet can be transmitted to remote areas via various physical and socio-economic pathways (Benzie et al., 2019), including trade (exchange and transportation of goods and services), finance (private and public capital), biophysical transfers (such as spatially extensive hydrological systems), and people's behavioral responses. The societal impacts are not only governed by the physical hazard and the resulting effect cascades but are also strongly linked to the societal risk response (Simpson et al., 2021). The COVID-19 pandemic has contributed to a growing awareness of transboundary implications and considerable complexity of systemic risks (Phillips et al., 2020; Ringsmuth et al., 2022), including climate change (Challinor et al., 2017; Gaupp, 2020; IPCC, 2022).

Assessment of impacts resulting from remote climate change features requires an analysis framework that embraces a "systemic risk" approach (Hochrainer-Stigler et al., 2020) and acknowledges complex interactions between risk attributes (Piontek et al., 2021; Simpson et al., 2021). Globalized, systemic shocks originating from extreme weather or climate conditions have been documented and analyzed for a wide range of events, for instance the 2003 and 2010 breadbasket disruption (Gaupp et al., 2020; Falkendal et al., 2021), global supply chain interruptions (Abe and Ye, 2013; Haraguchi and Lall, 2015) and financial exposure (Woo, 2019; Tesselaar et al., 2020). A systemic risk approach includes the need for a comprehensive definition of the system boundaries, relevant climate features, the risk propagation mechanism, quantitative hazard impact evaluation, and specification of alternative scenarios (Carter et al., 2021). It also requires the development of thorough interdisciplinary analytical and modelling approaches that succeed in making the large complexity and uncertainty of impact chains manageable for societal uptake (Piontek et al., 2021).

However, a generalization of complex cascading events, in order to evaluate societal risk or preparedness, is not trivial (Cutter, 2018, 2021). The topic is complicated by the nearly unlimited spatial extent over which risk transmission can take place, and the numerous pathways, triggers, event cascades and dependencies on boundary conditions. A formal probabilistic assessment of the associated risk is virtually impossible: impacts of climate events propagate through a complex and dynamic network of highly conditional cause-effect chains, and quantitative analysis of signal strength and cascading probabilities is conceptually far from being straightforward (Dessai and Hulme, 2004; Stainforth and Calel, 2020).

Alternatively, the exploration of specific risk-transmission pathways can provide useful information on socio-economic sensitivities to remote and cascading climate events, especially when interactions are very complex and subject to many conditional dependencies, which is a form of deep uncertainty (also framed as "radical uncertainty"; (Kay and King, 2020)). For this, well-designed physical climate storylines triggered by specific climate events (Shepherd et al., 2018; Lloyd and Shepherd, 2020; Sillmann et al., 2021) offer a helpful framework for analyzing how impacts can be diagnosed and resilience to climate change can be enhanced. A description of selected historic events that have been experienced by individuals can give more meaningful insights than a quantitative uncertainty assessment across a complex chain of causes and effect (Shepherd and Lloyd, 2021). Event-oriented physical climate

storylines (or in brief: climate event storylines) generate insights that can lead to better preparedness, for instance by developing stress-tests conditioned on plausible and verifiable boundary conditions, or by revealing previously unexplored risk propagation pathways or responses to emerging risks (Baldissera Pacchetti et al.; Albano et al., 2021).

However, similar to probabilistic approaches an effective application of climate event storylines requires a credible and traceable approach to construct them (Stainforth et al., 2007). The number of potential event-chains that could be chosen is infinite, and also the underlying assumptions, tools and metrics require explicit documentation and justification in order to be useful as a resource for climate risk assessments. Therefore, some standardization of storyline construction and evaluation criteria is desirable.

In this paper we outline a development protocol for climate event storylines that is designed to map impacts of global climate features on selected European socio-economic sectors. We propose a generic structure for the definition, engagement and quantitative analysis of the climate event storylines, and include examples of the use of such a protocol in various contexts. The approach is not free of ethical considerations reflecting stakeholder's perspectives and values as they refer to choices of events, impact transmission pathways and analysis protocol (Baldissera Pacchetti et al.). Stakeholder inputs are addressed here in the scoping of the climate event storylines, but a detailed analysis of the ethical aspects is out of scope of this study. However, to facilitate the societal uptake of this scientific information, a set of criteria ("realistic", "relevant" and "risk-informative") has been formulated and evaluated, broadly similar to those proposed by (Cash et al., 2003) for climate services.

We first outline the criteria and core ingredients of the analysis framework in section 2 and elaborate on storyline ingredients and processing steps in section 3, followed by an illustrative description of a number of storylines (section 4). Methodological concepts including the involved data and modelling approaches, and the role of alternative realizations of the storylines – referred to as "counterfactuals" – are described in section 3 and illustrated on a case-by-case basis in section 4. The storylines are constructed using different types of sources of evidence (e.g., models, data, expert judgment) that can be manipulated (perturbed) such that the result assesses the particular context at hand (i.e., societal risk to climate change). We conclude with a reflection on methodological approaches and application domains (section 5), and finally provide further outlooks to the future development of these and related event-based climate storylines.

## 2. Criteria for climate event storylines

In order to be a useful source of information supporting the assessment of climate change implications for a specific target domain, the criteria realism, relevance and risk-orientation are used as guidelines. The construction of "realistic" storylines is promoted by using historic event chains that demonstrated the European exposure to worldwide climatic features in practice, or events generated by models with epistemic reliability (Baldissera Pacchetti, 2021). The description of the impact transmission pathway is guided by the use of observations and witness testimonials focusing on key indicators and processes that characterize the storyline. We use or adapt fit-for-purpose modelling concepts that are evaluated for their ability to reproduce the relevant processes and interactions, and set up experiments that allow reproduction, verification and comparison (see (Baldissera Pacchetti, 2021) for a discussion on quality



dimensions for forward looking regional climate information). Illustrations of choices and evaluation of modelling concepts are given in the storyline example section below.

The “relevance” (or “salience”) of the event storylines is promoted by a number of design principles. First, a storyline scoping and selection process is carried out involving stakeholder insights, documentation of drivers and direct and indirect sectoral impacts of historic events and screening the relative importance of subjects in the socio-economical domain of interest. To allow analysis of the effect of remote climatic features on European sectors, we compare the outcome of multiple versions of constructed storylines with a reference configuration, and one or more “counterfactuals” with perturbed characteristics derived from predefined climate and socio-economic scenarios. A level of standardization across these scenarios is imposed by making explicit linkages to global warming levels and Shared Socio-economic Pathways (SSPs), matching the boundary conditions used in many national or European-wide climate risk assessments (see e.g. (Talebian et al., 2021)). Finally, the representativity of the storylines for stakeholders can be enriched by adding “micro-stories”, illustrating impacts by responses of specific actors related to the stakeholder community.

The climate event storylines are not designed to quantify the probability of the occurrence of impact pathways, which is duly impossible given the complexity of events and their consecutive impact cascade (Sillmann et al., 2021). Rather, the approach focuses on the plausibility (being not demonstrably inconsistent) of the event chains conditioned on specified climatological and socio-economical boundary conditions. They are still designed to be “risk-informative” by revealing or understanding the (sometimes hidden) relationships between climatic hazards and their remote impacts. Also, the storylines support the discovery element in exploratory foresight studies designed for informing present day policy making on future implications (Termeer et al., 2017; Wiebe et al., 2018). The assumptions used to select the storyline components need to be documented in order to allow evaluation of the realism of the findings, and reproduction of the storyline in other contexts and by different analysts. In addition, probabilistic context can be added by quantifying the (conditional) occurrence frequency of large-scale climate features giving rise to the hazard event included in the storyline (Shepherd, 2019).

### 3. Construction of event-based climate storylines

We define climate event storylines as “physically self-consistent unfoldings of past events, or of plausible future events or pathways” (Shepherd et al., 2018; Sillmann et al., 2021). In our context, a sequence of events with an underlying causal relationship forms a logical narrative that links climate hazards at a given location in the world with a socio-economic impact materialized in Europe. The storyline is captured in an analysis framework (using models, data or expert judgment) that can be interpreted, perturbed and explained in the context of a societal risk due to global climate change.

The climate event storylines described here connect geographical domains (of climate hazards and (remote) impacts), time scales (for precursors, events, impacts and response actions), process cascades (combining the physical, economic, ecological and social domains) and actors (including those that are directly impacted in the region of climate hazards, contributing to the impact transmission, and experiencing or responding to remote impacts). (Carter et al., 2021) identified similar connecting elements while exploring an analysis framework for remote climate impact chains. In our study, these elements are brought together in the construction of climate event storylines in order to identify a common structure that spans the entire chain between the remote climatic hazards and the final (socio-

economic) European impact. The common elements are illustrated for each of the selected storyline examples below. They consist of (see Figure 1):

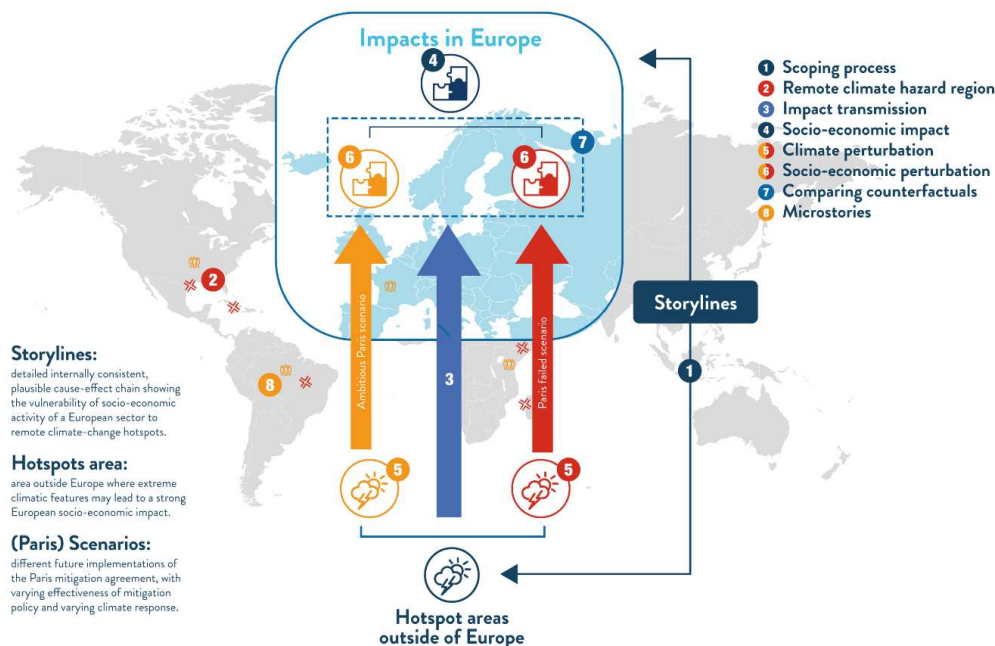


Figure 1 : Design steps for climate event storylines (see text for details)

1. A *scoping process*: from the diversity of historic events, societal sectors and physical and socio-economic transmission pathways, a selection of storylines is made that reveal relevant and recognizable impact transmission pathways. This includes an inventory of interested societal stakeholders, analysis of macro-economic global networks and supply/demand chains, inspiration from recent climate events and evidence of shock propagation in the globalized world. Stakeholder feedback by means of interviews and workshops is sought to collect relevant information on impacts, vulnerabilities and non-climatic drivers that are of interest for climate event storylines. This feedback is subsequently analyzed in conjunction with evidence from “top-down” climate and socio-economic scenario information archives (Berkhout et al., 2013; Cairns et al., 2013);
2. The *remote climate hazard region*: the geographical area where the initial climate triggers are manifested. The selection of hazard regions aims to identify remote regions where climate perturbations have a demonstrable impact on European socio-economic conditions and is carried out using historical evidence or extractions from model projections. Their description includes their causal drivers, hydrometeorological variables aggregated to an appropriate time and space scale, and an assessment of the level of scientific understanding (LOSU) of the link between climate change and their plausibility of occurrence. Climate hazards of interest usually

are common features which are expected to change in intensity/frequency, timing or domain in future climate conditions. Assessment of the likelihood of occurrence in the region is derived from historic observation records, ensembles of model projections, or ensemble techniques exploring alternative event realizations, so-called “downward counterfactuals” (Woo, 2019). However, the hazard occurrence at that location may be unprecedented due to an uncommon hazard pathway, atmospheric circulation pattern or combination of precursors. Multiple hazard regions can emerge simultaneously, for instance by a common large-scale driver such as ENSO or other SST anomaly patterns;

3. The *impact transmission pathway*: the process chain that links the hazard region to the impact on European stability, growth or resilience. The potential pathways vary widely, and can consist of trade networks, supply/demand chains of food and commodities, financial exposure portfolios (by investors, insurance or liability configurations), or geophysical teleconnections (sea level rise induced by remote ice mass loss or impacts cascading across transboundary watersheds) (Benzie et al., 2019). Also, the potential number of methodological approaches to characterize these pathways is large and varies strongly across applications (Piontek et al., 2021). Inputs can for instance be provided by the stakeholder feedback during the scoping phase, or statistical data on, for instance, historic trade records (Kuhla et al., 2021);
4. The *socio-economic impact* of the transmitted disturbances evolving from the remote climate hazard: quantitative measure of consequences for a specified set of societal actors (such as financial damage, anomalies in volume of trade or consumption) are mapped using acknowledged modelling and analysis frameworks. The applied model or data concepts are selected for their ability to define targeted socio-economic metrics for direct or indirect impacts, and to assess dependencies on ancillary conditions (such as different background population, economic structures or financial policies). As for the impact transmission pathway the number of available analysis concepts is large, and selection of these is subject to requirements raised during the scoping phase and stakeholder inputs. Illustrations of model and analysis concepts are provided in the storyline examples below. The combination of the remote climate hazard region, the transmission pathway and the European socio-economic impact metric represents the reference configuration, in which present day (adverse) climate features can be linked to socio-economic impacts;
5. The *climate perturbation*: the purpose of our climate event storylines is to identify impacts of remote climate change. For this the comparison between different climatic background states is organized by construction of a so-called (*climate*) *counterfactual* evolution of the event chain. The construction of perturbed climate event storylines is designed to describe the change of the physical characteristics of the climate feature(s) in the remote hazard region as a plausible response to changing levels of global warming, for which a reasonable LOSU exists (Hazeleger et al., 2015). This can be an observed analogue (for instance in an historic, cooler, climate episode), or a perturbation applied to a modelled representation of the event, for instance by applying a temperature-based scaling (Te Linde et al., 2010), regional modelling (Lenderink et al., 2021), model nudging (Van Garderen et al., 2021), conditional sampling of circulation patterns (Zappa and Shepherd, 2017) or analogue hazards (Hegdahl et al., 2020; Schaller et al., 2020), statistical resampling (Ward et al., 2014; Li et al., 2018) and other techniques. The comparison of different unfoldings of events is inherent to various techniques for climate event attribution (Hannart et

al., 2016; van Oldenborgh et al., 2021), including the analysis of the attribution of impacts of these events (see for instance (Mengel et al., 2020));

6. *A socio-economic perturbation*: as indicated in step 4 (socio-economic impacts), changes in the socio-economic background state may strongly affect the European impacts of remote climate hazards. This can include trends in economic structure, population or implementation of adaptation measures. To promote consistency across storylines or benchmarking against widely used global socio-economic projections, local interpretations of Shared Socio-economic Pathways (SSPs) (O'Neill et al., 2014) are carried out. SSPs sketch the global evolution of macro-economic and social indicators (such as GDP, population, industry, land use) following a set of narratives on global cooperation, technology and energy consumption. In many national or regional assessments of future socio-economic developments these SSPs are interpreted for the local context, feeding into projections of spatial developments, employment, mobility, economic structure and other attributes (Frame et al., 2018; Talebian et al., 2021). These downscaled projections usually don't include recursive or planned (adaptation) responses to environmental or socio-economic developments (Andrijevic et al., 2020; Chen et al., 2020). Responses to socio-economic impacts arising from (remote) climate pressures, such as implementing adaptation policies or changing exposure or vulnerability to high-impact shocks may be included in the socio-economic perturbation that is part of the counterfactual event-based storyline, depending on the application scope of the storyline (see subsection on "storyline application domain" below);
7. *Comparison between reference and counterfactual(s)*: a reference storyline is defined to document the baseline (current) transmission pathway that sets the scope of the analysis. One or multiple counterfactuals allow to explore impacts of perturbed climatological or socio-economic conditions on the baseline impact pathway, leading to a "climate change narrative". Quantitative and qualitative understanding can be derived from following the altered background state through the storyline components: a perturbation of the triggering climate features (an imposed link to global warming) may or may not lead to significant changes in the local impact, downstream transmission, or socio-economic impact, depending on assumptions on specific properties of the causal network chain and its dynamic responses. This requires a careful selection of data and models used, a thorough documentation of conditions and assumptions, and a targeted experimental (model) design to generate the reference and counterfactual storylines;
8. *Accompanying micro-stories*: these are complementary narrative elements to enrich the climate event storylines by providing additional detail or context. The event storylines usually contain events, transmissions and impacts whose selection is highly conditional, rendering the storylines adaptable for alternative representations, sensitivities to choices, and diversity in perspectives. "Micro-stories" can be helpful to make occasional excursions from the main storyline narrative, for instance to explore the sensitivity of the processes in the event-cascade to subtle changes in the used assumptions. Also inputs from individuals and stakeholders, for instance "witness reports" from people affected by historic event impacts, or stakeholders involved in the design in impact assessment or adaptation, may be added as micro-stories to the storyline package (see for instance (Jack et al., 2020)).

#### 4. Overview of illustrative storylines

To illustrate the common storyline elements discussed above we describe three storylines in detail:

- Concurrent drivers of disrupted food security in the Horn of Africa;
- Impacts of tropical cyclones on the European Union Solidarity Fund (EUSF);
- Soybean production for European food supply.

The three storylines together encompass a wide range of geographical, climatological and socio-economic contexts. However, the collection of potential scopes of these storylines is virtually unlimited. To provide additional illustration we also describe three additional storylines briefly, providing cross-references to published documentation.

Each storyline describes sector-specific socio-economic impacts of remote climate change features and the insights derived from it. Approaches, modelling concepts, scenario choices and application domains are outlined following the logic of the protocol steps and summarized in a dedicated table. Section 5 reflects on methodological approaches and application domains of the event storylines.

##### Storyline #1: Concurrent drivers of disrupted food security in the Horn of Africa

*Scoping process.* Beneath conflict and social instability, many countries in the Horn of Africa are facing frequent drought- or pest-induced domestic harvest failures, which, in combination with relatively small grain reserves (Laio et al., 2016), makes them dependent upon grain imports, or even food aid in crisis situations (ICPAC and WFP, 2018). Food security and humanitarian wellbeing in African (and other) countries are relevant to a wide range of European policies concerning development aid and humanitarian support (such as the formal partnership agreements with the African, Caribbean and Pacific states, ACP (Hurt 2003)). However, potential impacts of climate change are very strongly intertwined with compounding pressures and responses, and an analysis of the “net” impact of climate change on food security is far from straightforward. Therefore, a storyline is developed that analyzes the local food security crisis during the 2019/2021 locust outbreak in the region but put in the context of a compounding weather-induced global food price crisis of the year 2007/08 that explores the unfolding of a local food security crisis in a different climatic context. The main short-term driver of the 2007/08 crisis was compounding weather-induced crop failures of the main food crops wheat, maize, and rice in several main producing regions. In response to the resulting production failures, world market prices rose, and market uncertainties increased. In response, many import dependent countries raised unilateral and uncoordinated export restrictions to protect their domestic consumers by insulating them from the price hikes in global markets (Trostle et al., 2011; Challinor et al., 2018). These restrictions further aggravated the crises, especially for import dependent low-income countries in Africa and Asia and pushed an estimated 63 to 80 million people into food insecurity, and sparked food riots around the globe (Tiwari and Zaman, 2010).

We consider two counterfactual storylines, one where the local locust-induced production failures coincide with the global production failures of the 2007/08 crisis, and another where we additionally consider the impact of the escalating export restrictions of the 2007/08 crisis. The scoping process of this storyline was driven by analyses of food security statistics, revealing national and regional cereal import dependencies of countries rendering them vulnerable to global supply failures and associated price hikes at international markets (Figure 2).

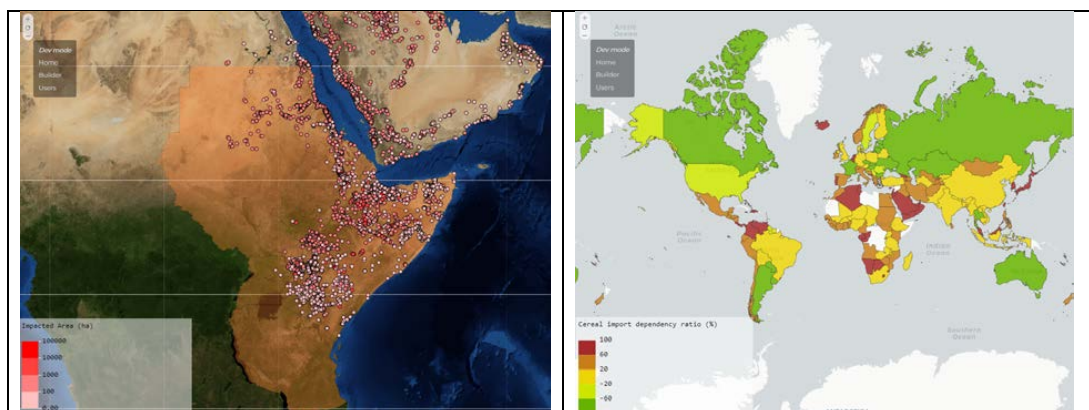


Figure 2: Source material used for the scoping of the storyline addressing food security crisis in Greater Horn of Africa and Arabic peninsula. Left: area impacted by locust infestation during 2019/21 (source: (FAO, 2021)); Right: global cereal import dependency ratio in 2017 (source:(FAO, 2017)).

**Remote climate hazard region.** In the **reference scenario**, we consider the food security risks from locust-induced crop failures in the Greater Horn of Africa region experienced in 2019. Desert locusts found ideal breeding conditions on both sides of the Red Sea due to three landfalling tropical cyclones bringing unusual amounts of precipitation. Additionally, response measures were delayed by the COVID-19 pandemic, and large swarms were able to form that spread not only across the Horn of Africa region but also across the Arabian Peninsula and Southeast Asian Countries.

**Impact transmission pathway.** The impact transmission of the regional food security crises to the EU is governed by historically grown trade dependencies (d'Amour et al., 2016) and development cooperation (Langlois, 2014). Global production of main food crops such as wheat, maize, and rice are concentrated in a few main breadbasket regions such as the EU. The resulting import dependencies of many developing countries of the Global South such as countries in the Greater Horn of Africa, render these countries vulnerable to remote supply failures and associated price hikes at world markets. Further, many people in these countries strongly depend on international humanitarian aid for their well-being. For instance, in 2020 and 2021 the European Union allocated nearly €200 million for a broad humanitarian-development approach, from which more than €20 million were mobilized to support the United Nations and partner countries in fighting the locust infestation (European Commission).

**Socio-economic impact.** The socio-economic impact is measured with various metrics: 1) world market price volatility (a potential precursor for insufficient accessibility to food); 2) impaired supply at the national level arising from the harvest failures and export restrictions (which urges countries to tap into their reserves or rely on international markets or humanitarian aid); and 3) the ratio of impaired supply to reserves (an indication for risk to limited food availability at the national level; see Figure 2).

**Climate perturbation.** To assess the vulnerability of the Greater Horn of Africa to a (plausible) worst-case combination of local and global food security crises, we superimpose the global production anomalies of the 2007/08 world food price crisis with the locust-induced production failures for 2019/21. In this way, the climate perturbation is applied by combining the food trade and production conditions in the region where the locust infestation was dominant with the implications of the multi-breadbasket failure

experienced during the major global food crisis of 2007/08. This defines a **first counterfactual storyline** for this analysis: what if the 2019/21 locust infestation would have occurred simultaneously with the production failures of 2007/08? (Gaupp et al., 2019) analyzed potential impacts of further global warming to 1.5 or 2°C on the likelihood of simultaneous crop failures and found that global wheat production failures are particularly sensitive to the degree of global warming. In the current storyline set-up these future warming levels are not explicitly imposed, but the counterfactual combining a factual 2019/21 reference scenario with the 2007/08 global production failure serves as an indication of event cascades impacted by global warming. This climatic counterfactual storyline involving a global food supply failure does not have a single climate hotspot but is linked to modes of climate variability with the potential to disrupt near-simultaneously cereal production in the major breadbasket regions around the world, specifically El Niño-Southern Oscillation, the Indian Ocean Dipole, Tropical Atlantic Variability, and the North Atlantic Oscillation (Anderson et al., 2019; Gaupp et al., 2020).

*Socio-economic perturbation.* There was no strong and coordinated response of the international community to the 2007/08 world food crisis. Many exporting countries wanted to make sure that they protected domestic consumers from high world market prices, so they overreacted by raising export taxes and imposing severe export restrictions. This further reduced the grain availability at world markets, drove the prices high, and had unintended consequences of exacerbated hunger in the Greater Horn of Africa. A socio-economic perturbation is therefore addressed in a **second counterfactual storyline**: what if the 2019/21 locust infestation would have occurred simultaneously with the production failures of 2007/08 and the uncoordinated export restrictions?

*Comparison between reference and counterfactual(s):* The comparison of counterfactuals allows the evaluation of the effectiveness of regulating the unilateral policy responses on the food security indicators. The analysis of the local locust infestation of 2019/21 shows that the locust infestation had severe impacts on food security at the Greater Horn of Africa, which however remained limited to this region. From the two counterfactuals, we see that the compounding impact of local and global food security crises can be devastating. Grain supply for many import-dependent middle- and low-income countries in Africa and Asia would be reduced by one-third. Food security consequences would be especially severe for countries in the Greater Horn of Africa being struck in parallel by locust-induced production declines. Many import-dependent countries would not be able to buffer the failures with their own reserves and may not be able to buy grain at world markets due to prices reaching the level of the 2007/08 crisis. This highlights the importance for the international community to ensure food deliveries and aid for vulnerable populations in import-dependent developing countries.

*Micro-stories* allow assessing food security implications at the sub-national level using the INFORM Severity Index framework (Poljanšek et al., 2020). This framework also allows analyzing the impact of compounding crisis situations such as the ongoing conflict in Ethiopia as well as the efficacy of different humanitarian response options.

*Implications and application:* The analysis reveals that the global food security implications of the 2007/08 multi-breadbasket failures would be strongly exacerbated by the escalating export restrictions. Already the export restrictions of a few key middle-income exporters such as Argentina, Russia, and Ukraine are enough to jeopardize food security, globally. This highlights the importance for the international community to provide targeted help to these vulnerable key exporters. There needs to be a global coordinated effort to reduce market uncertainties and keep markets open in times of crisis. The



analyses show that substantial mitigation potential exists in better coordinating policy responses in times of global food crises (Falkendal et al., 2021).

Integration and dissemination of the information in this storyline via the INFORM Severity Index framework ensures its propagation to a range of INFORM partner organisations. The INFORM platform is operated by the European Commission Joint Research Centre and is coordinated by the United Nations Office for the Coordination of Humanitarian Aid (UN-OCHA, 2023).

A summary of methodological approaches for this storyline is given in Table 1.

Table 1: Overview of modelling options and data sources of information for the Africa food security storyline

Storyline development step	Modelling approach	Data sources
1. Scope	Risk indices (INFORM), stakeholder input	Statistics on food security and trade are released by FAOSTAT (FAOSTAT, 2021), World Bank (Worldbank, 2021), and USDA's PSD database (USDA, 2021)
2. Remote climate hazard regions	Local and global crises in the Greater Horn of Africa <i>Local crisis:</i> The 2019/21 locust infestation <i>Global crisis:</i> The 2007/08 world food crisis	Statistics on food security and trade are released by FAOSTAT (FAOSTAT, 2021), World Bank (Worldbank, 2021) and USDA's PSD database (USDA, 2021)
3. Impact transmission	The Greater Horn of Africa region is highly vulnerable during global food crises, and the EU is one of the main providers of humanitarian aid to the region.	Data on bi-lateral aid flows are provided by the Financial Tracking Service of the United Nations' Office for the Coordination of International Affairs (UN-OCHA, 2023)
4. Socio-economic impacts	Three impact metrics: 1) World market price volatility; 2) National level impaired supply arising from the harvest failures and export restrictions; and 3) The ratio of impaired supply to reserves.	A global model for world market prices of staple crops accounting for trade policies and storage (Schewe et al., 2017) and a food supply network model (Falkendal et al., 2021)
5. Climate perturbations	In 2007/08, drought conditions in several breadbasket regions reduced grain production globally. Such multi-breadbasket failures are projected to become more frequent under global warming.	FAOSTAT (FAOSTAT, 2021) and USDA's PSD database (USDA, 2021)
6. Socio-economic perturbations	In response to the multi-breadbasket failures of 2007/08 many exporting countries restricted exports aiming to ensure food security domestically. This dramatically reduced grain availability at world markets leading to price spikes and had unintended consequences of exacerbated hunger in the Greater Horn of Africa.	The Agricultural Market Information System (OECD, 2023) provides information on export restrictions during the 2007/08 world food price crisis
7. Comparison	<i>Reference</i> – The factual locust infestation of 2019/21	

THE FORMALIZATION OF STORYLINES

reference/counterfactual	<p><i>Counterfactual #1</i> – what if the 2019/21 locust infestation occurred simultaneously with ONLY the production failures of 2007/08</p> <p><i>Counterfactual #2</i> – what if the 2010/21 events occurred simultaneously with the production failures AND the export restrictions of 2007/08</p>	
--------------------------	--	--

Storyline #2: Impacts of tropical cyclones on the European Union Solidarity Fund (EUSF)

*Scoping process.* An extraordinarily active Atlantic hurricane season in 2017 (Klotzbach et al., 2018) directly affected the European Union’s outermost regions in the Caribbean. Particularly the island of St Martin (French overseas collectivity) and Guadeloupe were strongly hit by hurricanes Irma and Maria, with severe damage to human life, property and mangrove ecosystems (Walcker et al., 2019). The events in the Caribbean and mainland Europe are connected to the European Union (EU) via the European Union Solidarity Fund (EUSF) (Hochrainer-Stigler et al., 2017) which arranges payouts to member states (including their overseas territories) in response to disasters due to extreme natural hazards such as floods, forest fires, earthquakes, storms and droughts. In 2017 payouts due to disasters in the Caribbean and (particularly) the earthquakes in central Italy led to a potential negative EUSF capital position, which was avoided by using capital originally allocated for 2016 and 2018. This occasion triggered the question whether alternative, unprecedented yet plausible, realizations of past hurricane events could have compromised the EUSF. If so, this may reveal weak spots in the system impact causal chains and serve as guidance for further stress-testing under climate and socio-economic changes. This question is not readily answered by following generic probabilistic climate attribution approaches (Frame et al., 2020), but acknowledges the highly conditional problem statement required for this particular context. During the scoping process of this storyline, procedures for the assessment of risk of the EUSF capital being compromised were explored. Possible situations were investigated in which the EUSF would not be able to fund recovery and emergency operations efforts; the identification of such scenarios can be helpful to prevent the depletion of the fund. To this aim, alternative hurricane trajectories (or “downward counterfactuals”, (Woo, 2019)), generated with natural catastrophe assessment models, were used to develop storylines of spatial and temporal compound events (Ciullo et al., 2021).

*Remote climate hazard region.* The remote climate hotspots for this storyline are the hurricane-prone territories of the Eastern Atlantic (Canary Islands, Azores, Madeira), Western Atlantic (Saint Martin, Guadeloupe, Martinique and French Guiana) and the West Indian Ocean. In 2017, the hurricane season was active with 17 storms, including Irma and Maria; EUSF contributed €48.9 million to recovery efforts. However, other tropical cyclones almost led to damages in the EU overseas territories in the Eastern Atlantic and the West Indian Ocean. The annual number of hurricanes in these areas varies considerably (Knapp et al., 2010), and overall, there is no clear trend in the observed frequency of hurricane development. However, an increasing trend in intensity with global warming is becoming apparent (IPCC, 2021).

*Impact transmission pathway.* The impact transmission of the intense hurricane season in the EU overseas territories reaches the European continent via (among others) the payout scheme of the EUSF.

*Socio-economic impact.* For this storyline, the main impact indicator is the capital availability of the EUSF fund, particularly the possibility of the fund not having enough capacity to cope with requested payouts. The amount that EUSF pays is based on recorded damages and the GDP of the affected region. If payouts are higher than the funds available, the EUSF can no longer fulfill its function. This scenario may become reality if multiple disasters coincide and/or persist over consecutive years.

*Climate perturbation.* The historic damage recorded for the tropical cyclones Irma and Maria was nearly €2 billion, and the EUSF sent nearly €50 million in aid. Meanwhile, efforts to recover from the major earthquakes in Central Italy received €1.2 billion from EUSF.

Figure 3 shows that in 2017 the funds dipped below €0. The EUSF coped with this by exceptionally anticipating funding allocated to 2018. With only €294 million in funds available for disaster relief this was left without major consequences as there were minimal payouts in 2018.

The storyline explores what could have happened if large payouts due to the 2017 earthquakes in Italy coincided with even more tropical cyclone damages abroad in 2017/18. The plausibility of this counterfactual scenario is illustrated by some near-misses in the 2017/18 season. Three hurricanes occurred in the Eastern Atlantic (Ophelia, 2017) and in the West Indian Ocean (Enawo, 2017, and Berguita, 2018). Luckily, these hurricanes did not make landfall on EU outermost regions. The construction of downward counterfactuals showed that they could have reached these territories, and could have been disastrous enough to require EUSF aid. In that case the fund would not have been able to help. Due to the costly earthquakes in Italy, the EUSF's capital was depleted in 2017. Had the large payouts due to the 2017 earthquakes in Italy coincided with even more tropical cyclone damages abroad in 2017/18 would have resulted in nearly €500 million in deficit (orange line in Figure 3).

Climate perturbations are used to simulate such “alternative past” tropical cyclones. The perturbations are applied in two steps. First, interesting cyclone tracks are selected from a catalog of historic events and their alternative trajectories. The selection is made based on the maximum damage the alternative trajectories may cause in one of the target regions. The second step addresses global warming. With 2°C global surface warming, the intensity of tropical cyclones may increase by up to 10% (Knutson et al., 2021). This general range of intensity increases was used to simulate various tropical cyclones. The level of scientific understanding of the relationship between ambient atmospheric and oceanic temperatures and hurricane intensity justifies the exploration of intensified hurricanes and their potential damage via an adopted hurricane intensity range setting up a range of climate counterfactuals.

*Socio-economic perturbations* are applied by adopting different levels of (future) GDP to the overseas target regions, which affects the value of exposed objects to extreme events and the calculated EUSF payouts. Average GDP in the EU has increased by about 20% since the EUSF was established in 2002. A range of increases in GDP of 0% up to 20% was used to simulate future socio-economic changes. In addition, policy changes are explored by changing the capitalization of the EUSF. The available EUSF capital depends on the amount contributed to it by EU member states. Currently, the EU annually contributes €500 million. Future increases between 0% and 150% were analyzed.

## THE FORMALIZATION OF STORYLINES

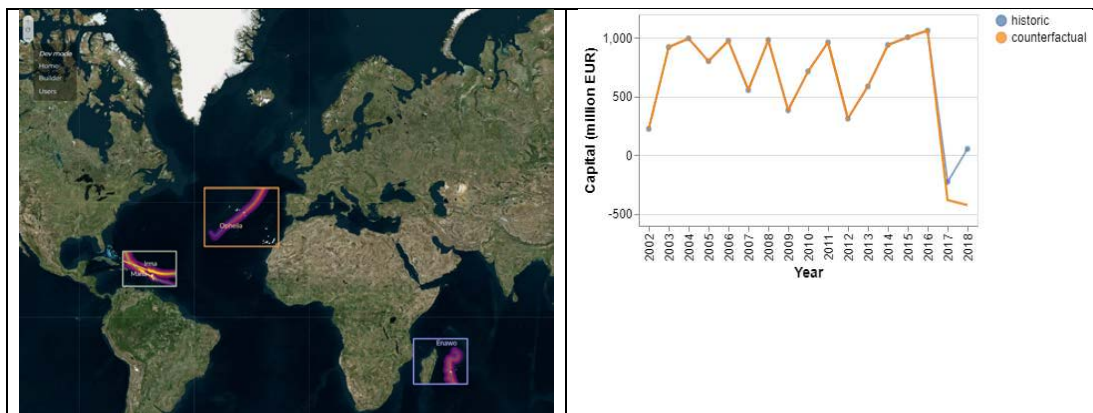


Figure 3: Left: remote climate hazard regions for the EUSF storyline with historic and reconstructed cyclone pathways; right: development of historic and counterfactual capital level of the EUSF fund (Ciullo et al., 2021)

Direct economic damages from tropical cyclones were estimated using the CLIMADA impact model (Aznar-Siguan and Bresch, 2019). Direct damages were assessed as a function of weather-related hazards, exposure of people and goods to such hazards, and vulnerability of the exposed entities. The exposed economic value was calculated by downscaling regional GDP using nighttime lights data.

*Comparison between reference and counterfactual(s):* The comparison of counterfactuals allows mapping the boundaries of the tolerable operating space of the EUSF. The counterfactuals incorporate a range of increased hurricane intensity levels (0% up to 10%), GDP increases of 0% up to 20% and annual EUSF capital increases of 0% up to 150%. Critical EUSF capital conditions will occur when in subsequent years rare (and high-damage) events are combined.

The analysis of the occurrence of the historic storms Irma and Maria together with the “alternative past” tropical cyclones Enawo, Ophelia and Berguitta, reveals that the European Union Solidarity Fund (EUSF) capital may undergo severe stress unless the fund is recapitalized. When the fund is not additionally capitalized, the EUSF may be in deficit by up to €1 billion. A 50% increase in EUSF capital may result in either a surplus or a deficit in the availability of funds, depending on the considered counterfactual. The capital level in 2017 is sufficient for all scenarios when the funds are increased by 150% per year in capital. However, there are trade-offs underlying the policy negotiations for this level of capitalization increase.

Potential *micro-stories* can relate to the longer-term impact on these small islands of such worst-case events and focus on the long-term sustainability of these regions.

*Implication and application:* Payouts due to tropical cyclones can deplete the EUSF fund if large payouts abroad occur concurrently with disasters in mainland Europe. In a 2°C warmer world in which cyclones are more frequent and more intense, it is wise to anticipate fund depletion. In 2021, the tasks of EUSF tasks have been transferred to the Solidarity and Emergency Aid Reserve (SEAR). The results of this storyline can inform how SEAR can cope with maintaining sufficient funds given the increasing climate risks. This storyline shows that the EU should increase disaster funds by at least 50%.

A summary of data and modelling concepts is given in Table 2.

Table 2: Overview of modelling approaches and data sources of information for the European Solidarity Fund storyline

Storyline development step	Modelling approach	Data sources
1. Scope	Recent Atlantic hurricane season in 2017 and related EUSF payouts	Historic payouts from the European Union Solidarity Fund (European Commission, 2023)
2. Remote climate hazard regions		Hazard data about historic tropical cyclone tracks are retrieved from the International Best Track Archive for Climate Stewardship (IBTrACS) dataset (Knapp et al., 2010). Hazard data on counterfactual tropical cyclones are simulated by using forecast data retrieved by the THORPEX Interactive Grand Global Ensemble (TIGGE) program (Swinbank et al., 2016).
3. Impact transmission	Natural catastrophe assessment model CLIMADA (Aznar-Siguan and Bresch, 2019)	Nightlight data from the the DMSP-OLS Nighttime Lights Time Series (Lloyd, 2016) provided by NOAA until 2013 and NASA's Black Marble data (Román et al., 2018) after 2013. Vulnerability functions are provided by (Eberenz et al., 2021)
4. Socio-economic impacts	Capital availability of the EUSF fund is simulated, based on the fund's payouts and capitalization rules.	
5. Climate perturbations	Tropical cyclones' intensity increases	Tropical cyclone intensity can increase between 1 % to 10 % in a 2-degrees warmer world based on expert knowledge (Knutson et al., 2020).
6. Socio-economic perturbations	<i>Socio-economic</i> : derived from GDP projections <i>Policy</i> : increase in the fund's annual capitalization	<i>Socio-economic</i> : Increase up to 20%, based on the average GDP increase registered in Europe since the establishment of the fund (i.e., 2002) assessed using regional GDP data taken from (EUROSTAT, 2023)  <i>Policy</i> : Annual capitalization increase up to 150 %, based on the pre-2014 reform capitalization levels
7. Comparison reference/counterfactual	<i>Reference</i> : combination of historic tropical cyclones (Ciullo et al., 2021)  <i>Counterfactuals</i> : simulated scenarios with ranges of combinations for: <ul style="list-style-type: none"> <li>• exposure increases due to potential increases in tropical cyclone intensity of 0% up to 10%</li> <li>• GDP increases of 0% up to 20%</li> <li>• EUSF annual capital increases of</li> </ul>	

	0% up to 150%	
--	---------------	--

### Storyline #3: Soybean production for European food supply

*Scoping process.* The vast majority of all soybeans consumed and processed in Europe is produced in areas concentrated in the Midwest US, Brazil and Argentina, together accounting for over 90% of the total global soybean export (Wellesley et al., 2017). These main soybean production areas are exposed to varying patterns of climate variability and trends, having pronounced impacts on regional production volume and world trade volumes (Anderson et al., 2017; Torreggiani et al., 2018).

In addition, various societal responses to climate and environmental change affect the sector strongly. Rainforest conservation policies in importing countries impose additional criteria on the spatial extent of soybean exploitation and are considered to constrain options of producers to expand or transfer production regions (Gibbs et al., 2015; Heilmayr et al., 2020; Bager et al., 2021). Also changes in dietary preferences in importing countries may affect demand and hence trade volumes and prices (Willett et al., 2019; Ortiz et al., 2021).

This climate event storyline explores the potential climate change impact on temporary production declines in major soybean producing areas in the US and South America. It reconstructs a number of weather-induced soybean losses that occurred in 2012 and their impacts on global and European prices, trade and consumption patterns, and explores how these events could unfold in a future warmer world. In addition, counterfactual storylines also account for impacts of diet changes towards less meat consumption and forest conservation policies. The scoping process was guided by a consultation with NGOs representing local soybean producers, shaping the analysis of local climate impacts and the various counterfactuals.

*Remote climate hazard region.* A survey of global climate hotspots for agricultural drought in major food production areas (Ercin et al., 2019) contributed to the selection of the remote target regions and identification of climatic drivers of yield losses in South America and US. Weather events in Brazil, Argentina and the US affect the EU through soy transmission links, as was seen in the 2012 drought and the correlated trade responses. The storyline focuses on the 2011/2012 growing season which displayed an unprecedented loss in soybean yields that resulted from a combination of low precipitation and high summertime temperature in the US (Goulart et al., 2021; Hamed et al., 2021) (see Figure 4).

*Impact transmission pathway.* The dramatic increase in global demand for soybeans has led to a surge in supply from Brazil and Argentina. Large shares of agricultural land in both countries produce this crop, often at the expense of highly biodiverse areas. The concentrated production to these regions makes soybeans vulnerable to large shocks related to weather and crop disease. Consequently, the entire supply chain is vulnerable to disturbances in the local production sides. The EU is highly dependent on soybean as a livestock feed, for biofuels and in the food industry. Each year, the EU imports 14 million tons of soy, making it the second biggest importer worldwide and thereby highly vulnerable to global shortages.

*Socio-economic impact.* Soybean shortages lead to different socio-economic impacts, including shocks and anomalies on commodity prices, trade, imports and exports, consumption, and food security risk around the world. These socio-economic impact metrics are assessed with the global biosphere

management model GLOBIOM (Havlík et al., 2014; Soterroni et al., 2018; Jägermeyr et al., 2021), and here include changes in bilateral trade flows, prices and value added, and changes in the consumption of soy for food, feed and other products (see Figure 4 for an illustration).

*Climate perturbation.* A simulation of yield loss for future weather anomalies similar to 2012 was carried out for different global warming scenarios. From scenario simulations of the UKESM1-0-LL model (Sellar et al., 2019) under two Representative Concentration Pathways (RCP2.6 and 8.5), 30-year time slices were selected around the mid-century (2035-2065) and the late century (2066-2096). These climate simulations were used to simulate yield anomalies using the crop model EPIC-IIASA (Balkovič et al., 2014). Climate counterfactuals are created by selecting extreme events defined as seasons with equivalently large yield losses from the selected time slices for selected global warming levels (2.5°C and 3°C relative to the pre-industrial mean global temperature).

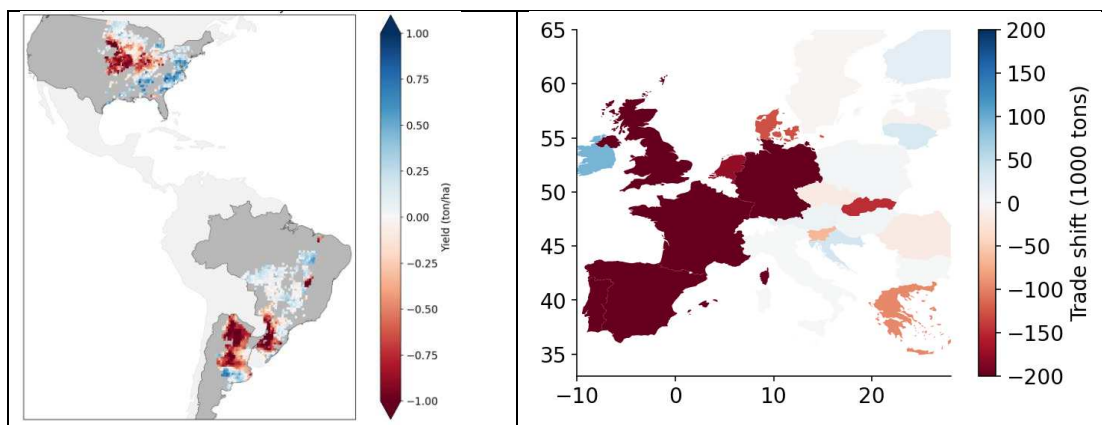


Figure 4: Left: 2012 production shock of soybean in major producing areas relative to the 2000/15 mean (source: (Goulart et al.)); Right: Changes in imported soybeans by European country in 2013 compared to the average of the 2011/15 period. Source: BACI bilateral trade data (Gaulier and Zignago, 2010)

*Socio-economic perturbation.* A number of socio-economic counterfactuals were designed to explore the impact of implementation of alternative policies: i) a “diet-oriented policy”, where EU citizens change to a more plant-based diet to reduce their livestock consumption by 50% as of 2030 (reducing the dependency on soy imports), and ii) “no deforestation perspective”, which enforces producer countries to prohibit conversion of primary forests to cropland (as of 2030 in the US, Argentina and Brazil). Socio-economic calculations were carried out using the GLOBIOM model forced with a SSP2 emission scenario (Havlík et al., 2014).

*Comparison between reference and counterfactual(s).* The different climate and societal alternatives reveal several relevant impacts. In the 2011/2012 reference scenario, European imports of soybeans decreased by 11% compared to the year 2010. At the same time, producer prices in Europe increased by 21%. Under the warmer climate counterfactuals larger soybean production losses are generated, cascading into larger market distortions. A “diet-oriented policy” reduces the European dependency on soybean consumption for its own markets. A “no deforestation policy” will modify the geographical distribution of local production regions. A reduced market sensitivity to climate impacts can be a result

## THE FORMALIZATION OF STORYLINES

of protecting drought prone regions which currently contribute significantly to the trade volume to the EU.

*Micro-stories* can be used to describe specific implications for one of the many actors in this sector, for instance addressing conflicts on water use in soybean production areas with other sectors under sustained drying (Flach et al., 2020), shifts in employment in the agri-food business both in production areas and within Europe, drought impacts on domestic transportation (Marengo et al., 2021), risk of depreciated investments (Chain Reaction Research, 2018), trends in predictability of climatic and technological impacts on yields, the interactions between regional deforestation and increased magnitude and frequency of soybean losses (Flach et al., 2021) and the role of carbon pricing to reduce deforestation pressures.

*Implication and application:* a climate-induced reduction in soybean supply to the EU leads to an increase in prices of both meat and soybeans and therefore leads to a decrease in consumption. The “no deforestation policy” helps mitigate negative environmental impacts in the production areas from soybean trade. If successful policies and adaptation measures are adopted the future impacts of extreme events will be considerably reduced.

Table 3 shows an overview of the models and concepts used for this storyline.

*Table 3: Overview of modelling approaches and data sources of information for the soybean production storyline*

Storyline development step	Modelling approach	Data sources and references
1. Scope	Trade statistics. BACCI bilateral trade data (Gaulier and Zignago, 2010) were used to calibrate the GLOBIOM model to the historical reference event.	FAOSTAT statistics (FAOSTAT, 2019) were used to assess import dependency
2. Remote climate hazard regions	Climate reanalysis archives and hydrological water resource modelling are used to generate spatial distributions of soybean production areas, water footprints (water use intensity) and agricultural drought.	Ercin et al. (2019). SPAM data (SPAM, 2019) and subnational statistics were used to identify harvested areas.
3. Impact transmission	The weather to crop yield variability transmission was done with a hybrid data/forecast model, combining machine learning and outputs from the global gridded crop model EPIC-IIASA.  The impact transmission of socio-economic dynamics was simulated with the GLOBIOM model.	(Balkovič et al., 2014; Havlík et al., 2014; Goulart et al., 2021)
4. Socio-economic impacts	Socio-economic impacts were simulated using the global biosphere management model GLOBIOM	(Havlík et al., 2014; Soterroni et al., 2018; Jägermeyr et al., 2021).
5. Climate perturbations	Simulated soybean yields are generated by EPIC-IIASA, with climatological forcing from UKESM1-0-LL model under RCP 2.6 and 8.5 for mid 21 <sup>st</sup> century.	CMIP6/ISIMIP3B model ensemble, UKESM1-0-LL (Sellar et al., 2019)
6. Socio-economic perturbations	Alternative socio-economic scenarios are imposed by driving the GLOBIOM model with SSP2	(Havlík et al., 2014)
7. Comparison	<i>Reference</i> – the anomaly of the 2011/2012 season	



reference/counterfactual	relative to a 30-yr time series of selected metrics.  <i>Physical counterfactuals</i> – anomaly of 2011/2012 combined with the expected mean yield at a 2.5°C and 3°C warming relative to pre-industrial.  <i>Socio-economic counterfactuals</i> – “diet-oriented policy” / “no deforestation policy”	
--------------------------	---	--

Short descriptions of other storylines involving complex impact cascades

Apart from the collection of illustrative storylines described above, an increasing number of storyline studies appear in scientific literature. Below a small sub-selection is presented without the elaborate description of each of the storyline ingredients.

**Impact of TC landfalls in the US on European consumption and trade.** Major tropical cyclones making landfall – besides causing devastating local damage and economic losses (the direct impact) – can result in macro-economic trade shocks and ripples through trade loss propagation (indirect impact). (Middelani et al., 2021) analyzed the potential indirect impact on global (final) consumption by the New York/New Jersey landfall of hurricane Sandy (2012), showing that both downstream and upstream interactions can result in losses or gains of consumption in other parts of the world that are not directly affected. (Middelani et al., 2022) focused on shock propagation in the trade network induced by the direct effects from the landfall of tropical cyclone Harvey (2017) and its global indirect economic repercussions, including impacts on the European economy. These studies include an impact assessment of climate change due to the response of intensity and size of tropical cyclones to global warming. Propagation and cumulative economic shocks by tropical cyclones are specific to many attributes of the event cascade. An event storyline built using a trade network modelling framework supports the mapping and quantification of climate changes footprints on specific steps in the impact cascades.

**Flood-induced displacement caused by Tropical Cyclone Idai.** (IPCC, 2022) concluded with high confidence that climate and weather extremes in all world regions are increasingly determining human displacement and contributing to humanitarian crises where hazards overlap with high vulnerability. Beyond financial considerations, the EU’s responsibility to protect people from vital threats also requires that displacement risk, and the means to reduce it, is factored into EU policymaking. Displacement can lead to a cascade of mutually reinforcing effects, increasing urbanization stress and fueling internal or transboundary conflicts (Desai et al., 2021). A tool to assess different drivers of humanitarian risk is the INFORM Risk Severity Index (Poljanšek et al., 2020). An analysis of the 2019 landfall of tropical cyclone Idai in Mozambique triggered national and international disaster relief funding and interventions of NGOs including the International Red Cross Red Crescent Movement. Apart from COVID19 and various reasons for blocking access to humanitarian relief resources, the effect of climate change features on the specific INFORM risk assessment were analyzed using dedicated event storylines by (Mester, B. et al., 2023). A set of historical counterfactuals is created by removing the effects of anthropogenic climate change on storm intensity and sea level, which are main drivers of coastal flooding and its consequences.

**Impacts of Storm Xaver on infrastructure damage in German Bight.** Global warming and sea level rise will continue to increase the frequency and severity of flood hazards across European coastal regions.

Together with continued development of the coastal floodplains, coastal risk is projected to grow by a factor of two by 2050 (Jongman et al., 2014). Storm Xaver made landfall in the German Bight on 6 December 2013. The coinciding surge and tide created “record breaking water levels for large parts of the southwestern German North Sea coastline” (Dangendorf et al., 2016), which boosted the estimate of the water level with a 1:200-year probability exceedance by 40 cm. Although the storm led to large direct damage in United Kingdom (UK), Netherlands, Germany and Denmark (Wadey et al., 2015; Rucińska, 2019), the considerable improvements in coastal protection and disaster risk reduction management significantly reduced the total damage and number of people affected compared to a similar storm in 1953 (Spencer et al., 2015; Wadey et al., 2015). Both the large anomaly of the storm and the complex cascade of impacts (particularly relating to the macroeconomic losses from long-term business interruption, damage to transportation networks and other critical infrastructure) create deep uncertainty that is difficult to assess using probabilistic approaches. A storyline analysis by (Koks et al., 2023) quantified the local direct physical damages to critical infrastructure and the (indirect) macroeconomic losses due to infrastructure failure for different sea level scenarios, developments of the spatial extent of risk prone assets and adaptation strategies.

## 5. Reflection on methodological approaches and application domains of event-based storylines

This gallery of climate event storylines illustrates the wide diversity of impact-pathways of climate change features. The pathways connect locations separated by long distances via complex physical and socio-economic cause-effect chains propagating over multiple time scales. Diagnosing the impact of climate change on the impact cascades involves a methodological approach that generally involves synthetic model outcomes and makes the (inevitably) subjective choices on assumed boundary conditions, uncertainty estimates and analysis tools explicit.

To make the construction of the storylines and its climate analyses transparent and reproducible, we have introduced a methodological protocol that distinguishes a set of predefined storyline development steps and have applied this protocol to three examples. The purpose of this inventory is to illustrate the practical implementation of the physical climate event storylines (Shepherd et al., 2018; Sillmann et al., 2021), and discuss concrete choices made to include stakeholder views, select analysis tools, interpret findings, represent uncertainty and provide useful information to societal actors.

For each of the storylines several criteria were evaluated assessing their potential to facilitate societal uptake (Table 4). All three storylines are built on historic events and have used impact mapping tools that have either been shown to give realistic results in earlier applications or show good correspondence with observed impacts. The counterfactuals are rooted in historic climate trends or apply well-documented climate projections or physical scaling protocols, which provides *realism* to the storylines. Apart from a broad societal interest in the topic of analysis most storylines have gained *relevance* by concrete contributions by stakeholders. An explicit analysis of potential adaptation strategies is included in a few storylines, and standard risk reporting tools are used to support *risk-assessments*. Risk-oriented information is derived from the exploration of expected future climate and/or socio-economic conditions.

Table 4: Evaluation of the criteria for societal uptake of the climate event storylines

Criterion	Africa food security	European Solidarity Fund	Soybean production
Realism	Evidence of plausible joint occurrence of multiple drivers of local food security	Historic event selection; evidence of consecutive active hurricane seasons	Historic event and subsequent impacts; stakeholder reports; physically based climate projections; documented agronomy models
Relevance	Broad concern of food security and societal instability and displacement	Stakeholder participated in storyline development	Societal attention for environmental impacts, land allocation and forest conservation
Risk-informativeness	Exploration of future resilience and mitigation strategies	Explore different GDP and climate conditions	Visualization of illustrative metrics on soy consumption, trade and prices

The storylines explored in this paper are intended to map risks to the European socio-economy that emerge from an immensely complex cascading set of event-impact chains (triggered by remote climate features), which cannot be analysed without a very stringent set of constraints imposed on available projection outputs from climate and impact assessment models. The concept does not rely on a standardized climate modelling toolset such as CMIP6 (Touzé-Peiffer et al., 2020), but instead combines stakeholder evidence, historic events and a mix of data analysis and model experiment techniques to arrive at evidence-based narratives of “unfoldings of events and their hypothetical future counterfactuals” (Shepherd et al., 2018). As such it combines quantitative and qualitative elements (Shepherd and Lloyd, 2021), where the quantitative information gives a meaningful contribution to the risk assessment from complex climate change processes, and the qualitative elements provide insights in relevant pathways of risk transmission. By exploring a range of present-day or future counterfactual conditions in most storylines, crucial climatic elements in the storylines are complemented with a quantification of the underlying uncertainty. However, given that the event cascades and a large number of compounding boundary conditions or contextual settings are prescribed, any probabilistic statement on the outcome of the storylines is highly conditioned on these assumptions, and thus heavily constrained. Storylines like these may serve as a stress-test for particular critical societal functions or contribute to exploratory foresight analyses of future societal developments (Wiebe et al., 2018). However, a review of storyline applications in the climate change domain is out of scope of this paper (Baldissera Pacchetti et al.).

The prime purpose of this paper is to document a methodological protocol to construct storylines that can contribute to the exploration of potential implications of climate change for a collection of societal topics. The steps in the protocol are organized around a central narrative of the chosen storyline, which is segmented into more or less standard scripting building blocks. Surrounding this central narrative, the communicative power of the storylines can be promoted by a carefully designed visual and textual language (Jack et al., 2020), application of story maps (Vollstedt et al., 2021), enhancing personal context by use of personas or actors (Moezzi et al., 2017), and other attributes. However, a standardization of the storyline approach has to appreciate the sheer variety of approaches and analysis needs within a specific storyline, emerging from the inherent complexity of the topic of analysis. Even with a structured outline of the storylines, methodological approaches to assess scope, remote hazard regions, impact metrics, perturbations and comparison of counterfactuals show variability as a result of significant variability of the nature of the considered impact pathways and application domains. A standardization of storyline ingredients is a necessary basis to channelize efforts and connect different impact domains and stakeholder groups.

The synthesis of a collection of storylines does allow extraction of generic principles, calibration of crucial parameters in for instance macro-economic supply-demand interaction models (Robinson and Roland-Holst, 1988; Partridge and Rickman, 2010; Otto et al., 2017), or to build conceptual system dynamics or Bayesian network models (Bala et al., 2017) exploring key dynamics, vulnerabilities and adaptation options under specific sets of assumptions. Also integrated or cross-sectoral climate change assessments carried out by these approaches rely on explicit or implicit choices on scope, boundary conditions and interactions between drivers and impacts. As such, a storyline structure as described above can also be applied to this cross-sectoral climate impact assessment.

**Practical guidelines to meet application criteria**

Adopting a generic structure for the development of climate event storylines allows to identify a number of practical guidelines to support future applications of the storyline concept for the understanding of complex climate risks.

The selection and design process of complex event-impact chains is usually triggered by historic events and the presence of a societal stakeholder group that is particularly exposed to such type of event cascades. This introduces a subjective element in the chosen transmission pathways, boundary conditions and impact metrics. Making these assumptions explicit provides a powerful tool to enhance awareness of conditional dependence, compounding drivers and sources of uncertainty. To utilize this tool due attention needs to be paid to the robust documentation of assumptions, reasoning, and methodology (Sillmann et al., 2021).

The reference storylines are based on historical events linked to remote climate impacts on a European socio-economic sector. Possible impacts of climate change are estimated by perturbing the reference storylines in multiple ways: climate change can affect intensity or frequency of climatic drivers, the transmission pathways and the societal response. Ideally, stakeholders are central to the selection of storylines, to ensure the relevance of the analysis and promote the uptake of results. However, for some storylines illustrated above, it is not immediately obvious what societal actor should be considered to be the prime “stakeholder” invited to respond to the analysis findings. Socio-economic impacts may affect a very broad range of societal actors, or lead to unclear or even divergent optimal responses by different stakeholder groups. In practice an iterative approach with long-term engagement with stakeholder groups is usually necessary and simultaneously challenging. Most of the storylines illustrated in section 4 followed a staged iterative approach consisting of showcasing initial science-based storylines compiled by the researchers, and subsequent finetuning of boundary conditions and impact metrics based on stakeholder experience. While this is a good baseline for storyline co-creation, the approach is rather stakeholder-informed than stakeholder-driven.

During the development of the storylines illustrated here several key elements were experienced to contribute particularly to the criteria that should be met to be a useful source of information supporting the assessment of climate change implications for a specific target domain (see section 2). These elements are presented in Table 5.

*Table 5: Key elements contributing to the storyline application criteria described in section 2*

Criterion	Storyline development elements contributing to criteria
Realism	<ul style="list-style-type: none"> <li>• use historic event and impact-chains as a starting point; this provides a realistic reference to plausible</li> </ul>

	<p>situations</p> <ul style="list-style-type: none"> <li>• anticipate divergent levels of understanding and intrinsic interests by different categories of stakeholders</li> <li>• invest in efforts to create bridges of confidence and trust, to make complexity of remote climate risks tangible and manageable by day-to-day business of stakeholders</li> <li>• an iterative storyline development enhances stakeholder involvement; mutual learning can be promoted by testing prototype storylines with stakeholders</li> </ul>
Relevance	<ul style="list-style-type: none"> <li>• careful documentation of drivers, boundary conditions and impact metrics of historic events using stakeholder experience as input</li> <li>• improve reference to broadly accepted scenario frameworks by making explicit linkages to global warming levels and Shared Socio-economic Pathways (SSPs)</li> <li>• use observations and witness testimonials from stakeholders in a “micro-stories” format; they stimulate empathy and consideration of multiple perspectives, contributing to awareness raising and appreciation of the multiple dimensions of climate risks</li> </ul>
Risk-orientation	<ul style="list-style-type: none"> <li>• demonstrate the plausibility of the event chains conditioned on specified climatological and socio-economical boundary conditions</li> <li>• consider including risk mitigation options as counterfactuals in the event storylines, to illustrate the impacts of taking risk reduction measures</li> </ul>

The standardization of storyline characteristics and criteria also proved to support the (usually required) interdisciplinarity of the research teams. The protocol contributed to mutual understanding and adjustment of disciplinary science output to create the comprehensive interdisciplinary storylines aligning the multiple elements (remote climate hazard regions, impact transmission, socio-economic responses). Selected insights from the storyline development teams may further inform practical guidelines for storyline development and are shared in Table 6.

Table 6: Practical insights from the storyline development teams

Main topic	Practical insights
Why or when can a storyline approach be helpful?	<p>Storylines...</p> <ul style="list-style-type: none"> <li>• can help to connect previously disconnected variables (e.g. crop yield and price);</li> <li>• allow to focus on ‘unseen’ extreme events that may be relevant to society;</li> <li>• allow exploration of climate change impacts on complex event-impact chains that are otherwise difficult to resolve;</li> <li>• allow unpacking ‘black-box’ interactions for stakeholders, illustrating cause and effect rather than risks and uncertainties;</li> <li>• enable formulation of a wide range of societal stress-tests using extreme – yet plausible – events which can be visualized, communicated and connected to history, experience and memory of the affected parties;</li> <li>• offer the possibility to explore both worst-case and optimal response scenarios in a transparent, realistic and consistent manner.</li> </ul>

## THE FORMALIZATION OF STORYLINES

Main difficulties or obstacles	<ul style="list-style-type: none"><li>• Storylines are highly context-specific, giving the risk of narrowing the perspective on climate change features (e.g. by focusing on worst-case scenarios);</li><li>• Reaching out to potential stakeholders can prove difficult when limited data is available;</li><li>• Trade-offs need to be made between rich qualitative event descriptions and quantitative modeling limitations;</li><li>• Difficulty in finding selection criteria for representative events from large data ensembles;</li><li>• Risk of making arbitrary assumptions on the magnitudes, geographical locations, or event-impact chains;</li><li>• Occasionally not straightforward to scale the magnitude of the impact with level of global warming.</li><li>• Balancing detailed versus simplistic assumptions on combined and cascading uncertainties across all storyline elements;</li><li>• Difficult to manage expectations and/or requirements of stakeholders.</li></ul>
--------------------------------	--

### Storyline visualization

The storylines illustrated in Section 4 are supported by a storyline visualizer platform, which was structured according to the protocol described in section 3 (RECEIPT project team, 2023). The visualizer greatly supported the standardization and harmonization of the storyline approach across different disciplines and application domains and structured the adjustment process of the interdisciplinary storyline production teams by the application of a coherent and well-defined narrative and its supporting elements. This has facilitated the explicit formulation and justification of storyline assumptions and structure. The documentation of subjective assumptions does enable the storyline approach to reduce complexity by selecting representative scenarios that are relevant for specific societal applications.

### Application domains

Climate risk assessments are supporting a numerous number of societal applications and sectors. The climate event storylines described in this study generally serve the assessment of complex risks emerging from transboundary transmission of climate hazards to socio-economic impacts, that can materialize in many different manners (Carter et al., 2021). A coherent description of potential application domains is not straightforward, so again we use the gallery of storyline illustrations to provide a selective overview.

The storyline on the Greater Horn of Africa provides information on cascading food security triggers, including the potential implications of major climate-induced global cereal production declines. The World Food Program enriches their subnational food shock impact assessments with global drivers of these impacts. The INFORM risk framework is used by the European Commission to prioritize humanitarian and emergency assistance and anticipate, prevent and prepare for famines and food crisis, including through development agreements such as the new EU-OACPS (Organisation of African, Caribbean and Pacific States (OACPS) Partnership Agreement). Evidence on trends in risk for humanitarian crises can support policy formulation on risk management building on enhanced climate attribution of hazards and impacts (see (IPCC, 2021, 2022)), and initiatives to protect people displaced

across borders in the context of disasters and climate change, such as the Platform on Disaster Displacement (PDD). Causal event pathways similar to the one explored here can serve as a blueprint for mapping impacts of geopolitical disruptions like the Russian-Ukraine 2022 war on African food security, as illustrated by (Gbadamosi, 2022).

The EUSF storyline is used to stress-test the EUSF, which is to be merged with a newly formed European emergency aid fund, the European Support Instrument. It provides support to choices regarding the fund capitalization and pay-out protocols. However, major hurricane event cascades have the potential to affect other European policies and regulations, including financial disclosure schemes, national catastrophe financial protection and solvency (e.g., stress and sensitivity tests performed by the European Insurance and Occupational Pension Authority (EIOPA, 2021)), and identification of remote climate risks in national and European climate risk assessments and adaptation strategies.

The soy market has many actors, including soybean producers, traders, food processing companies, but also consumers, policy makers, financing industry and NGOs addressing environmental or social wellbeing aspects. The relevance of the storyline is supported by the large economic value, the contribution to food supply in Europe, evidenced exposure to climatic pressures, and societal attention to efficient land allocation and environmental impacts of soybean production and consumption. The illustration of the impact of changing characteristics of climate extremes and socio-economic interventions in well-constrained climate event storylines are used in policy simulations to support for instance development of international policies on land management or food security (van Meijl et al., 2020). It also serves as a stress-test in activities aimed at preparing for global shocks in one or more major food sectors, both for public and private company responses. And it can assist in shaping the communication and intervention policies of NGOs active in the field.

## 7. Conclusions

A methodological protocol is proposed to construct climate event climate storylines, designed to analyze and document complex cascading event-impact chains contributing to societal climate risk. The protocol distinguishes a number of standardized steps in the narrative, connecting a (remote) climate hotspot region to a particular socio-economic impact to be explored for a baseline and one of more alternative realizations of the storyline. It includes stakeholder input to define the scope, allows for the exploration of alternative response options, and mixes qualitative and quantitative components to construct the storyline.

Baseline versions of the storyline are usually rooted in historic events where documented hazards and consecutive impacts are captured in data analysis and modelling tools that are able to represent essential dynamics of the event evolution. Climate change perturbations and alternative societal configurations are derived from plausible projections and scenarios, and resulting impacts are mapped for one or multiple counterfactual realizations of the storyline.

A set of criteria is defined to promote the societal relevance and uptake of the storylines. They should be expected to be realistic, relevant and risk informative. A list of three example storylines is described and explored in this paper, to illustrate the protocol and the application of the criteria.

The protocol and criteria checklist are shown to enable covering a wide range of storylines for a diverse set of sectoral applications and help to standardize the design and application of climate event climate storylines.

### Acknowledgements

This paper is compiled by RECEIPT (REmote Climate Effects and their Impact on European sustainability, Policy and Trade) which received funding from the European Union’s Horizon 2020 Research and Innovation Programme under Grant agreement No. 820712.

### References

- Abe, M., and Ye, L. (2013). Building Resilient Supply Chains against Natural Disasters: The Cases of Japan and Thailand. *Glob. Bus. Rev.* 14, 567–586. doi:10.1177/0972150913501606.
- Albano, C. M., McCarthy, M. I., Dettinger, M. D., and McAfee, S. A. (2021). Techniques for constructing climate scenarios for stress test applications. *Clim. Change* 164, 1–25. doi:10.1007/s10584-021-02985-6.
- Anderson, W. B., Seager, R., Baethgen, W., Cane, M., and You, L. (2019). Synchronous crop failures and climate-forced production variability. *Sci. Adv.* 5, 1–9. doi:10.1126/sciadv.aaw1976.
- Anderson, W., Seager, R., Baethgen, W., and Cane, M. (2017). Life cycles of agriculturally relevant <sc>ENSO</sc> teleconnections in North and South America. *Int. J. Climatol.* 37, 3297–3318. doi:10.1002/joc.4916.
- Andrijevic, M., Crespo Cuaresma, J., Muttarak, R., and Schleussner, C. F. (2020). Governance in socioeconomic pathways and its role for future adaptive capacity. *Nat. Sustain.* 3, 35–41. doi:10.1038/s41893-019-0405-0.
- Aznar-Siguan, G., and Bresch, D. N. (2019). CLIMADA v1: A global weather and climate risk assessment platform. *Geosci. Model Dev.* 12, 3085–3097. doi:10.5194/gmd-12-3085-2019.
- Bager, S. L., Persson, U. M., and dos Reis, T. N. P. (2021). Eighty-six EU policy options for reducing imported deforestation. *One Earth* 4, 289–306. doi:10.1016/j.oneear.2021.01.011.
- Bala, B. K., Arshad, F. M., and Noh, K. M. (2017). *System Dynamics*. Singapore: Springer Singapore doi:10.1007/978-981-10-2045-2.
- Baldissera Pacchetti, M. (2021). Structural uncertainty through the lens of model building. *Synthese* 198, 10377–10393. doi:10.1007/s11229-020-02727-8.
- Baldissera Pacchetti, M., Coulter, L., Dessai, S., van den Hurk, B. J. J. M., Sillmann, J., and Shepherd, T. G. The logics of physical climate storylines. *tbd*.
- Balkovič, J., van der Velde, M., Skalský, R., Xiong, W., Folberth, C., Khabarov, N., et al. (2014). Global wheat production potentials and management flexibility under the representative concentration pathways. *Glob. Planet. Change* 122, 107–121. doi:10.1016/j.gloplacha.2014.08.010.
- Benzie, M., Carter, T. R., Carlsen, H., and Taylor, R. (2019). Cross-border climate change impacts:



- implications for the European Union. *Reg. Environ. Chang.* 19, 763–776. doi:10.1007/s10113-018-1436-1.
- Berkhout, F., van den Hurk, B., Bessembinder, J., de Boer, J., Bregman, B., and Van Drunen, M. (2013). Framing climate uncertainty: socio-economic and climate scenarios in vulnerability and adaptation assessments. *Reg. Environ. Chang.* 14. doi:10.1007/s10113-013-0519-2.
- Cairns, G., Ahmed, I., Mullett, J., and Wright, G. (2013). Scenario method and stakeholder engagement: Critical reflections on a climate change scenarios case study. *Technol. Forecast. Soc. Change* 80, 1–10. doi:10.1016/j.techfore.2012.08.005.
- Carter, T. R., Benzie, M., Campiglio, E., Carlsen, H., Fronzek, S., Hildén, M., et al. (2021). A conceptual framework for cross-border impacts of climate change. *Glob. Environ. Chang.* 69, 102307. doi:10.1016/j.gloenvcha.2021.102307.
- Cash, D. W., Clark, W. C., Alcock, F., Dickson, N. M., Eckley, N., Guston, D. H., et al. (2003). Knowledge systems for sustainable development. *Proc. Natl. Acad. Sci. U. S. A.* 100, 8086–8091. doi:10.1073/pnas.1231332100.
- Chain Reaction Research (2018). No Title. Available at: <https://chainreactionresearch.com/report/cerrado-deforestation-disrupts-water-systems-poses-business-risks-for-soy-producers/> [Accessed May 4, 2021].
- Challinor, A. J., Adger, W. N., and Benton, T. G. (2017). Climate risks across borders and scales. *Nat. Clim. Chang.* 7, 621–623. doi:10.1038/nclimate3380.
- Challinor, A. J., Adger, W. N., Benton, T. G., Conway, D., Joshi, M., and Frame, D. (2018). Transmission of climate risks across sectors and borders. *Philos. Trans. R. Soc. A Math. Phys. Eng. Sci.* 376. doi:10.1098/rsta.2017.0301.
- Chen, H., Matsushashi, K., Takahashi, K., Fujimori, S., Honjo, K., and Gomi, K. (2020). Adapting global shared socio-economic pathways for national scenarios in Japan. *Sustain. Sci.* 15, 985–1000. doi:10.1007/s11625-019-00780-y.
- Ciullo, A., Martius, O., Strobl, E., and Bresch, D. N. (2021). A framework for building climate storylines based on downward counterfactuals: The case of the European Union Solidarity fund. *Clim. Risk Manag.* 33, 100349. doi:10.1016/j.crm.2021.100349.
- Cutter, S. L. (2018). Compound, cascading, or complex disasters: What’s in a name? *Environment* 60, 16–25. doi:10.1080/00139157.2018.1517518.
- Cutter, S. L. (2021). The Changing Nature of Hazard and Disaster Risk in the Anthropocene. *Ann. Am. Assoc. Geogr.* 111, 819–827. doi:10.1080/24694452.2020.1744423.
- d’Amour, C. B., Wenz, L., Kalkuhl, M., Steckel, J. C., and Creutzig, F. (2016). Teleconnected food supply shocks. *Environ. Res. Lett.* 11, 35007. doi:10.1088/1748-9326/11/3/035007.
- Dangendorf, S., Arns, A., Pinto, J. G., Ludwig, P., and Jensen, J. (2016). The exceptional influence of storm “Xaver” on design water levels in the German Bight. *Environ. Res. Lett.* 11, 054001. doi:10.1088/1748-9326/11/5/054001.
- Desai, B., Bresch, D. N., Cazabat, C., Hochrainer-Stigler, S., Mechler, R., Ponsérre, S., et al. (2021). Addressing the human cost in a changing climate. *Science (80-. ).* 372, 1284–1287.

doi:10.1126/science.abh4283.

Dessai, S., and Hulme, M. (2004). Does climate adaptation policy need probabilities? *Clim. Policy* 4, 107–128. doi:10.1080/14693062.2004.9685515.

Eberenz, S., Lüthi, S., and Bresch, D. N. (2021). Regional tropical cyclone impact functions for globally consistent risk assessments. *Nat. Hazards Earth Syst. Sci.* 21, 393–415. doi:10.5194/nhess-21-393-2021.

EIOPA (2021). | Eiopa. Available at: <https://www.eiopa.europa.eu/> [Accessed February 22, 2022].

Ercin, E., Chico, D., and Chapagain, A. K. (2019). Vulnerabilities of the European Union’s Economy to Hydrological Extremes Outside its Borders. *Atmosphere (Basel)*. 10, 593. doi:10.3390/atmos10100593.

European Commission EU increases support to fight severe Desert Locust outbreak. Available at: [https://ec.europa.eu/commission/presscorner/detail/en/IP\\_20\\_1148](https://ec.europa.eu/commission/presscorner/detail/en/IP_20_1148) [Accessed February 22, 2022].

European Commission (2023). EU Solidarity Fund. Available at: [https://ec.europa.eu/regional\\_policy/funding/solidarity-fund\\_en](https://ec.europa.eu/regional_policy/funding/solidarity-fund_en) [Accessed February 2, 2023].

EUROSTAT (2023). EUROSTAT. Available at: <https://ec.europa.eu/eurostat> [Accessed February 2, 2023].

Falkendal, T., Otto, C., Schewe, J., Jägermeyr, J., Konar, M., Kummu, M., et al. (2021). Grain export restrictions during COVID-19 risk food insecurity in many low- and middle-income countries. *Nat. Food* 2, 11–14. doi:10.1038/s43016-020-00211-7.

FAO (2017). FAOSTAT. Available at: <https://www.fao.org/faostat/en/#data/FS> [Accessed February 2, 2023].

FAO (2021). FAO Locust Hub. Available at: <https://locust-hub-hqfao.hub.arcgis.com/> [Accessed February 2, 2023].

FAOSTAT (2019). Food Balance Sheets. *FAO Stat. Databases*.

FAOSTAT (2021). *World Food and Agriculture – Statistical Yearbook 2021*. FAO doi:10.4060/cb4477en.

Flach, R., Abrahão, G., Bryant, B., Scarabello, M., Soterroni, A. C., Ramos, F. M., et al. (2021). Conserving the Cerrado and Amazon biomes of Brazil protects the soy economy from damaging warming. *World Dev.* 146, 105582. doi:10.1016/j.worlddev.2021.105582.

Flach, R., Skalský, R., Folberth, C., Balkovič, J., Jantke, K., and Schneider, U. A. (2020). Water productivity and footprint of major Brazilian rainfed crops – A spatially explicit analysis of crop management scenarios. *Agric. Water Manag.* 233, 105996. doi:10.1016/j.agwat.2019.105996.

Frame, B., Lawrence, J., Ausseil, A. G., Reisinger, A., and Daigneault, A. (2018). Adapting global shared socio-economic pathways for national and local scenarios. *Clim. Risk Manag.* 21, 39–51. doi:10.1016/j.crm.2018.05.001.

Frame, D. J., Wehner, M. F., Noy, I., and Rosier, S. M. (2020). The economic costs of Hurricane Harvey attributable to climate change. *Clim. Change* 160, 271–281. doi:10.1007/s10584-020-02692-8.

Gaulier, G., and Zignago, S. (2010). BACI: International Trade Database at the Product-Level. The 1994–2007 Version. Available at: <http://dx.doi.org/10.2139/ssrn.1994500> .

- Gaupp, F. (2020). Extreme Events in a Globalized Food System. *One Earth* 2, 518–521. doi:10.1016/j.oneear.2020.06.001.
- Gaupp, F., Hall, J., Hochrainer-Stigler, S., and Dadson, S. (2020). Changing risks of simultaneous global breadbasket failure. *Nat. Clim. Chang.* 10, 54–57. doi:10.1038/s41558-019-0600-z.
- Gaupp, F., Hall, J., Mitchell, D., and Dadson, S. (2019). Increasing risks of multiple breadbasket failure under 1.5 and 2 °C global warming. *Agric. Syst.* 175, 34–45. doi:10.1016/j.agsy.2019.05.010.
- Gbadamosi, N. (2022). How the Russia-Ukraine War Impacts Africans. *Africa Br. - Foreign Policy*. Available at: <https://foreignpolicy.com/2022/03/02/russia-ukraine-war-african-students-border-crisis/> [Accessed March 5, 2022].
- Gibbs, H. K., Rausch, L., Munger, J., Schelly, I., Morton, D. C., Noojipady, P., et al. (2015). Brazil's Soy Moratorium: Supply-chain governance is needed to avoid deforestation. *Science* (80-. ). 347, 377–378. doi:10.1126/science.aaa0181.
- Goulart, H. M. D., van der Wiel, K., Folberth, C., Balkovic, J., and van den Hurk, B. (2021). Storylines of weather-induced crop failure events under climate change. *Earth Syst. Dyn.* 12, 1503–1527. doi:10.5194/esd-12-1503-2021.
- Goulart, H. M. D., Wiel, K. van der, Folberth, C., Boere, E., and van den Hurk, B. J. J. M. Increase of simultaneous soybean failures due to climate change. *Earth's Futur.*
- Hamed, R., Van Loon, A. F., Aerts, J., and Coumou, D. (2021). Impacts of compound hot-dry extremes on US soybean yields. *Earth Syst. Dyn.* 12, 1371–1391. doi:10.5194/esd-12-1371-2021.
- Hannart, A., Pearl, J., Otto, F. E. L., Naveau, P., and Ghil, M. (2016). Causal counterfactual theory for the attribution of weather and climate-related events. *Bull. Am. Meteorol. Soc.* 97, 99–110. doi:10.1175/BAMS-D-14-00034.1.
- Haraguchi, M., and Lall, U. (2015). Flood risks and impacts: A case study of Thailand's floods in 2011 and research questions for supply chain decision making. *Int. J. Disaster Risk Reduct.* 14, 256–272. doi:10.1016/j.ijdr.2014.09.005.
- Havlik, P., Valin, H., Herrero, M., Obersteiner, M., Schmid, E., Rufino, M. C., et al. (2014). Climate change mitigation through livestock system transitions. *Proc. Natl. Acad. Sci. U. S. A.* 111, 3709–3714. doi:10.1073/pnas.1308044111.
- Hazeleger, W., Van Den Hurk, B. J. J. M., Min, E., Van Oldenborgh, G. J., Petersen, A. C., Stainforth, D. A., et al. (2015). Tales of future weather. *Nat. Clim. Chang.* 5. doi:10.1038/nclimate2450.
- Hedlund, J., Fick, S., Carlsen, H., and Benzie, M. (2018). Quantifying transnational climate impact exposure: New perspectives on the global distribution of climate risk. *Glob. Environ. Chang.* 52, 75–85. doi:10.1016/j.gloenvcha.2018.04.006.
- Hegdahl, T. J., Engeland, K., Müller, M., and Sillmann, J. (2020). An event-based approach to explore selected present and future atmospheric river-induced floods in Western Norway. *J. Hydrometeorol.* 21, 2003–2021. doi:10.1175/JHM-D-19-0071.1.
- Heilmayr, R., Rausch, L. L., Munger, J., and Gibbs, H. K. (2020). Brazil's Amazon Soy Moratorium reduced deforestation. *Nat. Food* 1, 801–810. doi:10.1038/s43016-020-00194-5.
- Hochrainer-Stigler, S., Colon, C., Boza, G., Poledna, S., Rovenskaya, E., and Dieckmann, U. (2020).

- Enhancing resilience of systems to individual and systemic risk: Steps toward an integrative framework. *Int. J. Disaster Risk Reduct.* 51, 101868. doi:10.1016/j.ijdr.2020.101868.
- Hochrainer-Stigler, S., Linnerooth-Bayer, J., and Lorant, A. (2017). The European Union Solidarity Fund: an assessment of its recent reforms. *Mitig. Adapt. Strateg. Glob. Chang.* 22, 547–563. doi:10.1007/s11027-015-9687-3.
- Hurt, S. R. (2003). Co-operation and coercion? The Cotonou Agreement between the European Union and ACP states and the end of the Lomé Convention. *Third World Q.* 24, 161–176. doi:10.1080/713701373.
- ICPAC, and WFP (2018). Greater Horn of Africa Climate and Food Security Atlas 2018. Available at: <https://www.icpac.net/publications/greater-horn-africa-climate-and-food-security-atlas/>.
- IPCC (2021). *Climate Change 2021: The Physical Science Basis. Contribution of Working Group I to the Sixth Assessment Report of the Intergovernmental Panel on Climate Change.*, eds. V. Masson-Delmotte, P. Zhai, A. Pirani, S. L. Connors, C. Péan, S. Berger, et al. Cambridge University Press.
- IPCC (2022). *Climate Change 2022: Impacts, Adaptation, and Vulnerability. Contribution of Working Group II to the Sixth Assessment Report of the Intergovernmental Panel on Climate Change.*, eds. H.-O. Pörtner, D. C. Roberts, M. Tignor, E. S. Poloczanska, K. Mintenbeck, A. Alegría, et al. Cambridge University Press.
- Jack, C. D., Jones, R., Burgin, L., and Daron, J. (2020). Climate risk narratives: An iterative reflective process for co-producing and integrating climate knowledge. *Clim. Risk Manag.* 29, 100239. doi:10.1016/j.crm.2020.100239.
- Jägermeyr, J., Müller, C., Ruane, A. C., Elliott, J., Balkovic, J., Castillo, O., et al. (2021). Climate impacts on global agriculture emerge earlier in new generation of climate and crop models. *Nat. Food* 2, 873–885. doi:10.1038/s43016-021-00400-y.
- Jongman, B., Hochrainer-Stigler, S., Feyen, L., Aerts, J. C. J. H., Mechler, R., Botzen, W. J. W., et al. (2014). Increasing stress on disaster-risk finance due to large floods. *Nat. Clim. Chang.* 4, 264–268. doi:10.1038/nclimate2124.
- Kay, J., and King, M. (2020). *Radical Uncertainty: Decision-Making Beyond the Numbers.* W. W. Norton & Co.
- Klotzbach, P. J., Schreck, C. J., Collins, J. M., Bell, M. M., Blake, E. S., and Roache, D. (2018). The extremely active 2017 North Atlantic hurricane season. *Mon. Weather Rev.* 146, 3425–3443. doi:10.1175/MWR-D-18-0078.1.
- Knapp, K. R., Kruk, M. C., Levinson, D. H., Diamond, H. J., and Neumann, C. J. (2010). The international best track archive for climate stewardship (IBTrACS). *Bull. Am. Meteorol. Soc.* 91, 363–376. doi:10.1175/2009BAMS2755.1.
- Knutson, T., Camargo, S. J., Chan, J. C. L., Emanuel, K., Ho, C.-H., Kossin, J., et al. (2020). Tropical Cyclones and Climate Change Assessment: Part II: Projected Response to Anthropogenic Warming. *Bull. Am. Meteorol. Soc.* 101, E303–E322. doi:10.1175/BAMS-D-18-0194.1.
- Knutson, T. R., Chung, M. V., Vecchi, G., Sun, J., Hsieh, T.-L., and Smith, A. J. P. (2021). Climate change is probably increasing the intensity of tropical cyclones. Available at: <https://news.sciencetribune.org/cyclones-mar2021/> [Accessed May 10, 2021].

- Koks, E. E., Le Bars, D., Essenfelder, A. , Nirandjan, S., and Sayers, P. (2023). The impacts of coastal flooding and sea level rise on critical infrastructure: a novel storyline approach. *Sustain. Resilient Infrastruct.* 8, 237–261. doi:10.1080/23789689.2022.2142741.
- Kuhla, K., Willner, S. N., Otto, C., Geiger, T., and Levermann, A. (2021). Ripple resonance amplifies economic welfare loss from weather extremes. *Environ. Res. Lett.* 16, 114010. doi:10.1088/1748-9326/ac2932.
- Laio, F., Ridolfi, L., and D’Odorico, P. (2016). The past and future of food stocks. *Environ. Res. Lett.* 11, 35010. doi:10.1088/1748-9326/11/3/035010.
- Langlois, M. de (2014). The comprehensive approach and the European Union : a case study of the Horn of Africa. IRSEM Available at: [https://www.defense.gouv.fr/content/download/285159/3671139/file/NRS\\_numero\\_10.pdf](https://www.defense.gouv.fr/content/download/285159/3671139/file/NRS_numero_10.pdf).
- Lenderink, G., de Vries, H., Fowler, H. J., Barbero, R., van Ulft, B., and van Meijgaard, E. (2021). Scaling and responses of extreme hourly precipitation in three climate experiments with a convection-permitting model. *Philos. Trans. A. Math. Phys. Eng. Sci.* 379, 20190544. doi:10.1098/rsta.2019.0544.
- Li, X., Meshgi, A., Wang, X., Zhang, J., Tay, S. H. X., Pijcke, G., et al. (2018). Three resampling approaches based on method of fragments for daily-to-subdaily precipitation disaggregation. *Int. J. Climatol.* 38, e1119–e1138. doi:10.1002/joc.5438.
- Lloyd, C. T. (2016). WorldPop Archive Global Gridded Spatial Datasets. Version Alpha 0.9. 100m Nightlights v4 (Tiled). *Harvard Dataverse*. doi:10.7910/DVN/VO0UNV.
- Lloyd, E. A., and Shepherd, T. G. (2020). Environmental catastrophes, climate change, and attribution. *Ann. N. Y. Acad. Sci.* 1469, 105–124. doi:10.1111/nyas.14308.
- Marengo, J. A., Cunha, A. P., Cuartas, L. A., Deusdará Leal, K. R., Broedel, E., Seluchi, M. E., et al. (2021). Extreme Drought in the Brazilian Pantanal in 2019–2020: Characterization, Causes, and Impacts. *Front. Water* 3, 639204. doi:10.3389/frwa.2021.639204.
- Mengel, M., Treu, S., Lange, S., and Frieler, K. (2020). ATTRICI 1.0 - counterfactual climate for impact attribution. *Geosci. Model Dev. Discuss.* 2020, 1–26. doi:10.5194/gmd-2020-145.
- Mester, B., Vogt, T., Bryant, S., Otto, C., Frieler, K., and Schewe, J. (2023). Human displacements from tropical cyclone Idai attributable to climate change. *Egusph*. Available at: <https://doi.org/10.5194/egusphere-2022-1308>.
- Middelani, R., Willner, S. N., Otto, C., Kuhla, K., Quante, L., and Levermann, A. (2021). Wave-like global economic ripple response to Hurricane Sandy. *Environ. Res. Lett.* 16, 124049. doi:10.1088/1748-9326/ac39c0.
- Middelani, R., Willner, S. N., Otto, C., and Levermann, A. (2022). Economic losses from hurricanes cannot be nationally offset under unabated warming. *Environ. Res. Lett.* 17, 104013. doi:10.1088/1748-9326/ac90d8.
- Moezzi, M., Janda, K. B., and Rotmann, S. (2017). Using stories, narratives, and storytelling in energy and climate change research. *Energy Res. Soc. Sci.* 31, 1–10. doi:10.1016/j.erss.2017.06.034.
- O’Neill, B. C., Kriegler, E., Riahi, K., Ebi, K. L., Hallegatte, S., Carter, T. R., et al. (2014). A new scenario

- framework for climate change research: The concept of shared socioeconomic pathways. *Clim. Change* 122, 387–400. doi:10.1007/s10584-013-0905-2.
- OECD (2023). Agricultural Market Information System. Available at: <https://www.oecd.org/agriculture/amis-policy-database/>.
- Ortiz, A. M. D., Outhwaite, C. L., Dalin, C., and Newbold, T. (2021). A review of the interactions between biodiversity, agriculture, climate change, and international trade: research and policy priorities. *One Earth* 4, 88–101. doi:10.1016/j.oneear.2020.12.008.
- Otto, C., Willner, S. N., Wenz, L., Frieler, K., and Levermann, A. (2017). Modeling loss-propagation in the global supply network: The dynamic agent-based model acclimate. *J. Econ. Dyn. Control* 83, 232–269. doi:10.1016/j.jedc.2017.08.001.
- Partridge, M. D., and Rickman, D. S. (2010). Computable general equilibrium (CGE) modelling for regional economic development analysis. *Reg. Stud.* 44, 1311–1328. doi:10.1080/00343400701654236.
- PDD About Us. Available at: <https://disasterdisplacement.org/about-us> [Accessed February 22, 2022].
- Phillips, C. A., Caldas, A., Cleetus, R., Dahl, K. A., Declet-Barreto, J., Licker, R., et al. (2020). Compound climate risks in the COVID-19 pandemic. *Nat. Clim. Chang.* 10, 586–588. doi:10.1038/s41558-020-0804-2.
- Piontek, F., Drouet, L., Emmerling, J., Kompas, T., Méjean, A., Otto, C., et al. (2021). Integrated perspective on translating biophysical to economic impacts of climate change. *Nat. Clim. Chang.* 11, 563–572. doi:10.1038/s41558-021-01065-y.
- Poljanšek, K., Disperati, S., Vernaccini, L., Nika, A., Marzi, S., and Essenfelder, A. H. (2020). *INFORM severity index: concept and methodology*. LU: Publications Office of the European Union Available at: <https://data.europa.eu/doi/10.2760/94802>.
- RECEIPT project team (2023). RECEIPT storyline visualizer. Available at: <https://www.climateimpactstories.eu/> [Accessed February 2, 2023].
- Ringsmuth, A. K., Otto, I. M., van den Hurk, B., Lahn, G., Reyer, C. P. O., Carter, T. R., et al. (2022). Lessons from COVID-19 for managing transboundary climate risks and building resilience. *Clim. Risk Manag.* 35, 100395. doi:10.1016/j.crm.2022.100395.
- Robinson, S., and Roland-Holst, D. W. (1988). Macroeconomic structure and computable general equilibrium models. *J. Policy Model.* 10, 353–375. doi:10.1016/0161-8938(88)90027-0.
- Rucińska, D. (2019). Describing Storm Xaver in disaster terms. *Int. J. Disaster Risk Reduct.* 34, 147–153. doi:10.1016/j.ijdrr.2018.11.012.
- Schaller, N., Sillmann, J., Müller, M., Haarsma, R., Hazeleger, W., Hegdahl, T. J., et al. (2020). The role of spatial and temporal model resolution in a flood event storyline approach in western Norway. *Weather Clim. Extrem.* 29, 100259. doi:10.1016/j.wace.2020.100259.
- Schewe, J., Otto, C., and Frieler, K. (2017). The role of storage dynamics in annual wheat prices. *Environ. Res. Lett.* 12, 54005. doi:10.1088/1748-9326/aa678e.
- Sellar, A. A., Jones, C. G., Mulcahy, J. P., Tang, Y., Yool, A., Wiltshire, A., et al. (2019). UKESM1: Description and Evaluation of the U.K. Earth System Model. *J. Adv. Model. Earth Syst.* 11, 4513–

4558. doi:10.1029/2019MS001739.
- Shepherd, T. G. (2019). Storyline approach to the construction of regional climate change information. *Proc. R. Soc. A Math. Phys. Eng. Sci.* 475. doi:10.1098/rspa.2019.0013.
- Shepherd, T. G., Boyd, E., Calel, R. A., Chapman, S. C., Dessai, S., Dima-West, I. M., et al. (2018). Storylines: an alternative approach to representing uncertainty in physical aspects of climate change. *Clim. Change* 151, 555–571. doi:10.1007/s10584-018-2317-9.
- Shepherd, T. G., and Lloyd, E. A. (2021). Meaningful climate science. *Clim. Change* 169, 17. doi:10.1007/s10584-021-03246-2.
- Sillmann, J., Shepherd, T. G., van den Hurk, B., Hazeleger, W., Martius, O., Slingo, J., et al. (2021). Event-Based Storylines to Address Climate Risk. *Earth's Futur.* 9, e2020EF001783. doi:10.1029/2020EF001783.
- Simpson, N. P., Mach, K. J., Constable, A., Hess, J., Hogarth, R., Howden, M., et al. (2021). A framework for complex climate change risk assessment. *One Earth* 4, 489–501. doi:10.1016/j.oneear.2021.03.005.
- Soterroni, A. C., Mosnier, A., Carvalho, A. X. Y., Câmara, G., Obersteiner, M., Andrade, P. R., et al. (2018). Future environmental and agricultural impacts of Brazil's Forest Code. *Environ. Res. Lett.* 13, 074021. doi:10.1088/1748-9326/aaccbb.
- SPAM (2019). Spatial Production Allocation Model. Available at: <https://mapspam.info/>.
- Spencer, T., Brooks, S. M., Evans, B. R., Tempest, J. A., and Möller, I. (2015). Southern North Sea storm surge event of 5 December 2013: Water levels, waves and coastal impacts. *Earth-Science Rev.* 146, 120–145. doi:10.1016/j.earscirev.2015.04.002.
- Stainforth, D. A., Allen, M. R., Tredger, E. R., and Smith, L. A. (2007). Confidence, uncertainty and decision-support relevance in climate predictions. *Philos. Trans. R. Soc. A Math. Phys. Eng. Sci.* 365, 2145–2161. doi:10.1098/rsta.2007.2074.
- Stainforth, D. A., and Calel, R. (2020). New priorities for climate science and climate economics in the 2020s. *Nat. Commun.* 11, 1–3. Available at: <https://doi.org/10.1038/s41467-020-16624-8>.
- Swinbank, R., Kyouda, M., Buchanan, P., Froude, L., Hamill, T. M., Hewson, T. D., et al. (2016). The TIGGE project and its achievements. *Bull. Am. Meteorol. Soc.* 97, 49–67. doi:10.1175/BAMS-D-13-00191.1.
- Talebian, S., Carlsen, H., Johnson, O., Volkholz, J., and Kwamboka, E. (2021). Assessing future cross-border climate impacts using shared socioeconomic pathways. *Clim. Risk Manag.* 32, 100311. doi:10.1016/j.crm.2021.100311.
- Te Linde, A. H., Aerts, J. C. J. H., and Kwadijk, J. C. J. (2010). Effectiveness of flood management measures on peak discharges in the Rhine basin under climate change. *J. Flood Risk Manag.* 3, 248–269. doi:10.1111/j.1753-318X.2010.01076.x.
- Termeer, C. J. A. M., Dewulf, A., and Biesbroek, G. R. (2017). Transformational change: governance interventions for climate change adaptation from a continuous change perspective. *J. Environ. Plan. Manag.* 60, 558–576. doi:10.1080/09640568.2016.1168288.
- Tesselaar, M., Botzen, W. J. W., and Aerts, J. C. J. H. (2020). Impacts of Climate Change and Remote

- Natural Catastrophes on EU Flood Insurance Markets: An Analysis of Soft and Hard Reinsurance Markets for Flood Coverage. *Atmosphere (Basel)*. 11, 146. doi:10.3390/atmos11020146.
- Tiwari, S., and Zaman, H. (2010). The Impact of Economic Shocks on Global Undernourishment. Rochester, NY: Social Science Research Network Available at: <https://papers.ssrn.com/abstract=1559733>.
- Torreggiani, S., Mangioni, G., Puma, M. J., and Fagiolo, G. (2018). Identifying the community structure of the food-trade international multi-network. *Environ. Res. Lett.* 13, 054026. doi:10.1088/1748-9326/aabf23.
- Touzé-Peiffer, L., Barberousse, A., and Le Treut, H. (2020). The Coupled Model Intercomparison Project: History, uses, and structural effects on climate research. *Wiley Interdiscip. Rev. Clim. Chang.* 11. doi:10.1002/wcc.648.
- Trostle, R., Marti, D., Stacey, R., and Westcott, P. (2011). Why have food commodity prices risen again? Available at: <https://www.ers.usda.gov/publications/pub-details/?pubid=40482>.
- UN-OCHA (2023). No Title. Available at: <https://fts.unocha.org/content/fts-public-api> [Accessed February 2, 2023].
- USDA (2021). PSD Online. Available at: <https://apps.fas.usda.gov/psdonline/app/index.html#/app/home> [Accessed February 22, 2022].
- van der Geest, K., and van den Berg, R. (2021). Slow-onset events: a review of the evidence from the IPCC Special Reports on Land, Oceans and Cryosphere. *Curr. Opin. Environ. Sustain.* 50, 109–120. doi:10.1016/j.cosust.2021.03.008.
- Van Garderen, L., Feser, F., and Shepherd, T. G. (2021). A methodology for attributing the role of climate change in extreme events: A global spectrally nudged storyline. *Nat. Hazards Earth Syst. Sci.* 21, 171–186. doi:10.5194/nhess-21-171-2021.
- van Meijl, H., Shutes, L., Valin, H., Stehfest, E., van Dijk, M., Kuiper, M., et al. (2020). Modelling alternative futures of global food security: Insights from FOODSECURE. *Glob. Food Sec.* 25, 100358. doi:10.1016/j.gfs.2020.100358.
- van Oldenborgh, G. J., van der Wiel, K., Kew, S., Philip, S., Otto, F., Vautard, R., et al. (2021). Pathways and pitfalls in extreme event attribution. *Clim. Change* 166, 1–27. doi:10.1007/s10584-021-03071-7.
- Vollstedt, B., Koerth, J., Tsakiris, M., Nieskens, N., and Vafeidis, A. T. (2021). Co-production of climate services: A story map for future coastal flooding for the city of Flensburg. *Clim. Serv.* 22, 100225. doi:10.1016/j.cliser.2021.100225.
- Wadey, M. P., Haigh, I. D., Nicholls, R. J., Brown, J. M., Horsburgh, K., Carroll, B., et al. (2015). A comparison of the 31 January–1 February 1953 and 5–6 December 2013 coastal flood events around the UK. *Front. Mar. Sci.* 2, 84. doi:10.3389/fmars.2015.00084.
- Walcker, R., Laplanche, C., Herteman, M., Lambs, L., and Fromard, F. (2019). Damages caused by hurricane Irma in the human-degraded mangroves of Saint Martin (Caribbean). *Sci. Rep.* 9, 1–11. doi:10.1038/s41598-019-55393-3.
- Ward, P. J., van Pelt, S. C., de Keizer, O., Aerts, J. C. J. H., Beersma, J. J., van den Hurk, B. J. J. M., et al.



# Discussion and conclusions

As Earth's climate continues to warm due to anthropogenic greenhouse gas emissions, understanding the impacts of this change and its many facets is of ever-increasing importance. In particular, more frequent and intense weather extremes have the potential to harm society and disrupt economic activity. Therefore, understanding their economic implications is essential to allow for tailored measures that mitigate negative repercussions. With this thesis, I add to this emerging research area, expanding on the scientific understanding of local impacts under current and future climate, the resulting global economic response, and the methods and tools to analyze this response. This final chapter combines the results of the conducted research, highlights the contributions of this thesis, discusses its limitations, and gives outlooks on potential future work.

## I Assessing current and future local impacts

A probabilistic assessment of extreme snowfall intensity in the Northern Hemisphere is conducted in [article 1](#). To this end, extreme percentiles of daily snowfall, as well as the expected extreme magnitude measuring the mean snowfall intensity above a certain percentile, are investigated in an ensemble of climate model projections until the end of the century and under a strong global warming scenario. The results yield an increase of the 99th and 99.9th percentiles, especially for North America and Northern Asia, while mean snowfall decreases. Similarly, the defined expected extreme magnitude increases for large areas, which again indicates an intensification of the most extreme snowfall events. The results thus confirm previous findings on the divergence between snowfall extremes and mean snowfall ([O'Gorman 2014](#); [Danco et al. 2016](#)). While the models show good regional agreement for the sign of the change in extreme percentiles, model agreement for the expected magnitude of extremes is comparatively low. This reveals the difficulty of predicting changes of the most severe extremes with confidence at a regional level using climate model ensembles. However, the increasing trend of snowfall extremes in larger regions is consistent across the model ensemble, and regional model disagreement in the tail risk might be due to natural variability of very rare extremes.

## DISCUSSION AND CONCLUSIONS

Within storylines, the unfolding of impacts from an individual historical extreme event is assessed under observed as well as counterfactual conditions. This necessitates estimates of the historical local impact as well as of plausible counterfactual local impacts. In [article 2](#), I present an approach to estimate the local direct economic losses of a historical hurricane in the USA. With this approach, an initial decrease in economic output of affected states in the USA is derived from the share of the local economy that is physically exposed to the hurricane. Focusing on inundation from storm surge and precipitation, this share is calculated from the gross domestic product of counties with reported high water marks attributable to the hurricane. Recovery from the initial shock is fitted as an exponential decay such that its duration matches observed increases in initial unemployment claims. I extend this approach in [article 3](#), whereby estimates of losses due to the hurricane are projected to future levels of global warming. To this end, the initial shock and the duration of the exponential decay are scaled with expected increases in size and precipitation intensity, respectively.

While the simplicity of this approach makes it flexible and allows for a straightforward adaptation to different hazards, it introduces some simplifications. In particular, it does not differentiate between individual sectors but estimates losses across the entire economy of the affected states. Moreover, the calculation of the exposed gross domestic product at county level is rather coarse. However, these simplifications are reasonable given the intended use of the estimates as direct losses in the *Acclimate* model. These simulations aim to qualitatively assess loss propagation effects rather than quantitatively measure exact costs and impacts. In other contexts, the method could easily be adapted to include proxy variables of higher sectoral or spatial resolution.

Similarly, the projection of hurricane losses to future warming levels is subject to uncertainty. This concerns the increases of both hurricane size and precipitation intensity. Despite some evidence for increasing storm size ([Lin, Zhao, and Zhang 2015](#)) and slower decay on land ([Li and Chakraborty 2020](#)), the effect of climate change on tropical cyclone size and rainfall area is subject to ongoing research ([Knutson, Camargo, et al. 2020](#)). While the effect of stronger precipitation is less debated, the exact change per degree Celsius of additional global warming is subject to uncertainty. For Hurricane Harvey, literature values of rainfall attributable to the  $\sim 1^\circ\text{C}$  global warming at the time of the hurricane's landfall in 2017 in the considered area range between an absolute lower bound of 7% given by the Clausius-Clapeyron relation and estimates of up to 24% ([Wehner and Sampson 2021](#)). As such, the projections should not be understood as predictions of future losses (which is not plausible for a single past event in any case). Rather, the uncertainties can be seen as a range of different plausible local economic impacts under different climate conditions, making the obtained estimates well-suited for assessments within the storyline framework. In the storyline constructed in [article 3](#), multiple simulations are conducted under different size increase scenarios and a wide range of temperature increases. These

scenarios allow to assess qualitative changes in the global economic response when direct losses change in the future due to global warming.

## 2 Simulating the global economic response

The developed loss estimates are used further to construct storylines to investigate the global economic response to hurricanes in the USA. In [article 2](#), I use loss estimates for Hurricane Sandy and analyze the resulting global dynamics of consumption prices. The simulations reveal a global three-phase consumption price ripple which affects also regions that are not directly exposed to the hurricane. First, an initial upstream effect causes consumption prices to drop and, therefore, consumption to increase. This is followed by a second phase, whereby an opposing, slower downstream effect results in a price increase and reduced consumption. The upstream phase is generally short in comparison to the downstream phase, which ends shortly before the direct shock has fully decayed. Thus, the duration of the first two phases is determined by the temporal evolution of the direct shock. Finally, prices and consumption levels resume to pre-hazard levels in a normalization phase. These findings of [article 2](#) emphasize the importance of the temporal dimension for disaster aftermath prices, as sustained by recent empirical findings ([Faccia, Parker, and Stracca 2021](#)). The evolving dynamic depends on the direct shock as I demonstrate by counterfactual variations of the shock duration. With a longer direct shock, more regions show net consumption losses due to a dominating downstream effect. Thus, in line with a recent study by [Cantelmo \(2022\)](#), the shock propagation dynamic has an overall positive or negative effect on consumption when either the upstream or downstream phase dominates. Adding to previous studies, my modeling approach allows the expansion of analysis beyond the exposed region. I find that price anomalies can be observed globally, but that a region's trade intensity with the exposed USA influences the overall consumption effect of the price ripple for this region. The results presented here thereby expand on existing literature of price impacts from natural disasters ([Heinen, Khadan, and Strobl 2019](#); [Parker 2018](#); [Cavallo, Cavallo, and Rigobon 2014](#)) and shed light on the related complex interactions of supply and demand effects in the economic network. If consumers behave rationally and maximize their utility within a constrained budget, these interactions may even yield temporarily positive consumption price elasticities as demonstrated in [article 5](#).

Using loss projections, I simulate the global production response to Hurricane Harvey under a reference and multiple counterfactual scenarios in [article 3](#). I find that not directly affected regions increase their production to offset, or compensate for, direct losses in the exposed regions. These compensation effects are in alignment with previous modeling results on a global level ([Willner, Otto, and Levermann 2018](#)), where direct production losses can be mitigated by regions that are not directly exposed. Such positive spillover

effects from tropical cyclones have been demonstrated on a regional level by the use of night-light data (Felbermayr et al. 2022), showing that local losses from extreme weather can be offset by surrounding regions. I show that the USA are able to compensate for the direct hurricane losses at the national level in the reference scenario without additional climate change. This complements previous econometric analyses of landfalling hurricanes in the USA that show negative growth effects on a county level being netted out at the state level (Strobl 2011). The results of article 3 further indicate that this effect extends beyond the national bounds of the USA, and to a global level.

Clearly, with intensifying direct and indirect economic effects under continued global warming (Zhang, Li, et al. 2018), compensation as simulated here will become of increasing importance. This is sustained by the counterfactual simulations, showing that the USA will no longer be able to fully compensate for direct losses nationally, once a certain level of additional warming is reached. In addition, shifts in the global distribution of compensation indicate that regions not directly affected eventually reach soft limits of what they can cost-effectively offset, owing to nonlinear production increases when economic sectors extend their production beyond the usual level. As a consequence, compensation shares decrease for regions that are large in terms of global exports, while they increase for smaller regions. In sum, the results of article 3 underline the ability of the economy to flexibly balance out losses to a certain extent, even though direct losses may not be fully compensated for. At the same time, they also reveal the vulnerability that arises for regions that are exposed to weather extremes. This is particularly pronounced for locally aggregated industries. Analyzing compensation in the mining and quarrying sector specifically, I find that the USA is under no scenario — neither reference nor counterfactuals — able to compensate losses nationally in this sector due to little alternative production capacity for compensation within the country.

Finally, a third storyline is constructed in article 4. Here, I assess the effect of global economic stress, as observed during the recent Covid-19 pandemic, on loss propagation from tropical cyclones, heat stress, and river floods worldwide. To this end, I compare the global economic response to these weather extremes between a stressed and a counterfactual unstressed scenario. The results demonstrate that consumption losses in response to weather extremes increase strongly when the global economy is under stress. I find that this loss increase is due to an intensified price response to the simulated extremes. Under global economic stress, the capacity for loss compensation is globally hampered, leading to an aggravated scarcity of goods. The resulting consumption loss increases are particularly pronounced in China and the USA, where losses triple and double, respectively, under global economic stress. Losses in the European Union increase by 35%, which is close to the global average of 37%. I show that this regional heterogeneity results from different exposure to the simulated shocks. The European Union suffers comparatively small direct domestic shocks, and is mostly exposed indirectly to repercussions within the economic network. Direct shocks in the USA and China are stronger, in addition to being similarly

exposed to indirect shocks as the European Union. These results indicate an increased vulnerability for consumption losses from both domestic and remote shocks when the global economy is under stress. Varying direct losses within the simulated ensemble reveal that vulnerability further increases when weather extremes grow stronger. Thus, my findings show an amplifying role of the interaction between weather extremes and their socio-economic backdrop. With this, [article 4](#) adds on the literature of impacts from consecutive disasters, which are of ever-increasing importance ([de Ruiter et al. 2020](#)). Specifically, my research demonstrates the need to consider the wider socio-economic background for a more comprehensive assessment of disaster impacts and risk.

In the used modeling chain for all three storylines, uncertainties arise from the representation of weather extremes. The uncertainties associated with the hurricane loss estimates and projections as used in [articles 2 and 3](#) have been discussed above. In addition to these, using *total* local losses as direct losses in the *Acclimate* model necessitates the rather strong assumption that in the directly affected regions, total losses are dominated by direct losses and locally confined higher-order losses. Of course, the historically observed local economic impact can also include indirect effects from the overall global economic response and interaction with regions not directly affected. However, the assumption holds when comparing simulated total and direct losses. In case of Hurricane Sandy, the ratio of total to direct losses lies above 90% for both directly affected states New York and New Jersey. Thus, the estimates are rather conservative and tend to underestimate direct losses, which can partly be mitigated by production extension.

Also the representation of the pandemic in [article 4](#) is subject to uncertainty and not all pandemic factors that affect economic activity can be included in a single indicator like the stringency index ([Hale et al. 2021](#)) used here. However, I emphasize that the analysis should not be understood as a hind-casting exercise that aims to quantitatively reproduce what has happened during the pandemic. To begin with, such an analysis would require historical records of global weather extremes during the pandemic instead of the used projected impacts. Rather, the contribution of the analysis lies in the conceptual findings gained from plausible scenarios. As such, the results are more generally informative of economic risk during a major global crisis that affects economic activity worldwide. The mechanisms found are likely applicable to other global economic stressors against which weather extremes unfold.

Generally, the results of all three storylines are of a qualitative nature. In particular, simulations with the *Acclimate* model should not be regarded as quantitative statements on what has happened or will happen. To interpret absolute values, including price anomalies, production changes, and impacts on consumption, calibration of the model with real-world data would be required. This is challenging on multiple levels ([Fagiolo, Guerini, et al. 2019](#)), including the availability of observational data at sufficient spatio-temporal resolution and coverage, the amount of model parameters, and the large number of possible output variables to calibrate on. Still, the direct loss estimation of historical

major hurricanes undertaken here may be seen as a first step in the direction of hind-casting and model calibration. Such calibration may well equip models like the one used here with the ability to provide quantitative estimates of loss propagation effects. For this, the approaches presented here would need to be combined with historical loss propagation effects from a past event like Hurricanes Sandy or Harvey. While this remains for future work, the simulation results already provide useful insights into economic mechanisms that otherwise cannot be studied in real-world data. Since the used model dynamics evolves from plausible micro-economic assumptions, the gained insights are informative also for the real world within the boundaries of these assumptions. As discussed, the simulated effects can provide conceptual explanations for empirical findings. The chosen model is thus well-suited to qualitatively study loss propagation from weather extremes in conjunction with climate change or major socio-economic drivers.

Overall, the findings obtained from the simulations conducted here advance the understanding of economic loss propagation mechanisms from weather extremes. As such, they are likely relevant for policy makers who aim to mitigate adverse economic repercussions from weather extremes under climate change and large-scale socio-economic drivers. To this end, my results can inform the development of adaptation measures that increase resilience of supply chains against weather extremes (Levermann 2014). These adaptation measures should account for the complex interactions in the economic network as discovered here.

### 3 Advancing on methods and tools

Modeling economic dynamics requires certain assumptions, which necessarily introduce simplifications. Improving on the previously simplistic representation of consumers, an extension of the *Acclimate* model is presented and applied in [article 5](#). With this extension, consumers are disaggregated into five income levels and maximize their utility within a constrained budget. This yields *market-emerging elasticities*, rather than exogenously prescribed price elasticities and allows for a more detailed and realistic representation of consumption. Maximizing a utility function under budget constraints, consumers can substitute goods within and between three groups of commodities; defined as necessary, relevant, and other goods. Thus, the extension to *Acclimate* presented in [article 5](#) allows for more nuanced analyses of indirect economic effects on consumption by providing a more detailed and realistic representation of consumers in the model. This is demonstrated by simulations of loss propagation from weather extremes. The resulting temporarily positive consumption price elasticities are analytically explained by a self-stabilizing feedback mechanism in the out-of-equilibrium state of the economy.

Though significantly extending the representation of the consumer, simplifying behavioral assumptions must still be made. This pertains in particular to the assumption



of purely rational *homo oeconomicus* consumption behavior. In reality, more factors, like personal taste, influence consumer behavior. Yet, the assumptions match the central characteristic of agents in *Acclimate* with regards to rational behaviour, which is similarly assumed for producing agents. The results obtained under these assumptions allow to study complex economic interactions and can be used to extend existing economic theory as demonstrated for the occurrence of positive price elasticities. While these are commonly assumed to be inherent to so-called Giffen (Jensen and Miller 2008) or Veblen (Bagwell and Bernheim 1996) goods, article 5 shows the general possibility for such behavior as a result of market dynamics. With this, the model extension allows for more nuanced analyses of the consumption response to economic shocks both within and outside of storyline assessments.

The studies presented in articles 2-4 of this thesis are part of a diverse storyline landscape, covering a wide range of hazards, interdisciplinary impact chains, and approaches to construct counterfactual scenarios. This landscape is explored in article 6. To this end, common elements across a set of presented storylines are derived to provide a formalization of the storyline framework, which may be used as a guideline to conduct analyses within this approach. Together with other researchers from a multidisciplinary research community using storylines, I propose the following eight elements to construct a storyline. Initially, storyline candidates of past events and associated impact chains with evidence for impacts from climate change or socio-economic drivers are collected in a (1) *scoping process*. This process can be guided by recent hazards with evidence for shock propagation, or by the involvement of relevant stakeholders. For the selected storyline, the (2) *remote climate hazard region* is defined as the geographical area of the hazard. For this region, information is collected on the impact that climate change has on the considered hazards, e.g., with regards to regional boundary conditions. The impact chain that links the hazard region to other impact areas is defined by the (3) *impact transmission pathway*. A wide range of pathways can be considered, including investment flows, supply chains for specific goods, or loss propagation in the global economic network as considered in the three storylines of this thesis. The (4) *socio-economic impact* specifies a quantitative measure for entities that experience consequences from the hazard through impact transmission. Together with the remote climate hazard region and the transmission pathway, the socio-economic impact defines the reference scenario of the storyline. A (5) *climate perturbation* describes the counterfactual evolution of the event chain with changed physical impacts of the hazard as a plausible response to climate change. Counterfactuals can also include a (6) *socio-economic perturbation* that considers economic and societal trends like population development, adaptation policies, or changing socio-economic vulnerability and exposure to hazards in the future. A (7) *comparison* of one or more constructed counterfactuals to the reference yields the impact of perturbed climate or socio-economic conditions. The resulting narrative can be qualitative or quantitative and may concern the local hazard impact, the impact transmission, or the indirect socio-economic impact. Finally, (8) *ac-*

*companying micro-stories* can be included as complementary narratives, for example to probe sensitivities to changes in different elements of the storyline.

As becomes apparent from the range of choices for each of the outlined elements, the presented standardization needs to appreciate the huge diversity of possible storylines. For this reason, the formalization can only provide a guiding structure for generic steps and no specific tool or method to execute these steps. Thus, the proposed formalization streamlines the assessment of storylines without constraining its broad applicability. Of course, many of the elements require making assumptions, often introducing a subjective element in the process. This pertains in particular to the choice of a historical event, the impact transmission, and the impact metric. However, even if desirable, it can be argued that subjectivity generally cannot be fully eliminated. The latest IPCC report states with high confidence that “the construction of climate change information and communication of scientific understanding are influenced by the values of the producers, the users and their broader audiences” (IPCC 2021). The presented storyline protocol cannot dispose of this subjectivity. However, implementing storylines guided by the outlined elements requires all assumptions to be made explicit. It thus increases the transparency of the resulting studies with respect to inevitably subjective choices.

## 4 Storylines for assessing the economic response

This thesis focuses on the assessment of weather extreme impacts within the storyline framework. In the previous sections, the supporting articles have been discussed with regards to the contributions they make for impact assessments of weather extremes. Bringing these aspects of my thesis together, I here discuss the connecting elements of all presented articles within the storyline framework. Embedding articles 1–5 in the storyline framework as described in article 6, I here lay out their common and diverging structural elements (Fig. 2). While articles 1 and 5 do not constitute full self-contained storylines, they cater to the overall narrative, framing the storylines in articles 2–4.

Evidently, not all eight elements are present in each of the constructed storylines in articles 2–4, with differing coverage of elements 5–8. Note that the elements themselves and, in particular, the distinction of counterfactuals into climate perturbation, socio-economic perturbation, and micro-stories, have been defined ex-post from the juxtaposition of multiple complete storylines after their completion. Therefore, the alteration of the shock duration in article 2 constitutes a micro-story, rather than a full counterfactual setup. Similarly, the analysis of the mining and quarrying sector in article 3 and varying intensity of climate extremes in article 4 qualify as micro-stories. A climate perturbation is considered in article 3 in the form of projected direct losses from Hurricane Harvey under counterfactual climate scenarios. Similarly, the results of article 1 can be mapped to the climate perturbation element. While this study in fact uses the more traditional proba-



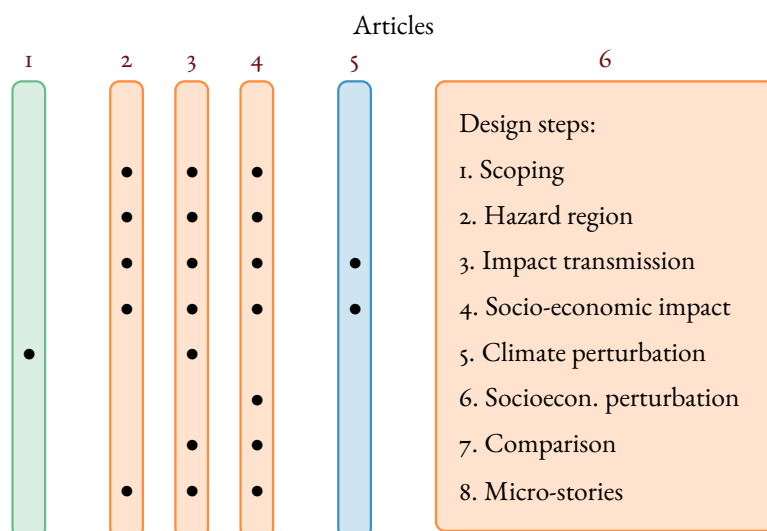


Figure 2: Embedding of articles 1–5 into the storyline framework as described in article 6. Bullet points indicate the coverage of storyline elements.

bilistic approach, the findings can be used to support the climate perturbation element of a possible future storyline on snowfall extremes. A socio-economic perturbation is applied in article 4, where global economic stress during Covid-19 is considered to construct a counterfactual.

Elements 1–4 of the formalization, on the other hand, are included in all of the three constructed storylines. Each individual article contains rationales for the scope of the storyline and associated hazard region, the applied perturbations to construct counterfactuals, the comparison to reference scenarios, and the creation of micro-stories. In this, article 4 stands out in that it does not focus on a single historic natural hazard in a specific region, but rather investigates indirect economic effects from synthetic representations of weather extremes, globally. Indeed, the historic event in this storyline is the Covid-19 pandemic with the resulting global economic stress, i.e., the socio-economic perturbation itself. Across all storylines, a common choice has been made with regards to using the agent-based model *Acclimate* to simulate the impact transmission pathway of economic loss-propagation and compute the resulting socio-economic impact. Thus, the model extension provided in article 5 expands on elements 3 and 4 of the storyline formalization.

Put together, the individual articles with self-contained scientific contributions and analyses blend into an overall coherent story and allow to form a narrative for the unfolding of weather extreme impacts in the economic network. Thereby, each article covers different aspects of this story. Arguably, from a technical perspective the economic mechanisms discovered in the constructed storylines do not depend on the storyline framework as such and could also be discovered by, e.g., simulating different stylized economic shocks in the *Acclimate* model, and observing the response. Such analyses would, of course, lack

realism, and therefore, relevance and risk-informativeness. Conversely, storylines provide a narrative that ensures these criteria and thus facilitates the investigation of specific elements in complex and partly uncertain impact chains. At the same time, this specific narrative necessarily lacks the comprehensive perspective. Therefore, storylines must be considered complementary to other approaches, each of them assessing economic impacts from a different angle.

## 5 Conclusions

With the research presented in this thesis, I contribute to the ever-growing body of literature that documents, investigates, and projects the economic impacts of climate change. As a central approach, I use the concept of storylines and conducted three core storyline assessments on economic loss propagation from weather extremes. Accompanying these storylines, I also employ the traditional approach of probabilistic impact assessments, thus highlighting its usefulness but also the limitations that ultimately promoted the emergence of storylines. Within the three storylines, I demonstrate distinct economic mechanisms of loss propagation from weather extremes in the global economic network. In particular, I show a wave-like global price ripple in the aftermath of a major hurricane and analyze the compensation of disaster output losses by regions that are not directly affected. These two mechanisms support my findings of increasing consumption losses from weather extremes under global economic stress, whereby an intensified price response results from a reduced capacity for compensation.

Using the techniques of agent-based modeling within the storyline framework, I assess the economic risks of weather extremes from a systemic perspective, while also advancing on these techniques. Of course, the results obtained here only represent a small piece to a bigger picture. The diverse landscape of storyline assessments illustrates the multitude of relevant hazards, affected regions, possible impact channels, and resulting socio-economic repercussions. As such, only a small subset of these aspects can be considered in this thesis. The conducted storyline assessments thus may be understood as stress-tests to plausible extreme scenarios that may inform the development of adaptation strategies. For a comprehensive understanding, the insights gained here need to be accompanied and extended by a plethora of complementing analyses. The findings in this thesis, therefore, are embedded in a wide and interdisciplinary scientific field. Further research informed by theory, modelling, and observation of both physical and socio-economic processes will be necessary to tell a more comprehensive story of the economic impacts of climate change generally, and weather extremes specifically. My thesis has added another chapter to this story.

## References

- Acemoglu, D. et al. (2012). “The network origins of aggregate fluctuations”. In: *Econometrica* 80.5, pp. 1977–2016.
- Bagwell, L. S. and B. D. Bernheim (1996). “Veblen effects in a theory of conspicuous consumption”. In: *The American economic review*, pp. 349–373.
- Barton-Henry, K. and L. Wenz (2022). “Nighttime light data reveal lack of full recovery after hurricanes in Southern US”. In: *Environmental Research Letters* 17.11, p. 114015.
- Bonadio, B. et al. (2021). “Global supply chains in the pandemic”. In: *Journal of international economics* 133, p. 103534.
- Botzen, W. W., O. Deschenes, and M. Sanders (2020). “The economic impacts of natural disasters: A review of models and empirical studies”. In: *Review of Environmental Economics and Policy*.
- Briguglio, L. et al. (2009). “Economic vulnerability and resilience: concepts and measurements”. In: *Oxford development studies* 37.3, pp. 229–247.
- Burke, M., S. M. Hsiang, and E. Miguel (2015a). “Climate and conflict”. In: *Annu. Rev. Econ.* 7.1, pp. 577–617.
- (2015b). “Global non-linear effect of temperature on economic production”. In: *Nature* 527.7577, pp. 235–239.
- Cantelmo, A. (2022). “Rare disasters, the natural interest rate and monetary policy”. In: *Oxford Bulletin of Economics and Statistics* 84.3, pp. 473–496.
- Cavallo, A., E. Cavallo, and R. Rigobon (2014). “Prices and supply disruptions during natural disasters”. In: *Review of Income and Wealth* 60, S449–S471.
- Changnon, S. A. and D. Changnon (2006). “A spatial and temporal analysis of damaging snowstorms in the United States”. In: *Natural Hazards* 37, pp. 373–389.
- Ciullo, A. et al. (2021). “A framework for building climate storylines based on downward counterfactuals: The case of the European Union Solidarity fund”. In: *Climate risk management* 33, p. 100349.
- Danco, J. F. et al. (2016). “Effects of a warming climate on daily snowfall events in the Northern Hemisphere”. In: *Journal of Climate* 29.17, pp. 6295–6318.
- Dasgupta, S. et al. (2021). “Effects of climate change on combined labour productivity and supply: an empirical, multi-model study”. In: *The Lancet Planetary Health* 5.7, e455–e465.

- de Ruiter, M. C. et al. (2020). “Why we can no longer ignore consecutive disasters”. In: *Earth’s future* 8.3, e2019EF001425.
- Donat, M. G. et al. (2016). “More extreme precipitation in the world’s dry and wet regions”. In: *Nature Climate Change* 6.5, pp. 508–513.
- DWD (2017). *Tropical cyclones*. Accessed 20 Mar 2023.
- Emanuel, K. (2017). “Assessing the present and future probability of Hurricane Harvey’s rainfall”. In: *Proceedings of the National Academy of Sciences* 114.48, pp. 12681–12684.
- Emanuel, K. A. (1987). “The dependence of hurricane intensity on climate”. In: *Nature* 326.6112, pp. 483–485.
- Eyring, V. et al. (2016). “Overview of the Coupled Model Intercomparison Project Phase 6 (CMIP6) experimental design and organization”. In: *Geoscientific Model Development* 9.5, pp. 1937–1958.
- Faccia, D., M. Parker, and L. Stracca (2021). “Feeling the heat: extreme temperatures and price stability”. In:
- Fagiolo, G., M. Guerini, et al. (2019). “Validation of agent-based models in economics and finance”. In: *Computer simulation validation: fundamental concepts, methodological frameworks, and philosophical perspectives*, pp. 763–787.
- Fagiolo, G., P. Windrum, and A. Moneta (2006). *Empirical validation of agent-based models: A critical survey*. Tech. rep. LEM Working Paper Series.
- Fankhauser, S. et al. (2022). “The meaning of net zero and how to get it right”. In: *Nature Climate Change* 12.1, pp. 15–21.
- Felbermayr, G. et al. (2022). “The economic impact of weather anomalies”. In: *World Development* 151, p. 105745.
- Friedlingstein, P. et al. (2022). “Global carbon budget 2021”. In: *Earth System Science Data* 14.4, pp. 1917–2005.
- Guan, D. et al. (2020). “Global supply-chain effects of COVID-19 control measures”. In: *Nature human behaviour* 4.6, pp. 577–587.
- Guha-Sapir, D., R. Below, and P. Hoyois (2023). *EM-DAT: The CRED/OFDA International Disaster Database*. Université Catholique de Louvain, Brussels, Belgium.
- Hale, T. et al. (2021). “A global panel database of pandemic policies (Oxford COVID-19 Government Response Tracker)”. In: *Nature Human Behaviour* 5.4, pp. 529–538.
- Hallegatte, S. (2008). “An adaptive regional input-output model and its application to the assessment of the economic cost of Katrina”. In: *Risk Analysis: An International Journal* 28.3, pp. 779–799.
- Hallegatte, S. and A. Vogt-Schilb (2019). “Are Losses from Natural Disasters More Than Just Asset Losses?” In: *Advances in Spatial and Economic Modeling of Disaster Impacts*. Ed. by Y. Okuyama and A. Rose. Cham: Springer International Publishing, pp. 15–42. 10.1007/978-3-030-16237-5\_2.
- Hallegatte, S. and V. Przyluski (2010). “The economics of natural disasters: concepts and methods”. In: *World Bank Policy Research Working Paper* 5507.

- Hazeleger, W. et al. (2015). “Tales of future weather”. In: *Nature Climate Change* 5.2, pp. 107–113.
- Heinen, A., J. Khadan, and E. Strobl (2019). “The price impact of extreme weather in developing countries”. In: *The Economic Journal* 129.619, pp. 1327–1342.
- Hochrainer-Stigler, S. et al. (2020). “Enhancing resilience of systems to individual and systemic risk: steps toward an integrative framework”. In: *International Journal of Disaster Risk Reduction* 51, p. 101868.
- Hoffmann, R. et al. (2020). “A meta-analysis of country-level studies on environmental change and migration”. In: *Nature Climate Change* 10.10, pp. 904–912.
- Hsiang, S. M. and A. S. Jina (2014). *The causal effect of environmental catastrophe on long-run economic growth: Evidence from 6,700 cyclones*. Tech. rep. National Bureau of Economic Research.
- Hummels, D., J. Ishii, and K.-M. Yi (2001). “The nature and growth of vertical specialization in world trade”. In: *Journal of international Economics* 54.1, pp. 75–96.
- IPCC (2012). *Managing the Risks of Extreme Events and Disasters to Advance Climate Change Adaptation. A Special Report of Working Groups I and II of the Intergovernmental Panel on Climate Change*. Ed. by C. Field et al. Cambridge, United Kingdom and New York, NY, USA: Cambridge University Press.
- (2021). *Climate Change 2021: The Physical Science Basis. Contribution of Working Group I to the Sixth Assessment Report of the Intergovernmental Panel on Climate Change*. Ed. by V. Masson-Delmotte et al. Cambridge, United Kingdom and New York, NY, USA: Cambridge University Press. 10.1017/9781009157896.
- (2023). *Synthesis Report of the IPCC Sixth Assessment Report*. Ed. by H. Lee et al.
- Jensen, R. T. and N. H. Miller (2008). “Giffen behavior and subsistence consumption”. In: *American economic review* 98.4, pp. 1553–1577.
- Kemp, L. et al. (2022). “Climate Endgame: Exploring catastrophic climate change scenarios”. In: *Proceedings of the National Academy of Sciences* 119.34, e2108146119.
- Knutson, T., S. J. Camargo, et al. (2019). “Tropical cyclones and climate change assessment: Part I: Detection and attribution”. In: *Bulletin of the American Meteorological Society* 100.10, pp. 1987–2007.
- (2020). “Tropical cyclones and climate change assessment: Part II: Projected response to anthropogenic warming”. In: *Bulletin of the American Meteorological Society* 101.3, E303–E322.
- Knutson, T. R., J. J. Sirutis, et al. (2013). “Dynamical downscaling projections of twenty-first-century Atlantic hurricane activity: CMIP3 and CMIP5 model-based scenarios”. In: *Journal of Climate* 26.17, pp. 6591–6617.
- Koks, E. E. et al. (2022). “The impacts of coastal flooding and sea level rise on critical infrastructure: a novel storyline approach”. In: *Sustainable and Resilient Infrastructure*, pp. 1–25.

- Konapala, G. et al. (2020). “Climate change will affect global water availability through compounding changes in seasonal precipitation and evaporation”. In: *Nature communications* 11.1, p. 3044.
- Kossin, J. P. et al. (2020). “Global increase in major tropical cyclone exceedance probability over the past four decades”. In: *Proceedings of the National Academy of Sciences* 117.22, pp. 11975–11980.
- Kotz, M., A. Levermann, and L. Wenz (2022). “The effect of rainfall changes on economic production”. In: *Nature* 601.7892, pp. 223–227.
- Kotz, M., L. Wenz, et al. (2021). “Day-to-day temperature variability reduces economic growth”. In: *Nature Climate Change* 11.4, pp. 319–325.
- Kuhla, K. et al. (2021). “Ripple resonance amplifies economic welfare loss from weather extremes”. In: *Environmental Research Letters* 16.11, p. 114010.
- Lehmann, J., D. Coumou, and K. Frieler (2015). “Increased record-breaking precipitation events under global warming”. In: *Climatic Change* 132, pp. 501–515.
- Lenzen, M., K. Kanemoto, et al. (2012). “Mapping the structure of the world economy”. In: *Environmental science & technology* 46.15, pp. 8374–8381.
- Lenzen, M., A. Malik, et al. (2019). “Economic damage and spillovers from a tropical cyclone.” In: *Natural Hazards & Earth System Sciences* 19.1.
- Leontief, W. (1970). “Environmental repercussions and the economic structure: an input-output approach”. In: *The review of economics and statistics*, pp. 262–271.
- Levermann, A. (2014). “Climate economics: Make supply chains climate-smart”. In: *Nature* 506.7486, pp. 27–29.
- Li, L. and P. Chakraborty (Nov. 1, 2020). “Slower decay of landfalling hurricanes in a warming world”. In: *Nature* 587.7833, pp. 230–234. 10.1038/s41586-020-2867-7.
- Lin, Y., M. Zhao, and M. Zhang (2015). “Tropical cyclone rainfall area controlled by relative sea surface temperature”. In: *Nature Communications* 6.1, p. 6591.
- Lloyd, E. A. and T. G. Shepherd (2020). “Environmental catastrophes, climate change, and attribution”. In: *Annals of the New York Academy of Sciences* 1469.1, pp. 105–124.
- Mandel, A. (2012). “Agent-based dynamics in the general equilibrium model”. In: *Complexity Economics* 1.1, pp. 105–121.
- Marzeion, B. and A. Levermann (2014). “Loss of cultural world heritage and currently inhabited places to sea-level rise”. In: *Environmental Research Letters* 9.3, p. 034001.
- Middelanis, R., S. N. Willner, C. Otto, K. Kuhla, et al. (2021a). “Wave-like global economic ripple response to Hurricane Sandy”. In: *Environmental Research Letters* 16.12, p. 124049.
- Middelanis, R., S. N. Willner, C. Otto, and A. Levermann (2022a). “Economic losses from hurricanes cannot be nationally offset under unabated warming”. In: *Environmental Research Letters* 17.10, p. 104013.

- Mindlin, J. et al. (2020). “Storyline description of Southern Hemisphere midlatitude circulation and precipitation response to greenhouse gas forcing”. In: *Climate Dynamics* 54, pp. 4399–4421.
- NOAA (2022). *Costliest U.S. Tropical Cyclones*. Accessed 28 Feb 2023.
- (2023). *U.S. Billion-Dollar Weather and Climate Disasters*. Accessed 28 Feb 2023. 10.25921/stkw-7w73.
- O’Neill, B. C. et al. (2016). “The scenario model intercomparison project (ScenarioMIP) for CMIP6”. In: *Geoscientific Model Development* 9.9, pp. 3461–3482.
- O’Gorman, P. A. (2014). “Contrasting responses of mean and extreme snowfall to climate change”. In: *Nature* 512.7515, pp. 416–418.
- O’Neill, B. C. et al. (2014). “A new scenario framework for climate change research: the concept of shared socioeconomic pathways”. In: *Climatic change* 122, pp. 387–400.
- Okuyama, Y. and S. E. Chang (2012). “Economic and planning approaches to natural disasters”. In: *The Oxford Handbook of Urban Economics and Planning*. Ed. by N. Brooks, K. Donaghy, and G.-J. Knaap. New York: Oxford University Press.
- Okuyama, Y. and J. R. Santos (2014). “Disaster impact and input–output analysis”. In: *Economic Systems Research* 26.1, pp. 1–12.
- Otto, C. et al. (Oct. 2017). “Modeling loss-propagation in the global supply network: The dynamic agent-based model acclimate”. In: *Journal of Economic Dynamics and Control* 83, pp. 232–269. 10.1016/j.jedc.2017.08.001.
- Paris Agreement* (2015). FCCC/CP/2015/L.9/Rev1 (United Nations Framework Convention on Climate Change, 2015).
- Parker, M. (2018). “The impact of disasters on inflation”. In: *Economics of Disasters and Climate Change* 2.1, pp. 21–48.
- Patricola, C. M. and M. F. Wehner (2018). “Anthropogenic influences on major tropical cyclone events”. In: *Nature* 563.7731, pp. 339–346.
- Patz, J. A. et al. (2005). “Impact of regional climate change on human health”. In: *Nature* 438.7066, pp. 310–317.
- Pichler, A. et al. (2022). “Forecasting the propagation of pandemic shocks with a dynamic input-output model”. In: *Journal of Economic Dynamics and Control* 144, p. 104527.
- Przyluski, V. and S. Hallegatte (2011). “Indirect costs of natural hazards”. In: *CONHAZ report WP02 2*, pp. 383–398.
- Rahmstorf, S. and D. Coumou (2011). “Increase of extreme events in a warming world”. In: *Proceedings of the National Academy of Sciences* 108.44, pp. 17905–17909.
- Reed, K. A., A. Stansfield, et al. (2020). “Forecasted attribution of the human influence on Hurricane Florence”. In: *Science advances* 6.1, eaaw9253.
- Reed, K. A., M. F. Wehner, A. M. Stansfield, et al. (2021). “Anthropogenic influence on hurricane Dorian’s extreme rainfall”. In: *Bulletin of the American Meteorological Society* 102.1, S9–S15.

- Reed, K. A., M. F. Wehner, and C. M. Zarzycki (2022). “Attribution of 2020 hurricane season extreme rainfall to human-induced climate change”. In: *Nature communications* 13.1, p. 1905.
- Ringsmuth, A. K. et al. (2022). “Lessons from COVID-19 for managing transboundary climate risks and building resilience”. In: *Climate Risk Management*, p. 100395.
- Rose, A. (2004a). “Defining and measuring economic resilience to disasters”. In: *Disaster Prevention and Management: An International Journal* 13.4, pp. 307–314.
- (2004b). “Economic principles, issues, and research priorities in hazard loss estimation”. In: *Modeling spatial and economic impacts of disasters*, pp. 13–36.
- Shepherd, T. G. (2016). “A common framework for approaches to extreme event attribution”. In: *Current Climate Change Reports* 2, pp. 28–38.
- (2019). “Storyline approach to the construction of regional climate change information”. In: *Proceedings of the Royal Society A* 475.2225, p. 20190013.
- Shepherd, T. G. et al. (2018). “Storylines: an alternative approach to representing uncertainty in physical aspects of climate change”. In: *Climatic change* 151.3, pp. 555–571.
- Sillmann, J. et al. (2021). “Event-Based Storylines to Address Climate Risk”. In: *Earth’s Future* 9.2, e2020EF001783.
- Stechemesser, A., A. Levermann, and L. Wenz (2022). “Temperature impacts on hate speech online: evidence from 4 billion geolocated tweets from the USA”. In: *The Lancet Planetary Health* 6.9, e714–e725.
- Strauss, B. H. et al. (2021). “Economic damages from Hurricane Sandy attributable to sea level rise caused by anthropogenic climate change”. In: *Nature communications* 12.1, p. 2720.
- Strobl, E. (2011). “The economic growth impact of hurricanes: Evidence from US coastal counties”. In: *Review of Economics and Statistics* 93.2, pp. 575–589.
- Suarez-Gutierrez, L. et al. (2018). “Internal variability in European summer temperatures at 1.5 C and 2 C of global warming”. In: *Environmental Research Letters* 13.6, p. 064026.
- Tebaldi, C. et al. (2021). “Climate model projections from the scenario model intercomparison project (ScenarioMIP) of CMIP6”. In: *Earth System Dynamics* 12.1, pp. 253–293.
- Trenberth, K. E. et al. (2014). “Global warming and changes in drought”. In: *Nature Climate Change* 4.1, pp. 17–22.
- Van der Veen, A. (2004). “Disasters and economic damage: macro, meso and micro approaches”. In: *Disaster Prevention and Management: An International Journal*.
- Verschuur, J., E. E. Koks, and J. W. Hall (2021). “Observed impacts of the COVID-19 pandemic on global trade”. In: *Nature Human Behaviour* 5.3, pp. 305–307.
- Vicedo-Cabrera, A. M. et al. (2021). “The burden of heat-related mortality attributable to recent human-induced climate change”. In: *Nature climate change* 11.6, pp. 492–500.



- Villarini, G. and G. A. Vecchi (2012). “Twenty-first-century projections of North Atlantic tropical storms from CMIP5 models”. In: *Nature Climate Change* 2.8, pp. 604–607.
- Walsh, K. J. et al. (2016). “Tropical cyclones and climate change”. In: *Wiley Interdisciplinary Reviews: Climate Change* 7.1, pp. 65–89.
- Wehner, M. and C. Sampson (2021). “Attributable human-induced changes in the magnitude of flooding in the Houston, Texas region during Hurricane Harvey”. In: *Climatic Change* 166.1-2, p. 20.
- Weinkle, J. et al. (2018). “Normalized hurricane damage in the continental United States 1900–2017”. In: *Nature Sustainability* 1.12, pp. 808–813.
- Wenz, L. and A. Levermann (2016). “Enhanced economic connectivity to foster heat stress-related losses”. In: *Science advances* 2.6, e1501026.
- Wenz, L. and S. N. Willner (2022). “Climate impacts and global supply chains: an overview”. In: *Handbook on Trade Policy and Climate Change*, pp. 290–316.
- Wenz, L., S. N. Willner, et al. (2015). “Regional and sectoral disaggregation of multi-regional input–output tables—a flexible algorithm”. In: *Economic Systems Research* 27.2, pp. 194–212.
- Wiel, K. van der, G. Lenderink, and H. de Vries (2021). “Physical storylines of future European drought events like 2018 based on ensemble climate modelling”. In: *Weather and Climate Extremes* 33, p. 100350.
- Willner, S. N., A. Levermann, et al. (2018). “Adaptation required to preserve future high-end river flood risk at present levels”. In: *Science advances* 4.1, eaa01914.
- Willner, S. N., C. Otto, and A. Levermann (2018). “Global economic response to river floods”. In: *Nature Climate Change* 8.7, pp. 594–598.
- Young, H. R. et al. (2021). “Storylines for decision-making: climate and food security in Namibia”. In: *Climate and Development* 13.6, pp. 515–528.
- Zappa, G. and T. G. Shepherd (2017). “Storylines of atmospheric circulation change for European regional climate impact assessment”. In: *Journal of Climate* 30.16, pp. 6561–6577.
- Zhang, T., K. van der Wiel, et al. (2022). “Increased wheat price spikes and larger economic inequality with 2° C global warming”. In: *One Earth* 5.8, pp. 907–916.
- Zhang, Z., N. Li, et al. (2018). “Analysis of the economic ripple effect of the United States on the world due to future climate change”. In: *Earth’s Future* 6.6, pp. 828–840.



# Appendices

## Contents

---

Appendix for article 1: The intensification of snowfall extremes . . . . .	151
Appendix for article 2: The global economic response to Hurricane Sandy . . . . .	167
Appendix for article 3: The projected compensation response to Hurricane Harvey	191
Appendix for article 4: The response to extremes under global economic stress . .	221
Appendix for article 5: The utility maximizing consumer . . . . .	229

---



# Appendix for article 1: The intensification of snow-fall extremes

## Supplementary figures and tables

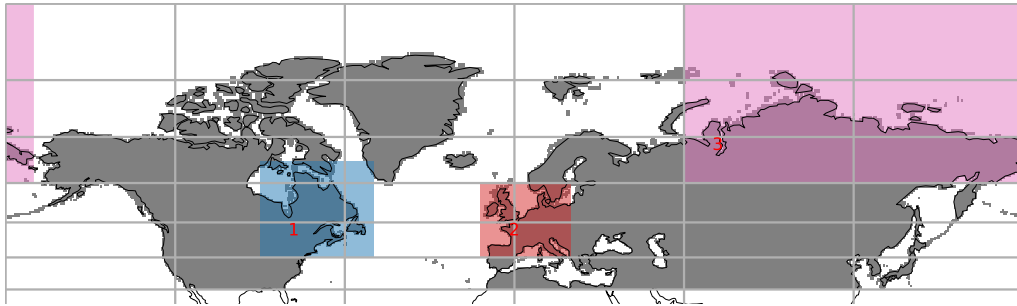


Figure S1: **Regions considered for localised analysis.** Only land area is Map created using the cartopy 0.17 Met Office n.d. library based on GSHHG shapes Wessel n.d.

Climate model
CanESM5
CNRM-CM6-1
CNRM-ESM2-1
EC-Earth3
GFDL-ESM4
IPSL-CM6A-LR
MIROC6
MPI-ESM1-2-HR
MRI-ESM2-0
UKESM1-0-LL

Table S1: **Climate models used in the ensemble**

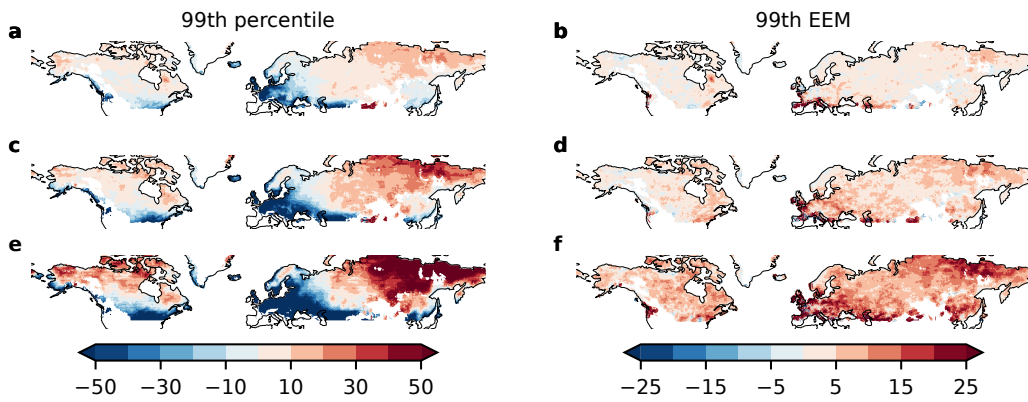


Figure S2: **99th percentile: Changes of daily snowfall metrics relative to historical baseline (1851–1920)**. Percentage change of **a,c,e** 99th percentile and **b,d,f** 99th expected extreme magnitude. **a,b** 2021–2030, **c,d** 2051–2060, **e,f** 2091–2100. Maps created using the cartopy 0.17 Met Office n.d. library based on GSHHG shapes Wessel n.d.

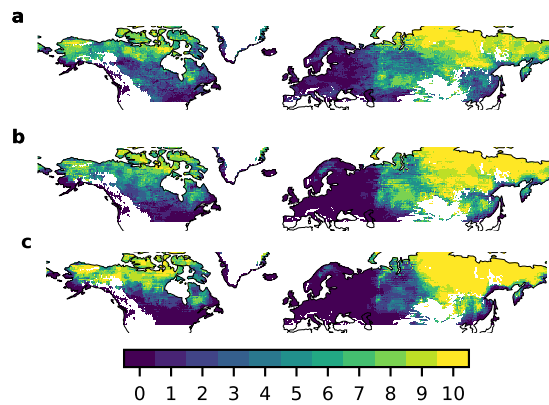


Figure S3: **High-model agreement on mean daily snowfall changes**. Number of models showing an increasing mean daily snowfall; **a** 2021–2030, **b** 2051–2060, **c** 2091–2100. Maps created using the cartopy 0.17 Met Office n.d. library based on GSHHG shapes Wessel n.d.

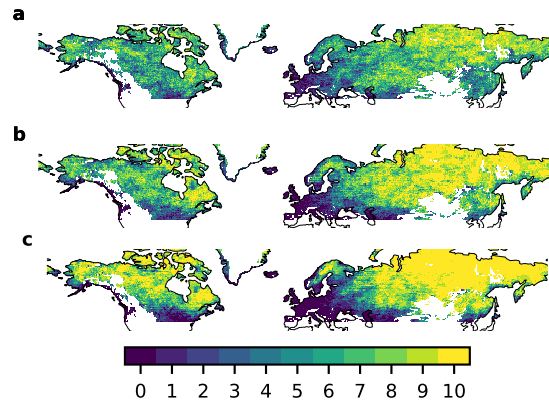


Figure S4: **High-model agreement on 99.9th percentile changes.** Number of models showing an increasing 99.9th percentile; **a** 2021–2030, **b** 2051–2060, **c** 2091–2100. Maps created using the cartopy 0.17 Met Office n.d. library based on GSHHG shapes Wessel n.d.

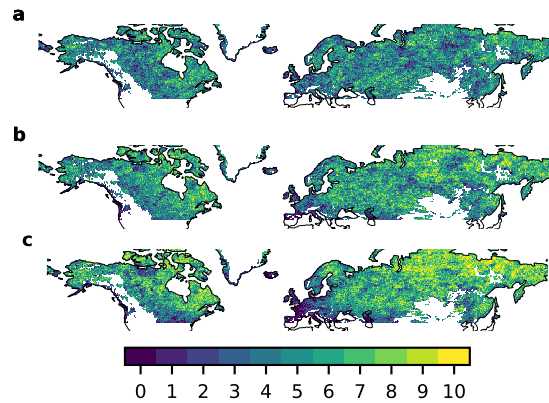


Figure S5: **Mixed model agreement on EEM above the 99.9th baseline percentile changes.** Number of models showing an increasing 99.9th EEM; **a** 2021–2030, **b** 2051–2060, **c** 2091–2100. Maps created using the cartopy 0.17 Met Office n.d. library based on GSHHG shapes Wessel n.d.

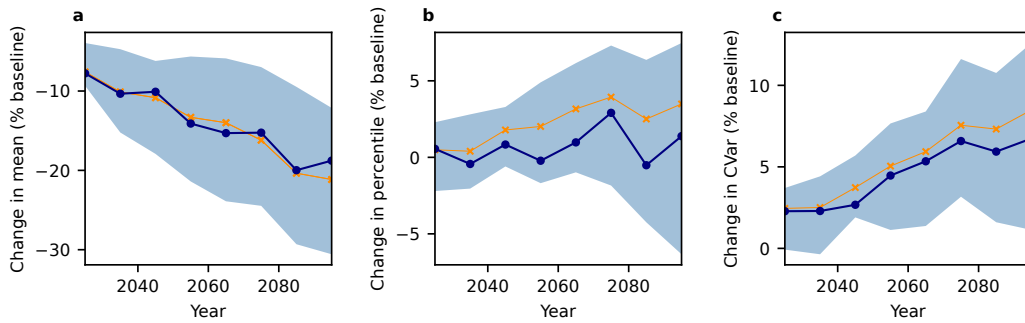


Figure S6: **Contrasting global trends of mean daily snowfall and extreme snowfall measures — using the current percentile as a threshold** (as in Fig. 3 with CVar instead of EEM, decadal statistics, Northern Hemisphere north of 40°N, for SSP5-RCP8.5). All values are area-weighted and relative to the baseline (1851–1920) climate. **a** Mean, **b** 99.9th percentile, **c** Conditional Value at Risk of the 99.9th percentile. Blue line shows the model ensemble median, shaded areas denote the likely range (16.7th to 83.3rd percentiles). Orange line shows statistics for all ten models combined into one time series ensemble.

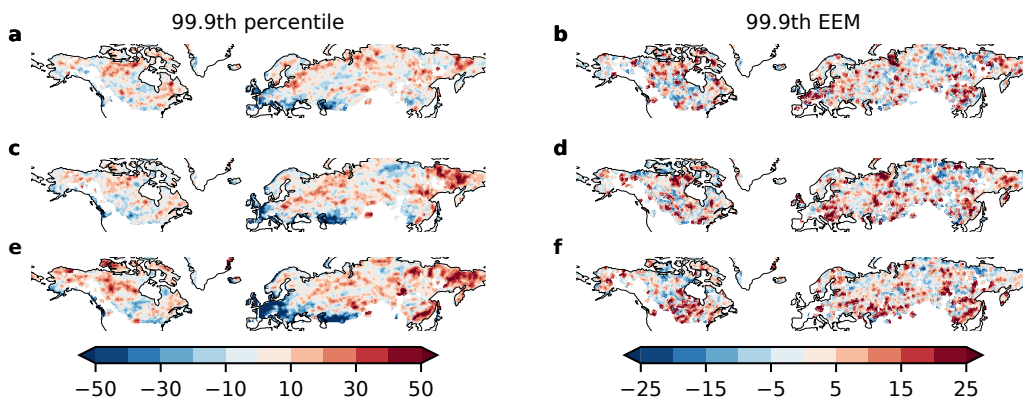


Figure S7: **Fig. 1 for CMIP MPI-ESM1-2-HR model without bias correction, SSP5-RCP8.5: Changes of daily snowfall metrics relative to historical baseline (1851–1920).** Percentage change of **a,c,e** 99.9th percentile and **b,d,f** 99.9th expected extreme magnitude. **a,b** 2021–2030, **c,d** 2051–2060, **e,f** 2091–2100. Maps created using the cartopy 0.17 Met Office n.d. library based on GSHHG shapes Wessel n.d.



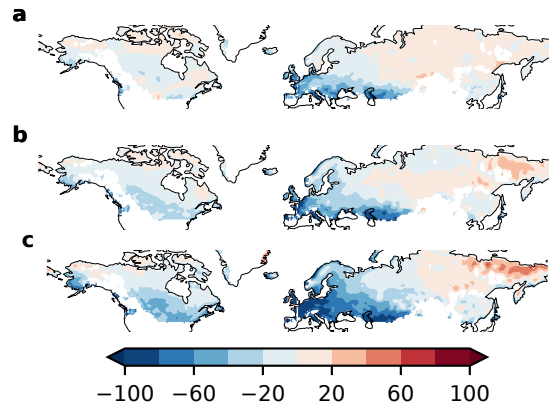


Figure S8: **Fig. 2** for CMIP MPI-ESM1-2-HR model without bias correction, SSP5-8.5: Changes of daily snowfall mean relative to historical baseline (1851–1920). **a** 2021–2030, **b** 2051–2060, **c** 2091–2100. Maps created using the cartopy 0.17 Met Office n.d. library based on GSHHG shapes Wessel n.d.

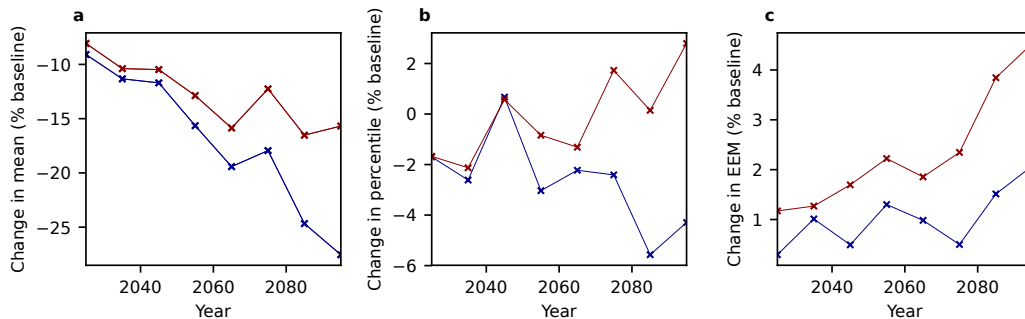


Figure S9: **Fig. 3** for CMIP without bias correction –blue line– and ISIMIP bias corrected –red line– MPI-ESM1-2-HR model, SSP5-8.5: Contrasting global trends of mean daily snowfall and extreme snowfall measures (elevation below 1000m, decadal statistics, Northern Hemisphere north of 40°N). All values are relative to the baseline (1851–1920) climate. **a** Mean, **b** 99.9th percentile, **c** Expected extreme magnitude above the 99.9th baseline percentile.

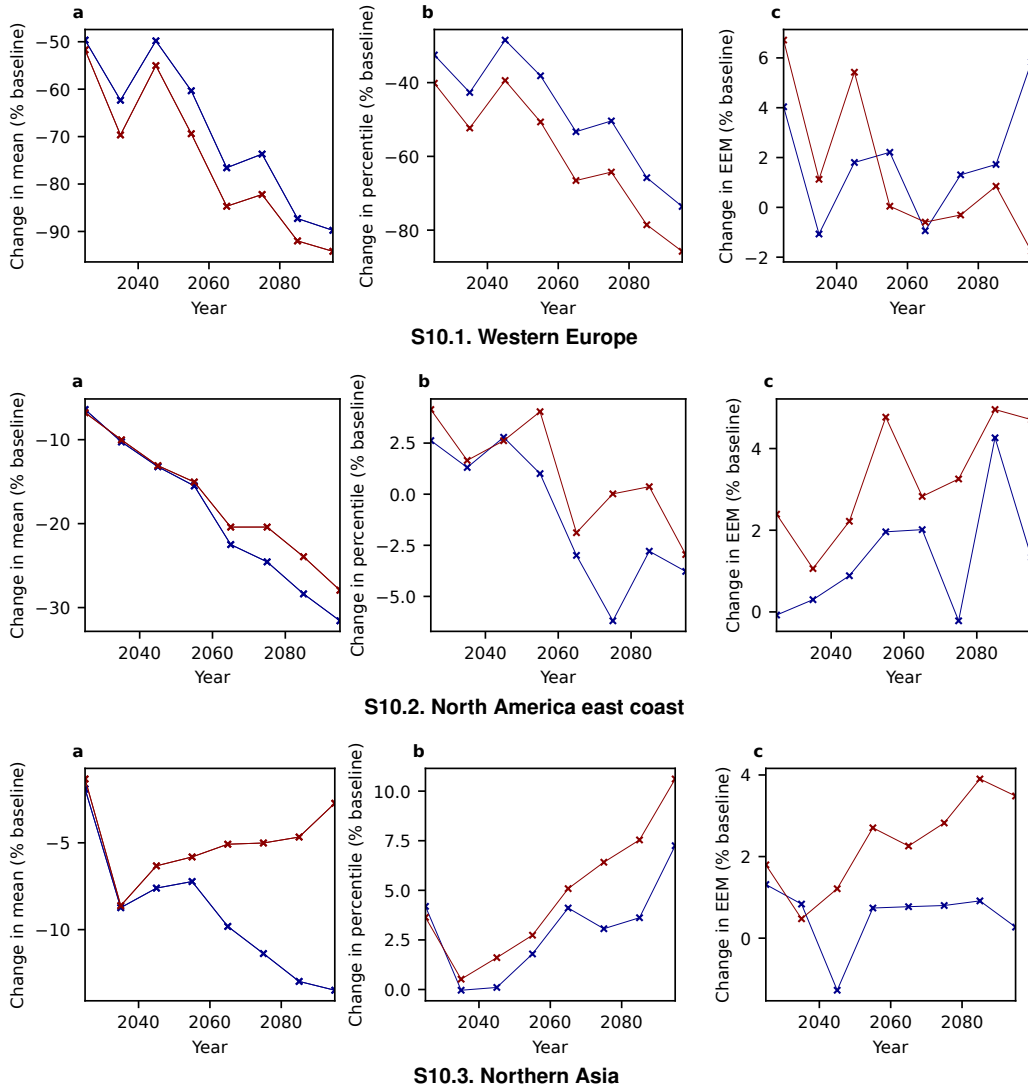


Figure S10: **Fig. 6 for CMIP without bias correction –blue line– and ISIMIP bias corrected –red line– MPI-ESM1-2-HR model: Regional differences of changes in daily snowfall statistics** (elevation below 1000m, decadal statistics, SSP5-RCP8.5). All values are relative to the baseline (1851–1920) climate. **a** Mean, **b** 99.9th percentile, **c** Expected extreme magnitude above the 99.9th baseline percentile.

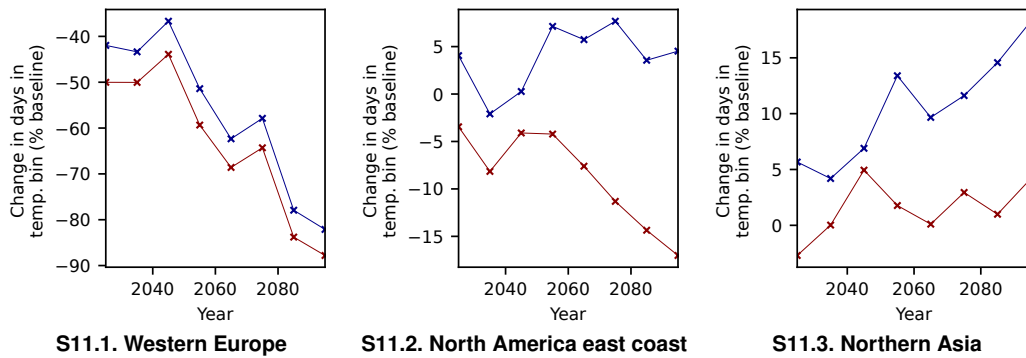


Figure S11: **Fig. 6 for CMIP without bias correction –blue line– MPI-ESM1-2-HR model and ISIMIP bias corrected –red line– MPI-ESM1-2-HR model, SSP5-8.5; Regional differences in trend of days with surface temperature between –2.5°C and –1.5°C.** For elevation below 1000m, decadal statistics. All values are relative to the baseline (1851–1920) climate.

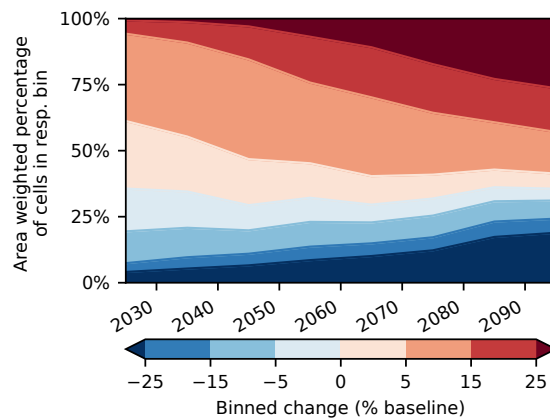


Figure S12: **Area exposed to strongly (more than 5 percentage points compared to baseline levels) intensifying snowfall events grows almost until the end of the century - Global area weighted trend of 99.9th percentile** (elevation below 1000m, decadal statistics, Northern Hemisphere north of 40°N, SSP5-RCP8.5). Binned according to change relative to the baseline (1851–1920) climate. Coloured area represents the area weighted percentage of cells in the respective bin.

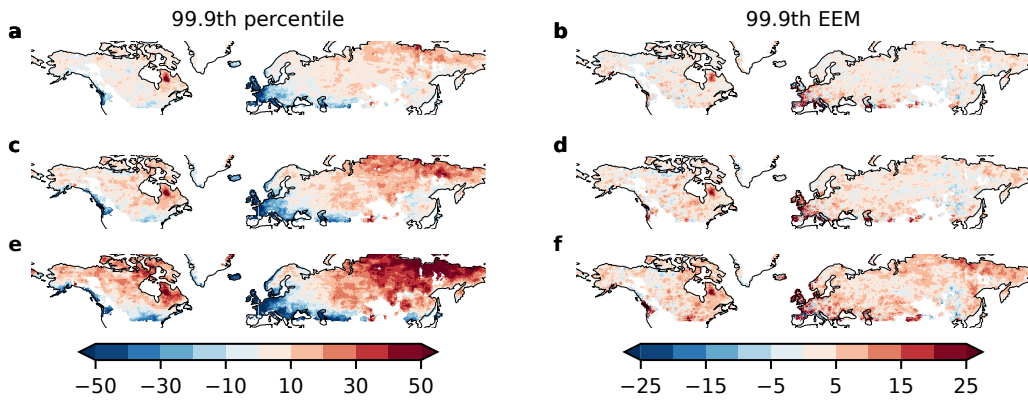


Figure S13: **SSP3-RCP7.0: Changes of daily snowfall metrics relative to historical baseline (1851–1920).** Percentage change of **a,c,e** 99.9th percentile and **b,d,f** 99.9th expected extreme magnitude. **a,b** 2021–2030, **c,d** 2051–2060, **e,f** 2091–2100. Maps created using the cartopy 0.17 Met Office n.d. library based on GSHHG shapes Wessel n.d.

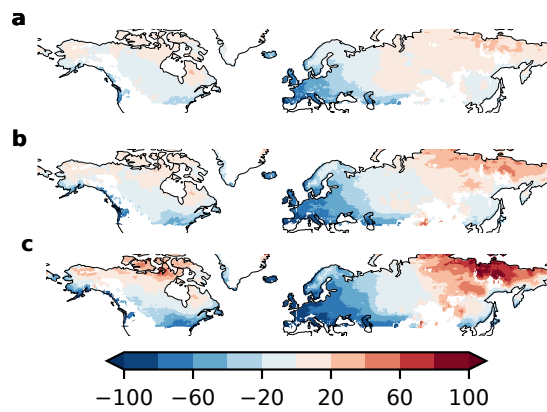


Figure S14: **SSP3-RCP7.0: Changes of daily snowfall mean relative to historical baseline (1851–1920).** **a** 2021–2030, **b** 2051–2060, **c** 2091–2100. Maps created using the cartopy 0.17 Met Office n.d. library based on GSHHG shapes Wessel n.d.

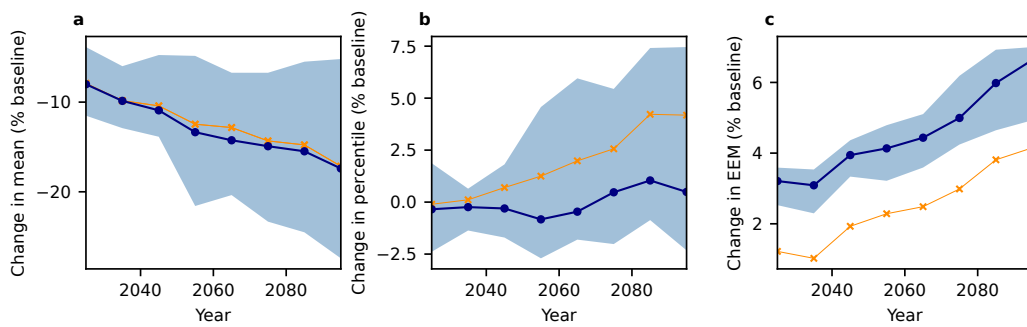


Figure S15: **SSP3-RCP7.0: Contrasting global trends of mean daily snowfall and extreme snowfall measures** (elevation below 1000m, decadal statistics, Northern Hemisphere north of 40°N). All values are relative to the baseline (1851–1920) climate. **a** Mean, **b** 99.9th percentile, **c** Expected extreme magnitude above the 99.9th baseline percentile. Blue line shows the model ensemble median, shaded areas denote the likely range (16.7th to 83.3rd percentiles). Orange line shows statistics for all ten models combined into one time series ensemble.

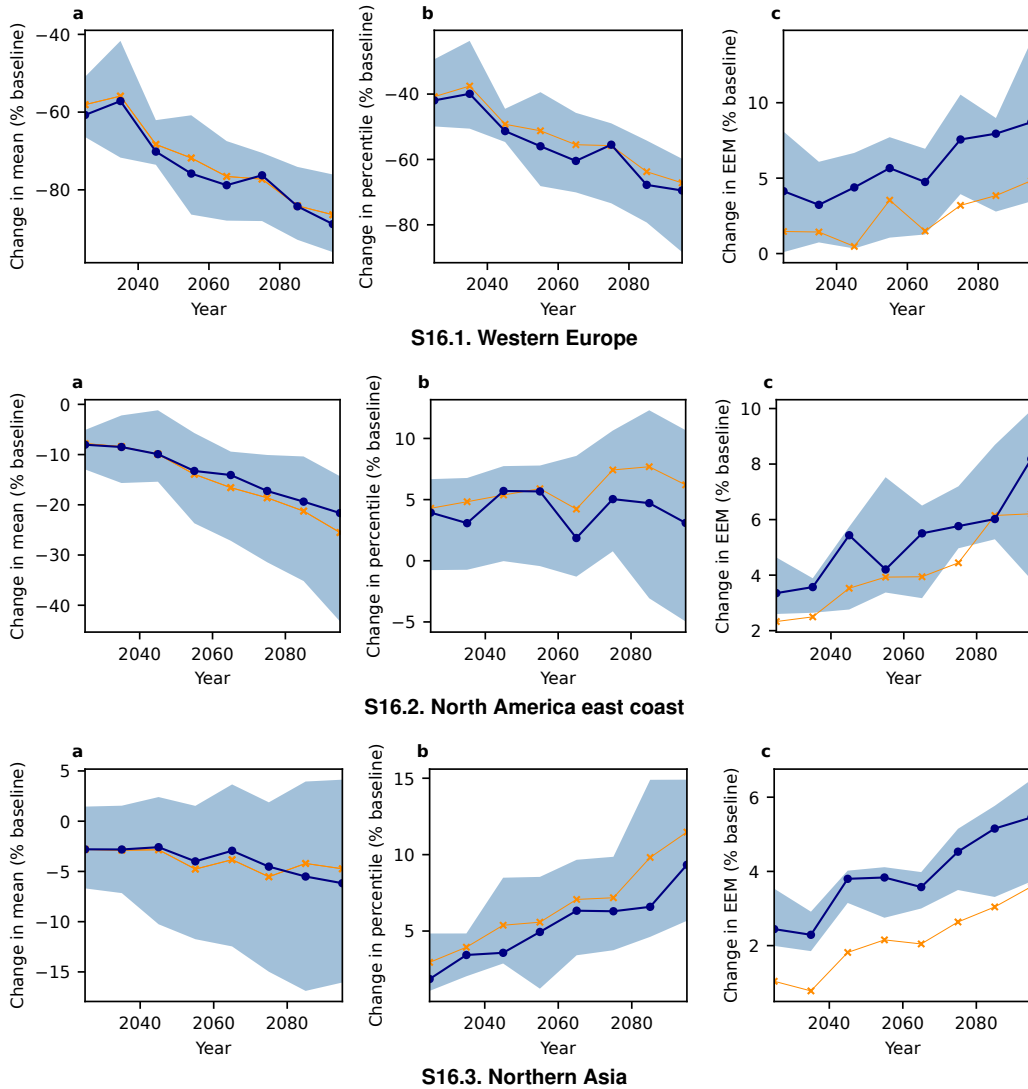


Figure S16: **SSP3-RCP7.0: Regional differences of changes in daily snowfall statistics** (elevation below 1000m, decadal statistics, SSP5-RCP8.5). All values are relative to the baseline (1851–1920) climate. **a** Mean, **b** 99.9th percentile, **c** Expected extreme magnitude above the 99.9th baseline percentile. Blue line shows the model ensemble median, shaded areas denote the likely range (16.7th to 83.3rd percentiles). Orange line shows statistics for all ten models combined into one time series ensemble.

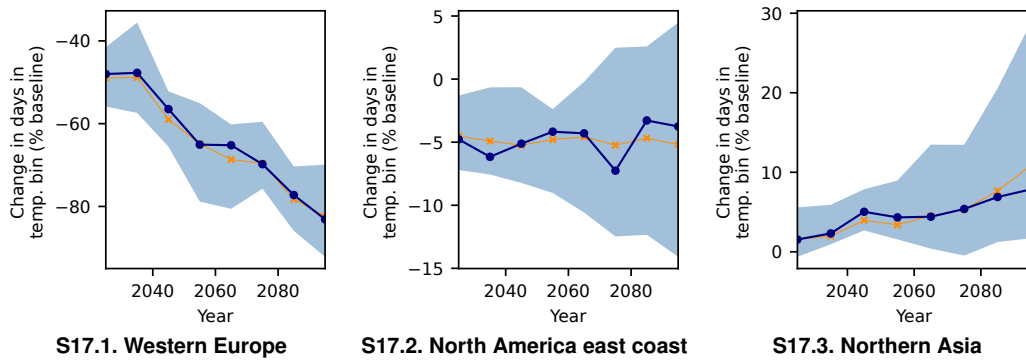


Figure S17: **SSP3-RCP7.0: Regional differences in trend of days with surface temperature between  $-2.5^{\circ}\text{C}$  and  $-1.5^{\circ}\text{C}$ .** For elevation below 1000m, decadal statistics. All values are relative to the baseline (1851–1920) climate. Blue line shows the model ensemble median, shaded areas denote the likely range (16.7th to 83.3rd percentiles). Orange line shows statistics for all ten models combined into one time series ensemble.

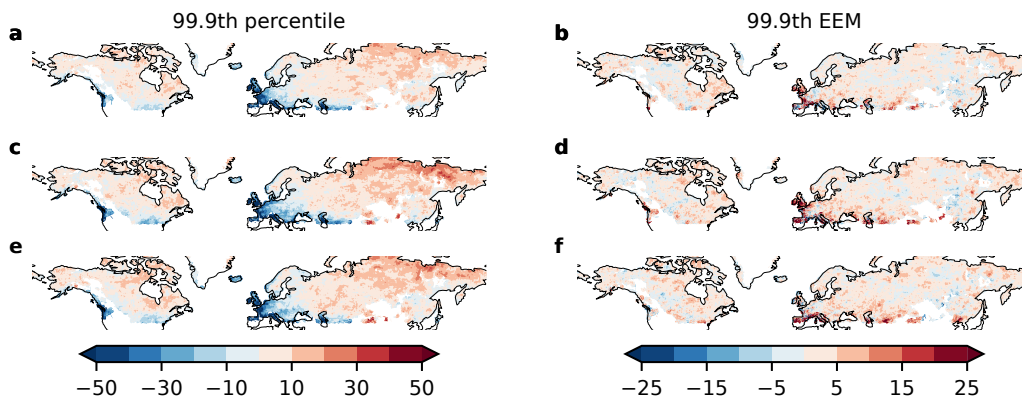


Figure S18: **SSP1-RCP2.6: Changes of daily snowfall metrics relative to historical baseline (1851–1920).** Percentage change of **a,c,e** 99.9th percentile and **b,d,f** 99.9th expected extreme magnitude. **a,b** 2021–2030, **c,d** 2051–2060, **e,f** 2091–2100. Maps created using the cartopy 0.17 Met Office n.d. library based on GSHHG shapes Wessel n.d.

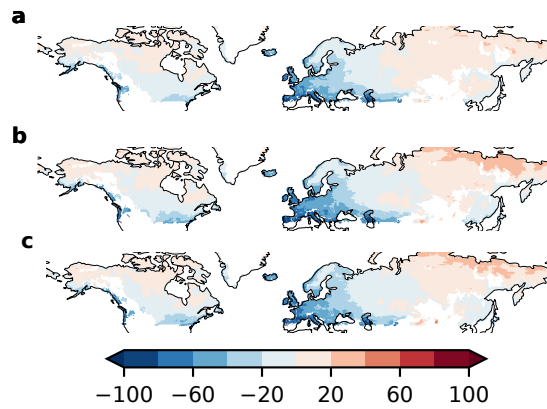


Figure S19: **SSP1-RCP2.6: Changes of daily snowfall mean relative to historical baseline (1851–1920).** **a** 2021–2030, **b** 2051–2060, **c** 2091–2100. Maps created using the cartopy 0.17 Met Office n.d. library based on GSHHG shapes Wessel n.d.

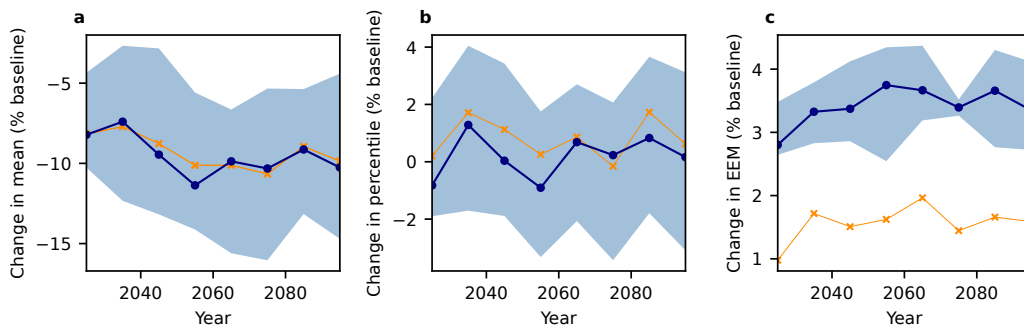


Figure S20: **SSP1-RCP2.6: Global trends of mean daily snowfall and extreme snowfall measures** (elevation below 1000m, decadal statistics, Northern Hemisphere north of 40°N). All values are relative to the baseline (1851–1920) climate **a** Mean **b** 99.9th percentile **c** Expected extreme magnitude above the 99.9th baseline percentile. Blue line shows the model ensemble median, shaded areas denote the likely range (16.7th to 83.3rd percentiles). Orange line shows statistics for all ten models combined into one time series ensemble.



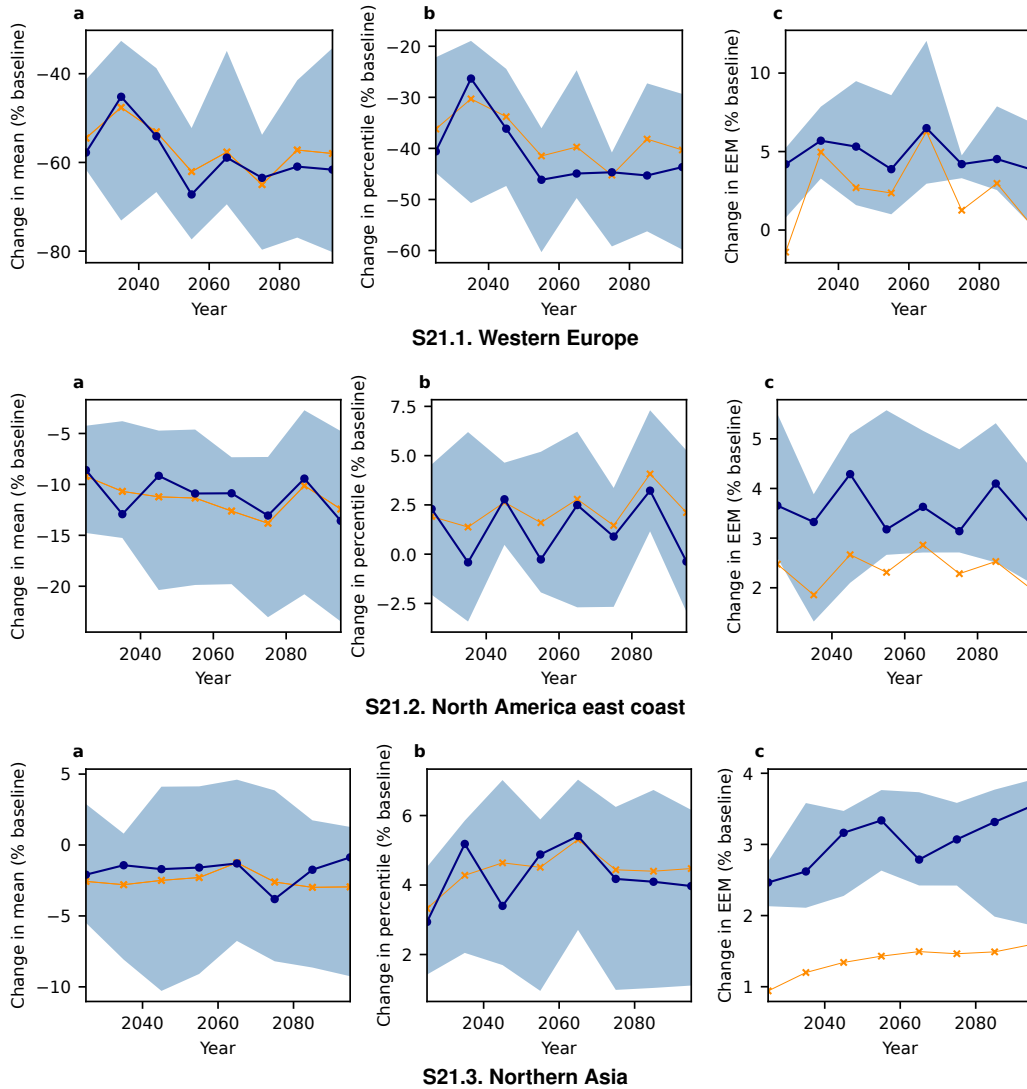


Figure S2I: **SSP1-RCP2.6: Regional differences of changes in daily snowfall statistics** (elevation below 1000m, decadal statistics, SSP5-RCP8.5). All values are relative to the baseline (1851–1920) climate. **a** Mean, **b** 99.9th percentile, **c** Expected extreme magnitude above the 99.9th baseline percentile. Blue line shows the model ensemble median, shaded areas denote the likely range (16.7th to 83.3rd percentiles). Orange line shows statistics for all ten models combined into one time series ensemble.

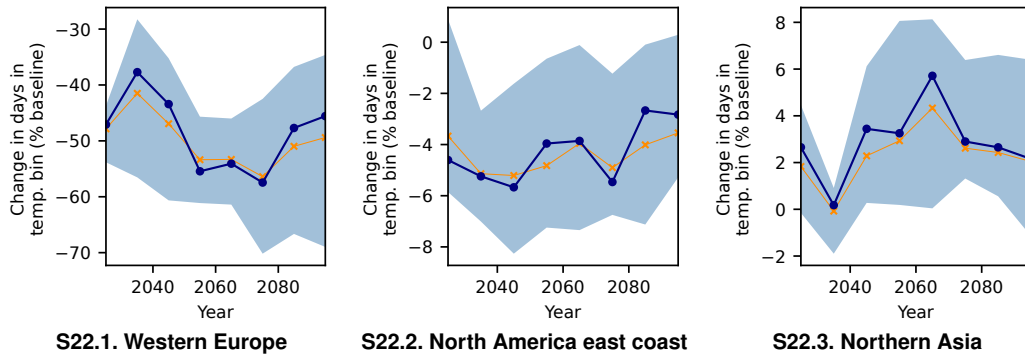


Figure S22: **SSP1-RCP2.6: Regional differences in trend of days with surface temperature between  $-2.5^{\circ}\text{C}$  and  $-1.5^{\circ}\text{C}$**  (elevation below 1000m, decadal statistics). All values are relative to the baseline (1851–1920) climate. Blue line shows the model ensemble median, shaded areas denote the likely range (16.7th to 83.3rd percentiles). Orange line shows statistics for all ten models combined into one time series ensemble.

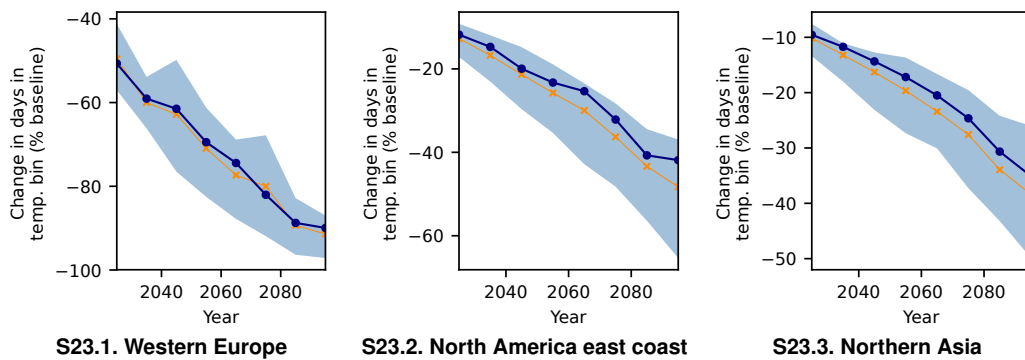
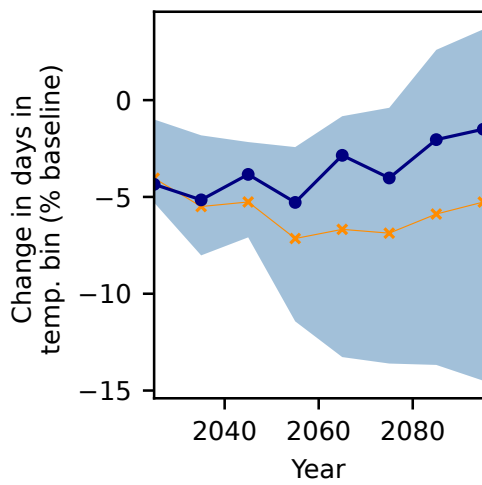
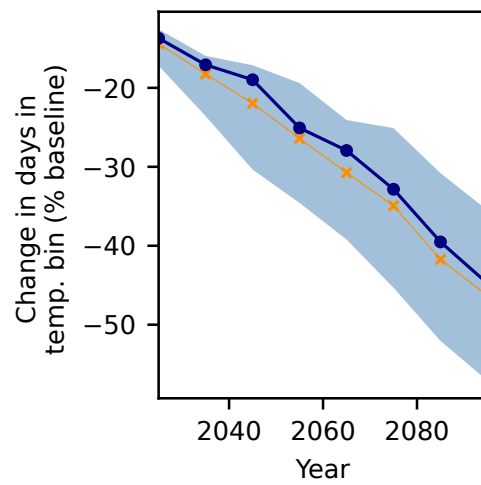


Figure S23: **Days with surface temperature below  $0^{\circ}\text{C}$**  (elevation below 1000m, decadal statistics, comparison between different regions, SSP5-RCP8.5). All values are relative to the baseline (1851–1920) climate. Blue line shows the model ensemble median, shaded areas denote the likely range (16.7th to 83.3rd percentiles). Orange line shows statistics for all ten models combined into one time series ensemble.



**S24.1. Temp. in [-2.5°C, -1.5°C]**



**S24.2. Temp. below 0°C**

Figure S24: **Comparison between different temperature bins.** Decadal statistics of days with surface temperature in given temperature range for elevation below 1000m for the Northern Hemisphere north of 40°N for SSP5-RCP8.5. All values are relative to the baseline (1851–1920) climate.

## References

- Met Office (n.d.). *Cartopy: a cartographic python library with a Matplotlib interface*. Exeter, Devon.
- Wessel, P. (n.d.). *gshhg - A Global Self-consistent, Hierarchical, High-resolution Geography Database*.

## Appendix for article 2: The global economic response to Hurricane Sandy

### Methods

#### Business interruption recovery

We assume the business interruption (BI) to be very strong but short, representing the short-term disruptions after the storm that can be quickly recovered from to an extent that most business processes are again functional, e.g. interruptions due to power outages, flooding, transportation disruption, and disturbance in communication. We set the initial intensity of this BI for NY and NJ to the GDP share of the respective state that is physically exposed to the hurricane. As damage from Sandy was primarily due to precipitation and flooding, we focus on this physical factor. For that, we calculate GDP exposure on a county level. We consider those counties as exposed for which the U.S. Geological Survey (USGS) reported at least one high water mark (USGS n.d.).

We then assume exponential recovery from the BI as is commonly done with disaster recovery (Hallegatte 2015; Baghersad and Zobel 2015), assuming a rather efficient recovery of the local economy (Koks et al. 2016) which we esteem realistic for the economically strong regions of NY and NJ. The intuitive reason for using exponential recovery in this case is that most effective measures of recovery can be believed to take place first. Subsequent measures may be less effective in comparison to their effort, resulting in an exponential path of recovery. As an example, power supply was restored exponentially after Hurricane Sandy (Kunz et al. 2013). We can also observe exponential recovery after Hurricane Katrina as measured by the Louisiana Coincident Economic Activity Index (Federal Reserve Bank of Philadelphia n.d.) (the index is based on non-farm payroll employment, the unemployment rate, average hours worked in manufacturing, and wages and salaries). However, this is a long-term recovery over about one year and therefore presumably cannot be explained by BI alone but potentially also reflects losses due to reconstruction efforts and capital stock losses. To estimate a time scale for the exponential decay of the BI shock, we similarly use unemployment as a proxy. The Federal Reserve Bank of New York found unemployment claims in NY and NJ to rise due to Sandy with the number of initial claims showing a roughly exponential decay (see Fig. 1 in Abel et al. 2021) after an initial peak. According to this report, “both states saw employment rebound to above October (pre-Sandy) levels by the end of the year” 2012. We therefore fit our BI recovery to end after 60 days. This time scale is also in accordance with a Downtown Alliance report (Downtown Alliance 2015)

which finds that over 95% of Manhattan office space was available again after Sandy by the end of the year 2012.

Note that our notion of recovery does not include any concept of growth, i.e. we consider recovery as completed once output quantities equal those before the disaster. Generally, disasters can have long-term or even permanent effects (Hallegatte and Przyluski 2010) and it has been shown that tropical cyclones have long-term impacts on economic growth (Strobl 2011) with effects lasting as long as 20 years (Hsiang and Jina 2014). Unlike for fluvial floods, countries with higher development are not well prepared against the impact of tropical cyclones and their associated long-term growth losses (Krichene et al. 2021). Since we focus here on the short-term impacts, we do not model growth and assume a constant baseline economy, resulting in much shorter recovery times.

We assume an initial production capacity reduction factor  $\lambda_0$  in the direct aftermath of the disaster as the share of state GDP that is exposed to the disaster. We use reported high water marks associated with the disaster to determine how severely individual states are affected. We retrieve high water marks from the USGS Flood Event Viewer (USGS n.d.). We consider each county within a state as affected by the disaster if it has at least one reported high water mark. We then calculate the relative GDP exposure, i.e. the initial production capacity reduction  $\lambda_0$ , of the entire state from

$$\lambda_0 = \frac{\sum_{c \in C} GDP_c}{GDP_s} \quad (1)$$

where  $GDP_c$  is the GDP of an affected county from the set of all affected counties  $C$  and  $GDP_s$  is the overall state's GDP.

While this approach to determine the initial production capacity reduction of a directly affected state is a rather simple one, we believe that it is still sufficiently good to achieve a realistic scenario of direct economic losses. Given that this initial reduction of production capacity level only prevails for a very short time and then is gradually relieved by the exponential recovery curve, we esteem variations in this value as less crucial for the outcome of the simulations than the direct economic loss which determines how long the production capacity reduction persists. For NY and NJ, we obtain initial production shock of  $\sim 80.2\%$  and  $\sim 69.3\%$ , respectively. This matches observations rather well. According to the Empire State Manufacturing Survey (Federal Reserve Bank of New York 2012) by the Federal Reserve Bank of New York, more than 90% of all businesses in the New York City area were shut down for at least one day due to Hurricane Sandy. For example, the New York stock exchange was shut down for two days after the hurricane.<sup>1</sup> The New York-Newark-Jersey City Metropolitan Statistical Area (NYMSA) accounts for a 2012 GDP of about \$1.4bn and counts mostly to the GDP of New York and New Jersey (and a negligible fraction for Pennsylvania with only one county). NY and NJ have

<sup>1</sup><https://www.theguardian.com/world/2012/oct/31/new-york-stock-exchange-opens-sandy>

a combined 2012 GDP of about \$1.8bn. Using GDP as a proxy for economic activity, we thus may assume that a 90% one-day shut down in the NYMSA is equivalent to a 68.4% one-day shutdown for both states combined. However, this number does not include businesses that were only partly disrupted and must hence be considered a lower bound for economic disruption. Our estimates for New York and New Jersey with 80.2% and 69.3% therefore seem reasonable for the day immediately following the hurricane.

After the disaster, we assume exponential recovery of the economy back to 100% from the initial production shock given by [equation \(1\)](#). Reduction in productive capacity is then given by

$$f(t) := 1 - \lambda_0 e^{-t/\tau} \quad (2)$$

with initial shock  $\lambda_0$  and characteristic time scale  $\tau$ . We assume that full recovery is given at time  $t_r$  once the shock has decayed to 0.1% or less, i.e.  $f_r = f(t_r) \geq 0.999$ . With a prescribed recovery time  $t_r$ , we thus can derive  $\tau$ :

$$\begin{aligned} f(t_r) = f_r &= 1 - \lambda_0 e^{-t_r/\tau} \\ \Rightarrow \tau &= -\frac{t_r}{\ln(\frac{1-f_r}{\lambda_0})}. \end{aligned} \quad (3)$$

The fully parametrised curve for the reduction of production capacity is then given by

$$f_{\lambda_0, f_r}(t) := \begin{cases} 1 - \lambda_0 e^{-t/\tau_{\lambda_0, f_r, t_r}} & \text{for } t \leq t_r \\ 1 & \text{for } t > t_r. \end{cases} \quad (4)$$

For the US states NY and NJ with recovery time  $t_r = 60$ , this yields the production capacity reduction curves shown in [Supplementary Fig. 1](#). The initial production capacity reduction values  $\lambda_0$  are listed in [Supplementary Tbl. 1](#).

## Indirect and consumption losses

To simulate indirect and consumption losses, we use the dynamic agent-based model *Acclimate* (Otto et al. 2017). This model has been presented in different versions previously (Bierkandt et al. 2014; Wenz, Willner, Bierkandt, et al. 2014; Otto et al. 2017) and was used in studies regarding the higher-order economic losses from extreme weather events (Willner, Otto, and Levermann 2018; Kuhla, Willner, Otto, Wenz, et al. 2021; Kuhla, Willner, Otto, Geiger, et al. 2021). We here use the latest model presented in Otto et al. (2017) (Otto et al. 2017). In this model, regional economic sectors are represented by individual agents that are interconnected through trade flows. The resolution of these regions is on a state-level in case of the United States, province-level in case of China and national level for all other

regions of the world, resulting in a total of 268 individual regions. The economy is split into 27 sectors, including the final consumer as one sector without production output. All sectors of a region that is directly affected by the hurricane are subjected to the same production reduction curves as per equation (4). Trade flows between the resulting total of 7,263 agents are taken from a disaggregated (Wenz, Willner, Radebach, et al. 2015) version of the EORA multi-regional input-output dataset (Lenzen et al. 2012). This data set contains annual monetary flows between the agents from the year 2012. We break this down to a monetary daily baseline flow by distributing equally over 365 days which we refer to as baseline equilibrium flow. This is the state around which *Acclimate* simulates deviations resulting from an externally enforced reduction of production capacity. This production shock results in perturbations of demand, supply and prices within the model, globally. The dynamics is a result from the profit maximisation that each individual agent performs by optimising production levels, demand distribution to suppliers and upstream demand to other agents. In this, increased demand from other agents can be addressed by activation of idle production capacities, resulting in elevated production prices. A comprehensive description of the model can be found in the original publication by Otto et al. (2017) (Otto et al. 2017).

For the present study, we look into the output variables of production, final consumption, and communicated demands along the supply chains as well as associated prices. Using the 2012 EORA dataset, the baseline flows must be considered influenced by the economic shock of Hurricane Sandy. However, this influence is small compared to the total volume of trade flows such that the introduced bias is negligible. For example, the impact of Hurricane Sandy on GDP in remote regions cannot be found in historic data.

While included in the simulations, for all calculations and analyses in this study, we exclude the EORA regions of Belarus, Moldova, Sudan, and South Sudan since the data quality for these regions is not reliable, especially with regards to final consumption.

Aggregate relative consumption changes  $\Delta \bar{C}_r$  in each simulated region  $r$  for the direct aftermath of the hurricane are calculated from the simulated consumption levels as follows:

$$\Delta \bar{C}_r = -1 + \frac{1}{(T - t_0)c_r^*} \sum_{t=t_0}^T c_r^{(t)} \quad (5)$$

where  $c_r^{(t)}$  is the final consumption in region  $r$  at time step  $t$ ,  $c_r^*$  is the baseline consumption and  $(T - t_0)$  is the time of aggregation after the disaster.

## Consumption prices

Consumers in the model, like other agents, purchase at a price which they propose to producers together with their demand request. This reservation price is oriented towards offer prices that producers advertise to their trade partners. The entirety of reservation



prices and the production quantity resulting from a producer's optimization process determine the final production price. The latter in turn influences the offer price that producers advertise. Therefore, in case of rising production prices, consumers also need to pay higher prices to ensure that their demand will be fulfilled. Production prices and consumer purchasing prices are therefore related. However, the measured consumption price is buffered by storage inventories that fill up and thus smooth production prices. Hence, the consumption price is an average of the goods' prices currently in storage and therefore averages production prices over a certain amount of time.

### Capacity utilisation and demand exceedance

Capacity utilization that is defined as the ratio of actual output to the output that would minimise production costs (Berndt and Morrison 1981). In the *Acclimate* model, the production output that would minimise production costs is given by the baseline production level. Beyond this production level, production costs increase super-linearly. However, for the directly affected regions of NY and NJ, the production capacity is diminished due to the hurricane. We therefore need to adjust the capacity utilization to the applied production capacity reduction. We calculate the change in capacity utilization  $u$  for region  $r$  at time step  $t$  from the applied production shock (i.e., the reduction in production capacity)  $f$ , the production level  $X$  and the baseline production level  $X^*$  as

$$u_r^{(t)} = \frac{X_r^{(t)}}{f_r^{(t)} X_r^*} - 1. \quad (6)$$

Hence, this measure quantifies if and by how much a region is in a state of overproduction, relative to the actual production capacity. In this, we need to adjust the baseline production level  $X^*$  with the production capacity reduction factor  $f_r$  in case of directly affected regions. A positive value means that the region is in a state of overproduction, causing production costs to increase super-linearly with the production quantity. Negative values indicate proportionality between production quantities and production prices.

Similarly, we define the demand exceedance  $e$  for region  $r$  at time step  $t$  as

$$e_r^{(t)} = \frac{d_r^{(t)}}{f_r^{(t)} X_r^*} - 1, \quad (7)$$

using the incoming demand  $d$  that the agent receives. Demand exceedance indicates if fulfilling the entire incoming demand at a given time step would drive the agent into overproduction (for positive values) or not (zero and negative values).

## Sectorial and regional aggregation

Sectors in regions are represented by individual agents in the *Acclimate* model. Thus we obtain simulated time series for each sector in every simulated region, individually. A time series of quantity variable  $q_{ir}$  of agent  $ir$  is classified by its pair of sector  $i$  and region  $r$ . However, to present comprehensive results, we aggregate time series for variables of interest over sectors or regions. For this we aggregate the quantity variables over the agents ensemble  $\{ir\}$ :

$$q_{\{ir\}} = \sum_{ir \in \{ir\}} q_{ir} \quad (8)$$

to obtain the sum of quantity values  $q_{\{ir\}}$ . Quantity variables are, for example, demand quantities or production quantities.

Aggregated price variables  $\langle p_{\{ir\}} \rangle$ , on the other hand, are calculated as the weighted average over all prices  $p_{ir}$  of the individual agents  $ir$ :

$$\langle p_{\{ir\}} \rangle = \frac{\sum_{ir \in \{ir\}} p_{ir} q_{ir}}{\sum_{ir \in \{ir\}} q_{ir}}. \quad (9)$$

We note that this aggregation can lead to apparent contradictions when considering, for example, demand exceedance and capacity utilization of aggregated agents. For example, in Fig. 5 the pooled region USA-OTH shows positive demand exceedance and simultaneous low capacity utilization during the first days after the disaster. This is simply a result of the aggregation that we perform over the US regions and their individual sectors. Some agents receive less demand due to the upstream network effect and others experience higher demand to compensate for NY and NJ production outages. While production levels react proportionally to demand changes if the demand exceedance is below zero, they are bound by supply or costs and potential revenue if the demand exceedance is positive. Therefore, the average production for all non-affected US regions is below baseline despite a positive average demand exceedance. However, the longer the scarcity situation prevails, the more agents in the non-affected US receive elevated demand and switch to overproduction, eventually resulting in an increased capacity utilization of USA-OTH as well.

## Consumer flexibility to price changes

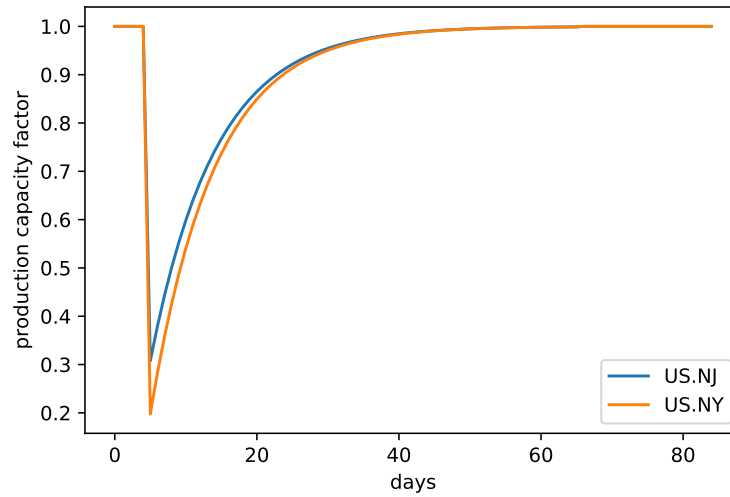
Consumers with different income tend to have a diverse flexibility if prices change for different commodities and services. This flexibility is integrated into our model by the regionally and sectorally dependent parameter of consumption price elasticity. We divide the regions used in our simulation into four income level groups: low, lower-middle,

upper-middle, high income level (Supplementary Tbl. 2). The classification of the income level groups is based on the gross national income (GNI) per capita (GNIPc) of each country. We use the annual, inflation-adjusted definition and classification of income level groups of the World Bank for the year 2012 (Khokhar n.d.). For this calibration, we only focus on average consumer income and do not consider other socio-economic structures (education, regional wealth distribution, etc.).

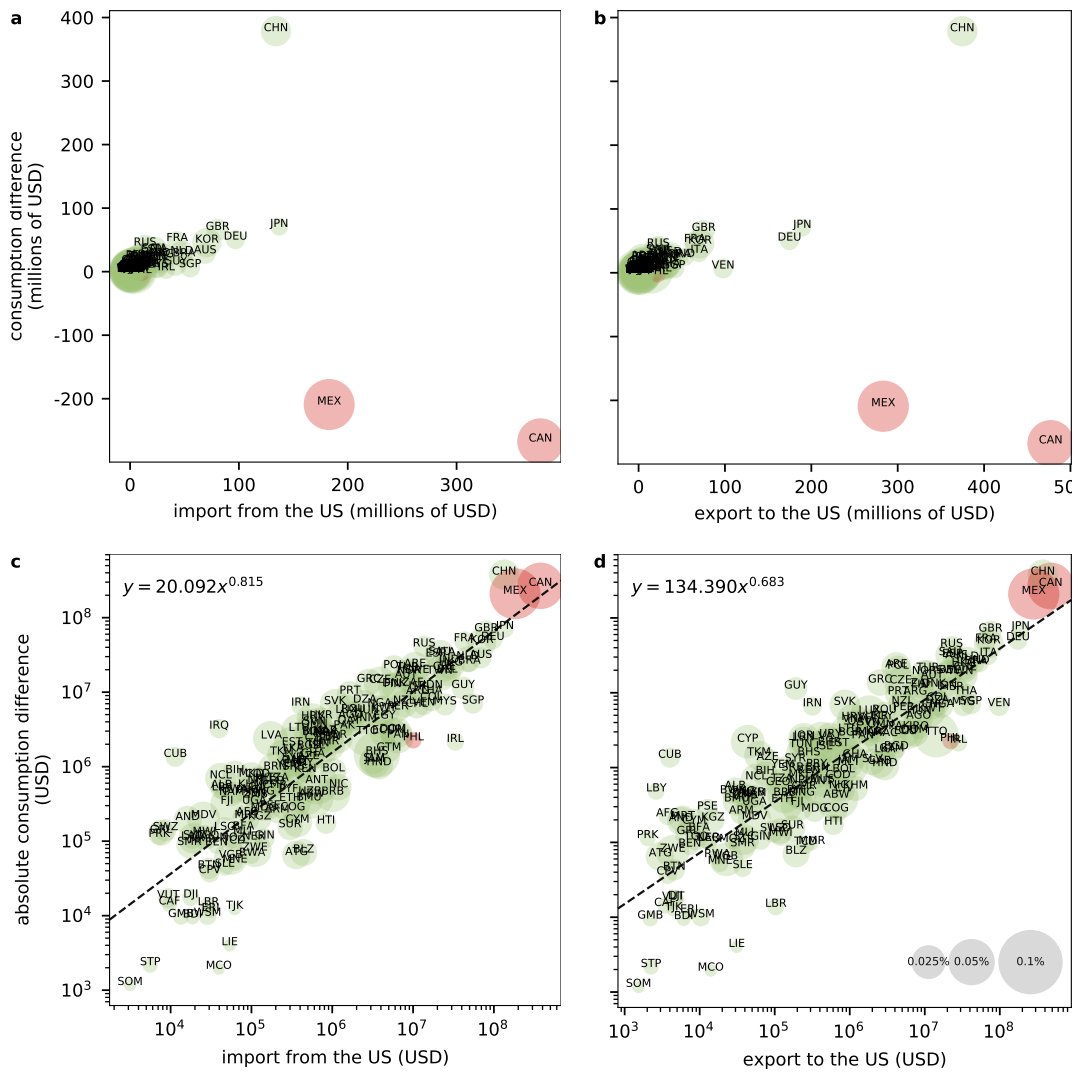
To obtain empirical parameters, we use the target income elasticities of demand for 140 regions and 10 commodity classes (Reimer and Hertel 2004) of the Global Trade Analysis Project (GTAP) (Ianchovichina and McDougall 2000). The regional resolutions of EORA and GTAP are not identical. To address this, we set the consumption price elasticities for non-GTAP-countries to the respective income level group parameter. Similarly, the sectoral resolutions of EORA and GTAP are not identical either. To handle this, we map EORA's economic sectors to the GTAP commodity classes and group them into three categories: vital, relevant and other (Supplementary Tbl. 3). Using these two classification parameters — income level groups of regions and economic relevance categories of sectors — we assign a specific consumption price elasticity from the GTAP data sets (Hertel and Mensbrughe n.d.) for any tuple of income level and sector category (Supplementary Tbl. 4).

With these price elasticities, flexibility to price changes increases with rising income. Therefore, wealthier countries are more resilient against price fluctuations. At the same time, consumers adapt less flexibly to price changes of more life essential goods and services. Since there is little or no substitutability for EORA's large and clearly distinguished sectors (Supplementary Tbl. 3), we do not consider cross-sector elasticities.

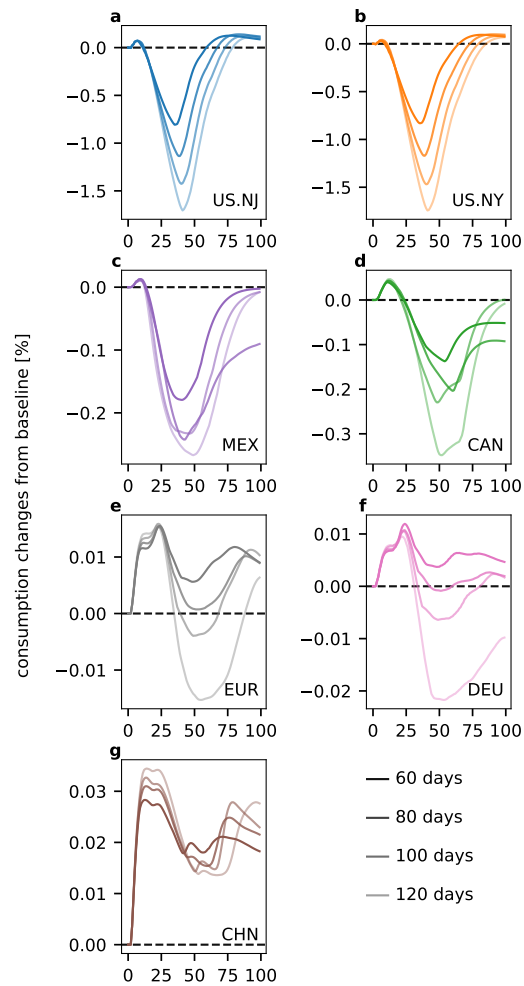
## Supplementary figures and tables



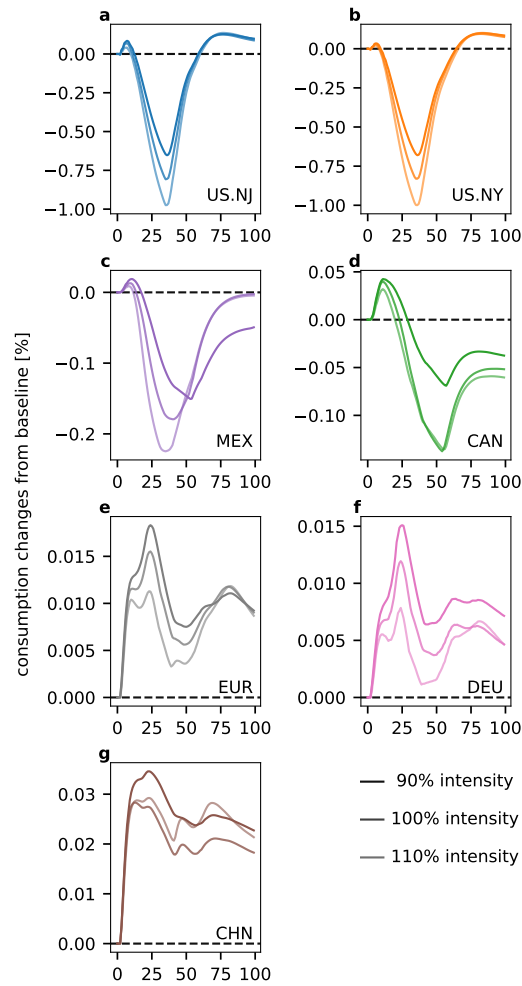
Supplementary Figure 1: **Production capacity reduction for Hurricane Sandy.** Time-dependent factor with which the production capacity is multiplied, representing the economic shock that results from the hurricane.



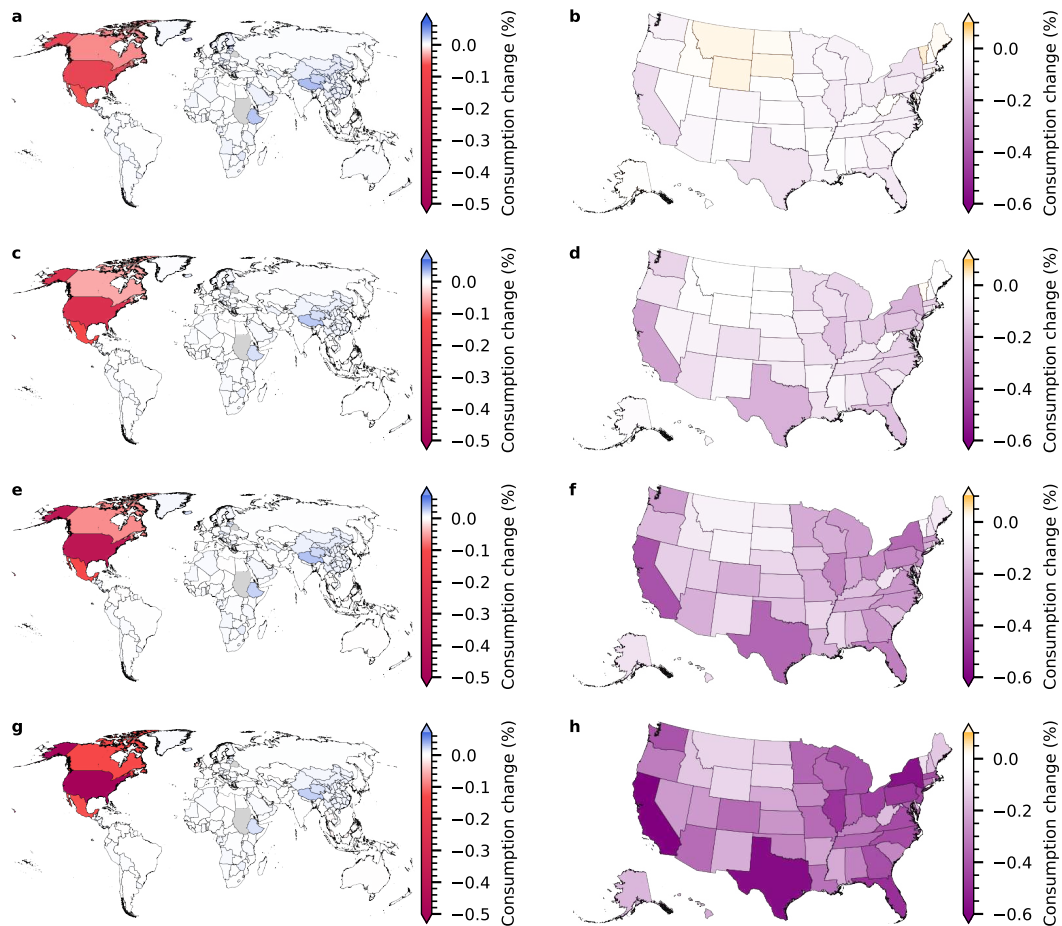
Supplementary Figure 2: **Consumption change for all simulated regions over their import and export volume with the US.** Consumption changes are cumulated for the first 100 days after the hurricane. Size of the scatters indicates the consumption change relative to what regions would consume under baseline conditions during this time. Green and red colors indicate consumption gains and losses, respectively. **a** consumption change over import volume from the US. **b** like panel a for export volume to the US. **c** absolute consumption change over import volume from the US on a log-log scale. Dashed line is the linear fit in the log-log space. **d** like panel c for export volume to the US.



Supplementary Figure 3: **Changes of consumption relative to baseline values with recovery time variation.** Same as Fig. 3 with longer recovery durations.



Supplementary Figure 4: **Changes of consumption relative to baseline values with initial shock intensity variation.** Same as Fig. 3 with slightly weaker and stronger initial shock intensity.



Supplementary Figure 5: **Global consumption changes after the hurricane with different shock durations.** Like Fig. 2 with longer BI recovery times. **left column** Global map. **right column** Detailed zoom on the United States. **a, b** 60 days, **c, d** 80 days, **e, f** 100 days, **g, h** 120 days. Region shapefiles retrieved from GADM (Global Administrative Areas 2018).



State	$\lambda_0$	$t_r$
New York	0.802032	60
New Jersey	0.693088	60

Supplementary Table 1: **Recovery curve parameters.**

Supplementary Table 2: **Regions used in the simulations.** Income level corresponds to Gross National Income per capita (GNIpc) of 2012 (Khokhar n.d.).

Income level 1:  $\text{GNIpc} < \$ 1,305$

Income level 2:  $\$ 1,036 < \text{GNIpc} < \$ 4,085$

Income level 3:  $\$ 4,086 < \text{GNIpc} < \$ 12,615$

Income level 4:  $\$ 12,616 < \text{GNIpc}$

ISO code	Name	Income level	Geographic region	Consumption change [%]
AFG	Afghanistan	1	Asia	0.004
ALB	Albania	3	Europe	0.010
DZA	Algeria	3	Africa	0.013
AND	Andorra	4	Europe	0.017
AGO	Angola	3	Africa	0.018
ATG	Antigua and Barbuda	4	North America	0.017
ARG	Argentina	3	South America	0.008
ARM	Armenia	2	Asia	0.009
ABW	Aruba	4	South America	0.047
AUS	Australia	4	Oceania	0.008
AUT	Austria	4	Europe	0.014
AZE	Azerbaijan	3	Asia	0.010
BHS	Bahamas	4	North America	0.053
BHR	Bahrain	4	Asia	0.029
BGD	Bangladesh	1	Asia	0.005
BRB	Barbados	4	North America	0.028
BLR	Belarus	3	Europe	0.115
BEL	Belgium	4	Europe	0.015
BLZ	Belize	3	North America	0.016
BEN	Benin	1	Africa	0.004
BMU	Bermuda	4	North America	0.017
BTN	Bhutan	2	Asia	0.008
BOL	Bolivia	2	South America	0.015
BIH	Bosnia and Herzegovina	3	Europe	0.013
BWA	Botswana	3	Africa	0.008
BRA	Brazil	3	South America	0.004
VGB	British Virgin Islands	4	South America	0.026
BRN	Brunei Darussalam	4	Asia	0.029
BGR	Bulgaria	3	Europe	0.017
BFA	Burkina Faso	1	Africa	0.005
BDI	Burundi	1	Africa	0.001
KHM	Cambodia	1	Asia	0.013
CMR	Cameroon	2	Africa	0.006
CAN	Canada	4	North America	-0.053
CPV	Cabo Verde	2	Africa	0.005
CYM	Cayman Islands	4	South America	0.019
CAF	Central African Republic	1	Africa	0.002
TCD	Chad	1	Africa	0.005

## APPENDIX FOR ARTICLE 2

ISO code	Name	Income level	Geographic region	Consumption change [%]
CHL	Chile	4	South America	0.010
CN.AH	Anhui	3	China, Asia	0.019
CN.BJ	Beijing	3	China, Asia	0.025
CN.CQ	Chongqing	3	China, Asia	0.021
CN.FJ	Fujian	3	China, Asia	0.024
CN.GS	Gansu	3	China, Asia	0.025
CN.GD	Guangdong	3	China, Asia	0.019
CN.GX	Guangxi	3	China, Asia	0.020
CN.GZ	Guizhou	3	China, Asia	0.024
CN.HA	Hainan	3	China, Asia	0.031
CN.HB	Hebei	3	China, Asia	0.017
CN.HL	Heilongjiang	3	China, Asia	0.019
CN.HE	Henan	3	China, Asia	0.017
CN.HU	Hubei	3	China, Asia	0.018
CN.HN	Hunan	3	China, Asia	0.018
CN.JS	Jiangsu	3	China, Asia	0.020
CN.JX	Jiangxi	3	China, Asia	0.020
CN.JL	Jilin	3	China, Asia	0.020
CN.LN	Liaoning	3	China, Asia	0.023
CN.NM	Nei Mongol	3	China, Asia	0.025
CN.NX	Ningxia Hui	3	China, Asia	0.034
CN.QH	Qinghai	3	China, Asia	0.036
CN.SA	Shaanxi	3	China, Asia	0.020
CN.SD	Shandong	3	China, Asia	0.020
CN.SH	Shanghai	3	China, Asia	0.024
CN.SX	Shanxi	3	China, Asia	0.020
CN.SC	Sichuan	3	China, Asia	0.017
CN.TJ	Tianjin	3	China, Asia	0.027
CN.XJ	Xinjiang Uygur	3	China, Asia	0.023
CN.XZ	Xizang	3	China, Asia	0.046
CN.YN	Yunnan	3	China, Asia	0.021
CN.ZJ	Zhejiang	3	China, Asia	0.021
COL	Colombia	3	South America	0.009
COG	Republic Congo	2	Africa	0.009
CRI	Costa Rica	3	North America	0.022
HRV	Croatia	4	Europe	0.023
CUB	Cuba	3	North America	0.007
CYP	Cyprus	4	Europe	0.026
CZE	Czech Republic	4	Europe	0.024
CIV	Côte d'Ivoire	2	Africa	0.008
PRK	North Korea	1	Asia	0.003
COD	Democratic Republic Congo	1	Africa	0.008
DNK	Denmark	4	Europe	0.014
DJI	Djibouti	2	Africa	0.004
DOM	Dominican Republic	3	North America	0.016
ECU	Ecuador	3	South America	0.016

## APPENDIX FOR ARTICLE 2

ISO code	Name	Income level	Geographic region	Consumption change [%]
EGY	Egypt	2	Africa	0.005
SLV	El Salvador	2	North America	0.015
ERI	Eritrea	1	Africa	0.002
EST	Estonia	4	Europe	0.032
ETH	Ethiopia	1	Africa	0.042
FJI	Fiji	3	Oceania	0.025
FIN	Finland	4	Europe	0.018
FRA	France	4	Europe	0.007
PYF	French Polynesia	4	Oceania	0.019
GAB	Gabon	3	Africa	0.017
GMB	Gambia	1	Africa	0.003
GEO	Georgia	2	Asia	0.012
DEU	Germany	4	Europe	0.006
GHA	Ghana	2	Africa	0.012
GRC	Greece	4	Europe	0.015
GRL	Greenland	4	North America	0.014
GTM	Guatemala	2	North America	0.011
GIN	Guinea	1	Africa	0.007
GUY	Guyana	2	South America	0.010
HTI	Haiti	1	North America	0.007
HND	Honduras	2	North America	0.017
HKG	Hong Kong	4	Asia	0.017
HUN	Hungary	3	Europe	0.015
ISL	Iceland	4	Europe	0.039
IND	India	2	Asia	0.005
IDN	Indonesia	2	Asia	0.005
IRN	Iran	3	Asia	0.005
IRQ	Iraq	3	Asia	0.006
IRL	Ireland	4	Europe	0.004
ISR	Israel	4	Asia	0.016
ITA	Italy	4	Europe	0.005
JAM	Jamaica	3	North America	0.022
JPN	Japan	4	Asia	0.004
JOR	Jordan	3	Asia	0.022
KAZ	Kazakhstan	3	Asia	0.006
KEN	Kenya	1	Africa	0.008
KWT	Kuwait	4	Asia	0.021
KGZ	Kyrgyz Republic	1	Asia	0.010
LAO	Lao PDR	2	Asia	0.005
LVA	Latvia	4	Europe	0.029
LBN	Lebanon	3	Asia	0.016
LSO	Lesotho	2	Africa	0.014
LBR	Liberia	1	Africa	0.004
LBY	Libya	3	Africa	0.004
LIE	Liechtenstein	4	Europe	0.000
LTU	Lithuania	4	Europe	0.027

## APPENDIX FOR ARTICLE 2

ISO code	Name	Income level	Geographic region	Consumption change [%]
LUX	Luxembourg	4	Europe	0.031
MAC	Macao	4	Asia	0.045
MDG	Madagascar	1	Africa	0.008
MWI	Malawi	1	Africa	0.007
MYS	Malaysia	3	Asia	0.009
MDV	Maldives	3	Asia	0.025
MLI	Mali	1	Africa	0.004
MLT	Malta	4	Europe	0.040
MRT	Mauritania	2	Africa	0.016
MUS	Mauritius	3	Africa	0.018
MEX	Mexico	3	North America	-0.065
MCO	Monaco	4	Europe	0.000
MNG	Mongolia	2	Asia	0.019
MNE	Montenegro	3	Europe	0.003
MAR	Morocco	2	Africa	0.009
MOZ	Mozambique	1	Africa	0.002
MMR	Myanmar	1	Asia	0.001
NAM	Namibia	3	Africa	0.010
NPL	Nepal	1	Asia	0.010
NLD	Netherlands	4	Europe	0.014
ANT	Netherlands Antilles	4	South America	0.044
NCL	New Caledonia	4	Oceania	0.022
NZL	New Zealand	4	Oceania	0.017
NIC	Nicaragua	2	North America	0.015
NER	Niger	1	Africa	0.004
NGA	Nigeria	2	Africa	0.009
NOR	Norway	4	Europe	0.017
PSE	West Bank and Gaza	2	Asia	0.008
OMN	Oman	4	Asia	0.019
PAK	Pakistan	2	Asia	0.005
PAN	Panama	3	South America	0.023
PNG	Papua New Guinea	2	Asia	0.010
PRY	Paraguay	2	South America	0.012
PER	Peru	3	South America	0.012
PHL	Philippines	2	Asia	-0.003
POL	Poland	4	Europe	0.014
PRT	Portugal	4	Europe	0.013
QAT	Qatar	4	Asia	0.011
KOR	South Korea	4	Asia	0.019
MDA	Moldova	2	Europe	0.083
ROU	Romania	3	Europe	0.009
RUS	Russian Federation	4	Asia	0.008
RWA	Rwanda	1	Africa	0.003
WSM	Samoa	2	Oceania	0.005
SMR	San Marino	4	Europe	0.015
STP	São Tomé and Príncipe	2	Africa	0.002

## APPENDIX FOR ARTICLE 2

ISO code	Name	Income level	Geographic region	Consumption change [%]
SAU	Saudi Arabia	4	Asia	0.020
SEN	Senegal	2	Africa	0.006
SRB	Serbia	3	Europe	0.007
SYC	Seychelles	3	Africa	0.021
SLE	Sierra Leone	1	Africa	0.005
SGP	Singapore	4	Asia	0.007
SVK	Slovak Republic	4	Europe	0.021
SVN	Slovenia	4	Europe	0.024
SOM	Somalia	1	Africa	0.000
ZAF	South Africa	3	Africa	0.011
SDS	South Sudan	1	Africa	0.000
ESP	Spain	4	Europe	0.007
LKA	Sri Lanka	2	Asia	0.008
SDN	Sudan	2	Africa	0.000
SUR	Suriname	3	South America	0.014
SWZ	Swaziland	2	Africa	0.009
SWE	Sweden	4	Europe	0.013
CHE	Switzerland	4	Europe	0.012
SYR	Syrian Arab Republic	2	Asia	0.007
TWN	Taiwan	4	Asia	0.028
TJK	Tajikistan	1	Asia	0.001
THA	Thailand	3	Asia	0.008
MKD	Macedonia	3	Europe	0.018
TGO	Togo	1	Africa	0.008
TTO	Trinidad and Tobago	4	South America	0.049
TUN	Tunisia	3	Africa	0.011
TUR	Turkey	3	Asia	0.008
TKM	Turkmenistan	3	Asia	0.019
UGA	Uganda	1	Africa	0.005
UKR	Ukraine	2	Europe	0.009
ARE	United Arab Emirates	4	Asia	0.020
GBR	United Kingdom	4	Europe	0.009
TZA	Tanzania	1	Africa	0.014
US.AL	Alabama	4	USA, North America	-0.078
US.AK	Alaska	4	USA, North America	0.017
US.AZ	Arizona	4	USA, North America	-0.106
US.AR	Arkansas	4	USA, North America	-0.028
US.CA	California	4	USA, North America	-0.219
US.CO	Colorado	4	USA, North America	-0.108
US.CT	Connecticut	4	USA, North America	-0.099
US.DE	Delaware	4	USA, North America	0.032
US.DC	District of Columbia	4	USA, North America	-0.031
US.FL	Florida	4	USA, North America	-0.172
US.GA	Georgia	4	USA, North America	-0.139
US.HI	Hawaii	4	USA, North America	-0.007
US.ID	Idaho	4	USA, North America	0.035

ISO code	Name	Income level	Geographic region	Consumption change [%]
US.IL	Illinois	4	USA, North America	-0.166
US.IN	Indiana	4	USA, North America	-0.115
US.IA	Iowa	4	USA, North America	-0.062
US.KS	Kansas	4	USA, North America	-0.054
US.KY	Kentucky	4	USA, North America	-0.074
US.LA	Louisiana	4	USA, North America	-0.097
US.ME	Maine	4	USA, North America	0.047
US.MD	Maryland	4	USA, North America	-0.121
US.MA	Massachusetts	4	USA, North America	-0.139
US.MI	Michigan	4	USA, North America	-0.135
US.MN	Minnesota	4	USA, North America	-0.112
US.MS	Mississippi	4	USA, North America	-0.021
US.MO	Missouri	4	USA, North America	-0.105
US.MT	Montana	4	USA, North America	0.073
US.NE	Nebraska	4	USA, North America	-0.022
US.NV	Nevada	4	USA, North America	-0.045
US.NH	New Hampshire	4	USA, North America	0.021
US.NJ	New Jersey	4	USA, North America	-0.150
US.NM	New Mexico	4	USA, North America	-0.010
US.NY	New York	4	USA, North America	-0.196
US.NC	North Carolina	4	USA, North America	-0.139
US.ND	North Dakota	4	USA, North America	0.050
US.OH	Ohio	4	USA, North America	-0.154
US.OK	Oklahoma	4	USA, North America	-0.071
US.OR	Oregon	4	USA, North America	-0.085
US.PA	Pennsylvania	4	USA, North America	-0.162
US.RI	Rhode Island	4	USA, North America	0.051
US.SC	South Carolina	4	USA, North America	-0.073
US.SD	South Dakota	4	USA, North America	0.073
US.TN	Tennessee	4	USA, North America	-0.108
US.TX	Texas	4	USA, North America	-0.200
US.UT	Utah	4	USA, North America	-0.046
US.VT	Vermont	4	USA, North America	0.120
US.VA	Virginia	4	USA, North America	-0.140
US.WA	Washington	4	USA, North America	-0.133
US.WV	West Virginia	4	USA, North America	0.016
US.WI	Wisconsin	4	USA, North America	-0.107
US.WY	Wyoming	4	USA, North America	0.080
URY	Uruguay	4	South America	0.018
UZB	Uzbekistan	2	Asia	0.003
VUT	Vanuatu	2	Oceania	0.007
VEN	Venezuela	3	South America	0.006
VNM	Vietnam	2	Asia	0.013
YEM	Yemen	2	Asia	0.010
ZMB	Zambia	2	Africa	0.007
ZWE	Zimbabwe	1	Africa	0.026

APPENDIX FOR ARTICLE 2

---

ISO code	Name	Income level	Geographic region	Consumption change [%]
----------	------	--------------	-------------------	------------------------

---



Supplementary Table 3: **Sectors used in the simulations.**

Code	Name	Category
AGRI	Agriculture	vital
FISH	Fishing	vital
MINQ	Mining and quarrying	other
GAST	Hotels and restaurants	relevant
WHOT	Wholesale trade	relevant
OTHE	Others	other
REPA	Maintenance and repair	other
RETT	Retail trade	relevant
FOOD	Food and beverages	vital
TEXL	Textiles and wearing apparel	relevant
TRAN	Transport	relevant
WOOD	Wood and paper	relevant
OILC	Petroleum, chemical & non-metallic mineral products	relevant
FINC	Financial intermediation and business activities	other
METL	Metal products	relevant
MACH	Electrical and machinery	relevant
TREQ	Transport equipment	relevant
MANU	Other manufacturing	relevant
REXI	Re-export and re-import	other
CONS	Construction	relevant
ADMI	Public administration	other
EDHE	Education, health and other services	vital
HOUS	Private households	other
COMM	Post and telecommunications	relevant
RECY	Recycling	other
ELWA	Electricity, gas and water	vital
FCON	Final consumption	relevant

Supplementary Table 4: **Consumption price elasticities per income level and sector category.** Values are based on GTAP (Hertel and Mensbrugghe n.d.).

Sector category	Income level			
	1	2	3	4
vital	-0.15	-0.2	-0.3	-0.45
relevant	-0.2	-0.3	-0.4	-0.65
other	-0.3	-0.4	-0.5	-0.75

## References

- Abel, J. R. et al. (2021). *The Region's Job Rebound from Superstorm Sandy*. Accessed 31 May 2021.
- Baghersad, M. and C. W. Zobel (2015). "Economic impact of production bottlenecks caused by disasters impacting interdependent industry sectors". In: *International Journal of Production Economics* 168, pp. 71–80.
- Berndt, E. R. and C. J. Morrison (1981). "Capacity utilization measures: underlying economic theory and an alternative approach". In: *The American Economic Review* 71.2, pp. 48–52.
- Bierkandt, R. et al. (2014). "Acclimate—A model for economic damage propagation. Part 1: Basic formulation of damage transfer within a global supply network and damage conserving dynamics". In: *Environment Systems and Decisions* 34.4, pp. 507–524.
- Downtown Alliance (2015). *Back to Business: The State of Lower Manhattan Four Months After Hurricane Sandy*. Accessed 31 May 2021.
- Federal Reserve Bank of New York (2012). *Empire State Manufacturing Survey Supplemental Report: Downstate Manufacturers Report Severe Disruptions from Sandy*. Accessed 14 May 2021.
- Federal Reserve Bank of Philadelphia (n.d.). *Coincident Economic Activity Index for Louisiana*. retrieved from FRED, Federal Reserve Bank of St. Louis, Accessed: 27 Apr 2021.
- Global Administrative Areas (2018). *GADM database of Global Administrative Areas, version 3.6*. Accessed 16 Dec 2020.
- Hallegatte, S. (2015). "The indirect cost of natural disasters and an economic definition of macroeconomic resilience". In: *World Bank Policy Research Working Paper* 7357.
- Hallegatte, S. and V. Przyluski (2010). "The economics of natural disasters: concepts and methods". In: *World Bank Policy Research Working Paper* 5507.
- Hertel, T. W. and D. van der Mensbrugge (n.d.). *Behavioral Parameters*. <https://www.gtap.agecon.purdue.edu/resources/download/8247.pdf>. Accessed 23 May 2020.
- Hsiang, S. M. and A. S. Jina (2014). *The causal effect of environmental catastrophe on long-run economic growth: Evidence from 6,700 cyclones*. Tech. rep. National Bureau of Economic Research.
- Ianchovichina, E. and R. McDougall (2000). *Theoretical Structure of Dynamic GTAP*. GTAP Technical Paper 17. Global Trade Analysis Project (GTAP).
- Khokhar, T. (n.d.). *Chart: Global Wealth Grew 66% Between 1995 and 2014*. <http://datatopics.worldbank.org/world-development-indicators/stories/the-classification-of-countries-by-income.html>. Accessed 23 Mar 2020.

- Koks, E. E. et al. (2016). “Regional disaster impact analysis: comparing input–output and computable general equilibrium models”. In: *Natural Hazards and Earth System Sciences* 16.8.
- Krichene, H. et al. (2021). “Long-term impacts of tropical cyclones and fluvial floods on economic growth – Empirical evidence on transmission channels at different levels of development”. In: *World Development* 144, p. 105475. [10.1016/j.worlddev.2021.105475](https://doi.org/10.1016/j.worlddev.2021.105475).
- Kuhla, K., S. N. Willner, C. Otto, T. Geiger, et al. (2021). “Ripple resonance amplifies economic welfare loss from weather extremes”. In: *Environmental Research Letters* 16.11, p. 114010.
- Kuhla, K., S. N. Willner, C. Otto, L. Wenz, et al. (2021). “Future heat stress to reduce people’s purchasing power”. In: *PloS one* 16.6, e0251210.
- Kunz, M. et al. (2013). “Investigation of superstorm Sandy 2012 in a multi-disciplinary approach”. In: *Natural Hazards and Earth System Sciences* 13.10, pp. 2579–2598.
- Lenzen, M. et al. (2012). “Mapping the structure of the world economy”. In: *Environmental science & technology* 46.15, pp. 8374–8381.
- Otto, C. et al. (Oct. 2017). “Modeling loss-propagation in the global supply network: The dynamic agent-based model acclimate”. In: *Journal of Economic Dynamics and Control* 83, pp. 232–269. [10.1016/j.jedc.2017.08.001](https://doi.org/10.1016/j.jedc.2017.08.001).
- Reimer, J. and T. W. Hertel (2004). “International Cross Section Estimates of Demand for Use in the GTAP Model”. In: *GTAP Technical paper* 23.
- Strobl, E. (2011). “The economic growth impact of hurricanes: Evidence from US coastal counties”. In: *Review of Economics and Statistics* 93.2, pp. 575–589.
- USGS (n.d.). *USGS Flood Event Viewer (FEV)*. Accessed 10 Jun 2020.
- Wenz, L., S. N. Willner, R. Bierkandt, et al. (2014). “Acclimate—a model for economic damage propagation. Part II: a dynamic formulation of the backward effects of disaster-induced production failures in the global supply network”. In: *Environment Systems and Decisions* 34.4, pp. 525–539.
- Wenz, L., S. N. Willner, A. Radebach, et al. (2015). “Regional and sectoral disaggregation of multi-regional input–output tables—a flexible algorithm”. In: *Economic Systems Research* 27.2, pp. 194–212.
- Willner, S. N., C. Otto, and A. Levermann (2018). “Global economic response to river floods”. In: *Nature Climate Change* 8.7, pp. 594–598.



## Appendix for article 3: The projected compensation response to Hurricane Harvey

### Methods

Our approach to project the historic TC to future climatic conditions is summarized in [supplementary figure 3](#). We assume a global mean temperature anomaly  $\Delta T$  (I) which adds up to the climatic conditions of the original Hurricane Harvey (which we also call the unscaled hurricane). This temperature increase leads to projected changed hurricane characteristics (which we then refer to as the counterfactual scenario with the projected or scaled hurricane) in terms of affected area and precipitation intensity (II). Based on this, we then estimate the resulting direct economic impact, i.e. an initial production shock and the duration of recovery (III). Finally, we use the direct economic impact as input for the *Acclimate* model and simulate global indirect economic impacts (IV).

### Climate projection

We assume changed climatic conditions (I in [supplementary figure 3](#)) simply as an increase of the global mean temperature ( $\Delta T$ ) relative to the climate of the original Hurricane Harvey in 2017. From this, we derive projected biophysical hurricane impacts. Because the Gulf of Mexico surface temperature controlled Harvey's moisture and wind speed, we first establish a relationship between future global mean temperature increase and the temperature of the Gulf of Mexico during hurricane season months (Jun-Nov). Using bias-corrected CMIP-6 near-surface air temperature (SAT) projections ([Eyring et al. 2016](#); [Lange and Büchner 2021](#)) for three shared socioeconomic pathways (SSP-126, SSP-370 and SSP-585) until the end of the century, we estimate how the Gulf of Mexico ([Flanders Marine Institute 2018](#)) SAT changes with the global mean temperature. We find good correlation ([supplementary figure 4](#)) and note that the Gulf of Mexico SAT increases faster with less optimistic SSPs. For our simulations, we assume, without loss of generality, factor 0.8 between the global mean and Gulf of Mexico temperature which is approximately the mean of the three SSP scenarios. In this study, we generally use changes in the global mean temperature change after Hurricane Harvey  $\Delta T$  (i.e., after the year 2017), implying herewith changes of Gulf of Mexico SAT with the chosen factor of 0.8. For our simulations, we choose  $\Delta T \in [0^\circ C, 4.0^\circ C]$ .

## Biophysical impact

From the in global mean temperature, we derive the corresponding increased biophysical hurricane impact (II in [supplementary figure 3](#)) which we define as the area affected by extreme precipitation and the intensity of this precipitation.

For the affected area of the original, unscaled hurricane, we first define a geographic envelope curve around high water marks related to Hurricane Harvey which are reported by the U.S. Geological Survey (USGS) (USGS n.d.). We then enlarge this area with our projections by different radius values  $\Delta r$  ([supplementary figure 6](#)) to account for the expectation that hurricanes will grow larger (Xu et al. 2020; Lin, Zhao, and Zhang 2015) and have extended decay time on land (Li and Chakraborty 2020) with increased sea surface temperature. However, since the relationship between SST and hurricane precipitation area is still subject to ongoing research, we can hardly assume a specific relationship of how changes in global mean temperature translate into hurricane size changes. For each considered temperature anomaly  $\Delta T$  we therefore assume a set of radius changes  $\Delta r \in [0km, 40km]$  in steps of  $2.5km$ . This way, we can assume arbitrary relationships between  $\Delta T$  and  $\Delta r$  within the given ranges.

For the precipitation increase we use the average best estimate of three studies on the precipitation of Hurricane Harvey attributable to climate change (Oldenborgh et al. 2017; Risser and Wehner 2017; Wang et al. 2018), i.e. about 19% per degree Celsius warming (Wehner and Sampson 2021). We express the amount of precipitation as

$$p_{\Delta T} = p(\Delta T) = 1.19^{\Delta T} \cdot p_{\Delta T=0} \quad (10)$$

with the (unknown) initial amount of precipitation  $p_{\Delta T=0}$  for the unscaled Hurricane Harvey.

## Direct economic impact

We derive the direct economic impact (III in [supplementary figure 3](#)) for Texas and Louisiana from the biophysical hurricane impact (II), using estimates of the initial economic shock and subsequent recovery (Middelanis et al. 2021) from the original Hurricane Harvey. This shock is defined as a reduction in productive capacity of areas affected by the hurricane due to business interruption. In particular, this does not include any notion of reconstruction of destroyed assets, which happens on longer time scales. We first derive the shock for the original Hurricane Harvey in 2017, before projecting it to future climate, using the previously estimated biophysical impact of Hurricane Harvey under climate change. Daily reduction in productive capacity is represented by a production capacity reduction factor  $f_{s,\Delta T,\Delta r}(t)$  for a given affected state  $s$  under projected biophysical impact of global warming  $\Delta T$  and radius change  $\Delta r$ . The initial production shock  $f_{s,\Delta r}^{(0)}$  directly

after the hurricane is given by the share of the state's economy that is physically exposed to the disaster. We assume that the recovery of the economy from this initial shock follows an exponential curve. The speed of recovery (i.e. the recovery time constant  $\theta_{\Delta T, \Delta r}$  of the exponential curve) is set to match the recovery duration  $t_{r, \Delta T}$  of an estimate for the business interruption that the hurricane resulted in. As a proxy for business interruption from the original hurricane, we use initial unemployment claims in Texas after the landfall of Hurricane Harvey ([supplementary figure 5](#)) and set  $t_{r, \Delta T=0} = 60$  for the unscaled scenario. Both parameters —  $f_{s, \Delta r}^{(0)}$  and  $t_{r, \Delta T}$  — of the original hurricane are then scaled with the changed biophysical impact under climate change. In this, we assume that  $f_{s, \Delta r}^{(0)}$  and  $t_{r, \Delta T}$  scale with the projected covered area and the increased precipitation, respectively.

The time-dependent factor  $f_{s, \Delta T, \Delta r}(t)$  by which productive capacity in state  $s$  is reduced, is given by the following equation:

$$f_{s, \Delta T, \Delta r}(t) := \begin{cases} 1 - f_{s, \Delta r}^{(0)} \cdot e^{\frac{-t}{\theta_{\Delta T, \Delta r}}} & \text{for } t \leq t_{r, \Delta T} \\ 1 & \text{for } t > t_{r, \Delta T} \end{cases} \quad (\text{ii})$$

with time constant

$$\theta_{\Delta T, \Delta r} = -\frac{t_{r, \Delta T}}{\ln\left(\frac{1-f_r}{f_{s, \Delta r}^{(0)}}\right)}. \quad (\text{12})$$

The parameter  $f_r$  in [equation \(ii\)](#) and [equation \(12\)](#) is the production reduction factor after which we assume full recovery. We set this factor to  $f_r = 0.999$ , i.e. we assume full recovery once the shock has decayed to 0.1% or less ([Middelanis et al. 2021](#)).

Since the initial production shock is the share of the economy that is exposed to the TC, it depends on the area affected by precipitation. We therefore calculate the scaled initial production shock  $f_{s, \Delta r}^{(0)}$  for an affected US state  $s$  as the share of the economy that geographically intersects with the affected area given a radius increase  $\Delta r$  of the biophysical impact. As a proxy for the exposure of a state's economy we use the gross state product (GSP) and calculate the share of GSP on a county level that intersects with the precipitation area. We refer to the GSP exposure as  $E$ , i.e. the GDP that is geographically exposed. GSP and county gross regional product (GRP) are obtained from BEA's Gross Domestic Product by County and Metropolitan Area table ([U.S. Bureau of Economic Analysis 2020](#)) for the year 2015. We use values from 2015 instead of 2017 to be consistent with the economic baseline data we use in our simulation model (see "Indirect economic impact"). We calculate  $E_s$  the exposure of an individual US state  $s$  as the sum over the GRP of all counties from this state that lie within or intersect with the precipitation area of the projected storm:

$$E_s(\Delta r) = \sum_{c \in C_{\Delta r} \cap C_s} X_c \quad (13)$$

with  $C_{\Delta r}$  the set of all counties affected by the precipitation area defined by  $\Delta r$ ,  $C_s$  the set of all counties in state  $s$  and  $X_c$  the GRP of county  $c$ . From the state-level exposure, we calculate the initial production shock as the exposed GSP within a particular state relative to the total GSP:

$$f_{s,\Delta r}^{(0)} = f_s^{(0)}(\Delta r) = \frac{E_s(\Delta r)}{X_s} \quad (14)$$

where  $X_s$  is GSP of state  $s$ .

We calculate initial production shocks for Texas and Louisiana for different values of  $\Delta r$  by sampling [equation \(14\)](#) with steps of  $10km$  in the range of  $\Delta r \in [0, 100km]$ . This yields the initial production shocks shown as scatters in the first panel of [supplementary figure 6](#). These intensities show good linearity with the radius extension and we therefore linearise the initial production shock for both states to obtain initial production shocks for Texas and Louisiana as a function of the radius extension:

$$\begin{aligned} f_{TX}^{(0)}(\Delta r) &= 0.3692 + \frac{1.901 \cdot 10^{-3}}{km} \Delta r \\ f_{LA}^{(0)}(\Delta r) &= 0.0443 + \frac{1.614 \cdot 10^{-3}}{km} \Delta r \end{aligned} \quad (15)$$

The speed of the recovery from business interruption, i.e. the time  $t_{r,\Delta T}$  to recover from the business interruption shock, depends on the amount of damage that needs to be (provisionally) fixed in the direct aftermath of the hurricane. This does not mean that the entire hurricane damage — in case of the unscaled Hurricane Harvey \$125bn — is reconstructed until this point. Instead, we assume that the amount of work needed to recover from business interruption, i.e. recovery to a state where business processes can mostly operate under normal conditions again, is proportional to the total amount of damage that the hurricane resulted in. Of course, this is not always true, especially when damages vary extremely. However, since we scale with Harvey an already strong hurricane with extremely large damages and an already long business interruption, we esteem linearity between recovery duration and total disaster damage in the environment of the large unscaled damage a valid assumption. In reality of course, damages of critical infrastructure can be an important source of nonlinearity which we do not account for here. In this, we assume that when the total damage increases by some factor, then the amount of damage to restore business productivity and hence the time needed to recover



from the business interruption shock increase by this same factor. Therefore, we scale  $t_{r,\Delta T}$  with the same factor by which we assume total damages of the projected Hurricane Harvey to grow with increased precipitation.

Damages from flooding are typically assessed as a function of inundation depth  $i$ , which again is a function of the precipitation intensity  $p$ . Since the latter is defined as the amount of water that is released per area, the proportionality  $i \sim p$  may reasonably be assumed. Following Frame et al. (2020) (Frame et al. 2020), we further assume a linear damage function that translates inundation depth  $i$  into damages  $D$ . This can be justified based on the damage functions published by Huizinga et al. (2017) (Huizinga, De Moel, Szweczyk, et al. 2017) which are reasonably linear for the range of inundation depths that Hurricane Harvey resulted in. We therefore can assume linearity between damage  $D$  and precipitation intensity  $p$  and thus  $t_{r,\Delta T} \sim p$ . Using equation (10), this results in the scaled recovery time:

$$\begin{aligned} t_{r,\Delta T} &\sim p \\ \Leftrightarrow \frac{t_{r,\Delta T}}{t_{r,\Delta T=0}} &= \frac{p_{\Delta T}}{p_{\Delta T=0}} \\ \Rightarrow t_{r,\Delta T} &= t_{r,\Delta T=0} \cdot 1.19^{\Delta T} \end{aligned} \tag{16}$$

and with  $t_{r,\Delta T=0} = 60$  we obtain

$$t_{r,\Delta T} = 60 \cdot 1.19^{\Delta T}. \tag{17}$$

Using equation (17) and equation (15) we can solve equation (12) and determine the time-dependent reduction factor for productive capacity for Texas and Louisiana according to equation (11).

## Indirect economic impact

We simulate the indirect economic impacts on production resulting from the original Hurricane Harvey as well as all projected scaled versions of the hurricane. For this, we use the agent-based model *Acclimate* (Otto et al. 2017) which simulates anomalies around an economic baseline network of a specific year as a response to an externally prescribed production capacity shock to the network (see supplementary table 4 for model parameters). This shock for the original or scaled hurricane is given by a reduction in productive capacity defined in equation (11). Agents in the network represent economic sectors of entire regions (on a country level, generally and on a state or province level for the United States and China, respectively). With a total of 268 regions and 27 sectors (including the final consumption as an individual economic sector), this results in a total of over

7,000 agents that are connected through a dense network of more than 1.8 million trade relations. While *Acclimate* can in principle handle different shocks for all agents (and thus for different sectors in a region), we assume all sectors within the affected regions Texas and Louisiana to be affected in the same manner. This can be argued because natural disasters affect different regional economic activities and typically do not concentrate on single sectors (West and Lenze 1994). In particular, the estimated business interruption in the direct aftermath of the disaster may be assumed to affect all sectors equally.

As economic baseline, we use the 2015 version (EORA simplified dataset v199.82) of the EORA multi-region input-output (MRIO) database (Lenzen et al. 2012) from the year 2015. While Hurricane Harvey made landfall in 2017, we consider the difference of two years sufficiently short to obtain meaningful results for the event. We disaggregate (Wenz et al. 2015) the United States and China trade flows to obtain flows on a state and province level, respectively. As a proxy, we use state-level GDP with an industry breakdown published by the US Beureau of Economic Analysis (BEA) (U.S. Bureau of Economic Analysis 2021) for the United States to obtain realistic sector weights for the disaggregation into individual US states. For this, we define a mapping (supplementary table 7) from the NAICS sector classification system (supplementary table 5) used by BEA to the 27 sectors of the EORA database (supplementary table 6). For China, we use GDP on a province-level (Statistics of China 2016) for disaggregation.

## Sensitivity analysis

In addition to the variation of the direct economic shock, we investigate how model parameters of *Acclimate* affect our findings. To this end, we perform a sensitivity analysis along three key model parameters. All model parameters and their values used in the main simulations can be found in [supplementary table 4](#). The parameters for the conducted sensitivity analysis are

1. storage fill factor  $\Psi$ : this parameter sets the size of storages and the storage levels that agents aim to refill,
2. unit extra variable production costs in production extension  $\Delta n^{in,v,>}$ : this parameter sets the slope of the linear increase of marginal production costs in production extension,
3. storage balance time scale  $\tau$ : the time scale at which agents aim to refill and empty their storages to reach the desired storage level.

We vary each of the aforementioned parameters while holding the others constant to investigate their individual effect on the reported findings. To this end, we use values  $\Psi \in [2, 3, \dots, 30]$ ,  $\Delta n^{in,v,>} \in [0.5, 1.0, \dots, 15.0]$  and  $\tau \in [1.0, 1.5, \dots, 15.0]$ . Another important parameter for the response dynamics of *Acclimate* is the production extension factor  $\beta$  which we do not vary here because throughout all main simulations, production is constantly well below the allowed production extension of 15%. The parameter variation is conducted both for the unscaled scenario ( $\Delta T = 0^\circ C$ ,  $\Delta r = 0km$ ) and the strongest counterfactual scenario ( $\Delta T = 4^\circ C$ ,  $\Delta r = 40km$ ).

We look into the temporal evolution of global net production in the direct aftermath of the hurricane (supplementary figures 7 and 8), the global gains and losses throughout the first 365 days after the hurricane (supplementary figures 9 and 10, similar to figure 3) as well as the distribution of gain shares among different groups of regions (supplementary figures 11 and 12, similar to figure 4).

We find that the storage fill factor  $\Psi$  does not significantly change the temporal evolution of the production anomaly for the unscaled scenario and, therefore, neither absolute gains and losses nor the distribution among groups of regions are affected by a change in this parameter. The strongest counterfactual scenario exhibits a slight increase of gains with this parameter — both globally and in the US alone ([supplementary figure 10a,b](#)) — because larger storages act as a buffer against scarcity of goods.

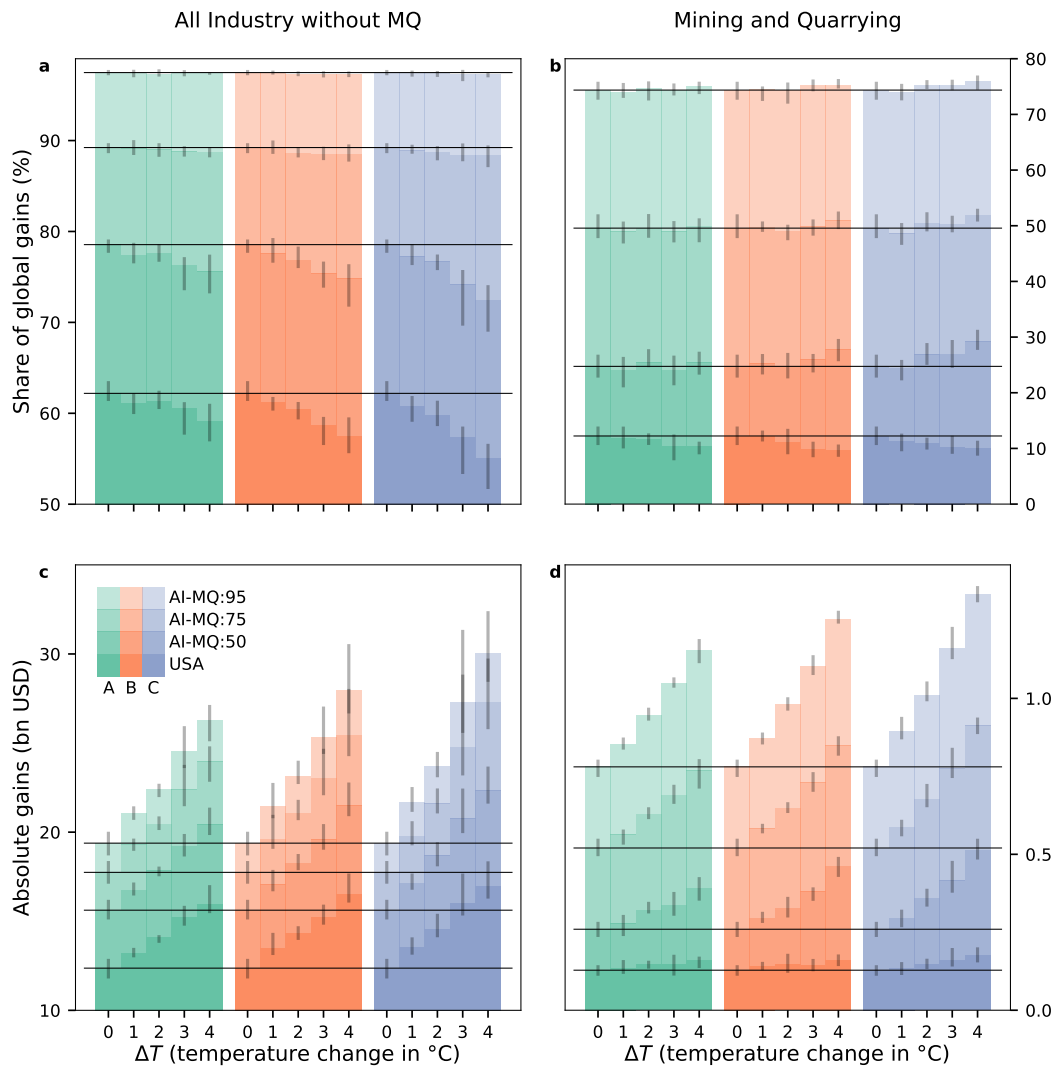
Variation of the unit extra variable production costs in production extension  $\Delta n^{in,v,>}$  on the other hand shows a significant impact on the temporal evolution of global production for both the unscaled and strongest counterfactual scenario. A (less) steep increase in marginal costs results in production extension being less (more) cost-efficient and thus a

weaker (stronger) production overshoot in the immediate aftermath of the disaster (panel b of supplementary figures 7 and 8). The higher the cost of production extension, the longer it takes for production losses to be offset. As a result, an increase in losses and decrease of gains, can be observed for the US (panel d of supplementary figures 9 and 10). However, we note that for the unscaled scenario, the impact of these parameters changing does not range in the same magnitude as the climate change impact in our simulations (figure 3). Higher production costs result in a lower compensation threshold, i.e., less production losses that a region can cost-efficiently compensate for. For very low values, the directly affected regions Texas and Louisiana can compensate for large shares of the losses themselves by production extension, hence the lower aggregated losses. On a global scale, gains never decrease with  $\Delta n^{in,v,>}$  in the unscaled case, indicating idle compensation capacities on a global level even for the largest parameters simulated. This is different for the strongest counterfactual, where a decrease in gains can even be observed on a global scale (supplementary figure 10c). In accordance with the findings of this work, production shifts from large to smaller exporters with increasing  $\Delta n^{in,v,>}$  (supplementary figure 11b), because increasing this parameter means lowering the capacity to compensate losses.

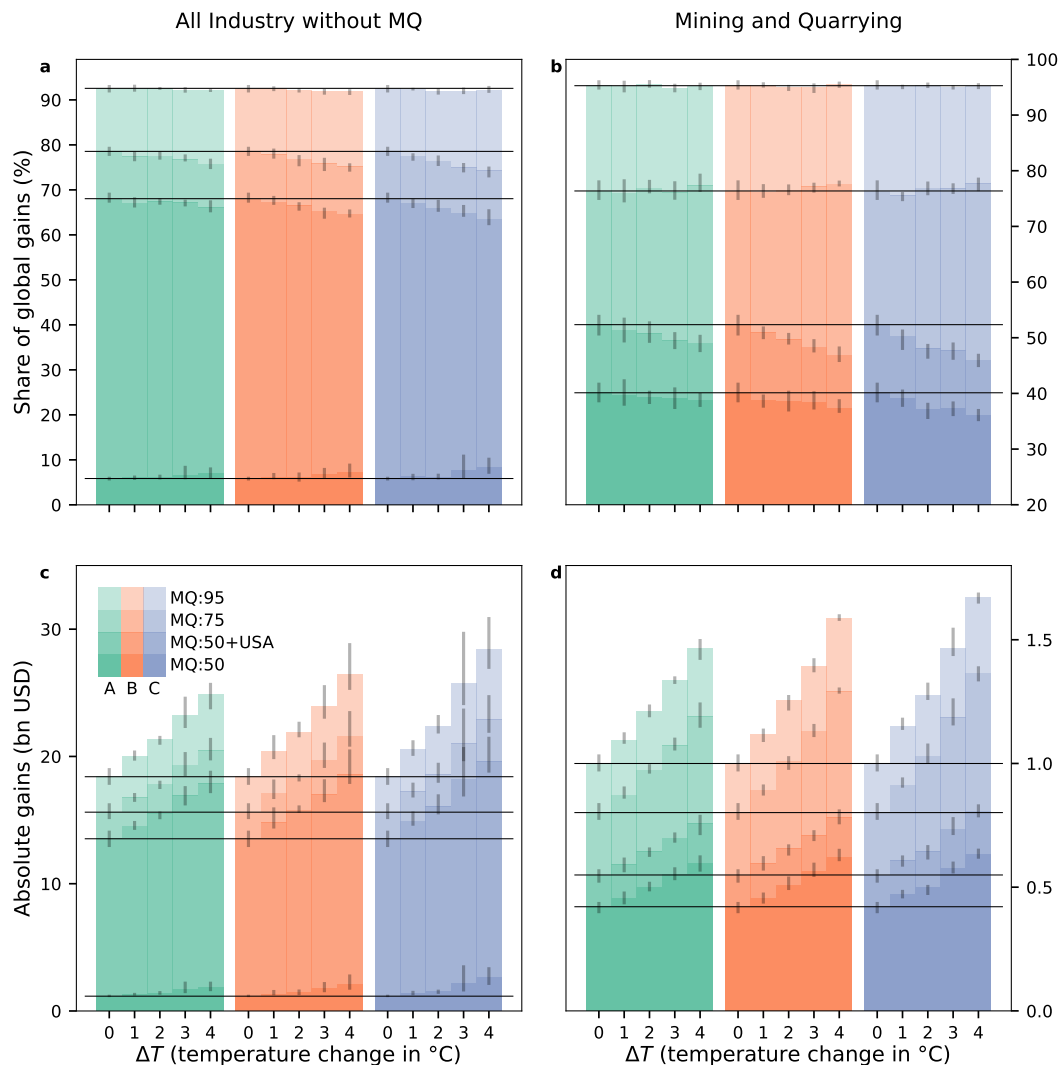
Varying the storage balance time  $\tau$  yields an effect on the time needed for loss compensation (supplementary figure 7c). Since this parameter steers how quickly agents aim to refill their storages, a larger parameter value shifts compensation efforts to later time steps. Allowing agents to refill their storages over longer time requires less production extension from regions not directly affected by the hurricane. Instead, compensation is distributed over a longer time frame, resulting in larger gains (supplementary figure 9e,f). However, because this is true for all regions, the shares of realized gains do not change with the storage balance time (supplementary figure 11c).

Overall, this sensitivity analysis shows that our qualitative results are robust under a wider range of key model parameters.

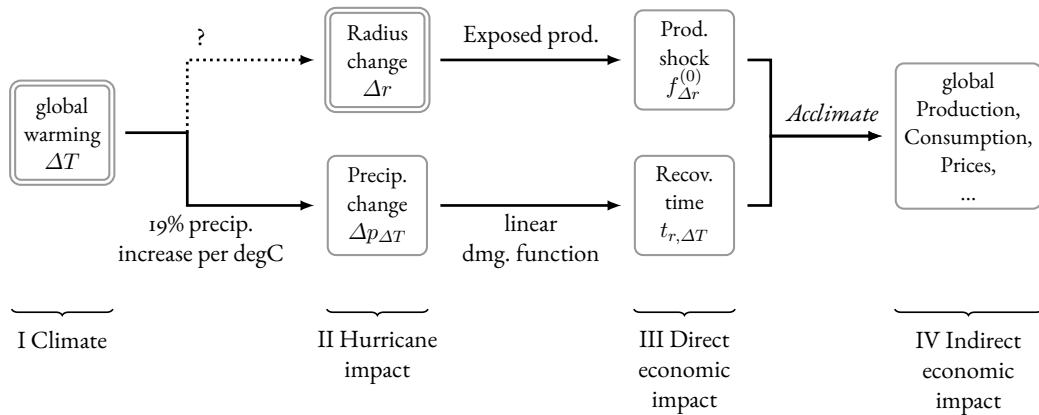
## Supplementary figures and tables



Supplementary Figure I: **Gains of regions grouped by total export volume excluding the mining and quarrying sector.** Gains are shown for groups of regions that make up 50%, 75% and 95% of global exports in all sectors except the mining and quarrying sector (AI-MQ, [supplementary table 1](#)). **(left)** Gains in all sectors aggregated except the mining and quarrying sector and **(right)** only the mining and quarrying sector. **(upper panels)** Relative shares of global gains and **(lower panels)** absolute values. Bar height denotes mean values of gains from the fine-grained simulations along slopes A, B, C and D as in figure 2, with the full range of values shown as vertical error bars. Horizontal lines mark mean values without global warming.

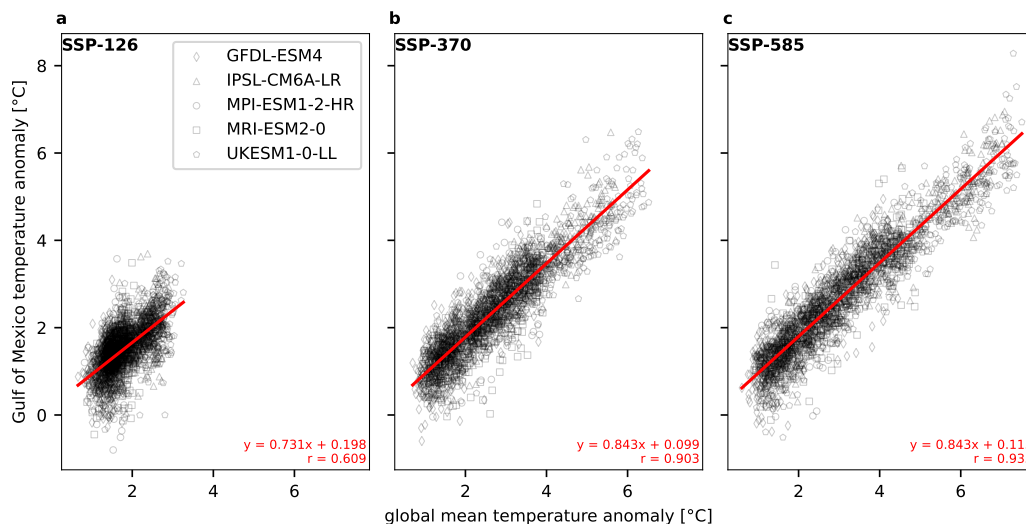


Supplementary Figure 2: **Gains of regions grouped by export volume in the mining and quarrying sector.** Gains are shown for groups of regions that make up 50%, 75% and 95% of global exports in the mining and quarrying sector (MQ, [supplementary table 2](#)). **(left)** Gains in all sectors aggregated except the mining and quarrying sector and **(right)** only the mining and quarrying sector. **(upper panels)** Relative shares of global gains and **(lower panels)** absolute values. Bar height denotes mean values of gains from the fine-grained simulations along slopes A, B, C and D as in figure 2, with the full range of values shown as vertical error bars. Horizontal lines mark mean values without global warming.

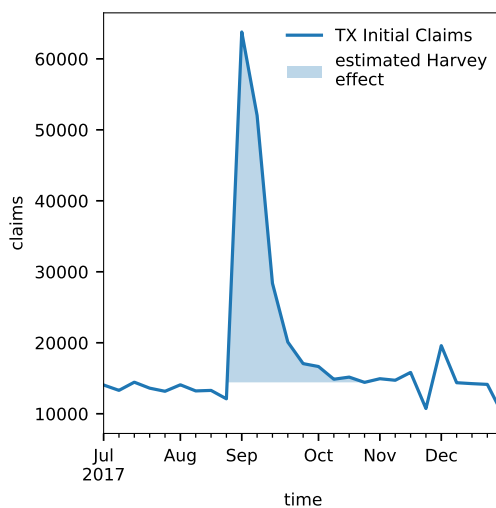


Supplementary Figure 3: **Flow diagram of the scaling approach.** We derive the possible global indirect economic effects (IV) of the historic Hurricane Harvey under changed climatic conditions (I). To this end, we use estimates of scaled hurricane impact characteristics (II) from which we derive direct economic impacts (III) to feed our simulation model *Acclimate* with. Boxed variables represent the descriptive variables in each step. Arrows between the boxes indicate the methods we use to derive variables from one another. The dotted arrow connecting the global temperature anomaly and a resulting change of the hurricane radius indicates that while there is evidence for a causal relationship between the two, we have no direct quantitative means to translate a temperature change into a radius change. For this reason, in our simulations also the radius change is an independent variable (double boxed) besides the temperature anomaly. This allows us to later assume arbitrary relationships between temperature anomaly and radius change.

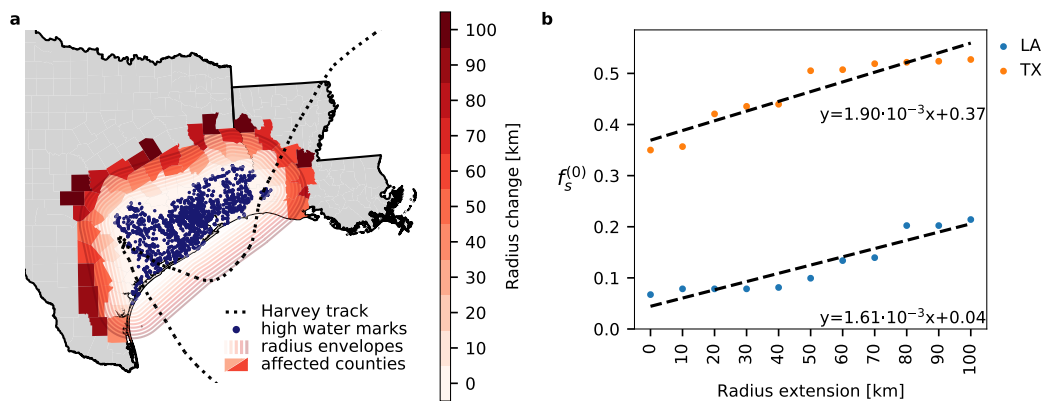




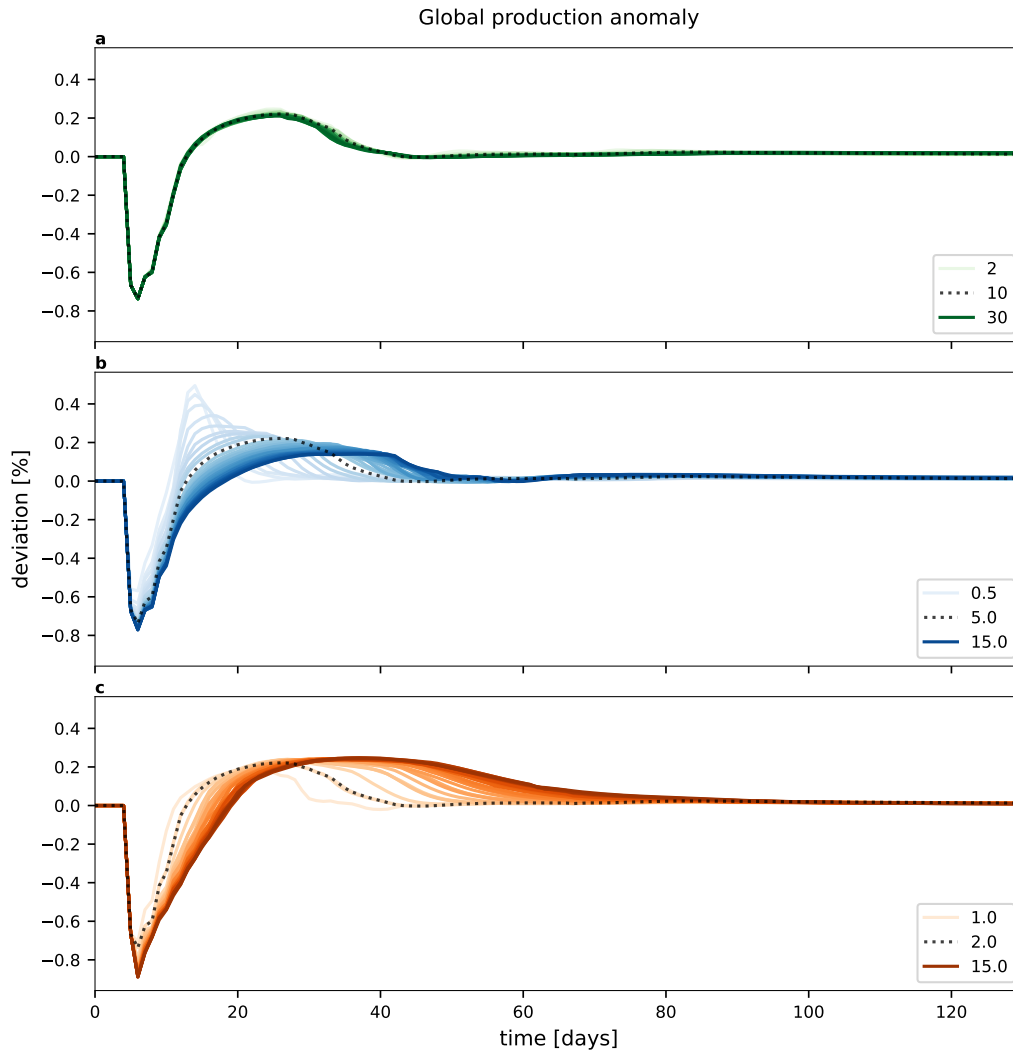
Supplementary Figure 4: **Estimated future relationship between global and Gulf of Mexico near-surface air temperature under different SSPs.** Analysis is based on bias-corrected temperature predictions from 5 CMIP-6 models for (a) SSP-126, (b) SSP-370 and (c) SSP-585. Data points are spatially and temporally averaged temperature differences to the baseline climate (1850-1899) for hurricane season months (Jun–Non) from 2015 to 2100 for each of the five considered models.



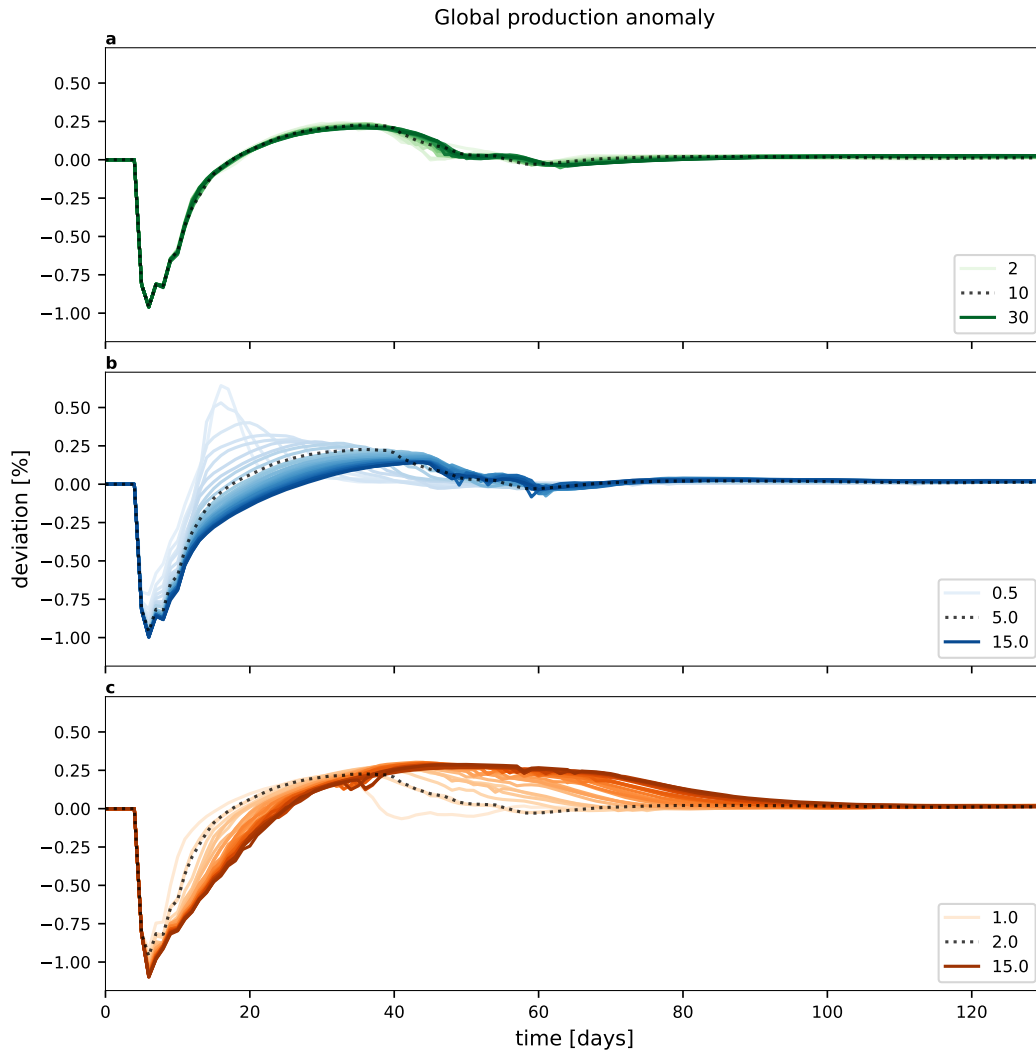
Supplementary Figure 5: **Initial jobless claims in Texas after Hurricane Harvey.** Data source: Federal Reserve Bank of St. Louis (U.S. Employment and Training Administration n.d.)



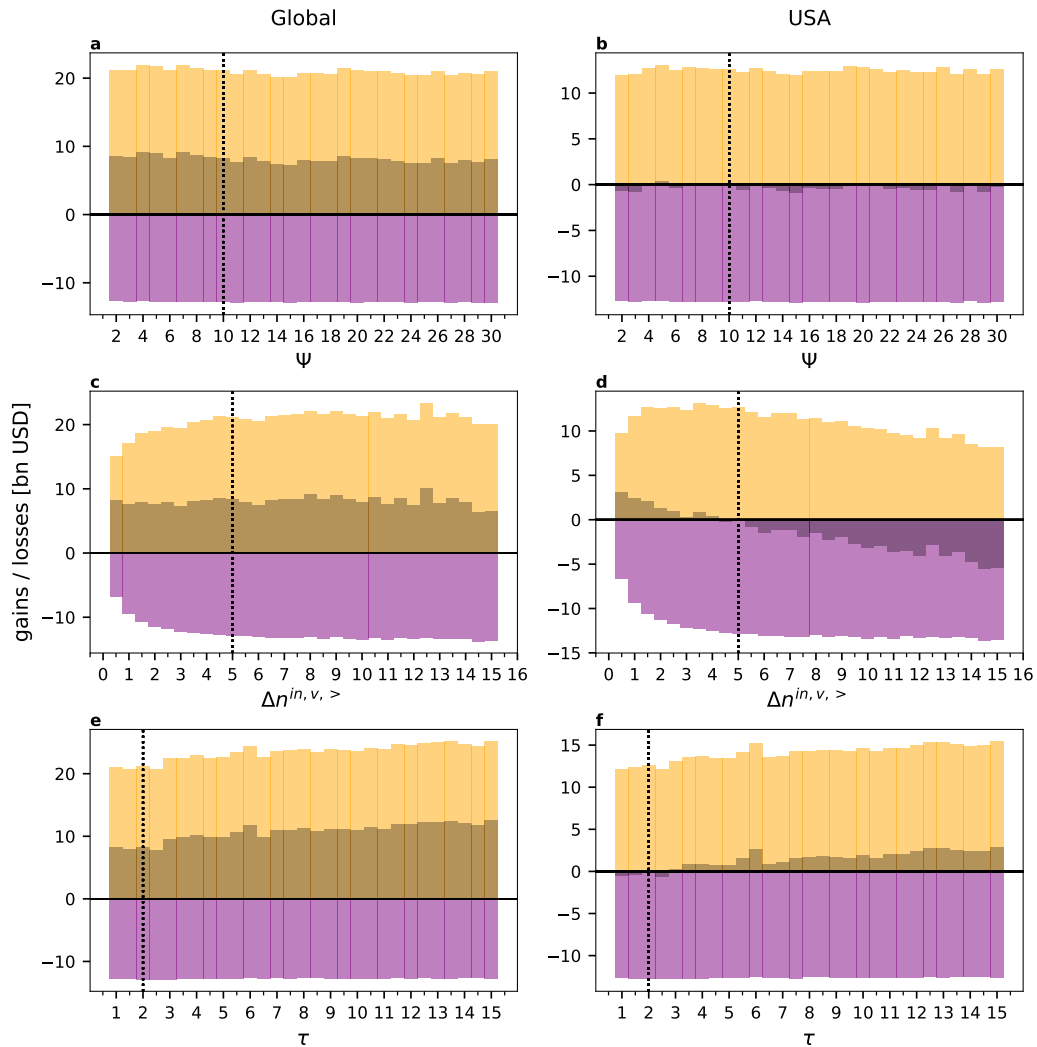
Supplementary Figure 6: **Radius extension impact.** (a) Simulated radius extensions and affected counties. Envelope curves (red shaded lines) are drawn around the reported high water marks (blue dots) of the original, unscaled Hurricane Harvey. Counties in Texas and Louisiana are colored in the shade of the largest radius they are affected by. (b) Impact of increased rainfall area radius. Solid lines show values obtained for discrete radius extension values, dashed lines show linearized functions. State and county shapefiles from GADM (Global Administrative Areas 2018), high water mark data from USGS (USGS n.d.), storm track from IBTrACS (Knapp et al. 2018).



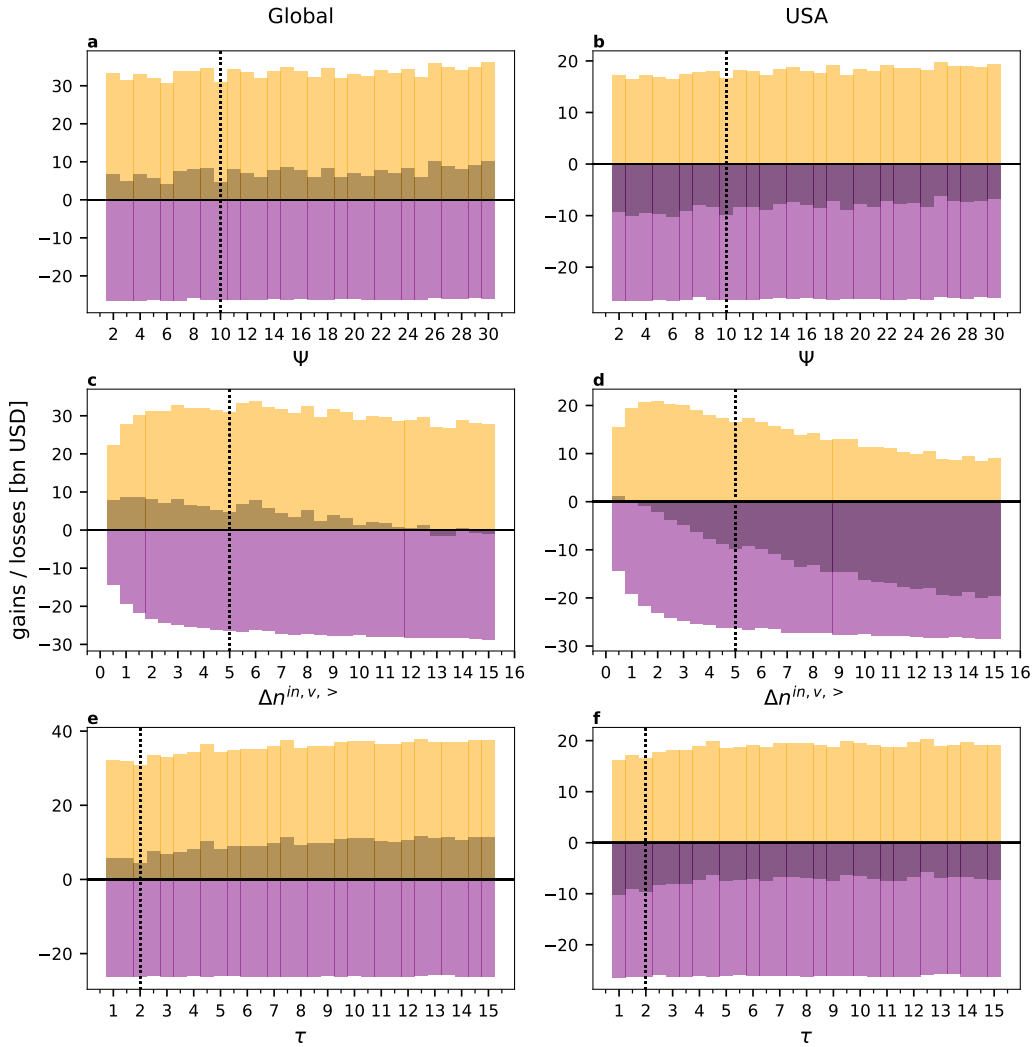
Supplementary Figure 7: **Production anomaly over time for the unscaled scenario under varied model parameters.** Time evolution for **(a)** storage fill factor  $\Psi \in [2, 3, \dots, 30]$ , **(b)** unit extra variable production costs in production extension  $\Delta n^{in,v,>} \in [0.5, 1.0, \dots, 15.0]$  and **(c)** storage balance time scale  $\tau \in [1.0, 1.5, \dots, 15.0]$ . Evolution of simulations with the original parameters are shown as dotted lines.



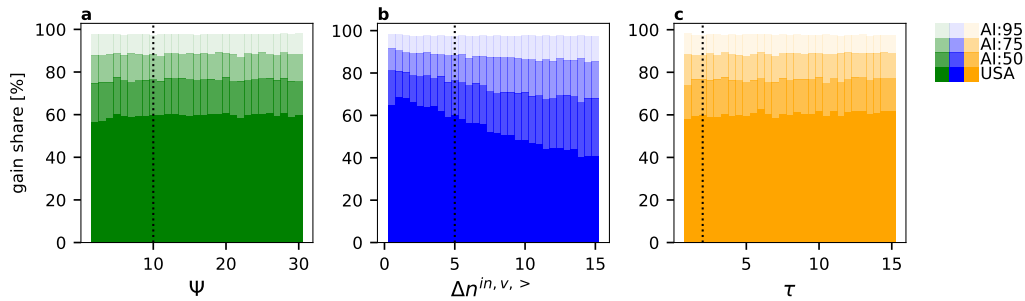
Supplementary Figure 8: **Production anomaly over time for the strongest counter-factual scenario under varied model parameters.** Time evolution for **(a)** storage fill factor  $\Psi \in [2, 3, \dots, 30]$ , **(b)** unit extra variable production costs in production extension  $\Delta n^{in,v,>} \in [0.5, 1.0, \dots, 15.0]$  and **(c)** storage balance time scale  $\tau \in [1.0, 1.5, \dots, 15.0]$ . Evolution of simulations with the original parameters are shown as dotted lines.



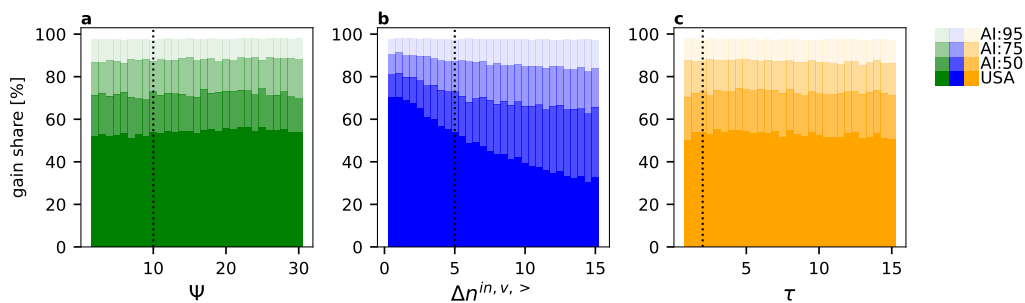
Supplementary Figure 9: **Gains and losses during the first 365 days after the hurricane for the unscaled scenario under varied model parameters.** Gains (orange), losses (purple) and their sum (grey) are shown (**left**) globally and (**right**) for the US. (**a, b**) storage fill factor  $\Psi$ , (**c, d**) unit extra variable production costs in production extension  $\Delta n^{in,v,>}$  and (**e, f**) storage balance time scale  $\tau$ . Original parameters are shown as dotted lines.



Supplementary Figure 10: **Gains and losses during the first 365 days after the hurricane for the strongest counterfactual scenario under varied model parameters.** Gains (orange), losses (purple) and their sum (grey) are shown **(left)** globally and **(right)** for the US. **(a, b)** storage fill factor  $\Psi$ , **(c, d)** unit extra variable production costs in production extension  $\Delta n^{in,v,>}$  and **(e, f)** storage balance time scale  $\tau$ . Original parameters are shown as dotted lines.



Supplementary Figure 11: **Gain shares for the unscaled scenario under varied model parameters.** (a) storage fill factor  $\Psi$ , (b) unit extra variable production costs in production extension  $\Delta n^{in,v,>}$  and (c) storage balance time scale  $\tau$ . Shadings denote US states that are not directly affected by the hurricane and groups of the top 50%, 75% and 95%, of global exporters. Original parameters are shown as dotted lines.



Supplementary Figure 12: **Gain shares for the strongest counterfactual scenario under varied model parameters.** (a) storage fill factor  $\Psi$ , (b) unit extra variable production costs in production extension  $\Delta n^{in,v,>}$  and (c) storage balance time scale  $\tau$ . Shadings denote US states that are not directly affected by the hurricane and groups of the top 50%, 75% and 95%, of global exporters. Original parameters are shown as dotted lines.

Supplementary Table 1: **Regional export shares in an aggregate of all sectors excluding the mining and quarrying sector.** Absolute exports, share of all exports and cumulative export share for the regions that make up 95% of global exports excluding the mining and quarrying sector, according to the EORA-2015 network. AI-MQ group denotes the smallest group a region is part of.

region	AI-MQ exports (bn USD)	global export share (%)	cumulative share (%)	AI-MQ group
DEU	2141.238	11.058	11.058	AI-MQ:50
CHN	1945.760	10.049	21.107	AI-MQ:50
USA	1712.343	8.843	29.950	AI-MQ:50
JPN	986.767	5.096	35.046	AI-MQ:50
FRA	960.773	4.962	40.008	AI-MQ:50
ITA	919.378	4.748	44.756	AI-MQ:50
GBR	785.761	4.058	48.814	AI-MQ:50
NLD	780.283	4.030	52.844	AI-MQ:75
BEL	627.375	3.240	56.084	AI-MQ:75
KOR	613.023	3.166	59.250	AI-MQ:75
CAN	578.090	2.986	62.236	AI-MQ:75
ESP	465.566	2.404	64.640	AI-MQ:75
SGP	377.616	1.950	66.590	AI-MQ:75
CHE	370.319	1.912	68.503	AI-MQ:75
MEX	334.413	1.727	70.230	AI-MQ:75
RUS	302.386	1.562	71.791	AI-MQ:75
IND	301.720	1.558	73.350	AI-MQ:75
MYS	293.228	1.514	74.864	AI-MQ:75
SWE	286.272	1.478	76.342	AI-MQ:95
AUT	265.416	1.371	77.713	AI-MQ:95
THA	247.053	1.276	78.989	AI-MQ:95
AUS	234.416	1.211	80.200	AI-MQ:95
BRA	224.392	1.159	81.359	AI-MQ:95
HKG	221.453	1.144	82.502	AI-MQ:95
IDN	210.033	1.085	83.587	AI-MQ:95
IRL	202.654	1.047	84.633	AI-MQ:95
CZE	181.321	0.936	85.570	AI-MQ:95
TWN	179.356	0.926	86.496	AI-MQ:95
DNK	173.550	0.896	87.392	AI-MQ:95
POL	153.913	0.795	88.187	AI-MQ:95
FIN	141.615	0.731	88.919	AI-MQ:95
HUN	124.685	0.644	89.563	AI-MQ:95
PHL	124.381	0.642	90.205	AI-MQ:95
TUR	112.338	0.580	90.785	AI-MQ:95
ZAF	98.491	0.509	91.294	AI-MQ:95
NOR	97.919	0.506	91.800	AI-MQ:95
ARG	84.014	0.434	92.233	AI-MQ:95
ISR	79.967	0.413	92.646	AI-MQ:95



## APPENDIX FOR ARTICLE 4

region	AI-MQ exports (bn USD)	global export share (%)	cumulative share (%)	AI-MQ group
ARE	78.996	0.408	93.054	AI-MQ:95
PRT	76.587	0.396	93.450	AI-MQ:95
SVK	70.721	0.365	93.815	AI-MQ:95
NZL	70.243	0.363	94.178	AI-MQ:95
SAU	66.602	0.344	94.522	AI-MQ:95
CHL	64.885	0.335	94.857	AI-MQ:95

Supplementary Table 2: **Regional export shares in the mining and quarrying sector.** Absolute exports, share of all exports and cumulative export share in the mining and quarrying sector (MQ) for the regions that make up 95% of global MQ exports according to the EORA-2015 network. MQ group denotes the smallest MQ-intensive group a region is part of.

region	MQ exports (bn USD)	global export share (%)	cumulative share (%)	MQ group
RUS	106.857	10.181	10.181	MQ:25
CAN	77.015	7.338	17.519	MQ:25
VEN	73.273	6.981	24.500	MQ:25
AUS	55.661	5.303	29.804	MQ:50
NOR	51.198	4.878	34.682	MQ:50
IDN	46.381	4.419	39.101	MQ:50
DZA	43.258	4.122	43.223	MQ:50
SAU	42.910	4.088	47.311	MQ:50
IRN	34.499	3.287	50.598	MQ:50
CHN	32.788	3.124	53.722	MQ:60
USA	29.806	2.840	56.562	MQ:60
KWT	28.014	2.669	59.231	MQ:60
GBR	25.144	2.396	61.627	MQ:75
BRA	23.426	2.232	63.859	MQ:75
NGA	22.698	2.163	66.021	MQ:75
AGO	20.623	1.965	67.986	MQ:75
ZAF	19.953	1.901	69.887	MQ:75
ARE	19.885	1.895	71.782	MQ:75
QAT	19.658	1.873	73.655	MQ:75
IND	15.853	1.510	75.165	MQ:75
MEX	15.512	1.478	76.643	MQ:95
IRQ	15.165	1.445	78.088	MQ:95
NLD	14.792	1.409	79.498	MQ:95
OMN	14.135	1.347	80.844	MQ:95
MYS	13.697	1.305	82.149	MQ:95
TTO	12.793	1.219	83.368	MQ:95
DEU	10.495	1.000	84.368	MQ:95
BEL	9.823	0.936	85.304	MQ:95
LBY	7.865	0.749	86.054	MQ:95
KAZ	7.794	0.743	86.796	MQ:95
CHL	7.144	0.681	87.477	MQ:95
VNM	6.713	0.640	88.116	MQ:95
FRA	6.641	0.633	88.749	MQ:95
ARG	6.516	0.621	89.370	MQ:95
BOL	6.216	0.592	89.962	MQ:95
DNK	6.186	0.589	90.552	MQ:95
COL	5.870	0.559	91.111	MQ:95
ESP	5.658	0.539	91.650	MQ:95

## APPENDIX FOR ARTICLE 4

region	MQ exports (bn USD)	global export share (%)	cumulative share (%)	MQ group
ITA	4.983	0.475	92.125	MQ:95
PER	4.827	0.460	92.585	MQ:95
BRN	4.688	0.447	93.031	MQ:95
UKR	4.500	0.429	93.460	MQ:95
ECU	4.142	0.395	93.855	MQ:95
SYR	4.038	0.385	94.240	MQ:95
JPN	3.805	0.363	94.602	MQ:95
CHE	3.596	0.343	94.945	MQ:95
YEM	3.248	0.309	95.254	MQ:95

Supplementary Table 3: **Texas shares of global exports.**

sector	global export share (%)
All industry	3.335
All industry without Mining and Quarrying	3.262
Mining and Quarrying	5.710

Supplementary Table 4: **Parameters used for the *Acclimate* simulation runs.**

Variable	Description	Unit	Scope	Value
$\Delta_t$	timestep	time	global	1 day
$\omega$	upper storage limit	–	sector	3
$\Psi$	storage fill factor	time	sector	10 days
$\beta$	production extension factor	–	sector	1.15
$\pi^*$	baseline monopolistic markup	price	sector	0.05
$\Delta n^{in,v,>}$	unit extra variable prod. costs in prod. extension	price	sector	5
$\Delta n^{tp}$	coefficient of quadratic transport penalty	value	sector	0.08 USD
$\tau$	storage balance time scale	time	storage	2 days
$\epsilon_{i \rightarrow js}^c$	consumption price elasticity	–	storage (consumer)	see ref (Middelanis et al. 2021)

Supplementary Table 5: **NAICS sectors.**

sector index	NAICS sector
1	Farms
2	Forestry, fishing, and related activities
3	Oil and gas extraction
4	Mining (except oil and gas)
5	Support activities for mining
6	Utilities
7	Construction
8	Wood product manufacturing
9	Nonmetallic mineral product manufacturing
10	Primary metal manufacturing
11	Fabricated metal product manufacturing
12	Machinery manufacturing
13	Computer and electronic product manufacturing
14	Electrical equipment, appliance, and component manufacturing
15	Motor vehicles, bodies and trailers, and parts manufacturing
16	Other transportation equipment manufacturing
17	Furniture and related product manufacturing
18	Miscellaneous manufacturing
19	Food and beverage and tobacco product manufacturing
20	Textile mills and textile product mills
21	Apparel, leather, and allied product manufacturing
22	Paper manufacturing
23	Printing and related support activities
24	Petroleum and coal products manufacturing
25	Chemical manufacturing
26	Plastics and rubber products manufacturing
27	Wholesale trade
28	Retail trade
29	Air transportation
30	Rail transportation
31	Water transportation
32	Truck transportation
33	Transit and ground passenger transportation
34	Pipeline transportation
35	Other transportation and support activities
36	Warehousing and storage
37	Publishing industries (except Internet)
38	Motion picture and sound recording industries
39	Broadcasting (except Internet) and telecommunications
40	Data processing, hosting, and other information services
41	Monetary Authorities- central bank, credit intermediation, and related services
42	Securities, commodity contracts, and other financial investments and related activities

APPENDIX FOR ARTICLE 4

sector index	NAICS sector
43	Insurance carriers and related activities
44	Funds, trusts, and other financial vehicles
45	Real estate
46	Rental and leasing services and lessors of nonfinancial intangible assets
47	Legal services
48	Computer systems design and related services
49	Miscellaneous professional, scientific, and technical services
50	Management of companies and enterprises
51	Administrative and support services
52	Waste management and remediation services
53	Educational services
54	Ambulatory health care services
55	Hospitals
56	Nursing and residential care facilities
57	Social assistance
58	Performing arts, spectator sports, museums, and related activities
59	Amusement, gambling, and recreation industries
60	Accommodation
61	Food services and drinking places
62	Other services (except government and government enterprises)
63	Federal civilian
64	Military
65	State and local

Supplementary Table 6: **EORA sectors.**

sector index	EORA sector
1	Agriculture
2	Fishing
3	Mining and Quarrying
4	Food & Beverages
5	Textiles and Wearing Apparel
6	Wood and Paper
7	Petroleum, Chemical and Non-Metallic Mineral Products
8	Metal Products
9	Electrical and Machinery
10	Transport Equipment
11	Other Manufacturing
12	Recycling
13	Electricity, Gas and Water
14	Construction
15	Maintenance and Repair
16	Wholesale Trade
17	Retail Trade
18	Hotels and Restaurants
19	Transport
20	Post and Telecommunications
21	Financial Intermediation and Business Activities
22	Public Administration
23	Education, Health and Other Services
24	Private Households
25	Others
26	Re-export & Re-import
27	Final Consumption

APPENDIX FOR ARTICLE 4

Supplementary Table 7: **NAICS to EORA sector mapping.**

NAICS sector index	EORA sector index
1	1
2	1; 2
3	3
4	3
5	3
6	13
7	14
8	6
9	7
10	8
11	8
12	9
13	9
14	9
15	10
16	10
17	11
18	11
19	4
20	5
21	5
22	6
23	6
24	7
25	7
26	7
27	16
28	17
29	19
30	19
31	19
32	19
33	19
34	19
35	19
36	19
37	20
38	20
39	20
40	20
41	21
42	21

NAICS sector index	EORA sector index
43	21
44	21
45	21
46	21
47	22
48	20
49	22
50	22
51	22
52	12
53	23
54	23
55	23
56	23
57	23
58	18
59	18
60	18
61	4
62	25
63	22
64	22
65	22



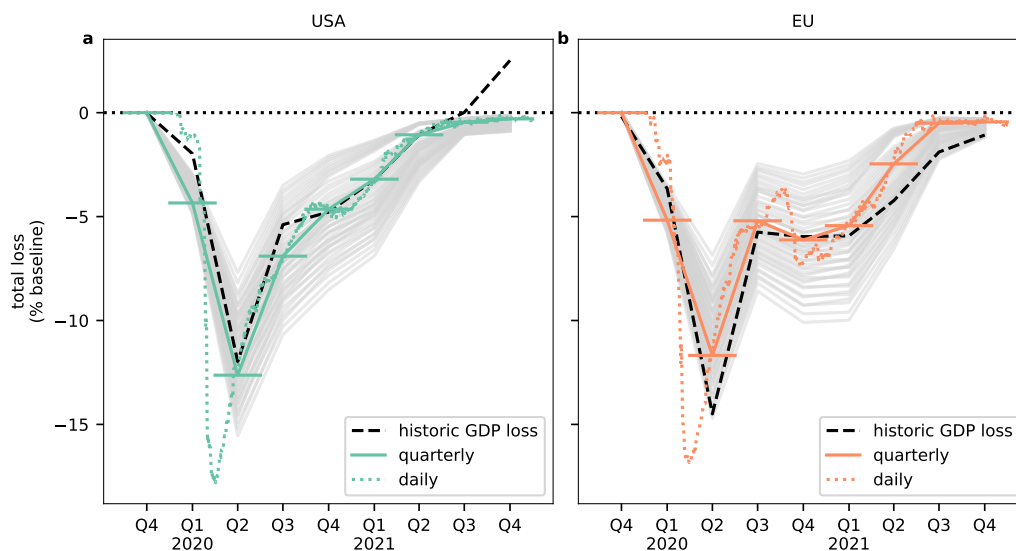
## References

- Eyring, V. et al. (2016). “Overview of the Coupled Model Intercomparison Project Phase 6 (CMIP6) experimental design and organization”. In: *Geoscientific Model Development* 9.5, pp. 1937–1958.
- Flanders Marine Institute (2018). *IHO Sea Areas, version 3*. (Accessed: 22 Apr 2022). <https://doi.org/10.14284/323>.
- Frame, D. J. et al. (2020). “The economic costs of Hurricane Harvey attributable to climate change”. In: *Climatic Change* 160.2, pp. 271–281.
- Global Administrative Areas (2018). *GADM database of Global Administrative Areas, version 3.6*. Accessed 16 Dec 2020.
- Huizinga, J., H. De Moel, W. Szewczyk, et al. (2017). *Global flood depth-damage functions: Methodology and the database with guidelines*. Tech. rep. Joint Research Centre (Seville site).
- Knapp, K. R. et al. (2018). *International Best Track Archive for Climate Stewardship (IB-TrACS) Project, Version 4*. NOAA National Centers for Environmental Information. Accessed 08 Aug 2020. <https://doi.org/10.25921/82ty-9e16>.
- Lange, S. and M. Büchner (2021). *ISIMIP3b bias-adjusted atmospheric climate input data (v1.1)*. (Accessed: 22 Apr 2022). <https://doi.org/10.48364/ISIMIP.842396.1>.
- Lenzen, M. et al. (2012). “Mapping the structure of the world economy”. In: *Environmental science & technology* 46.15, pp. 8374–8381.
- Li, L. and P. Chakraborty (Nov. 1, 2020). “Slower decay of landfalling hurricanes in a warming world”. In: *Nature* 587.7833, pp. 230–234. [10.1038/s41586-020-2867-7](https://doi.org/10.1038/s41586-020-2867-7).
- Lin, Y., M. Zhao, and M. Zhang (2015). “Tropical cyclone rainfall area controlled by relative sea surface temperature”. In: *Nature Communications* 6.1, p. 6591.
- Middelanis, R. et al. (2021). “Wave-like global economic ripple response to Hurricane Sandy”. In: *Environmental Research Letters* 16.12, p. 124049. [10.1088/1748-9326/aa9ef2](https://doi.org/10.1088/1748-9326/aa9ef2).
- Oldenborgh, G. J. van et al. (Dec. 1, 2017). “Attribution of extreme rainfall from Hurricane Harvey, August 2017”. In: *Environmental Research Letters* 12.12, p. 124009. [10.1088/1748-9326/aa9ef2](https://doi.org/10.1088/1748-9326/aa9ef2).
- Otto, C. et al. (Oct. 2017). “Modeling loss-propagation in the global supply network: The dynamic agent-based model acclimate”. In: *Journal of Economic Dynamics and Control* 83, pp. 232–269. [10.1016/j.jedc.2017.08.001](https://doi.org/10.1016/j.jedc.2017.08.001).
- Risser, M. D. and M. F. Wehner (2017). “Attributable human-induced changes in the likelihood and magnitude of the observed extreme precipitation during Hurricane Harvey”. In: *Geophysical Research Letters* 44.24, pp. 12–457.
- Statistics of China, N. B. of (2016). *Gross Regional Products and Indices*. (Accessed: 13 May 2022).

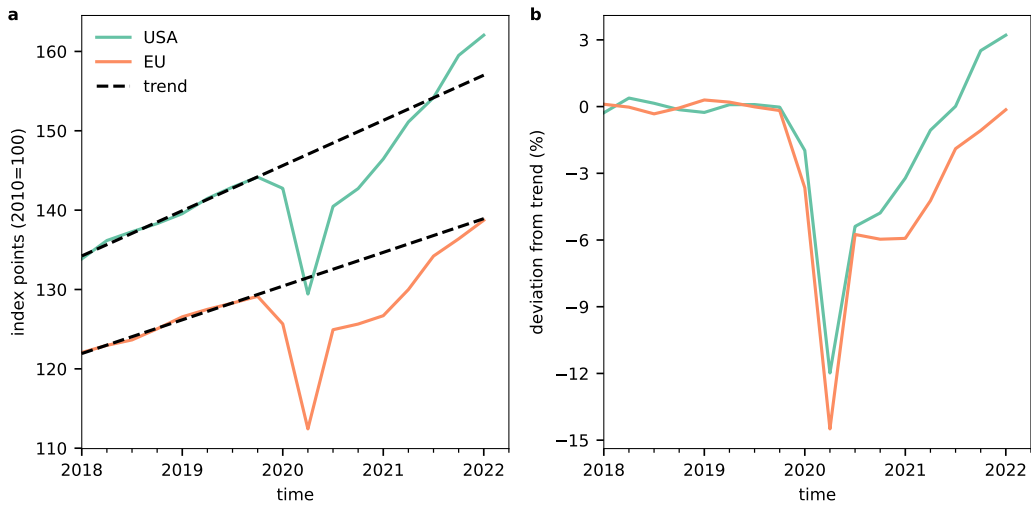
- U.S. Bureau of Economic Analysis (2020). *GROSS DOMESTIC PRODUCT (GDP) BY COUNTY AND METROPOLITAN AREA - GDP in current dollars (CAGDP2)*. (Accessed: 12 Oct 2020).
- (2021). *ANNUAL GROSS DOMESTIC PRODUCT (GDP) BY STATE - GDP in current dollars (CAGDP2)*. (Accessed: 24 Mar 2021).
- U.S. Employment and Training Administration (n.d.). *Initial Claims in Texas [TXI-CLAIMS]*. retrieved from FRED, Federal Reserve Bank of St. Louis, Accessed: 23 Jun 2021.
- USGS (n.d.). *USGS Flood Event Viewer (FEV)*. Accessed 10 Jun 2020.
- Wang, S. S. et al. (2018). “Quantitative attribution of climate effects on Hurricane Harvey’s extreme rainfall in Texas”. In: *Environmental Research Letters* 13.5, p. 054014.
- Wehner, M. and C. Sampson (2021). “Attributable human-induced changes in the magnitude of flooding in the Houston, Texas region during Hurricane Harvey”. In: *Climatic Change* 166.1-2, p. 20.
- Wenz, L. et al. (2015). “Regional and sectoral disaggregation of multi-regional input–output tables—a flexible algorithm”. In: *Economic Systems Research* 27.2, pp. 194–212.
- West, C. T. and D. G. Lenze (1994). “Modeling the regional impact of natural disaster and recovery: A general framework and an application to Hurricane Andrew”. In: *International regional science review* 17.2, pp. 121–150.
- Xu, Z. et al. (2020). “Tropical Cyclone Size Change under Ocean Warming and Associated Responses of Tropical Cyclone Destructiveness: Idealized Experiments”. In: *Journal of Meteorological Research* 34.1, pp. 163–175.

## Appendix for article 4: The response to extremes under global economic stress

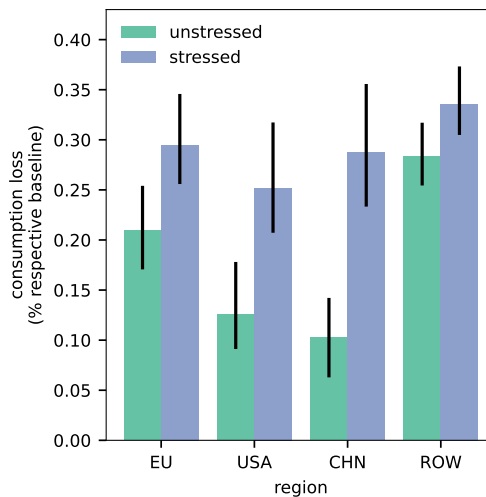
### Supplementary figures and tables



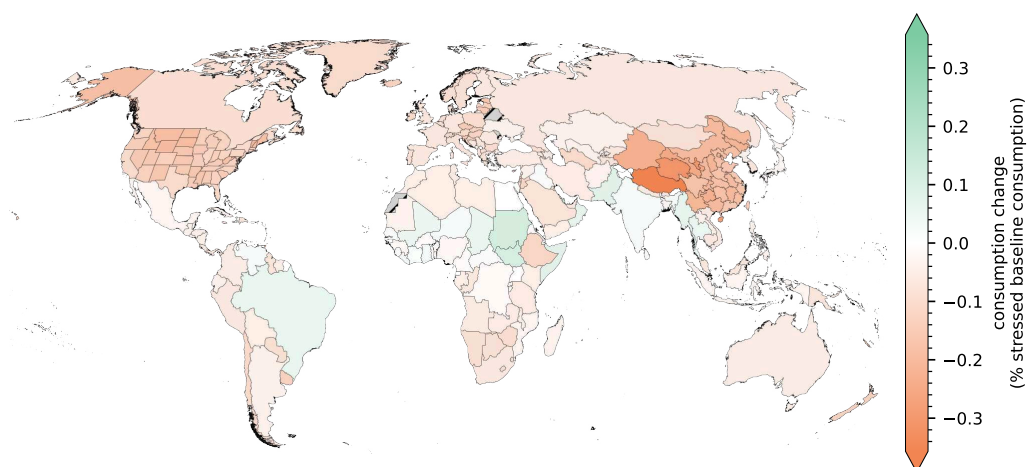
Supplementary Figure 1: **Calibration simulations.** Relative quarterly GDP loss from *Acclimate* simulations with different parameters for  $\alpha$  and  $\tau$  (solid lines) and historic GDP loss (dashed black lines) for **(a)** the US and **(b)** EU. Colored lines represent quarterly aggregated simulation results for selected parameters  $\alpha = 0.22$  and  $\tau = 9\text{mos}$  which best represent historical GDP loss (supplementary table 1). Aggregated quarters are highlighted with horizontal solid lines. Dotted lines are GDP losses with original, i.e. daily, simulation resolution of the selected calibration simulations.



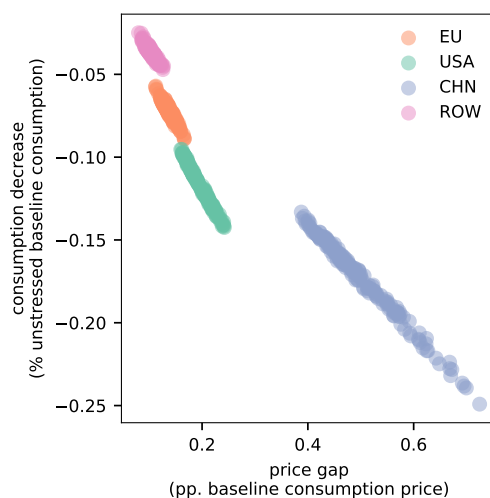
Supplementary Figure 2: **GDP and GDP loss due to the pandemic in the US and the EU.** (a) Quarterly GDP for the US and EU in index points, with index value 100 in the year 2010 and respective trends for the two years preceding the pandemic (dashed lines). (b) GDP loss as relative deviation from trend for the two regions.



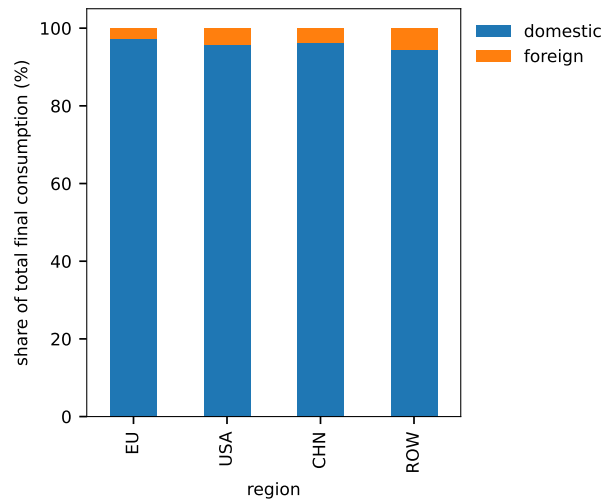
Supplementary Figure 3: **Consumption losses relative to baseline consumption.** Climate extreme-induced absolute consumption losses for the EU, US, and China under unstressed and stressed scenario, relative to the respective baseline consumption.



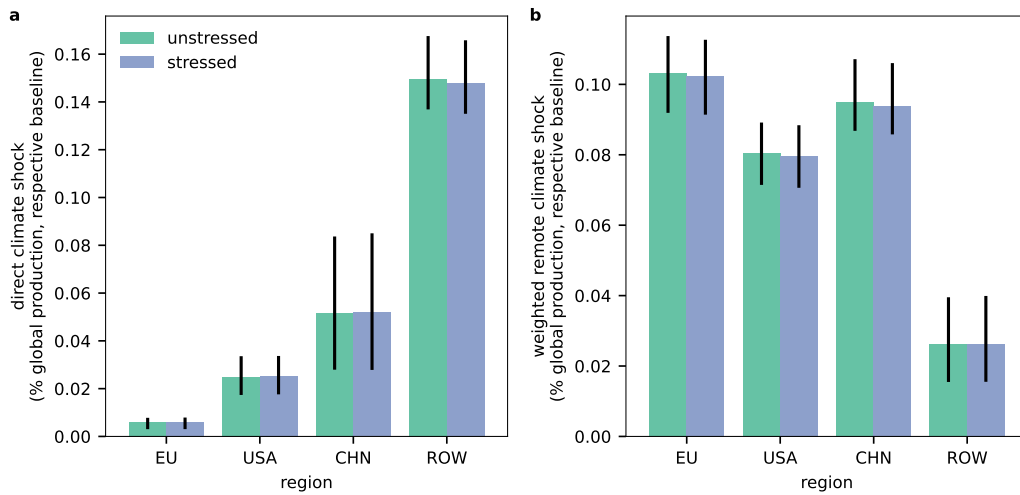
Supplementary Figure 4: **Consumption loss increase relative to stressed baseline consumption.** Same as panel c of Fig. 1 with normalization to stressed consumption baseline.



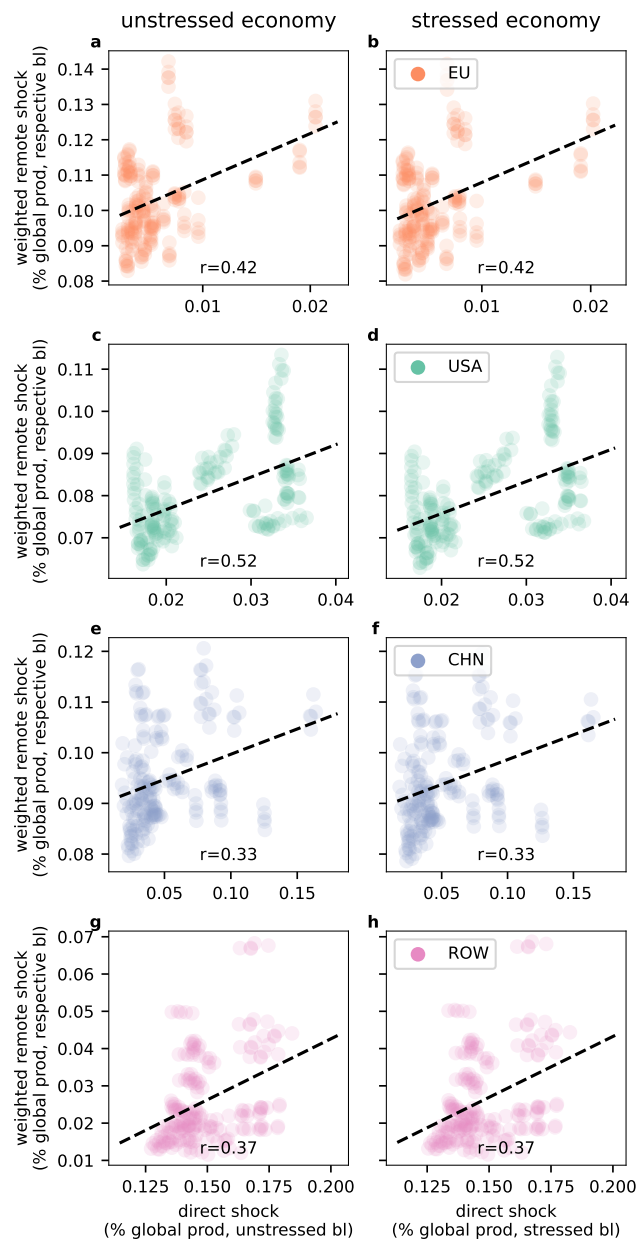
Supplementary Figure 5: **Consumption decrease in response to price gap changes.** Price gap is the pp. mean price difference between unstressed and stressed scenario. Consumption decrease in percent of unstressed scenario baseline consumption.



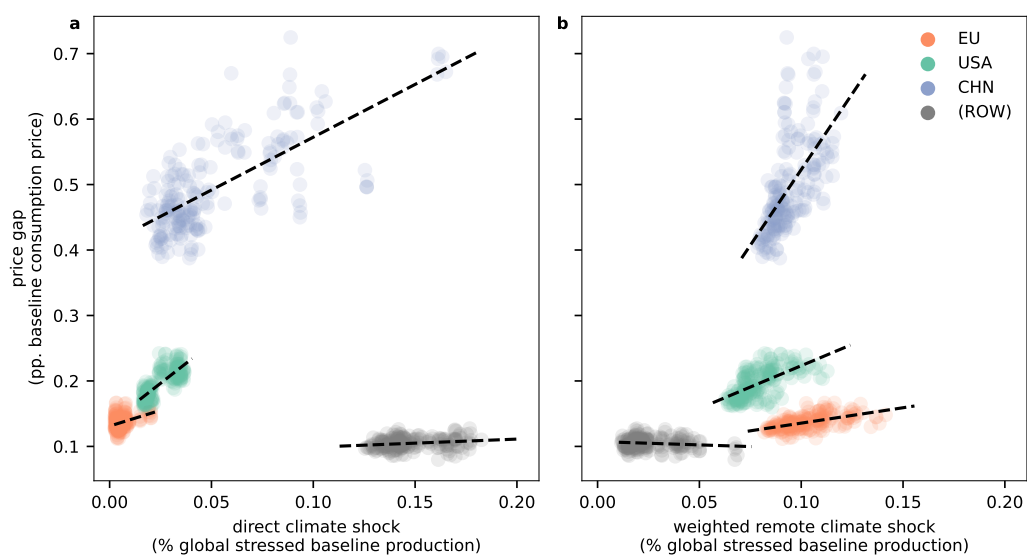
Supplementary Figure 6: **Shares of domestic and foreign consumption.** Share of total final consumption that is supplied domestically and by foreign producers. Shares are computed from the EORA (Lenzen, Kanemoto, et al. 2012) equilibrium economic state.



Supplementary Figure 7: **Direct and weighted remote climate shock under both scenarios.** Magnitudes of (a) direct and (b) weighted remote climate shock under both scenarios, expressed as percent of respective global baseline production.

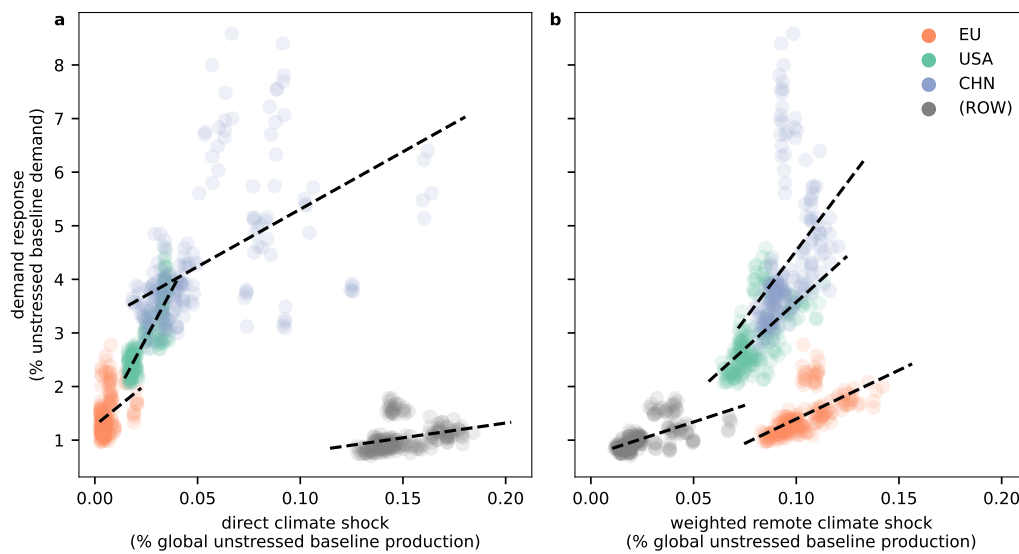


Supplementary Figure 8: **Linear correlation between direct and weighted remote shock.** Correlations are shown for **(a, b)** the EU, **(c, d)** the US, **(e, f)** China and **(g, h)** the rest of the world (ROW) in the **(left column)** unstressed and **(right column)** stressed scenario.



Supplementary Figure 9: **Price gap with regards to climate shocks normalized to stressed baseline production.** Same as Fig. 4 with shocks normalized to stressed global baseline production.





Supplementary Figure 10: **Demand response increases with climate shock intensity.** Demand response for the EU, US, China and rest of the world **(a)** with regards to the direct climate shock and **(b)** the weighted remote climate shock, relative to unstressed baseline demand. Points represent individual simulations from the ensemble, dashed lines are linear fits. Values for ROW are shown for completeness but should be interpreted with care due to the large number of aggregated regions.

Supplementary Table 1: **Evaluation of calibration simulations.** Mean squared error for all parameter sets of  $\alpha$  and  $\tau$ . Best parameter set across both regions highlighted in yellow.

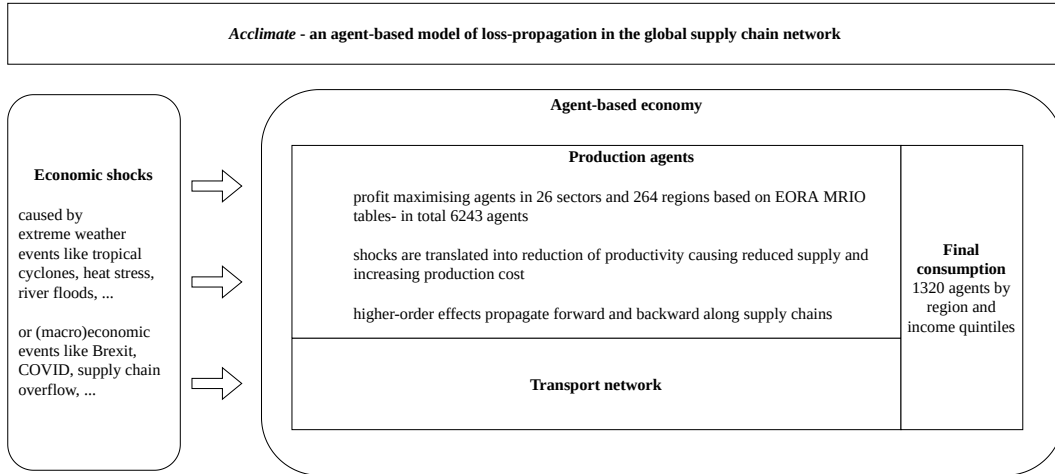
$\alpha$	$\tau$	total	USA	EU
0.15	182.50	8.22	4.58	11.86
0.15	273.75	4.89	2.48	7.29
0.15	365.00	3.47	1.97	4.97
0.15	456.25	2.91	2.07	3.76
0.15	547.50	2.87	2.47	3.27
0.16	182.50	7.32	4.02	10.62
0.16	273.75	4.13	2.09	6.17
0.16	365.00	2.83	1.75	3.92
0.16	456.25	2.48	2.04	2.93
0.16	547.50	2.63	2.65	2.61
0.17	182.50	6.53	3.54	9.53
0.17	273.75	3.45	1.83	5.08
0.17	365.00	2.39	1.63	3.14
0.17	456.25	2.24	2.15	2.34
0.17	547.50	2.62	3.03	2.22
0.18	182.50	5.91	3.12	8.71
0.18	273.75	2.91	1.58	4.24
0.18	365.00	2.06	1.69	2.43
0.18	456.25	2.19	2.45	1.93
0.18	547.50	2.81	3.57	2.05
0.19	182.50	5.23	2.73	7.73
0.19	273.75	2.47	1.50	3.43
0.19	365.00	1.89	1.88	1.91
0.19	456.25	2.29	2.89	1.68
0.19	547.50	3.18	4.23	2.14
0.20	182.50	4.68	2.48	6.89
0.20	273.75	2.13	1.51	2.76
0.20	365.00	1.87	2.18	1.56
0.20	456.25	2.60	3.56	1.65
0.20	547.50	3.78	5.16	2.41
0.21	182.50	4.19	2.30	6.08
0.21	273.75	1.94	1.64	2.24
0.21	365.00	2.00	2.66	1.34
0.21	456.25	3.05	4.30	1.79
0.21	547.50	4.55	6.17	2.92
0.22	182.50	3.79	2.18	5.41
0.22	273.75	1.82	1.83	1.81
0.22	365.00	2.28	3.26	1.30
0.22	456.25	3.68	5.18	2.18

$\alpha$	$\tau$	total	USA	EU
0.22	547.50	5.52	7.39	3.64
0.23	182.50	3.44	2.13	4.74
0.23	273.75	1.85	2.18	1.52
0.23	365.00	2.71	3.97	1.45
0.23	456.25	4.54	6.35	2.74
0.23	547.50	6.76	8.91	4.61
0.24	182.50	3.19	2.16	4.22
0.24	273.75	2.00	2.64	1.36
0.24	365.00	3.26	4.79	1.74
0.24	456.25	5.54	7.62	3.47
0.24	547.50	8.13	10.50	5.75



Supplementary Figure 2: **Schematic overview of the *Acclimate* agent-based economy**

The economy in the model consists of myopic, profit-maximizing producing agents as well as final consumers. All agents exchange goods via a transport network. Both production of individual agents and the transport network can be disturbed by external economic shocks, resulting e.g. from weather extremes.



## *Acclimate* – an agent-based model of loss-propagation in the global supply chain network

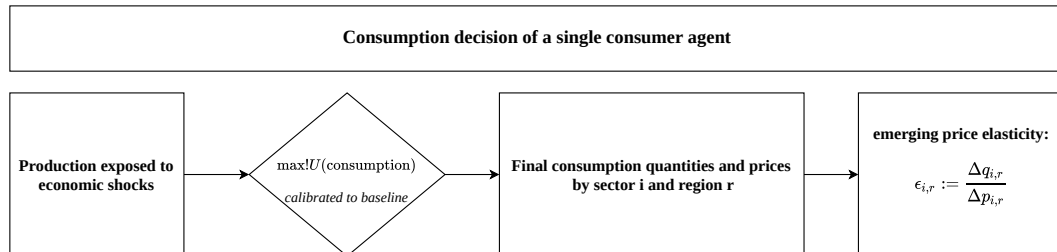
The *Acclimate* framework is described extensively in the original model description [Otto et al. 2017](#). Here, we focus on a brief introduction to the main components of the model relevant to our work.

First, the economic shocks are defined as an exogenous time-series of production capacity reductions. Here, we use a combined ensemble of heat stress, river floods, and tropical cyclone impacts [Kuhla, Willner, Otto, Geiger, et al. 2021](#) as discussed in the methods. This reduction in productive capacity propagates through the network and results in anomalies of production, prices, trade, and consumption. The dynamics of these anomalies results from the profit maximizing behavior of the producing agents, and the maximization of utility by representative consumers. Producing agents can mitigate lost outputs by extending their production beyond baseline capacity, resulting in a super-linear increase of production costs. Thus, a reduction of production capacity has upstream and downstream effects manifesting in demand and supply changes. If a shocked firm reduces production due to a shock, its suppliers experience reduced demand and the buyers of the produced goods experience reduced supply. Thus, these secondary affected firms have to

readjust their supply and demand as well and the effects of a local production shock thus propagate through the whole network.

An additional component of the *Acclimate* model is the transport network between agents, which can also be exposed to disruptions as in [Kuhla, Willner, Otto, and Levermann 2022](#). Here, goods are assumed to be transported either via road, ship, or air transport depending on distance and cost, such that the goods in delivery constitute a rolling inventory and re-balancing of demand might change the transport cost to be covered. Nota bene, that so far the network structure in the *Acclimate* model is assumed to be fixed, i.e. in accordance to the focus on short term reaction of the network to disruption it is not possible to establish new trade links. Finally, with our extension the final consumption is split into five income quintiles per region, who are calibrated based on World Bank income shares [Bank 2021](#). For this extension of the model, we refer to the detailed explanation in the methods section.

Supplementary Figure 3: **Single agent consumption decision:** Utility is maximized based on available quantities and prices of individual goods. The resulting flows can be used to deduce the market emergent elasticity as the ratio of relative change of quantities and prices.



Supplementary Table 1: Sector basket mapping

EORA sector	Basket	Description
AGRI	necessary	Agriculture
FOOD	necessary	Food and beverages
ELWA	necessary	Electricity, gas and water
FISH	necessary	Fishing
EDHE	necessary	Education, health and other services
OILC	relevant	Petroleum, chemical & non-metallic mineral products
TRAN	relevant	Transport
WOOD	relevant	Wood and paper
COMM	relevant	Post and telecommunications
RETT	relevant	Retail trade
TEXT	relevant	Textiles and wearing apparel
METL	relevant	Metal products
MACH	relevant	Electrical and machinery
TREQ	relevant	Transport equipment
MANU	relevant	Other manufacturing
CONS	relevant	Construction
WHOT	relevant	Wholesale trade
GAST	other	Hotels and restaurants
MINQ	other	Mining and quarrying
REXI	other	Re-export and re-import
RECY	other	Recycling
OTHE	other	Others
FINC	other	Financial intermediation and business activities
HOUS	other	Private households
ADMI	other	Public administration
REPA	other	Maintenance and repair

## References

- Bank, W. (Mar. 2021). *World Development Indicators DataBank*.
- Kuhla, K., S. N. Willner, C. Otto, and A. Levermann (2022). “Resilience of International Trade to Typhoon-Related Supply Disruptions”. Working paper.
- Kuhla, K., S. N. Willner, C. Otto, T. Geiger, et al. (Oct. 2021). “Ripple resonance amplifies economic welfare loss from weather extremes”. en. In: *Environmental Research Letters* 16.11, p. 114010. 10.1088/1748-9326/ac2932.

APPENDIX FOR ARTICLE 5

Otto, C. et al. (Oct. 2017). “Modeling loss-propagation in the global supply network: The dynamic agent-based model acclimate”. In: *Journal of Economic Dynamics and Control* 83, pp. 232–269. [10.1016/j.jedc.2017.08.001](https://doi.org/10.1016/j.jedc.2017.08.001).



# Danksagung

Ich bedanke mich bei all den großartigen Menschen, die ich im Laufe meiner Promotion kennenlernen durfte und mit denen ich das Vergnügen hatte, gemeinsam zu arbeiten und zu forschen. Ohne sie wäre diese Arbeit nicht möglich gewesen.

Zunächst möchte ich mich bei den beiden Betreuern meiner Arbeit bedanken. Bei Niels Landwehr, ohne dessen Hilfe ich diese Arbeit nie hätte einreichen können; sowie in besonderer Weise bei Anders Levermann, für seine Unterstützung während der Zeit meiner Promotion und alles, was ich von ihm gelernt habe.

Daneben hat wohl Sven Willner am meisten zum Gelingen dieser Arbeit beigetragen. Er war mir als Mentor in den vergangenen Jahren eine unglaubliche Hilfe und ich danke ihm für die vielen fruchtbaren Gespräche und seine verlässlich guten Ratschläge.

Eine große Freude war mir auch immer die Zusammenarbeit mit Lennart Quante, meinem Bürokollegen, sowie Kilian Kuhla und Christian Otto, mit denen ich die Tiefen komplexer ökonomischer Dynamik erkundet habe.

Bedanken möchte ich mich auch bei Anja Bruhn, die geduldig jeden Monat die Fehler in meinen Timesheets gefunden hat, die ich dort für sie versteckt habe. Vor allem aber dafür, dass sie jederzeit den organisatorischen Überblick behielt.

Ich bin überdies sehr dankbar für die Erfahrung, Teil einer festen und wachsenden Gruppe von Doktorandinnen und Doktoranden zu sein. Kelsey Barton-Henry, Timothé Beaufils, Anja Katzenberger, Max Kotz, Jakob Lochner, Anna Reckwitz, Annika Stechemesser und Maria Zioga – diese Menschen waren nicht nur großartige Kolleginnen und Kollegen, sondern sind mir auch gute Freunde geworden.

Mein besonderer Dank gilt meiner Familie; insbesondere meinen Eltern und meinem Bruder Lukas. Dafür, dass sie mich schon mein ganzes Leben lang begleiten und ich mich stets auf ihre Unterstützung und ihren Halt verlassen kann.

Ich bin außerdem sehr dankbar für all die Freundschaften, die über viele Jahre entstanden sind und ebenso lange andauern. Ich freue mich, dass wir uns trotz häufig großer räumlicher Distanz nie aus den Augen verlieren.

Und ich bedanke mich ganz besonders bei Uwe, für seine bedingungslose Unterstützung in den vergangenen drei Jahren und dass er mich stets daran erinnert, dass im Grunde eigentlich nichts schiefgehen kann.



# Erklärung

Diese Arbeit ist bisher an keiner anderen Hochschule eingereicht worden. Sie wurde selbständig und ausschließlich mit den angegebenen Mitteln angefertigt.

---

ROBIN MIDDELANIS

Berlin, April 2023

